AD NUMBER
AD921756
LIMITATION CHANGES

TO:

Approved for public release; distribution is unlimited.

FROM:

Distribution authorized to U.S. Gov't. agencies only; Test and Evaluation; 04 MAR 1973. Other requests shall be referred to HQ Space and Missile Systems Organization, P.O. Box 92960, Worldway Postal Center Los Angeles, CA 90009.

AUTHORITY

SAMSO ltr, 17 Jun 1977

WDL-TR5291
28 February 1974

SAMSO TR 74-183

AD921756

AD No. _____

DD FILE COPY

GLOBAL POSITIONING SYSTEM (GPS)
FINAL REPORT

PART II

VOLUME B
User Segment Trades and Analyses

new —
see AD 921 752

D D C
RECEIVED
AUG 22 1974
C

Submitted to:
DEPARTMENT OF THE AIR FORCE
HEADQUARTERS SPACE AND MISSILE SYSTEMS ORGANIZATION (AFSC)
P.O. Box 92960, Worldway Postal Center
Los Angeles, California 90009

TRW
SYSTEMS GROUP

PHILCO *Ford*

Philco-Ford Corporation
Western Development Laboratories Division
Palo Alto, California 94303

CONTROL DATA

SAMSO TR 74-183

WDL Technical Report 5291
28 February 1974

GLOBAL POSITIONING SYSTEM (GPS)
FINAL REPORT

PART II - VOLUME B
USER SEGMENT TRADES AND ANALYSES

Contract F04701-73-C-0296

Prepared for

DEPARTMENT OF THE AIR FORCE
HEADQUARTERS SPACE AND MISSILE SYSTEMS ORGANIZATION (AFSC)
Los Angeles, California 90009

ATTENTION: YEE $\mathcal{U}$

D D C
AUG 22 1974
C

DISTRIBUTION STATEMENT B

Distribution limited to U.S. Government
agencies only; Test and Evaluation;
4 March 1973. Other requests for this
document must be referred to SAMSO (YEEU).

PHILCO-FORD CORPORATION
Western Development Laboratories Division
Palo Alto, California 94303

PHILCO 🔵 *Ford*

Philco-Ford Corporation
Western Development Laboratories Division
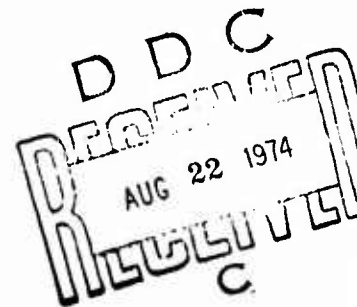
FOREWORD

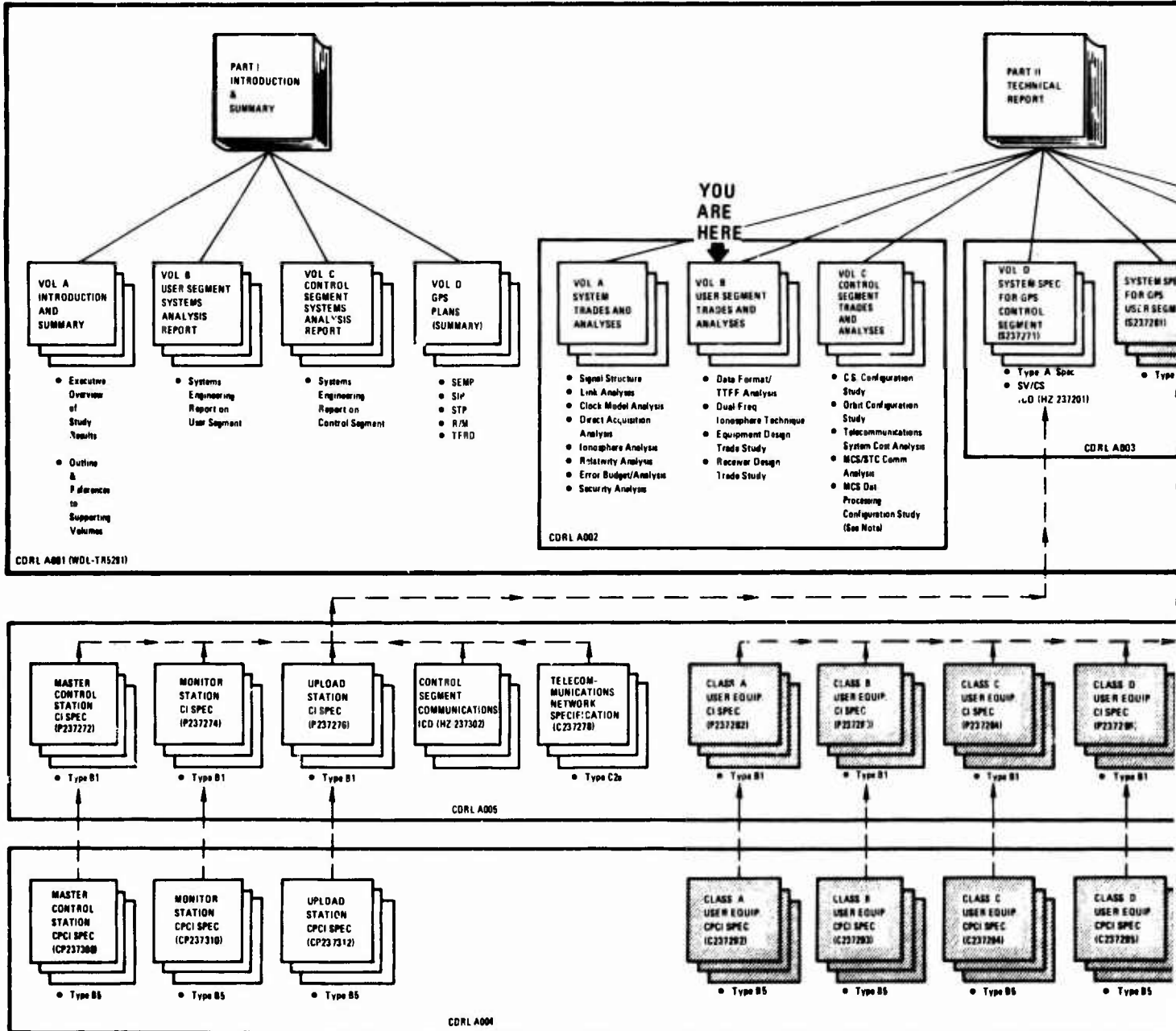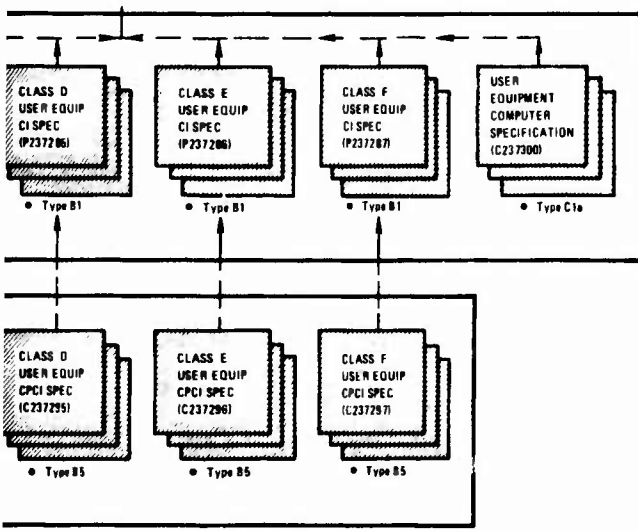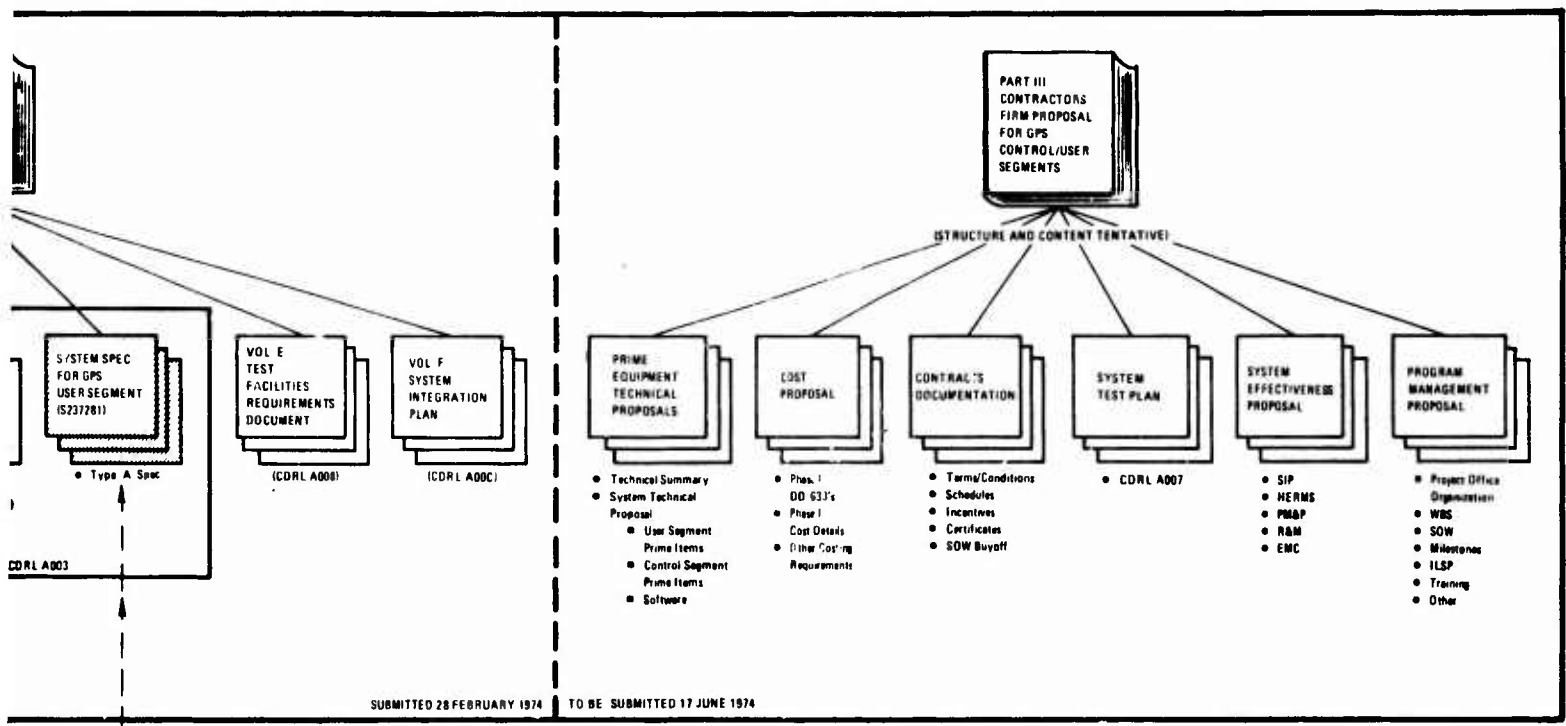This is Part II, Volume B, of the GPS Definition Study Final Report,
submitted by Philco-Ford in accordance with Sequence Number A002
of Exhibit A to Contract F04701-73-C-0296. The period of perform-
ance for the report submitted herein is from 28 June 1973 to 28 Feb-
ruary 1974. The following figure identifies the structure of the
Final Report and the relationship of this volume to other volumes
of this submittal.

1

WDL-TR5291
Part II
Volume B

PART I
INTRODUCTION
&
SUMMARY

PART II
TECHNICAL
REPORT

YOU
ARE
HERE

VOL A
INTRODUCTION
AND
SUMMARY

- Executive
  Overview
  of
  Study
  Results

- Outline
  &
  Reference
  to
  Supporting
  Volumes

VOL B
USER SEGMENT
SYSTEMS
ANALYSIS
REPORT

- Systems
  Engineering
  Report on
  User Segment

VOL C
CONTROL
SEGMENT
SYSTEMS
ANALYSIS
REPORT

- Systems
  Engineering
  Report on
  Control Segment

VOL D
GPS
PLANS
(SUMMARY)

- SEMP
- SIP
- STP
- R/M
- TFRD

CDRL A001 (WDL-TR5291)

VOL A
SYSTEM
TRADES AND
ANALYSES

- Signal Structure
- Link Analyses
- Clock Model Analysis
- Direct Acquisition
  Analysis
- Ionosphere Analysis
- Relativity Analysis
- Error Budget/Analysis
- Security Analysis

VOL B
USER SEGMENT
TRADES AND
ANALYSES

- Data Format/
  TTFF Analysis
- Dual Freq
  Ionosphere Technique
- Equipment Design
  Trade Study
- Receiver Design
  Trade Study

VOL C
CONTROL
SEGMENT
TRADES
AND
ANALYSES

- C.S. Configuration
  Study
- Orbit Configuration
  Study
- Telecommunications
  System Cost Analysis
- MCS/STC Comm
  Analysis
- MCS Data
  Processing
  Configuration Study
  (See Note)

CDRL A002

VOL D
SYSTEM SPEC
FOR GPS
CONTROL
SEGMENT
(S237771)

- Type A Spec
- SV/CS
  ICD (HZ 237201)

SYSTEM SPEC
FOR GPS
USER SEGMENT
(S237281)

- Type

CDRL A003

MASTER
CONTROL
STATION
CI SPEC
(P237272)

- Type B1

MONITOR
STATION
CI SPEC
(P237274)

- Type B1

UPLOAD
STATION
CI SPEC
(P237276)

- Type B1

CONTROL
SEGMENT
COMMUNICATIONS
ICD (HZ 237302)

TELECOM-
MUNICATIONS
NETWORK
SPECIFICATION
(C237279)

- Type C2a

CLASS A
USER EQUIP.
CI SPEC
(P237282)

- Type B1

CLASS B
USER EQUIP.
CI SPEC
(P237293)

- Type B1

CLASS C
USER EQUIP.
CI SPEC
(P237294)

- Type B1

CLASS D
USER EQUIP
CI SPEC
(P237295)

- Type B1

CDRL A005

MASTER
CONTROL
STATION
CPCI SPEC
(CP237308)

- Type B5

MONITOR
STATION
CPCI SPEC
(CP237310)

- Type B5

UPLOAD
STATION
CPCI SPEC
(CP237312)

- Type B5

CLASS A
USER EQUIP
CPCI SPEC
(C237292)

- Type B5

CLASS B
USER EQUIP
CPCI SPEC
(C237293)

- Type B5

CLASS C
USER EQUIP
CPCI SPEC
(C237294)

- Type B5

CLASS D
USER EQUIP
CPCI SPEC
(C237295)

- Type B5

CDRL A004

2

PHILCO

Philco-Ford Corporation
Western Development Laboratories Division

PART III
CONTRACTORS
FIRM PROPOSAL
FOR GPS
CONTROL/USER
SEGMENTS

(STRUCTURE AND CONTENT TENTATIVE)

SYSTEM SPEC
FOR GPS
USER SEGMENT
(S237281)

- Type A Spec

VOL E
TEST
FACILITIES
REQUIREMENTS
DOCUMENT

(CDRL A006)

VOL F
SYSTEM
INTEGRATION
PLAN

(CDRL A00C)

PRIME
EQUIPMENT
TECHNICAL
PROPOSALS

- Technical Summary
- System Technical
  Proposal
    - User Segment
      Prime Items
    - Control Segment
      Prime Items
  - Software

COST
PROPOSAL

- Phase I
  DD 633's
- Phase I
  Cost Details
- Other Costing
  Requirements

CONTRACTS
DOCUMENTATION

- Terms/Conditions
- Schedules
- Incentives
- Certificates
- SOW Buyoff

SYSTEM
TEST PLAN

- CDRL A007

SYSTEM
EFFECTIVENESS
PROPOSAL

- SIP
- HERMS
- PM&P
- R&M
- EMC

PROGRAM
MANAGEMENT
PROPOSAL

- Project Office
  Organization
- WBS
- SOW
- Milestones
- ILSP
- Training
- Other

CDRL A003

SUBMITTED 28 FEBRUARY 1974   TO BE SUBMITTED 17 JUNE 1974

CLASS D
USER EQUIP
CI SPEC
(P237285)

- Type B1

CLASS E
USER EQUIP
CI SPEC
(P237286)

- Type B1

CLASS F
USER EQUIP
CI SPEC
(P237287)

- Type B1

USER
EQUIPMENT
COMPUTER
SPECIFICATION
(C237300)

- Type C1a

INDICATES   30 JAN SUBMITTAL
(NOT INCLUDED IN THIS SUBMITTAL)

NOTE
ADD THESE ITEMS TO LIST
- MS Data Processing Configuration Study
- Reference Ephemeris Data Processing
  Cost Analysis
- Ephemeris Determination Analysis
- Signal Power Monitoring Techniques
- Ephemeris and Clock Processing
  Simulations

CLASS D
USER EQUIP
CPCI SPEC
(C237295)

- Type B5

CLASS E
USER EQUIP
CPCI SPEC
(C237296)

- Type B5

CLASS F
USER EQUIP
CPCI SPEC
(C237297)

- Type B5

Structure of Global Positioning System
Definition Study Final Report

CONTENTS

CONTENTS (Continued)

CONTENTS (Continued)

CONTENTS (Continued)

1. INTRODUCTION

In this volume of the final report, the analyses and results of the User Segment Trade Studies are shown. The studies fall into 4 main groups, as follows:

- Data message design
- Ionospheric correction techniques
- Equipment groups
- Receiver design.

Each of these main groups is further subdivided. The principal features of the trade studies are covered in the main body of this volume. Additionally, a number of appendices are included here, containing the more important of the back-up analyses which are referred to in the main body, and which are not available in the general literature.

2. DATA MESSAGE DESIGN TRADE STUDY

2.1 SCOPE

The data message which is the subject of this trade study is transmitted from the spacecraft and received by all users, and contains all the information needed by a user for navigation. This trade study is concerned with those aspects of the comparisons between alternate designs of the data message which are significant to the user equipment. In particular, it deals with

- Data rate
- Methods of transmitting ephemeris data
- Methods of transmitting reference data
- Handover words
- Frame sync patterns
- Parity
- Relationship between C- and P-data messages.

2.2 FUNCTIONAL AND TECHNICAL DESIGN REQUIREMENTS

The data message requirements are as follows:

a) Provide data with which the user can estimate the spacecraft's position and velocity with errors not exceeding 0.3 meters and 0.003 m/sec (one-sigma). These errors are those caused by the data transmission and the estimation processes, and do not include errors in the original determination of the satellite's ephemeris by the Control Segment.

b) Provide data with which the user can estimate the satellite's oscillator phase, relative to the GPS system time standard, with an error not exceeding 1 nsec (one-sigma). This error is the one caused by the data transmission and the estimation processes, and does not include the error in the original determination of the oscillator phase by the Control Segment.

c) Provide data with which the user can select the constellation of satellites he wishes to use.

3

d) Provide data with which the user can effect acquisition of the P-code after having acquired the C-code with little or no need for a P-code phase search.

e) Provide the means for a C-navigator to resolve the range ambiguities inherent in using the short C-code.

f) Provide the coefficients to be used in an ionospheric propagation correction model. The coefficients are computed by the Control Segment and the model is usable by navigators.

2.3 ALTERNATIVE APPROACHES

2.3.1 Data Rate

The data bit clock may be derived coherently from the same oscillator in the spacecraft which generates the carrier frequencies and the code clock signals, or it may be derived independently of these. The data rate may be selected over a wide range of values, subject only to the need to detect the data at low signal levels, resolve the range ambiguities, and minimize the frame duration.

2.3.2 Ephemeris Data

Alternative approaches to the method of transmitting the ephemeris data include sending a set of the orbital elements, from which the user will find the satellite position by doing an orbit integration calculation, or sending the coefficients of a set of polynomial expressions, in which time is the argument.

2.3.3 Reference Data

The reference data consist of the orbital elements of all satellites in the system (used for constellation selection), the coefficients of an ionospheric propagation correction model, and (possibly), rekey data for a TRANSEC device. There is also the possibility of including spacecraft telemetry data here, but this is not of concern to the User Segment, and will not be considered in this report.

The principal alternative methods are to include part of the reference data in each data frame (i.e., subcommutating the reference data), or substituting, on occasion, special reference frames for normal data frames.

2.3.4 Handover Words

There are two alternative methods for sending C-to-P handover data; either the state of the P-code generator which will become valid at some future specific time, is sent, or the time at which a specific state will become valid, is sent. Additionally, there is an alternative to sending the handover word once per frame, or more often.

2.3.5 Frame Sync Patterns

The tradeoff study in this area concerns the length of the sync pattern. The longer the pattern, the lower the false alarm rate, but this increases the missed detection rate too, as well as increasing the frame duration.

2.3.6 Parity

There is a tradeoff between error detecting and correcting techniques, and error detecting only. Further, there are the alternatives of parity check schemes which operate on small groups of bits, or on larger groups, up to a frame in size.

2.3.7 Relationship Between C- and P-Data Messages

One technique is to send identical messages simultaneously on both the C- and the P-signals. Alternatively, the messages can be identical but offset in phase, or they may even be of different content.

2.4 EVALUATION CRITERIA

2.4.1 Data Rate

The evaluation criteria here are twofold. The rate must be as slow as possible, so that the maximum jamming immunity during data collection can be achieved, but must not be so slow that the time to first fix (90 percent confidence) for a sequential P-navigator will exceed 5 min. Secondly, the preferred method of generating the data rate will be the one which reduces the user equipment complexity.

2.4.2 Ephemeris Data

The preferred method will be the one which reduces user equipment complexity (and hence cost), and which gives the longest allowable time of validity of a frame of data, subject always to satisfying the accuracy requirements.

2.4.3 Reference Data

Again, the evaluation criteria emphasize user equipment complexity and cost. Additionally, the criteria look at the effect of the method on the time to first fix.

2.4.4 Handover Words

The evaluation criteria are user equipment complexity and time to first fix.

2.4.5 Frame Sync Patterns

The evaluation criterion is to select a method which results in acceptable frame sync detection statistics, with a minimum of frame sync bits.

2.4.6 Parity

The evaluation criterion is simplicity of user equipment.

2.4.7 Relationship Between C- and P-Data Messages

The evaluation criteria are simplicity in user equipment and minimization of the time to first fix.

2.5 COMPARISON OF ALTERNATIVES

2.5.1 Data Rate

The question of generating the data clock coherently or noncoherently (relative to the carrier and code signals) can be dealt with first. With coherent generation, both the spacecraft processor and every user's receiver will be considerably less complex. Considering the receiver only, the noncoherent data clock will need a narrow band, frequency tracking, bit synchronizer, whereas the coherent method allows use of a simpler circuit,

since the correct data frequency can be synthesized from the carrier tracking loop's VCO. Even more importantly, if the data clock and the C-code clock are coherent (as they will be in the "coherent data rate" method), then the range ambiguities of the C-code can be resolved by very coarse ranging on the data bit transitions. With the noncoherent method, the resolution of range ambiguity would probably require a special signal. The one advantage that the noncoherent data enjoys is greater freedom in selecting the desired data bit frequency.

The advantages and disadvantages are summarized in Table 1. A weighting scheme has been selected and is shown in that table.

Table 1. Comparison of Coherent and Noncoherent
Data Bit Rates

Characteristic	Weight	Rating	
		Coherent	Noncoherent
Spacecraft processor complexity	5	5	0
Receiver bit synchronizer complexity	20	15	5
C-code range ambiguity resolution complexity	20	20	0
Freedom of design	5	0	5
Totals		40	10

The actual frequency is subject to a tradeoff between high data rates, which give low times-to-first fix, and low rates, which give improved jamming immunity.

For the time to first fix (TTFF) dependence on data rate, we have the following results from Appendix 1. The most critical case is that of

7

a sequential receiver, used for P-navigation. As was shown in that Appendix, the TTFF is given by

$$T = \sum_{i=1}^{4} (t_{1i} + t_{2i} + t_{3i} + t_{4i})$$

where t_{1i} = C-code search time

   t_{2i} = C-data frame sync wait time

   t_{3i} = time to collect navigation data

   t_{4i} = time for C $\rightarrow$ P handover

The four variates t_{1i} (i = 1, 2, 3, 4) are independently distributed. Their numerical values depend upon the received carrier-to-noise density ratio of the L_1-C signal. From Appendix 2, the minimum receiver power of the signal is -165 dBw and from Appendix 1, the worst case noise figure is shown to be -199. 6 dBw/Hz. Thus, as a minimum design point, we have, for the C/N_0 of the L_1-C signal, 34. 6 dB Hz. The means and standard deviations of the C-code search time (t_{1i}) are shown in Table 2 of Appendix 1 as a function of signal level; for 34. 6 dB Hz, they are, by interpolation, 28. 5 and 21. 5 sec, respectively.

The variates t_{2i} (i = 1, 2, 3, 4) are also independent; they are uniformly distributed between zero and the frame duration, T_f. Thus,

$$t_2 - \text{mean} = T_f/2$$

and t_2 - standard deviation = $T_f/\sqrt{12}$

Let the bit rate be B bits/sec, and the frame length be N_1 bits/frame.

Then

$$T_f = N_1/B$$

The variates t_{3i} (i = 1, 2, 3, 4) are fixed quantities, each equal to N_2/B, where N_2 is the number of bits from the beginning of frame sync until the end of the normal navigation data. If reference data are to be subcommutated, then $N_2 < N_1$; otherwise, $N_2 = N_1$.

Fixed values are also taken for the variates t_{4i}, equal to the time taken to collect the handover word (assumed to be 40 bits long) plus the time for P-loop pull-in and settling (assumed to be 0.3 sec). Thus,

$$t_4 = \frac{40}{B} + 0.3$$

Thus $\qquad$ T-mean $= 4\left\{28.5 + \frac{N_1}{2B} + \frac{N_2}{B} + \frac{40}{B} + 0.3\right\}$

$$= 115.2 + \frac{2}{B}\left(N_1 + 2N_2 + 80\right)$$

and $\qquad$ T-standard deviation $= \left|4(21.5)^2 + 4(N_1/B\sqrt{12})^2\right|^{\frac{1}{2}}$

$$= \left[1849 + \frac{1}{3}\left(\frac{N_1}{B}\right)^2\right]^{\frac{1}{2}}$$

The TTFF which is not exceeded on 90 percent of occasions is T_{90}, where

$$T_{90} = T_{mean} + 1.28\ T_{SD}$$

$$= 115.2 + \frac{2}{B}\left(N_1 + 2N_2 + 80\right) + 1.28\left[1849 + \frac{1}{3}\left(\frac{N_1}{B}\right)^2\right]^{\frac{1}{2}}$$
(seconds)

T_{90} is shown in Figure 1 as a function of B, for representative pairs of values of N_1 and N_2. The values shown for N_1 (the number of bits per frame) are 600, 900, 1200, 1500, and 1800, these being the lengths shown in the latest version of the System Specification. In each case, N_2 has been set at 600.

For the jamming immunity effect, we consider the L_1-P signal.

The bit energy-to-noise density ratio required for coherent PSK demodulation with a bit error rate of 10^{-5} is 9.5 dB. An allowance of 1.5 dB is made for the demodulation loss, so the required effective carrier-to-noise density ratio in L_1-P for data collection is

$$(C/N_o)_e = 10 \log B + 9.5 + 1.5$$

$$= 11 + 10 \log B \quad dBHz$$

Now, Appendix 2 shows that the L_1-P signal is 3 dB below the L_1-C signal, so the minimum design point for the C/N_o of the L_1-P is 31.6 dBHz, or 1445 Hz.

The relationship between the effective and jam-free carrier-to-noise density ratios for the L_1-P signal is

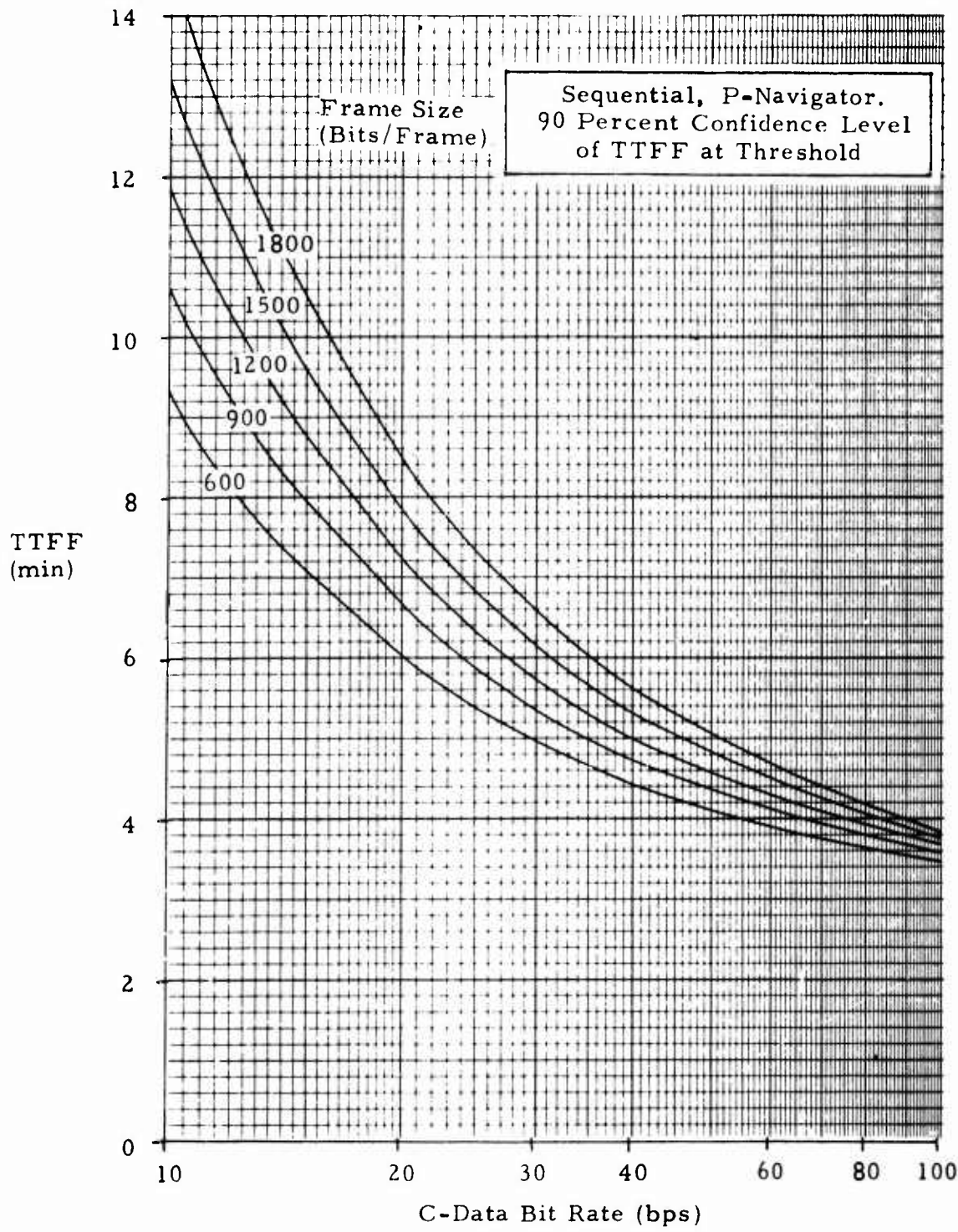$$(C/N_o)_e = \frac{C/N_o}{1 + (J/S)(C/N_o)(10.23 \times 10^6)^{-1}}$$

10

Figure 1. TTFF Versus Bit Rate

11

where J/S is the jammer-to-signal ratio, or, in other words, the jamming immunity.

Thus,
$$11 + 10 \log B = 10 \log\left[\frac{1445}{1 + \left(\frac{1445}{10.23 \times 10^6}\right)\left(\frac{J}{S}\right)}\right]$$

The jamming immunity is plotted as a function of the bit rate in Figure 2.

There is a third consideration to be taken into account, and that is the ease of using the data for C-code range ambiguities. The duration of the C-code is 1 msec, so that its range ambiguity is the distance moved by light in 1 msec, or 300 Km. The data bit duration is 1/B sec, so its ambiguity distance is 300,000/B Km. Quite evidently, with even the highest bit rates being considered (200 bps), this ambiguity distance (1500 Km) is easily resolvable with a priori navigation information. Thus, with all data bit rates in the range 10 - 200 bps, all range ambiguities are resolvable. The ease of doing this is related to the ratio of the durations, that is to the number of C-code ambiguities in one data bit. This number is 1000/B. Thus, without any other aid, the output phase jitter from the data bit synchronizer must be less than B/1000 cycles, or 0.36B degrees. Although this is possibly achievable if B = 100 bps (maximum allowable phase jitter is 36 degrees), it is impractical (in a low cost receiver) at B = 10 bps.

However, as a practical matter, ambiguity resolution should not be attempted with adjacent tone frequency ratios greater than, say, 6. Thus, for bit rates between 10 and 30 bps, two intermediate "tones" are required, and for bit rates between 30 and 160 bps, one "tone" is sufficient. (The "tone" is simulated by PCM-encoding each data bit; a 5:1 frequency ratio is equivalent to encoding with a 5-bit pulse pattern.)

The receiver complexity is considerably increased if two "tones" are required instead of one. Accordingly, from these considerations alone, the data bit rate should not be less than 30 bps.
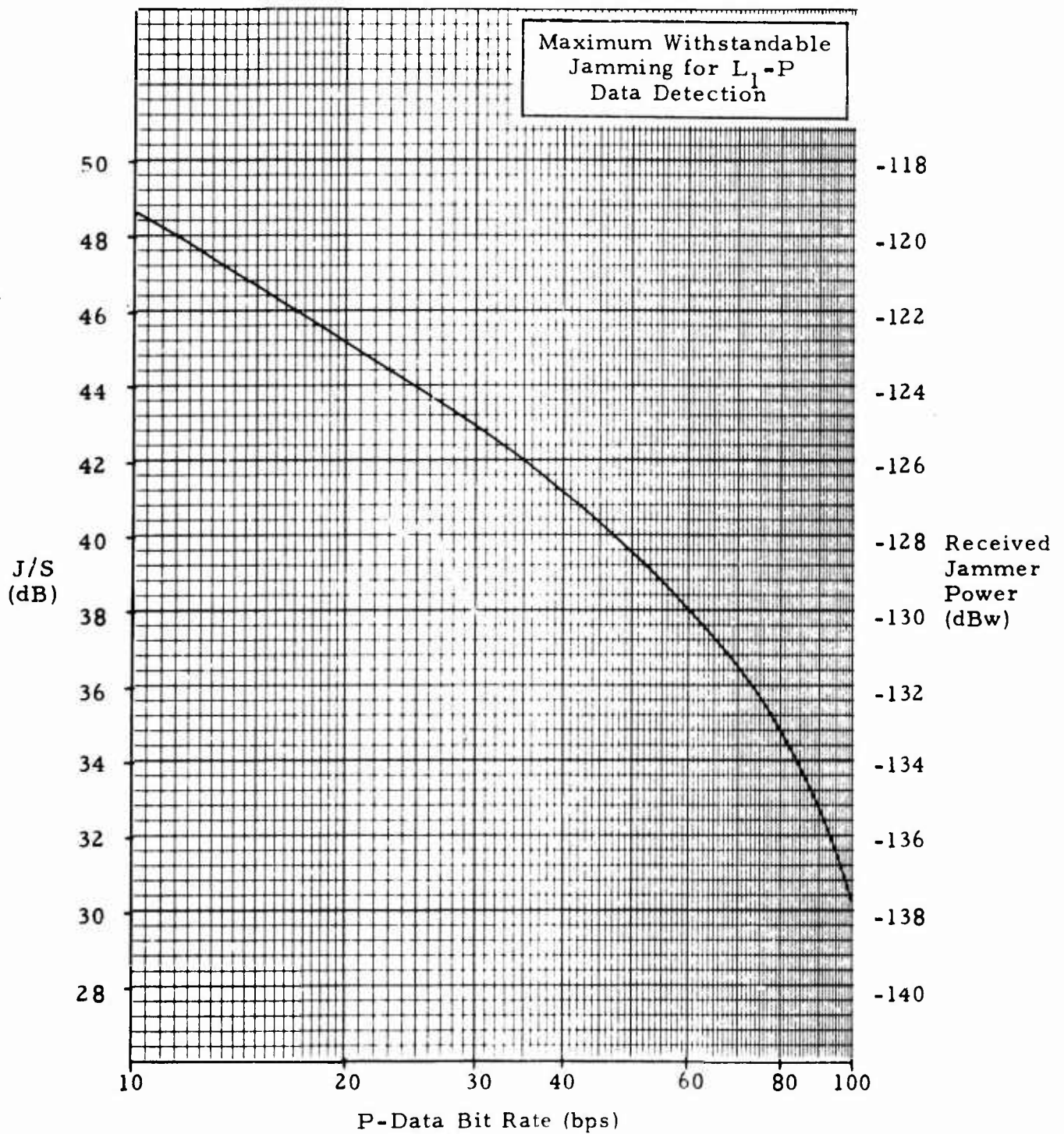
Figure 2. Jamming Immunity Versus Bit Rate

To summarize, the various considerations to be considered influencing the choice of the data bit rate are as follows:

a)   Time-to-First Fix - To achieve TTFFs of 5 min or less at the 90 percent confidence level, the minimum acceptable bit rates are as shown in Table 2.

Table 2.   Minimum Acceptable Bit Rates
for 5 Minutes TTFF

Frame Length (N_1 bits)	Minimum Acceptable Bit Rate (bps)
600	29
900	35
1200	40
1500	45
1800	50

b)   Ambiguity Resolution - To avoid the need of more than one intermediate "tone" for ambiguity resolution, the minimum acceptable bit rate is 30 bps.

c)   Jamming Immunity - For the best jamming immunity, the bit rate should be as low as possible.

d)   Ease of Synthesis - The bit rate should be a submultiple of the P- or C-code chipping rates (10.23 and 1.023 MHz, respectively).

It is evident that a good case can be made for having different bit rates in the P- and C-channels.   The TTFF and ambiguity resolution considerations call for a high C-data rate, whereas the jamming immunity calls for a low P-data rate.   Although two different bit rates can be easily handled in the receiver (since it will be working only one or the other, and never both simultaneously), there will be increased complexity in the

spacecraft. Thus, there is a tradeoff between spacecraft complexity and jamming immunity which can only be resolved at the GPS system level, and not here at the User Segment level. Accordingly, both the alternative solutions will be drawn up.

Firstly, if both C- and P-data bit rates are to be the same, then they should be equal to 50 bps, or more precisely,

$$B = \frac{F_c}{1023 \times 20}$$

where F_c = C-code chipping rate.

For ambiguity resolution, the 20:1 ratio between the C-code epoch rate and the data bit rate will require an intermediate "tone," which can be obtained by modulating each data bit with either a 4- or 5-bit sync pattern.

The TTFF will be less than 5 min (90 percent confidence level) with all the frame lengths being considered.

The C/N_o required for detecting the data at 50 bps is 28 dB Hz. Thus, there is a 6.6 dB margin for C-data detection (of which about 1 dB must be allocated for the multiple access loss). In the P-channel, the margin will be 3.6 dB, which may be used to withstand jamming to a J/S level of 39.6 dB (or a received jammer power of -128.4 dBw).

Secondly, if the added complexity in the spacecraft is tolerable, then there is a decided advantage to having different bit rates, as follows. The C-code bit rate will be 166.7 bps, or more precisely,

$$B = \frac{F_c}{1023 \times 6}$$

Since there will now be only six C-code epochs in each data bit duration, further encoding is not necessary for ambiguity resolution. This is a significant advantage to the User Segment, and, to some extent, also offsets the added complexity in the spacecraft.

The data ambiguity distance will be 1800 Kms, which is easily taken care of by the C-navigator's a priori knowledge of his location.

The TTFF will be well within requirements with this bit rate.

The C/N_o required for detecting data at 166.7 bps is 33.2 dB Hz. Since we are considering only the C-channel, a further 1 dB must be allocated for multiple access loss, bring the requirement up to 34.2 dB Hz. As was shown before, the minimum available C/N_o in the C-channel will be 34.6 dB Hz.

For the P-data bit rate, we do not have to concern ourselves with the requirements of TTFF and ambiguity resolution. Accordingly, this rate should be very low, so that the jamming immunity for P-data collection can approach, and be compatible with, the immunity for P-code range measurement (50 dB). For this, a bit rate of the order of 10 bps is needed. The actual rate must not only be easily derivable from the P-code chipping rate, but should also be a submultiple of the C-data rate. This latter point is important, since the spacecraft should change the data content of P and C simultaneously, and should do this at the ends of frames. Accordingly, the P-data bit rate will be 10.42 bps, or more precisely

$$B = \frac{F_p}{1023 \times 10 \times 6 \times 16}$$

where F_p = P-code chipping rate.

That is, the P-data bit rate will be exactly 16 times slower than the C-data bit rate.

The C/N_o required in the P-channel is 21.2 dB Hz. Since the minimum available C/N_o in this channel will be 31.6 dB Hz, the margin of 10.4 dB will provide a jamming immunity of $J/S = 48.4$ dB, or immunity against received jammer power of -119.6 dB w.

In summary, provided that the added complexity in the spacecraft is tolerable, the P- and C-data bit rates should be different, and equal to 10.4 and 166.7 bps, respectively. If they must be the same, then they should be 50 bps. The comparison between the two solutions is summarized in Table 3.

2.5.2 Ephemeris Data

Transmitting a set of orbital elements to each user is not a suitable technique for the ephemeris data for two reasons. Firstly, the calculations which the user would have to carry out in order to find the satellite's position and velocity would have to be iterative, rather than explicitly analytic, in order to meet the stringent accuracy requirements. Secondly, again to meet the accuracy requirements, these iterative calculations must take into account the many perturbations to the geopotential field, which increases both the computation time and the memory size needed. In all, if orbital elements were sent, the user computer would have to emulate the Control Segment ephemeris computer. Generally, it can be said that simple computations with orbital elements result in very coarse satellite position data (although the validity period of the elements is very long), and extremely complex computations result in very accurate positions. However, what is required of the ephemeris data in this application is that, with comparatively simple computation by the user, very accurate satellite position and velocity data can be derived, albeit over a short period of time.

This kind of requirement is best met by transmitting the coefficients of an expansion formula, in which the argument is time. In effect, the Control Segment computes a polynomial expression for each position coordinate of the satellite (x, y, z) which is a "best fit" to the best estimate of the trajectory. The coefficients of these polynomials, and the

17

Table 3. Summary Comparison of Alternative
Bit Rate Schemes

Characteristics	Same Bit Rate for C- and P-Data	Different Bit Rates
C-data rate P-data rate	50 bps 50 bps	166. 7 bps 10. 4 bps (= 166. 7/16)
C-code range ambiguity resolution	Data bit encoding needed	Resolution directly from C-data
Spacecraft complexity factors	Only one bit rate, needed, but data bit encoding too	Simultaneous transmission at 2 bit rates needed, but no data bit encoding
User receiver complexity factors	Need to detect bit encoding pattern	Simpler receiver
Ease of generating data bit rates (in both spacecraft and user equipment)	Equally simple	

Time to first fix (sequential, P-navigator, 90% confidence):
  with 600 bits/frame
  with 1800 bits/frame
	4. 10 min
	4. 99 min
		3. 22 min
		3. 46 min

C-data detection - worst case margin	5. 6 dB	0. 4 dB
P-data detection - J/S immunity	39. 6 dB	48. 4 dB

system time epoch for them all, constitute the ephemeris data. Each polynomial expression can also be used for velocity determination.

There are two tradeoff factors involved here. One concerns the order of the expressions. Generally, the higher the order the more bits have to be transmitted, but the accuracy of determination is improved and/or the period of validity is extended. The other tradeoff concerns the type of polynomial expression used; the alternatives include the continuous type (i. e. , Taylor expansions) or the discrete, or difference coefficient, type (such as the Gregory-Newton formula).

The effect of the order of the polynomial on accuracy and time of validity was extensively studied, first for the 24-hour period satellite orbits, and then, after redirection during the Study, for the 12-hour period orbits (Appendices 3 and 4). From the latter work, we have the numerical results reproduced here in Figures 3 and 4.

The zero-time epoch shown in these figures is not, necessarily, the system time at the start of the period of validity, but rather indicates when the time-argument in the expansion will be zero. (The time-argument is the actual system time minus the time epoch word sent with the ephemeris data.) Generally, the period of validity begins before this zero and ends after it. Accordingly, for the purposes of this trade study, the results shown in Figures 3 and 4 have been redrawn with time of validity as a parameter (in Figures 5 and 6). At the same time, the truncation and quantization errors have been RSS-added, instead of being shown separately, and the error has been shown in terms of its one-sigma value, rather than its maximum value (assumed to be 3-sigma.)

The requirements are that the errors should not exceed 0. 3 meters or 0. 003 m/sec. Clearly, the position accuracy requirement is the more stringent, and can be met with fifth differences for as long as 38 min, or with sixth differences for 62 min. As will be shown, 378 bits are needed for the fifth order difference coefficients, or 396 for the sixth order.
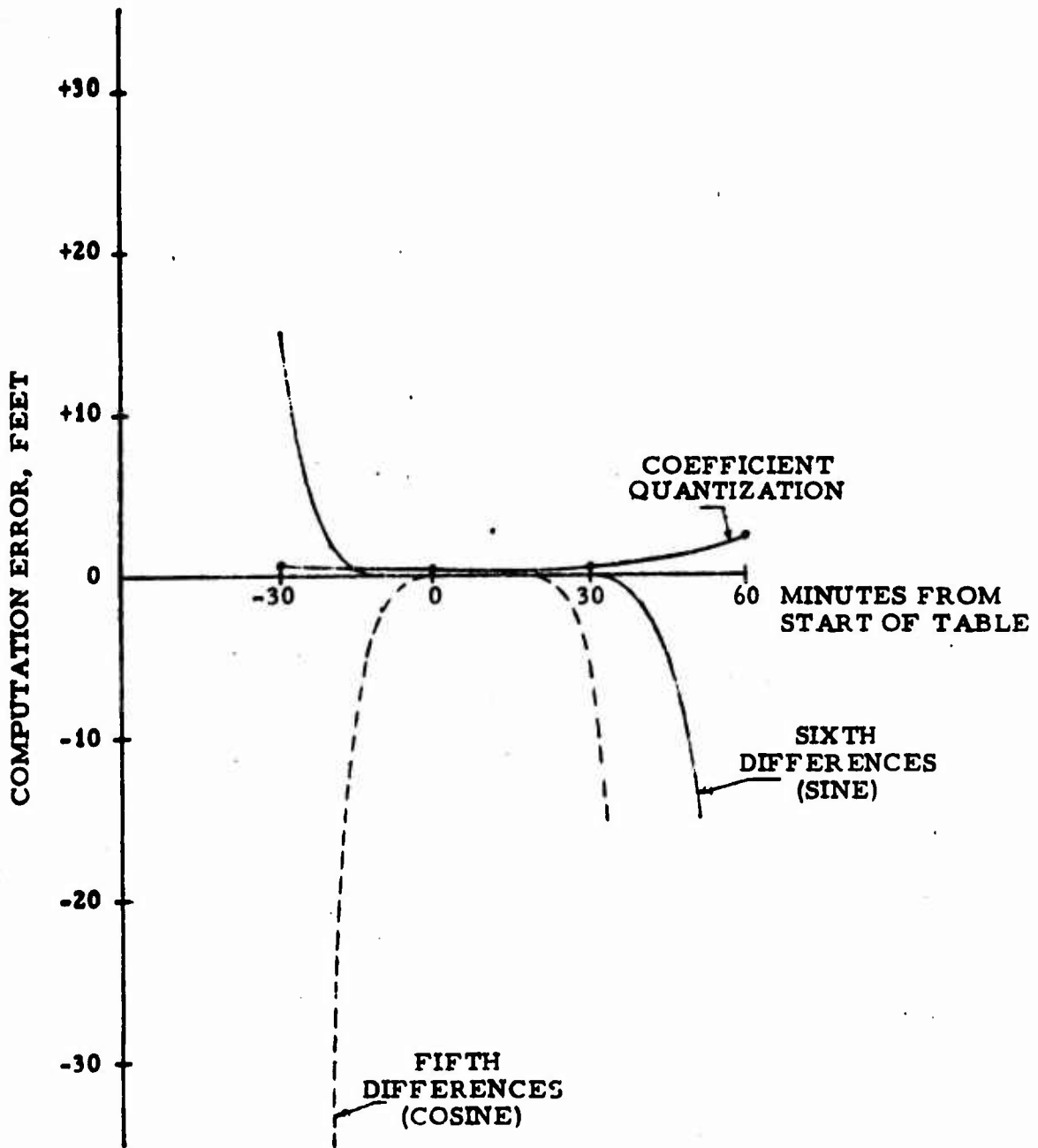
19

Figure 3. Error in Computation of Position Using Gregory-
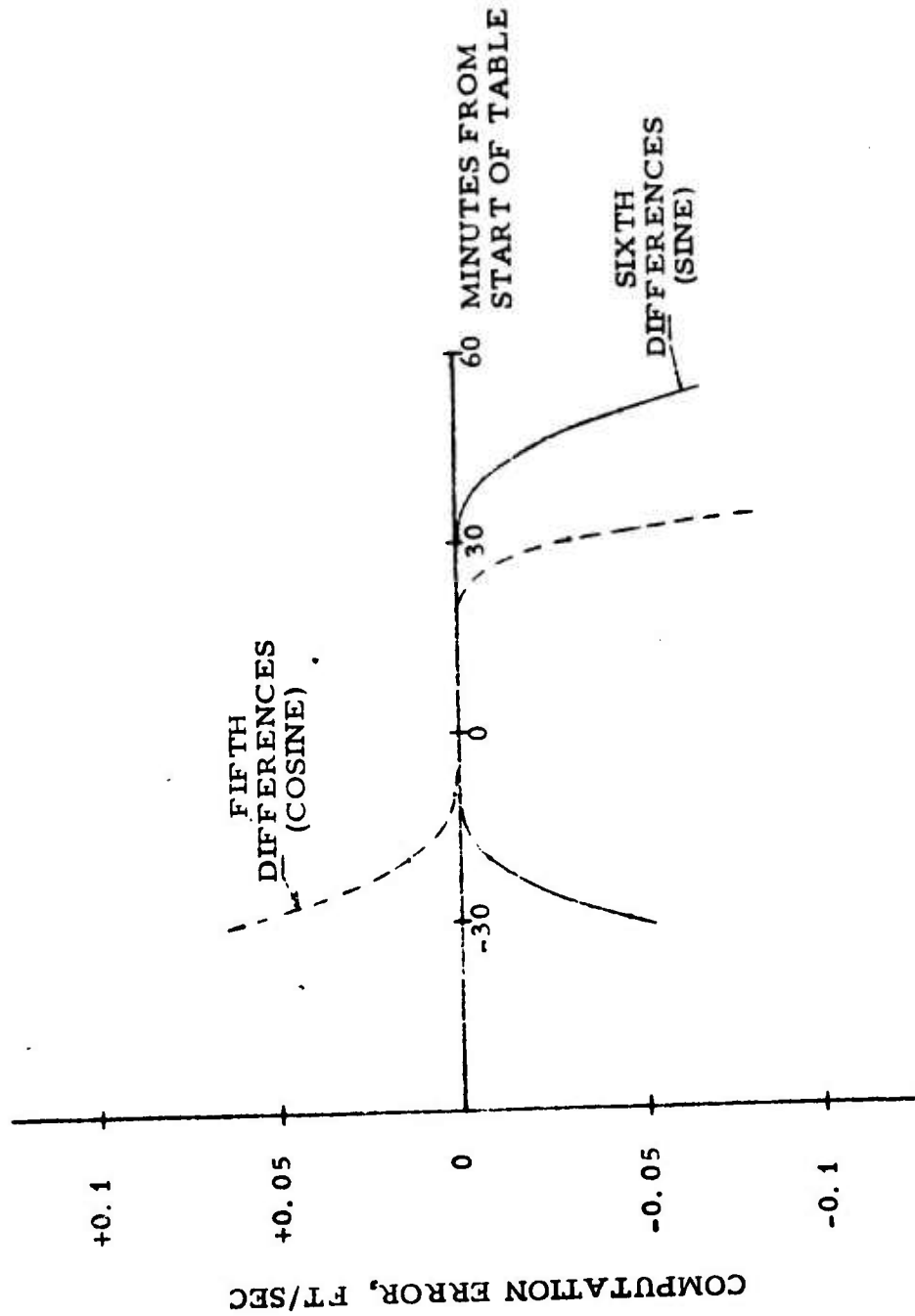Newton Formula for 12-Hour Orbits

20

Figure 4. Error in Computation of Velocity Using Gregory-Newton Formula for 12-Hour Orbits

21
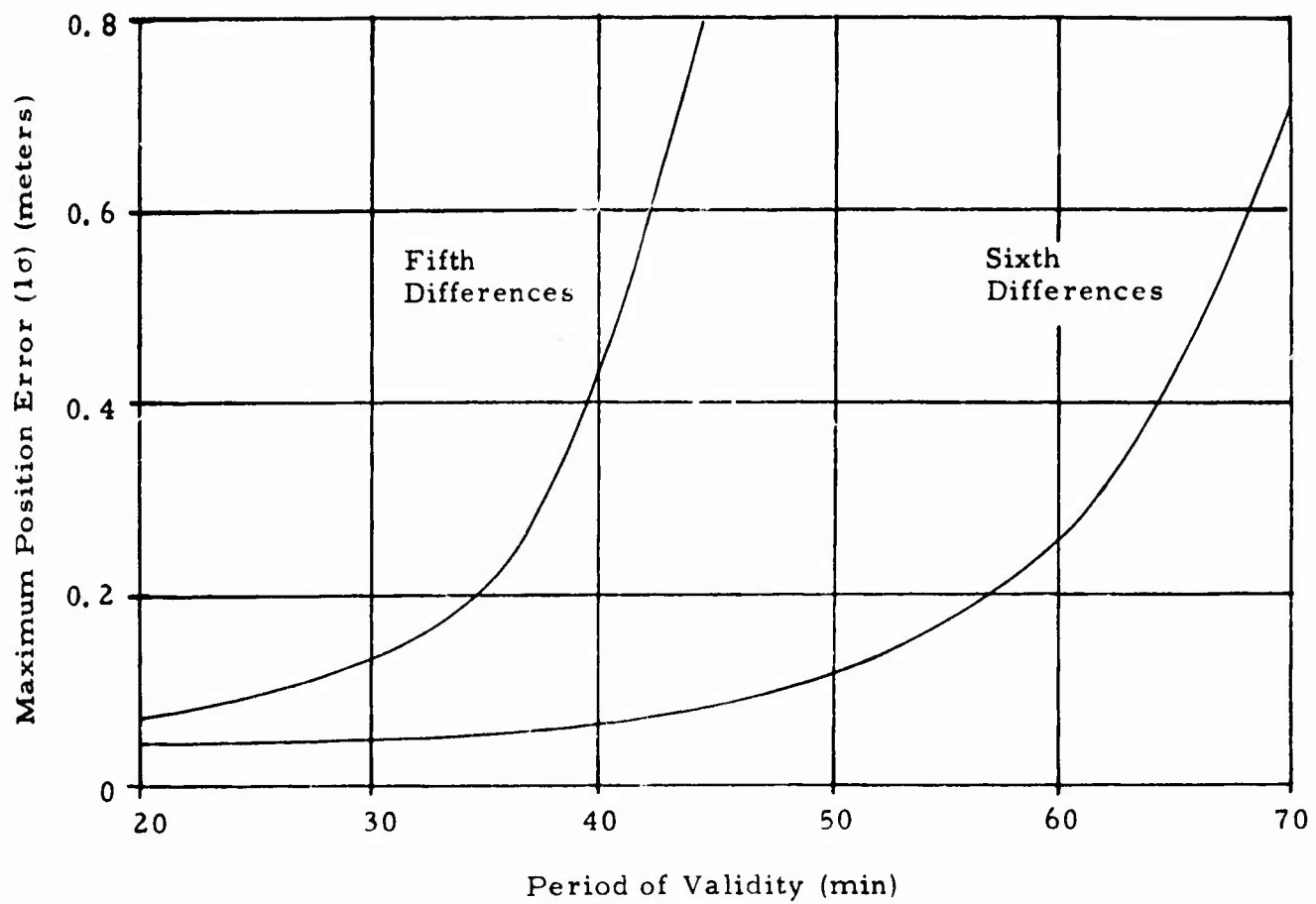
Figure 5.   Ephemeris Position Error

22
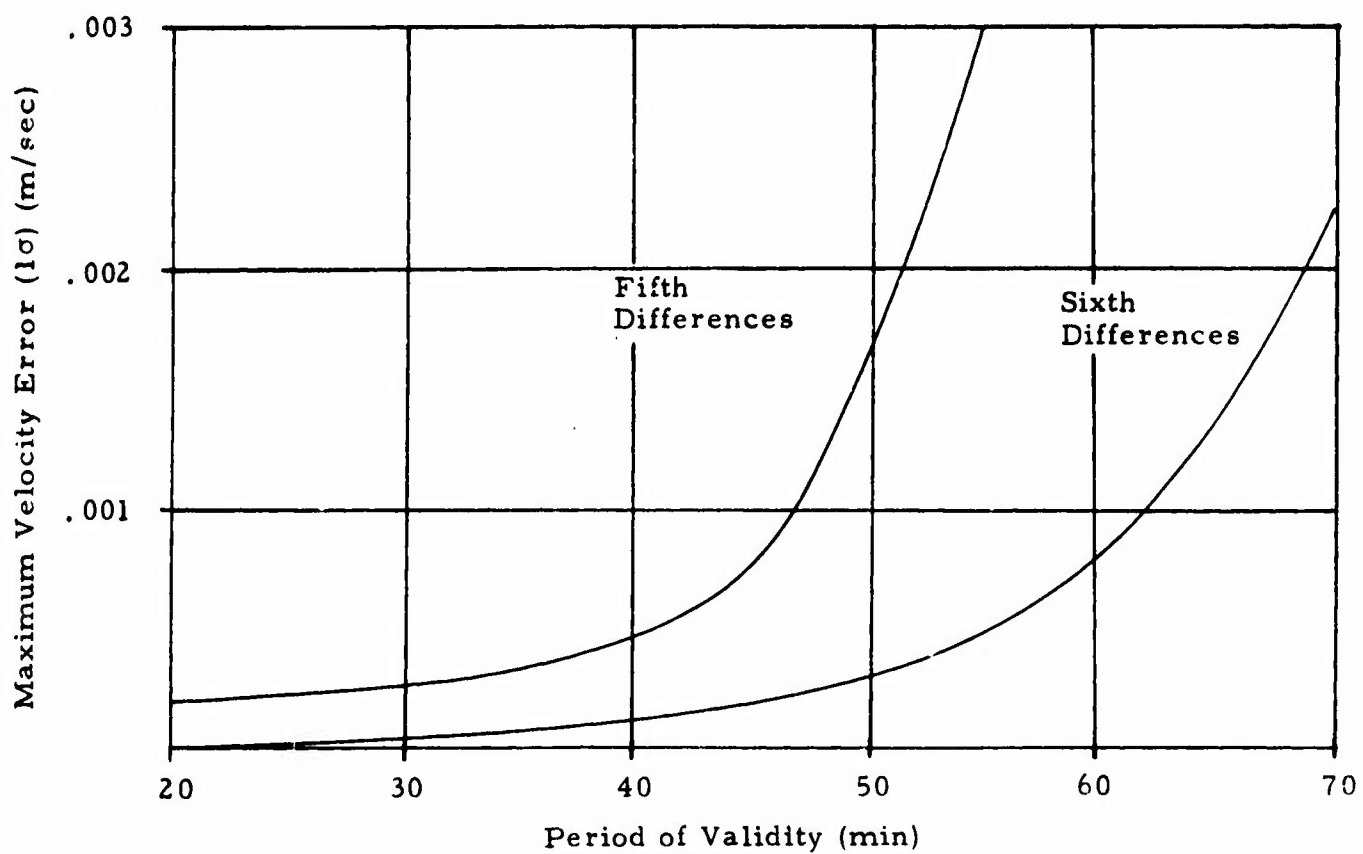
Figure 6. Ephemeris Velocity Error

23

Since it is not practical to fit these polynomial expressions to spans of orbit data longer than about 1 hr, it can be concluded that the requirements are met with one of two options. Either fifth difference expressions are used, updated every 38 min at the most, or sixth differences, updated every 62 min. The first option leads to a requirement to store, in the spacecraft, 14, 324 bits for each 24 hr of unattended operation, compared with 9, 197 bits for the second option. Clearly, the second option is the better choice and is the one here recommended.

For the tradeoff between the type of expression (polynomial or difference), we compare the number of bits needed for expressions of the same order (and hence having the same accuracy/validity performance). This comparison was studied in Reference 8, for fifth order and difference expressions with the results shown in Table 4.

Table 4. Comparison of Ephemeris Expressions

Coefficient	Required Number of Bits	
	Fifth Order Polynomial Expression	Newton-Gregory Fifth Difference Formula
a_0	31	30
a_1	27	27
a_2	18	23
a_3	18	19
a_4	18	16
a_5	18	11
Total (each axis)	130	126
Total (x, y and z)	390	378

24

This advantage in the number of bits required indicates the Newton-Gregory difference formula is preferable.

To complete the satellite ephemeris data message, we need the zero time epoch word (the system time when the argument in the formula is zero), and also data concerning the satellite oscillator.

Although system time will probably not be reset more often than once a week, it is not necessary to design for a maximum value of the zero time epoch word as large as this, since it will not differ from current time by more than 1 hr. However, the least significant bit must represent about 1 nsec. Thus, 42 bits are required.

The satellite oscillator phase and frequency will be computed using a second degree polynomial for phase, with time as argument. Thus, three coefficients are needed, representing the best estimate by the Control segment of the phase, frequency, and frequency rate at the zero time epoch (see Reference 1). In summary, the optimum satellite ephemeris message will be made up as shown in Table 5.

2.5.3 Reference Data

Only four types of reference data have been identified, namely, orbital elements, ionospheric coefficients, rekey data, and spacecraft telemetry.

The orbital elements are used for constellation selection. They are discussed in detail in Appendix 5, where it is shown that 2018 bits are needed, excluding ID and parity. These data will be valid for many months and will be changed quite infrequently.

In fact, they will need to be changed only under the following circumstances:

a) A new satellite has been placed in service. Assuming 24 satellites, each with a 7-year lifetime[*], this will

_____

[*] Note that, for this calculation, we do not have to consider infant mortality in the satellite's expected lifetime, since satellites which fail early never enter the operational system.

25

Table 5. Satellite Ephemeris Message

Word	Number of Bits (Incl. sign, excl. parity)
X_o	30
ΔX_o	27
$\Delta^2 X_o$	23
$\Delta^3 X_o$	19
$\Delta^4 X_o$	16
$\Delta^5 X_o$	11
$\Delta^6 X_o$	6
Total for x-axis formula	132
Total for y-axis formula	132
Total for z-axis formula	132
Zero time epoch	42
Satellite oscillator phase	31
Satellite oscillator frequency	21
Satellite oscillator frequency rate	4
Total	494

happen, in the operational system, every $3\frac{1}{2}$ months, on an average.

b) An existing satellite has been dropped from service. Since it is not absolutely vital that the users know of the event immediately it happens, the elimination of this satellite's orbital elements from these data may be delayed until the replacement satellite is placed in service, thus not causing an increase in the frequency of data change.

c) A satellite's orbit has drifted so far that its orbital elements must be updated. The required positional accuracy for constellation selection is of the order of several thousands of feet, so this change can always await the next placing into service of a new satellite, and hence will not increase the change rate. (This is an assumption; it is well beyond the scope of work of the User Segment Study to analyze satellite orbit drift rates.)

Thus, it can be concluded that changes to the content of the orbital element data message will not occur more frequently than once every 3.5 months, on an average.

There are three alternative methods of injecting these data into the user equipment, and the characteristics of each are summarized in Table 6. The first method considered is to use auxiliary support equipment, which will be located at the factory and at repair depots. It should be noted that this equipment will have to exist anyway, since it is also the method of injecting the computer program into the user equipment. Whenever data are changed (every 3.5 months), they will have to be distributed (physical distribution of magnetic tape) to all factories and repair depots.

The second method makes use of plug-in, read-only memories. Such devices are currently available; the nonrecurring cost (making the mask) is only a few thousand dollars, and the recurring cost, for a ROM of 4K bits, is less than $50 for large quantities.

The third method makes use of the data link from the satellites for updating (but still requires auxiliary support equipment at factories and repair depots). There is a variant to this alternative; these data may be

27

Table 6. Methods of Injecting Orbital Element Data Into User Equipment

Method	Impact on Satellite	Impact on User Equipment	Impact on Signal Structure	How Are Data Acquired Initially	How Are Data Acquired After Equipment Repair	How Are Data Updated (Infrequent Procedure)
Data injected with auxiliary support eqpt.	None	None	None	With auxiliary support eqpt at factory	With auxiliary support eqpt at repair depot	Equipment returned to repair depot. New data distributed to repair depots on magnetic tape
Data in replaceable plug-in ROM	None	Cost of ROM and ROM socket	None	ROM plugged-in at factory	ROM plugged-in at repair depot	New ROM distributed to all users, who plug it in themselves
Data obtained via the L-band link	Storage required in satellite Additional formatting requirement	More complex decoder	Frame length increased, or normal frames not sent continuously	With auxiliary support eqpt at factory	With auxiliary support eqpt at repair depot	Automatically, via the data link, whenever necessary and the eqpt is in use

sent quasi-continuously, subcommutated in normal data frames, or they may be sent intermittently, and indeed, on an as-needed basis, in special reference frames which replace normal frames.

From the standpoint of the User Segment (which is, admittedly, more limited than the overall GPS system point of view), the third method is the least desirable, since it offers, at significant cost and complexity, a facility infrequently used. Of the other two methods, the replaceable ROM is preferred, since it is anticipated that it is less costly to make and distribute ROMs every few months than it is to remove, send to repair depots, return, and replace major parts of the user equipment, at these same intervals. However, there are other considerations which are beyond the purview of this study, such as the possible need to change the data almost instantaneously if a new satellite is placed in service during an emergency period of hostilities. Because of these unknown factors, the ultimate decision cannot be made here.

The second type of reference data which has been identified to date consists of the coefficients of an ionospheric propagation correction model. This model would be quite complex (something like the Stanford or Bent models), makes a very significant and costly demand on the Control Segment, and will need about 1184 bits to describe all the coefficients (References 2 and 3). It is in addition to, and does not replace, the other two methods of ionospheric correction, namely, a simple algorithm which does not need data from the Control Segment, and the two-frequency method.

It has not been possible to obtain a reliable estimate of the accuracy attainable from such a model. It is extremely unlikely that it could even approach the accuracy of the two-frequency method (which is about 3-4 ft, see Appendix 6), and there is reason to believe that, on a worldwide basis, it will offer no improvement over the simple algorithm.

The third type of reference data contains the rekey for a TRANSEC device, and the fourth type contains spacecraft telemetry which is not

29

needed by users. (For the operational GPS, it would be desirable to send to all users a single bit describing the "go/no go" validity of the signal from the spacecraft. This bit could be incorporated with the spacecraft ID word). There is some question as to the need to send rekey data over the satellite downlink, and certainly telemetry data would not be sent on the navigation signal in the operational system.

Thus, for the reference data in general, it is concluded that, for the operational system, it is either undesirable or unlikely that the data should be sent via the L-band link.

In that case, should the data be sent over this link in the development configurations of GPS, they should be sent in such a way as to have minimum impact on the operational signal structure. This can be achieved by planning to send the data (if they are sent at all), on special reference frames, and not subcommutated in the normal data frames. Such reference frames should have the same length as the normal frames and begin with the same preamble.

2.5.4 Handover Words

We will first consider the alternatives between sending the state at a specific time, or the time at a specific state. The hardware required in the spacecraft for these two methods is about the same, but in the user receivers there is a significant difference, which is illustrated in Figure 7. In part a) of the figure, we show, in simplified functional form, the user receiver designed to use a handover word (HOW) which gives the state at a specific time. The "state" referred to is the state of the X2 replica code generator. The "specific time" is one P-chip duration after the "enable clock pulses" command, which itself is generated in the data decommutator at a fixed number of data bit transitions after frame sync. Between the time the HOW is received and this command is generated, the X2 generator is preset to the state contained in the HOW (that is, the HOW is read into the shift register), and the X1 generator is preset to its epoch state (all ones). Then, when the "enable clock pulses" command is sent,

a) **State at a Specific Time**
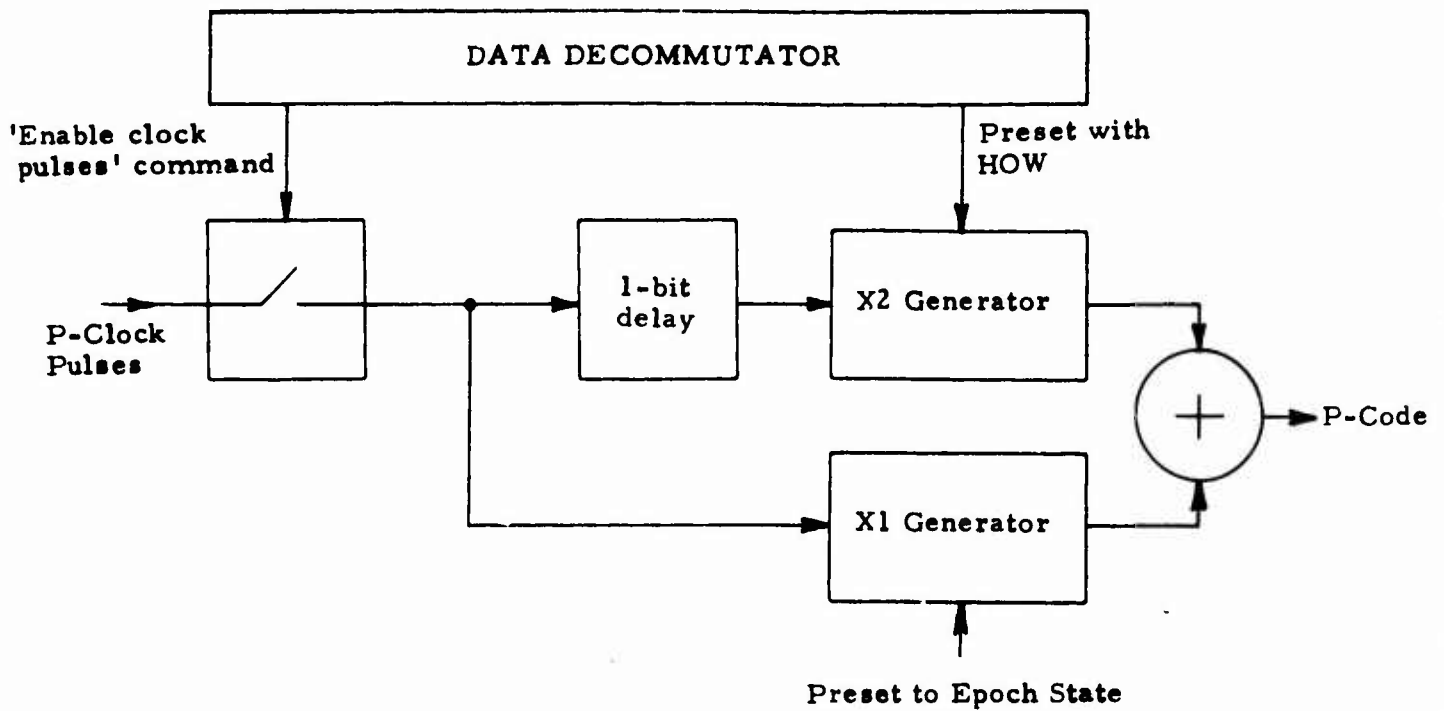
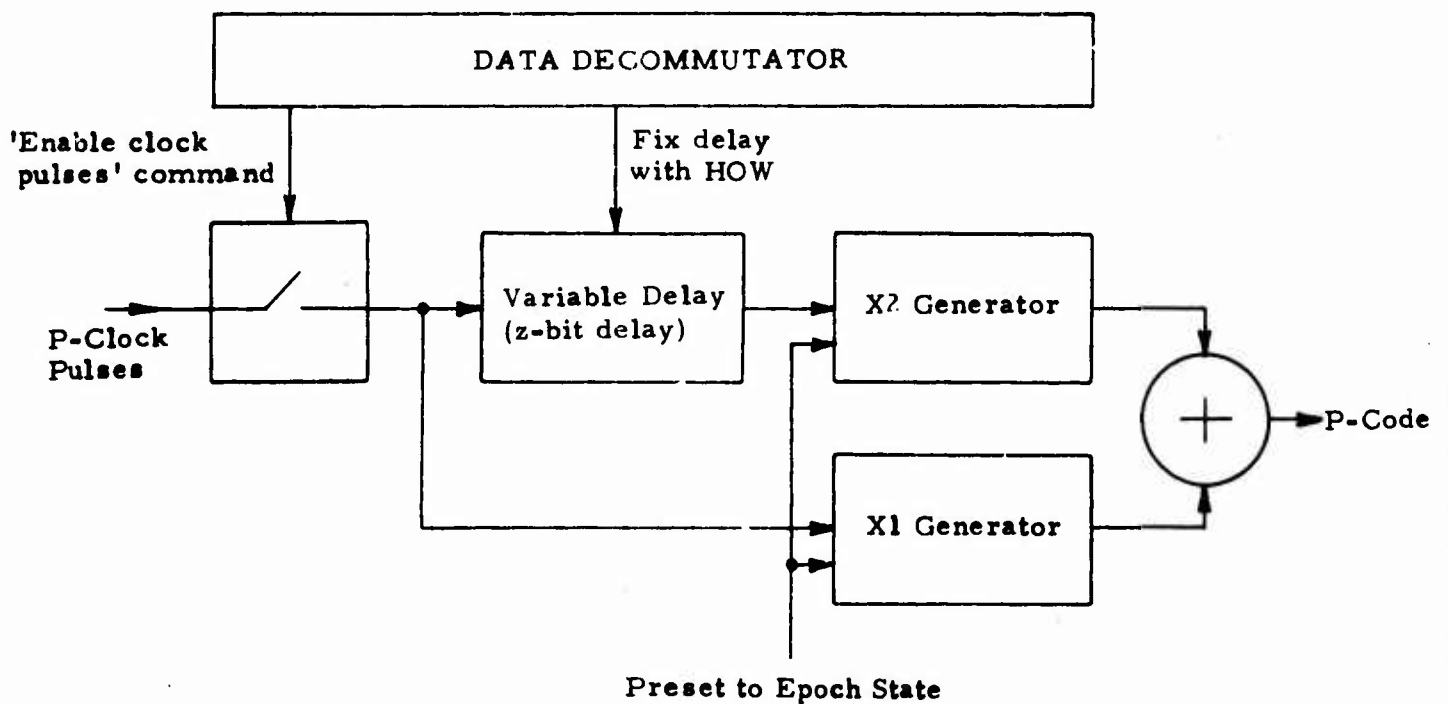
b) **Time at a Specific State**

Figure 7. Illustration of Handover Techniques in Receiver

31

the P-code clock pulses are immediately applied to the X1 generator, and after a 1 bit delay (in a one-stage shift register), to the X2 generator too.

For comparison, we shown in part b) of the figure, the alternative technique (time at a specific state). Both X1 and X2 are set to their epoch states (the "specific state "), and the HOW contains the value of the delay required. In all other respects, the techniques require the same circuitry. But now, the constant, 1-bit delay is replaced by a variable delay.

Although it is recognized that the variable delay is more complex than the constant 1-bit delay, they are both very simple devices. Nevertheless, if in all other respects the two techniques were alike, the better choice would be the one with less hardware, and so, by a small but observable margin, the first technique would be superior and be the one used.

However, the two techniques are not exactly alike, because the second technique has the potential of providing at least one, and perhaps two other capabilities to users. Both of these are derived from the meaning of the so-called Z-word (the amount of the delay), and from the fact that the variable divider consists of a countdown register and a gate, and that, after the handover has been effected, the register is not needed.

The Z-word is generated in the spacecraft and is the count of the number of X1-epochs since everything was initialized (which happens once every 7 days). Thus, in the spacecraft, it is system time, as best the spacecraft knows it, with a quantization level of, nominally, 1.5 sec, and a maximum range of 7 days. It is also, in the receiver, an approximate measure of GPS system time. The precision of this receiver system clock is of the order of tens of nsec (the jitter in the reconstituted P-code clock pulses), but it is not very accurate, since it is not corrected for spacecraft oscillator phase error, nor, more importantly, for transit time.

In fact, the uncompensated Z-word, in the receiver, represents GPS system time with an error of between .05 and .08 sec. As a frequency standard, it is somewhat more accurate, since the X1 code epochs

occur at a nominal frequency of $2/3$ Hz, with an error of up to ± 2 parts in 10^6. The information required for the compensation is, of course, available in the user computer.

Nevertheless, after handover to P, the Z countdown register can be used as a medium accuracy system time register, clocked by X1-code epoch pulses.

The second capability of the Z-word handover technique is for an automatic receiver reset at the 7-day reinitialization. Just as, in the spacecraft, when the Z-counter reaches the count of 403,200 (7 days/1.5 sec), it commands a complete reset, so in the receiver a replica Z-counter could command a complete reset of all the replica code generators. In this way, there will be no interruption to navigation at the 7-day resets.

Accordingly, it is concluded that these potential additional capabilities of the Z-word handover technique outweigh its slight added hardware complexity, and it is the preferred technique.

The second tradeoff for handover words is more significant in its impact. This concerns the number of HOWs in each data frame. One technique which has been recommended is that many of these words (about 6) should be used, uniformly distributed in the frame. The advantage claimed for this technique is that, at start-up, the time to wait for a HOW is greatly reduced, so reducing the time-to-first fix (TTFF).

The penalty paid for this is not inconsiderable. Firstly, the number of bits per frame needed for the HOWs is increased (by 56 bits for each HOW) which either reduces the spares holding, or even forces an increase in the frame length. Secondly, each HOW will have to be preceded by a sync pattern, which must be distinguishable from the sync pattern used at the beginning of each frame.

Although it can be argued that the advantage outweighs the disadvantage, it must be noted that the advantage is actually illusory and a shortened wait for HOW does not result in a shorter TTFF. This is because a complete set of navigation-data must be acquired before the first fix can be made. They may be acquired from either the C-or the P-data stream.

Suppose they are acquired from C. Then, after C-code acquisition, we must wait for main frame sync, collect the data, and then hand over to P. Thus, only one HOW per frame is needed, and it should follow as soon as possible after the navigation data. Alternatively, suppose the data are to be acquired from P. Then, although we can expect only a short wait between acquiring C-code and then handing over to P (with any one of the multiple HOWs), we then have to wait for P-data main frame sync before we can acquire the navigation data. As was rigorously shown, algebraically, in Appendix 1, the TTFF will be the same in both cases, that is, that the advantage of multiple HOWs is nonexistent.

Moreover, if the recommendation to use different bit rates in P and C is adopted, the use of multiple HOWs (implying, as it does, initial data collection in P rather than in C) will definitely increase the TTFF.

Accordingly, the tradeoff results in opting for only one HOW per frame.

2.5.5 Frame Sync Patterns

The tradeoff in the area of frame sync patterns is between long patterns, which have good detection and false alarm statistics, but which reduce channel capacity and require more detection circuitry, and short patterns, which are simple to implement at the cost of their performance statistics.

The performance of a frame sync pattern is measured by three quantities:

P_{md} = probability of missed detection

= probability of not detecting the sync pattern when it is received

P_{fa} = probability of false alarm

= probability of apparently detecting the sync pattern when it has not been received

P_{se} = probability of synchronization phase error

34

The performance characteristics of sync patterns have been described by Barker (Reference 4). He showed that the probabilities of missed detection and false alarm are dependent on the pattern length and not on the nature of the pattern. In the referenced paper, Barker analyzes the general case, and includes, as a parameter, the number of errors permitted the recognizer.

His results are

$$P_{md} = 1 - \sum_{\chi=0}^{k} C_{\chi}^{n} (1 - \epsilon)^{n-\chi} \epsilon^{\chi}$$

and

$$P_{fa} = 2^{-n} \sum_{\chi=0}^{k} C_{\chi}^{n}$$

where   n = length of sync pattern

k = number of errors permitted the recognizer

ϵ = bit error probability

The two performance parameters are shown in Figure 8 as a function of the pattern length, n, for discrete values of k, and for the bit error probability of 10^{-5}.

As can be seen from the figure, by allowing one or two errors in the recognition process, a very significant reduction in the probability of missed detection can be achieved at comparatively little cost in increased false alarm rate.

In the GPS application, the result of a missed frame sync detection is that the user must wait another frame duration before acquiring his data. Also, if he falsely detects frame sync, he will discover this one
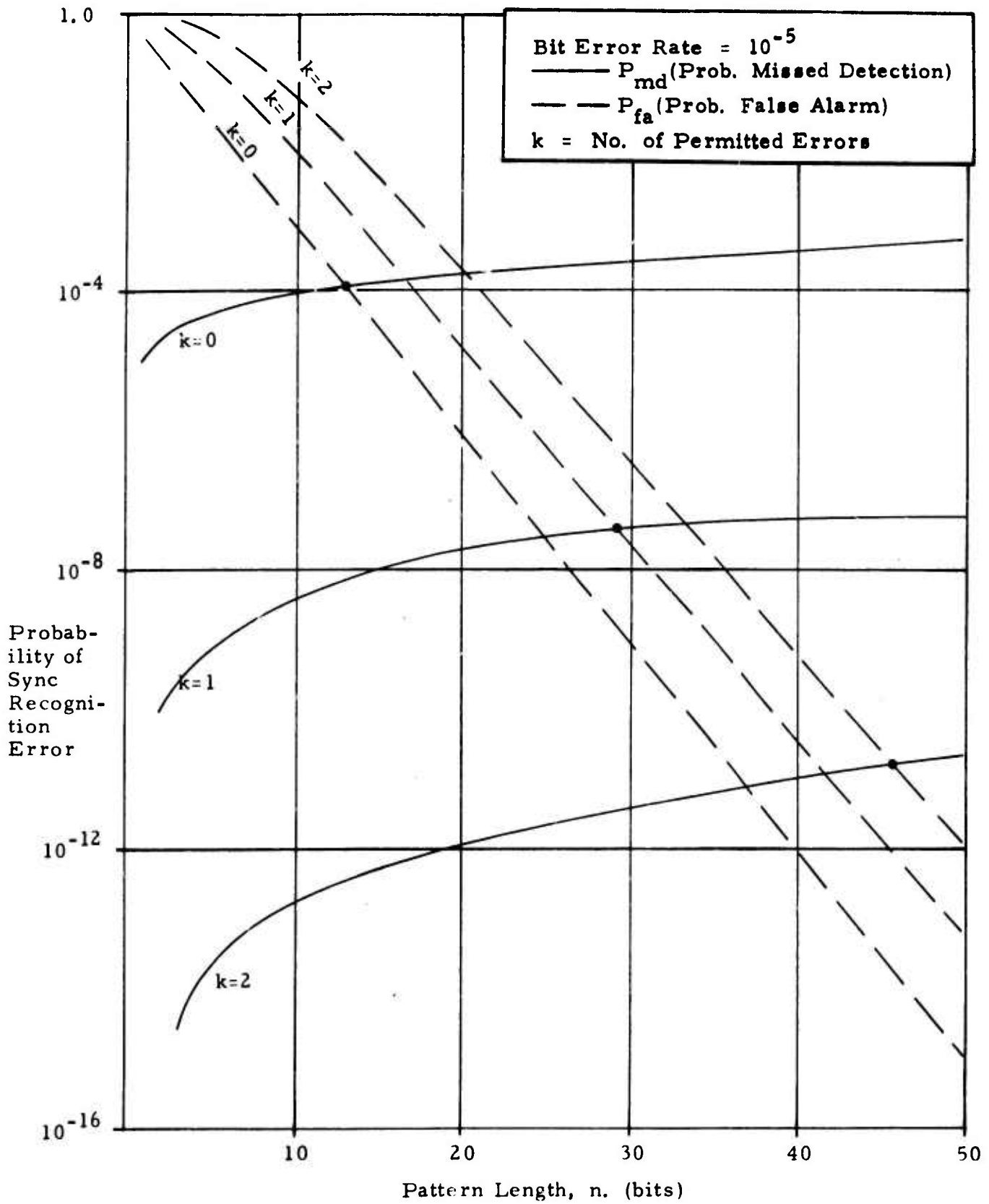
35

Figure 8. Sync Pattern Performance

frame duration later, when the data parity check fails. Actually, he will not know whether the parity check fails because of data transmission errors or because of false sync detection, but the result is the same: a delay of one frame duration. Thus, the effects of either missed detection or false alarm are the same. Accordingly, the design should attempt to minimize the greater of the two probabilities, P_{md} and P_{fa}. The combinations of n and k which do this are shown with large dots in Figure 8.

We must now take into account the third performance factor of frame sync patterns, the probability of synchronization phase errors. These are the errors in determining the correct end point of the pattern, caused by random pulses immediately adjacent to the sync word. This type of error is best understood by Barker's own example of a sync pattern consisting entirely of ones. Since there is a 50 percent probability that the bit which precedes the sync pattern is also a one, there is a 50 percent probability that the sync phase error will be 1 bit duration. Accordingly, the nature of the pattern itself must be such as to reduce the probability of this kind of error. Barker discovered such patterns, which have lengths

$$n = 3, 7, 9, 11, 21, 33, 49, 77 \text{ and } 121$$

Three of these (n = 3, 7, and 11) are "ideal" inasmuch as their auto-correlation sequence terms are zero and negative, except at one point in the center. The others are nearly ideal, since the off-center auto-correlation sequence times are no larger than +1.

Hence, it is highly desirable to use one of the Barker sync patterns. Using the criterion of selecting k (the number of errors permitted the recognizer) such that the larger of P_{md} and P_{fa} is minimized, a short list of the best possible combinations is shown in Table 7. Included in the table is a value of the mean time between errors. This is equal to the frame duration divided by the larger of P_{md} and P_{fa}. For the frame duration, we have assumed the worst case, which is a 600-bit frame, sent at the rate of 166.6 bps, resulting in a frame duration of 3.6 sec.

37

From this table, it is concluded that the best choice for GPS is to use the 33-bit Barker sync pattern, and to set the threshold of the recognizer so that it indicates sync when at least 32 bits of the pattern are matched.

Table 7. Best Combinations for Sync Patterns

n	k	P_{md}	P_{fa}	Mean Time Between Errors
11	0	1.1×10^{-4}	4.9×10^{-4}	2 hrs
21	1	2.1×10^{-8}	1.0×10^{-5}	100 hrs
33	1	5.3×10^{-8}	4.0×10^{-9}	786 days
49	2	2.0×10^{-11}	2.1×10^{-12}	5707 yrs

2.5.6 Parity

The principal choice for a parity scheme is between error detecting techniques and error correcting techniques. In general terms, error detection is comparatively simple, adds little to the frame length, and requires but simple hardware and/or software in the user equipment group. Its disadvantage is that it can but detect data errors, and results in data rejection. Error correction, on the other hand, is a more complex method, and, in particular, requires complex hardware/software in the receiving equipment.

Two important characteristics of GPS are critical to this tradeoff. Firstly, the most important selection criterion is simplicity in the user equipment, and this heavily mitigates against error correction techniques. Additionally, the GPS data are highly redundant, with frames being repeated many times. The number of repetitions will depend upon the final selection of bit rate, frame length and update interval, but will be at least

20 (10.4 bps, 1800 bits/frame, 1 hr intervals), and could be as many as 1000 (166.6 bps, 600 bits/frame, 1 hr intervals). Thus, if an error is detected but not immediately corrected, the penalty paid is time, and not complete loss of irreplaceable information.

Accordingly, it can be decided that, for GPS, the data need be coded only for error detection, and not also for error correction.

This, then, leads to the next tradeoff decision: which data should be error detection coded, and how should they be grouped. In this context, grouping refers to the block of data which share common error detection bits, and hence which must be rejected in toto if the parity check fails. The group could be as large as the frame, or smaller.

Using the reasonable criterion that data need be encoded only if the parity check decision can and should be used, it is clear that sync patterns do not need encoding. Not so evident is the case of the handover word. For a 2-channel, sequential receiver, there is no additional penalty paid if an erroneous handover word is used instead of rejected. However, in a continuous tracking receiver, the C-signal is dropped at the time of handover, so that if the HOW was in error, the P-signal will not be acquired, and the receiver will be forced to search for the C-signal all over again. Additionally, of course, there are other potential uses of the HOW which clearly require parity checking.

Hence, apart from the sync patterns, all data should be error detection encoded with parity check bits.

As far as grouping is concerned, it must be such that, at the user's choice, he may design his hardware/software for total frame rejection or part-frame (erroneous group only) rejection.

This is achievable by using the simplest of all error detection techniques, which consists of groups of (n-1) bits of data plus one parity bit. The user may then accept or reject groups in integral multiples of n bits. Very simple user software can then be designed to reject entire frames if any one of the group parity checks fail. More complex user

software can use the same GPS signal structure, but reject only the group (or group of groups) which fail the parity check, and then ensure that it searches for a replacement of only that part of the frame.

The size of the group (i.e., the value of n) depends upon the desired probability of error detection, and also on its convenience for use in computer handling. With these simple schemes, the probability of not detecting an error is, approximately, $(n\epsilon)^2/2$, where ϵ is the bit error rate. Typical values of this are shown in Table 8, for which $\epsilon = 10^{-5}$ has been assumed.

Table 8. Probability of Not Detecting an Error

Group Size	Probability
8	3×10^{-9}
12	7×10^{-9}
16	1×10^{-8}
24	3×10^{-8}
32	5×10^{-8}
36	6×10^{-8}
40	8×10^{-8}
48	1×10^{-7}
56	2×10^{-7}
60	2×10^{-7}
64	2×10^{-7}

For ease in user computer handling, the group size should be related to the computer's byte size. It is apparent that for many years to come, mini-computers will have byte sizes of 8, 12, 16, or 24 bits. Thus, a parity group size of 48 bits can be conveniently handled by any of these machines. And, from Table 8, it is seen that this group size gives an acceptably low probability (10^{-7}) of not detecting an error.

Finally, since most of the contents of a data frame are generated on earth and transmitted to the spacecraft for temporary storage there, and since this uplink will also require error detection encoding, it would be desirable that the parity bits for these data to be generated by the Control Segment, and transmitted and stored with the data, leaving the spacecraft processor the simpler task of preparing parity bits only for data generated in the spacecraft.

2.5.7 Relationship Between C- and P-Data Messages

In the optimum start-up sequence, navigation data are collected, for the first time, from the C-signal, and then the handover to P is made (see Appendix 1). There is no particular urgency in collecting the same data from P after handover, so there is no real advantage to be gained from phase offsetting the P- and C-data signals. Certainly it will be simpler in the spacecraft if they are not offset.

Most of the data are required in both the C- and P-data messages. The exceptions are the HOW, which is ignored in P, and the automatic rekey message, which (if it is sent at all) must not be sent in C. Accordingly, to avoid the cost of two hardwired decommutators in C/P receivers, the data formats should be identical in C and P. This will cause some small amount of channel capacity inefficiency in P (because the useless HOW is sent over that channel), and will require spacecraft logic to blank out the rekey word in C, but these are considered small penalties to pay for the major cost advantage of needing only one receiver decommutator.

2.6 CONCLUSIONS AND RECOMMENDATIONS

In summary, this trade study leads to the following conclusions and recommendations.

The data clock should be coherent with the carriers and the code clocks. The C-data rate should be six times slower than the C-code epoch rate (that is, it should be 166.7 bps, nominally), and the P-data rate should be 16 times slower than the C-rate (10.4 bps, nominally). It will not be necessary to further encode the data bits for C-code ambiguity resolution.

However, should it be decided that two different data rates will excessively complicate the spacecraft, then both should be 50 bps, and the C-data bits must be further encoded with either a 4 or 5 bit pattern.

The ephemeris data should be sent in the form of Newton-Gregory sixth difference formulae, one each for x, y, and z. The validity period will be 1 hr. The total navigation data message will consist of the three sets of six coefficients for the difference formula (3 x 132 bits), the zero time epoch word for the argument of these formulae (42 bits) and oscillator phase, frequency, and frequency rate words (56 bits). Thus, the navigation-data group consists of 494 bits, excluding parity.

From the standpoint of the User Segment, reference data should be made known to all users by the occasional distribution of plug-in read-only memories (ROMs). However, if from the GPS system-level point of view, it is decided that the reference data must be distributed via the L-band link, then they should be sent in special reference frames, which occasionally replace normal frames, and they should not be sub-commutated in the normal frames.

For the handover word, it is recommended that the time of validity of a specific state should be sent. Further, only one handover word per frame is required, and it should be located immediately following the navigation data. The optimum user strategy at start-up will be to collect the navigation-data in C before handing over to P.

It is concluded that, for GPS, the frame sync should be the 33-bit Barker synchronization pattern, and that the threshold in the user receiver's sync detector should allow 1 bit mismatch.

All data except the sync pattern should be parity bit encoded for error detection (but not for error detection and correction). The grouping should be one parity bit for each group of 47 information bits. Data which are generated by the Control Segment should be parity bit encoded on the ground, and these parity bits should also be stored in the spacecraft, along with their corresponding data. The spacecraft processor should generate parity bits only for data it itself generates.

The content of the P- and C-data frames should be identical, except that rekey data must be blanked out in C. Also, the start of each P frame should coincide with the start of a C frame.

3. IONOSPHERIC CORRECTION TECHNIQUE
TRADE STUDY

3.1 SCOPE

The scope of this trade study covers the alternative methods for a GPS user to correct his pseudorange measurements for the effect of the ionosphere. As far as possible, the scope has been limited to the User Segment, but in some instances, it has been found necessary to give consideration to the Control Segment too, and it must be recognized that, ultimately, ionospheric compensation technique tradeoffs have to be made at the GPS System level.

3.2 FUNCTIONAL AND TECHNICAL DESIGN REQUIREMENTS

The design requirement for ionospheric compensation is that the GPS signal must be such that users can obtain from it the magnitude of the correction they wish to make to their direct measurements of pseudorange. Further, the signal should be compatible with more than one compensation technique, so that users may select the least complex method consistent with their accuracy requirements.

3.3 ALTERNATIVE APPROACHES

Three principal techniques have been identified, as follows:

   a. Two frequency comparisons

   b. Correction algorithm with User Segment generated coefficients

   c. Correction algorithm with Control Segment generated coefficients.

There are minor variants within these principal classifications, especially in the last two, in which there are alternatives to the actual algorithm employed.

It should be noted that all of these methods are directed to compensating the pseudorange measurements only, and not the pseudorange rate. This is because, at the worst, the ionospheric error changes at

the rate of only 0. 0027 meters/sec (0. 53 ft/min) (see Reference 5).   Since
range rate measurements are made by differencing ranges over periods
considerably less than 1 second, the uncompensated ionospheric range rate
error is insignificant, and can be ignored.

3. 4 EVALUATION CRITERIA

The most important evaluation criterion for ionospheric compensation
is that the technique available to a user should introduce a minimum of
cost and complexity into his equipment, compatible with his accuracy
requirements.

This criterion forces GPS to provide more than one correction
technique, since a single common method would have to be the two
frequency comparison, this being the only one which provides the high
accuracy requirement demanded by Classes A, B and C.   Unfortunately,
two frequency techniques are significantly complex and costly, and so a
common method heavily penalizes medium and low accuracy navigators.

3. 5 COMPARISON OF ALTERNATIVES

3. 5. 1 Two Frequency Comparison

This technique consists of the transmission, by the satellite, of the
P-code modulated on carriers at two very different frequencies.   Since
the ionospheric delay is inversely proportional to the square of the carrier
frequency, there will be an easily observable difference in the pseudoranges
measured at each carrier frequency, and this difference is related to the
delay at any frequency.   Thus,

$$\rho_t = \rho_1 + \frac{k}{f_1^2}$$

and

$$\rho_t = \rho_2 + \frac{k}{f_2^2}$$

where ρ_t = true pseudorange

ρ_1 = measured pseudorange, with carrier
      frequency f_1

ρ_2 = measured pseudorange, with carrier
      frequency f_2

k = a factor which depends upon the integrated
      electron density along the radio path when
      the measurements are taken.

There are alternative formulas containing terms with f^4 and f^6 in the denominators, but the magnitude of these terms is insignificant.

In the simplest case, if we suppose that the two measurements are made simultaneously, it can be seen that

$$k = (\rho_1 - \rho_2) \ / \left(\frac{1}{f_2^2} - \frac{1}{f_1^2} \right)$$

In practice, the method is not so simply executed, partly because the two measurements are not made simultaneously, and partly because advantage can be taken of the short term time invariance of k. The practical method is exhaustively examined in Appendix 6, where it is shown that a satisfactory technique is:

- make L_2 measurements every 10 seconds

- adjust each L_2 measurement to the validity time of
  the closest L_1 measurement, using a second order polynomial

- compute the average pseudorange difference, using a moving
  arc, fixed weight filter, over the last 10 differences

- compute the correction factor (k/f_1^2) and apply it to every L_1
  measurement made in the next 10 seconds.

The only assumptions made in this technique concern the spatial and temporal invariance of the k-factor, that is, of the integrated electron density. We assume that it is nearly constant over a 100 second interval, and this is substantiated in Reference 5.

47

This technique adds considerably to the cost and complexity of the spacecraft, and to a lesser but still significant extent, to the user equipment (but only for those users who wish to use the technique). It has no impact on the Control Segment.

The technique is capable of performing very accurately. First and foremost, the error caused by the invalidity of the assumption of k-factor invariance, is insignificant. That is to say, the model is nearly perfect. The only significant errors are caused by the actual measurement errors themselves. In Appendix 6, it is shown that

$$\sigma 2(R_I) = \frac{\omega^2}{n} \left[\sigma^2(\rho_1) + \sigma^2(\rho_2) \right]$$

where

$\sigma(R_I)$ = S.D. of error in the correction

ω = a constant related to the ratio of carrier frequencies

= 0.613 (nominally)

$\sigma(\rho_1)$ = S.D. of L_1-P measurement error

$\sigma(\rho_2)$ = S.D. of L_2-P measurement error

n = number of differences used in moving arc average

= 10 (nominally)

The measurement errors have been evaluated and are here shown in Appendix 7, where it was shown that their standard deviation varied from 0.64 meters (2.1 feet) to 3.87 meters (12.7 feet), depending upon the effective carrier-to-noise density ratio.

Using the values of minimum received P-signal power of -168 dBw (for L_1-P) and -171 dBw (for L_2-P), and of maximum noise density of -199.6 dBw/Hz (See Appendix 2), we have

worst case C/N_0 - unjammed   31.6 dBHz (L_1-P)

28.6 dBHz (L_2-P)

48

Hence, without jamming, we have

$$\sigma(\rho_1) = 1.13 \text{ m.}$$

$$\sigma(\rho_2) = 1.74 \text{ m}$$

and

$$\sigma(R_I) = 0.40 \text{ m (worst case)}$$

with jamming (in both L_1 and L_2), we have

$$\sigma(\rho_1) = 3.87 \text{ m}$$

$$\sigma(\rho_2) = 3.87 \text{ m}$$

and

$$\sigma(R_I) = 1.06 \text{ m}$$

Thus, it may be seen that the two frequency technique is capable of very high accuracy. The complexity of the technique has been explored in detail in Appendix 8. Trade-offs are there shown between single and dual preamplifiers, single and dual first mixers, and between different filtering/channelizing schemes. It is concluded that a single preamplifier, combined with dual mixers, is the preferred approach, but the input filtering scheme will require further development. In that same Appendix, a trade-off is made between various frequency plans for an L_1/L_2 receiver. At the time the trade-off analysis was made, the L_1 and L_2 carrier frequencies were fixed at 1575 MHz and 1240 MHz, and the P-code clock rate was 10 MHz (so dictating the receiver's stable oscillator output frequency at 5 MHz). With those ground rules, and with the added constraint of operating the carrier loop VCO at either 40 MHz or 60 MHz (nominal), various frequency plans were traded-off, with special attention given to their spurious responses. It was found (and this is reported in Appendix 9) that for a 60 MHz VCO, the 2-frequency receiver needs triple conversion, and that for a 40 MHz VCO, this receiver has a choice of several frequency plans which require only double conversion.

The recent change of the P code rate from 10 MHz to 10.23 MHz (this changing the oscillator from 5 MHz to 5.115 MHz) has little effect

49

on the results of this frequency plan trade-off. However, the concurrent change which removed the fixed constraints on the carrier frequencies will allow even more frequency plans to be studied. Accordingly, the conclusions of the frequency plan trade-off must be considered provisional only at this stage in receiver development.

3.5.2 Correction Algorithm with User Segment Generated Coefficients

One expression for ionospheric error is (see Reference 6)

$$\Delta R = 1.32 \left(1 + \frac{H}{R}\right)\left(\frac{I_v}{f^2}\right)\left\{\sin^2 E + \frac{2H}{R} + \left(\frac{H}{R}\right)^2\right\}^{-\frac{1}{2}}$$

in which

ΔR = ionospheric range error, in feet

R = Earth's radius

H = ionospheric scale height (typically 350-400 Km)

f = RF frequency, in GHz

I_v = vertical integrated electron density, in hexams

E = elevation angle to satellite

The major weakness in this expression is that is assumes that the ionosphere is horizontally homogenous throughout the plane containing the center of Earth, user location and satellite location. Nevertheless, it forms the basis of a very simple correction technique, applicable to users with low accuracy requirements.

Eliminating all small terms, the expression reduces to

$$\Delta R \propto I_v \, \text{cosec} \, E$$

The value used for I_v will depend upon the user's latitude, the local time of day and the time of year, all of which are, of course, known with sufficient accuracy. It is also dependent on other factors, such as the solar activity index, which would not, normally, be available to the user.

Although it is tempting to conceive of more and more formulations for I_v in this technique, this is probably not worthwhile, since the major error source is the assumption of the homogenous ionoshpere. Accordingly, a simple expression for I_v in terms of latitude, season and time of day will probably be sufficient.

There is, at present, insufficient data about the ionosphere on a global basis to allow a reliable estimate of the errors associated with this correction technique. In fact, in all probability, the data will be obtained in the early development phases of GPS, when a number of two-frequency receivers become deployed around the World. However, as a rule of thumb, we may suppose that the residual error is no greater than one-third of the magnitude of the correction itse'f. (If the residual error were greater than this, then there would be little purpose in applying the correction in the first place.) In Appendix 9 it is shown that the largest ionospheric error (at 1575 MHz) is approximately 113 meters (368 feet), but there is a paucity of statistical distributional data. However, if we assume that this is the 3- sigma limit, and apply the rule of thumb, we can say that the standard deviation of residual error using this technique is 13 meters (41 feet).

It is noteworthy that the form of this ionospheric correction algorithm is the same as that for the tropospheric correction algorithm (see Appendix 10). Thus, a further virtual simplification results from its use.

3.5.3 Correction Algorithm with Control Segment Generated Coefficients

The status of investigations into these techniques is best summarized in Reference 7, where a model is described which requires 1184 bits (excluding parity and ID) every 24 hours for transmission of the coefficients. The software task to make use of this model is considerable, since a pair of double Fourier series have to be summed. Moreover, it is not presently known how accurate the resulting correction will be. In fact, Reference 7 makes the point that the GPS Development Phases I and II will themselves permit the statistical accuracy of the model to be evaluated.

3.5.4 Overall Comparison of Techniques

A full quantitive trade-off of the ionospheric correction techniques is not possible at this time, because the performance of the single frequency modeling methods is not yet known. A more general, qualitative, comparison is shown in Table 9.

Table 9. Overall Comparison of Ionospheric Correction Techniques

Characteristics	Two-Frequency Method	Model With User Generated Coefficients	Model With Ground Generated Coefficients
Impact on Control Segment	none	none	very high
Impact on Satellite	very high - second transmitter needed	none	very low - storage needed for 1200 bits
Impact on User Equipment (which uses the method)	high-two frequency capability needed	very low - simple software	considerable software impact
Impact on User Equipment (which does not use the method)	reduction in available L_1 power (satellite power must be split between L_1 and L_2)	none	some reduction in usable data link capacity
Accuracy (S.D. of residual error after correction)	0.4 meter	13 meters	not known

52

3.6 CONCLUSIONS AND RECOMMENDATIONS

The two frequency method of ionospheric correction is a firm requirement, since it is the only method capable of the accuracy needed by User classes A, B and F.

For lower accuracy users, it is not yet known if the simpler method, (a model with user-generated coefficients) will be adequately accurate on a global basis, or whether the more complex method will be satisfactory either. Both techniques should be investigated during Phase I at least and possibly beyond into Phase II.

4. EQUIPMENT GROUP DESIGN TRADE STUDY

4.1 SCOPE

Much of the equipment group tradeoff analysis is, of necessity, highly dependent upon the specific user installation under consideration. This is, indeed, one of the sought-for characteristics of GPS user equipment, namely that from a small number of standardized hardware and software components, various equipment group combinations can be made up, so as to match each user's specific requirements, including any requirements he may have to make continued use of components already in his inventory. Accordingly, the great bulk of these analyses will be carried out in a continuing manner in the early phases of the development program.

For this definition phase study, we concentrated on the higher level, and more general aspects of the equipment group tradeoffs, particularly those concerned with the selection of P or C navigation receivers, and the need for, and type of, auxiliary navigation sensors included in the group.

4.2 FUNCTIONAL AND TECHNICAL DESIGN REQUIREMENTS

The design requirements for a complete equipment group are complex and comprehensive, and are, at this time, best represented by the Prime Item Development Specifications for each user class (Spec No.'s P237282 through P237287). For the purposes of the trade-study, the significant design requirements can be summarized as shown in Table 10.

4.3 ALTERNATIVE APPROACHES

The alternative approaches important to the tradeoff study are that the GPS receiver can be a continuous or a sequential tracker, that it can operate on the C signal or the P signal, that it corrects for the ionosphere by the two frequency method or not and that the equipment group may include an inertial measurement sensor.

4.4 EVALUATION CRITERIA

The evaluation criterion is satisfaction of the basic requirements at the lowest user cost.

Table 10. Abbreviated Summary of Equipment Group Design Requirements

	CLASS A	CLASS B	CLASS C	CLASS D	CLASS E	CLASS F
ENVIRONMENTS						
DYNAMICS	4G, 2K FT/SEC	7G, 2K FT/SEC	2G, 800 FT/SEC	1G, 100 FT/SEC	1G, 100 FT/SEC	1G, 75 FT/SEC
JAMMING	80 DB	50 DB	20 DB	50 DB	50 DB	50 DB
VEHICLE	TACTICAL/ STRATEGIC	TACTICAL	TRANSPORT	GROUND VEHICLES, SHIPS	MAN	SUBMARINES
PERFORMANCE						
POSITION ACCURACY	15M	15M	45M	60M	60M	15M
TIME TO FIRST FIX (TTFF)	3 MIN	3 MIN	5 MIN	5 MIN	5 MIN	1 TO 2 MIN

4.5 COMPARISON OF ALTERNATIVES

4.5.1 Continuous/Sequential Tracking Receivers

There will certainly be users with some very specific requirements which, alone, will decide the choice of a continuous or a sequential tracking receiver. For example, a firm requirement for time-to-first fix less than 90 seconds, say, will be paramount in forcing the selection of a continuous tracking receiver, whereas a user with severe cost limitations will employ a sequential tracker, regardless of any performance penalty which that choice might incur.

Generally, however, the requirements do not so obviously lead to such an inflexible selection. Rather, it is the combination of all requirements which is the deciding factor. Particularly, it is the combination of user dynamics, required measurement accuracy, and required jamming immunity. This is demonstrated in Figures 9 and 10 which show how measurement accuracy and the desired jamming immunity are highly dependent on the choice of the receiver immunity.[*]

From a wide examination of the basic class requirements, the selection of continuous or sequential tracking for Phase I equipment groups is as shown in Table 11.

Table 11.   Continuous/Sequential Comparison Chart

Requirement	Better Choice for Receiver					
	Class A	Class B	Class C	Class D	Class E	Class F
User Dynamics	Cont	Cont	Seq	Seq	Seq	Seq
Measurement Accuracy	Cont	Cont	Seq	Seq	Seq	Cont
Jamming Immunity	Cont	Cont	Seq	Cont	Cont	Cont
TTFF	Cont	Cont	Seq	Seq	Seq	Cont
Overall	Cont	Cont	Seq	Seq	Seq	Cont

---

[*] These figures should be used with caution, since they were derived when a different signal structure was valid. Nevertheless, the general shape and dependence which they illustrate are still correct.

PSEUDO RANGE MEASUREMENT ERROR   PSEUDO RANGE RATE MEASUREMENT ERROR
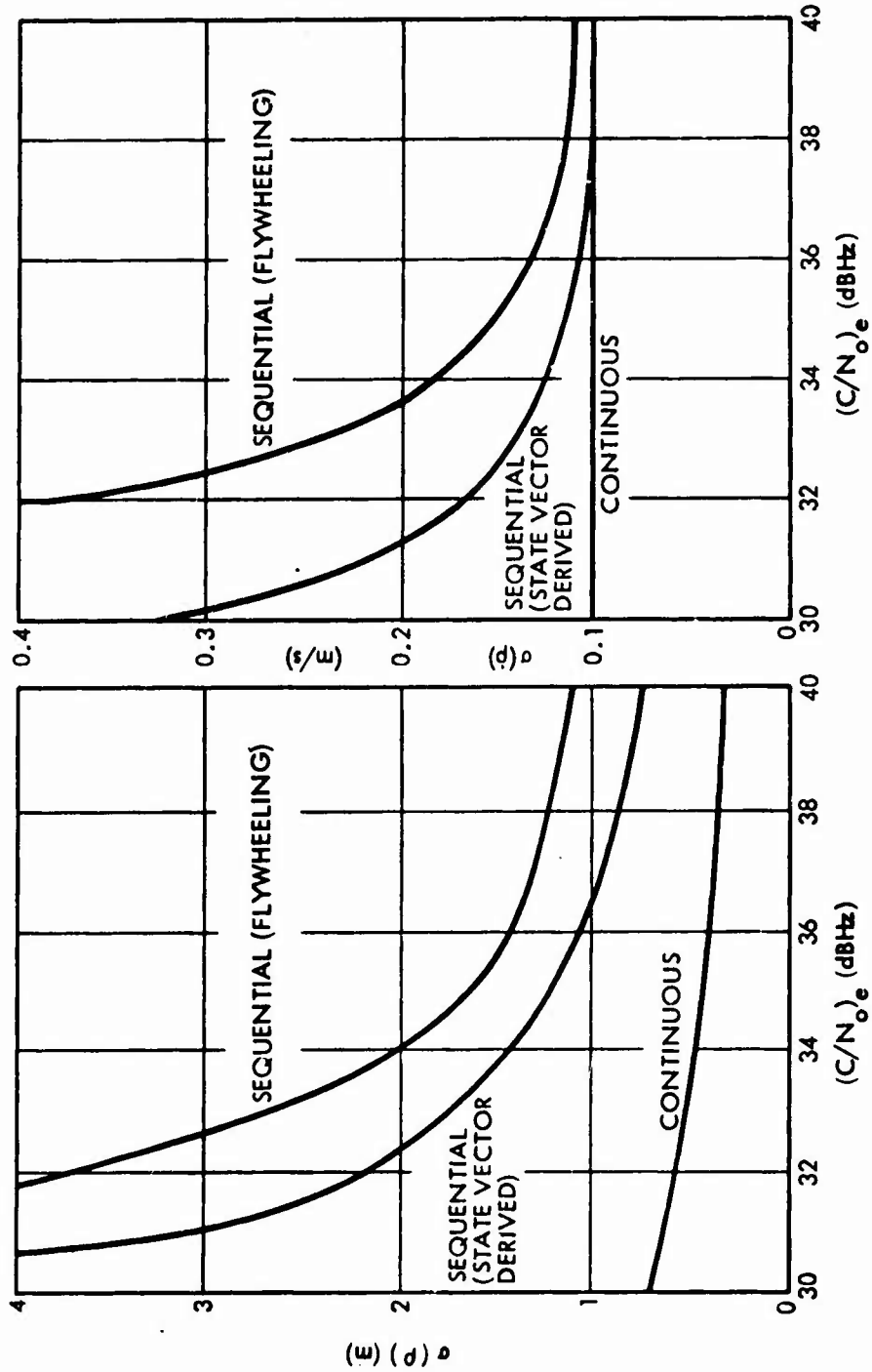
ACCELERATION = 1g   QUANTIZATION: 0.3m
TIME SLOT DURATION = .15 SEC   AND: 0.1 m/s

Figure 9. Typical Measurement Accuracies
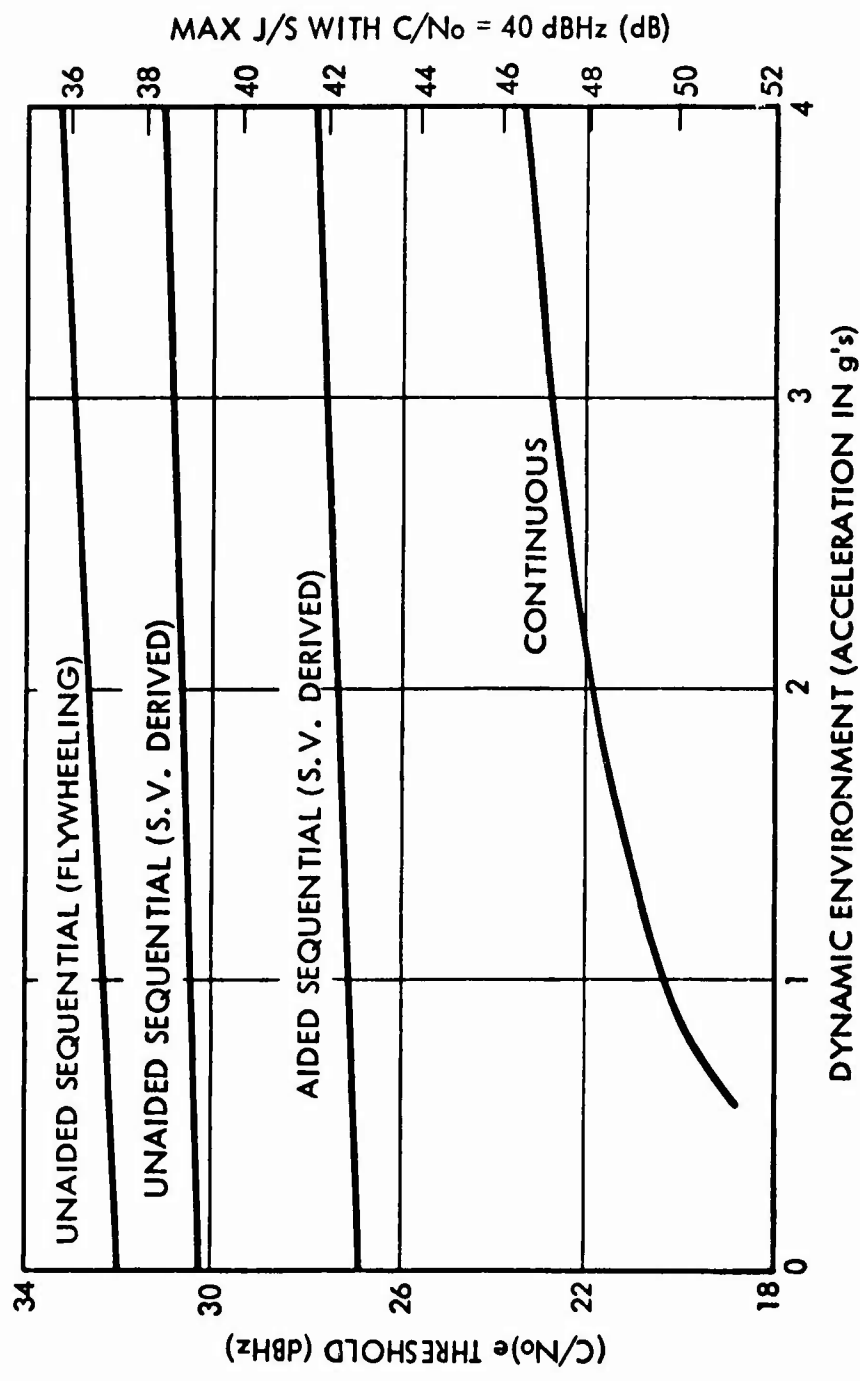
58

Figure 10. Typical Jamming Immunities

4.5.2 C/P Navigation

Generally, the two advantages that P-navigation offers over C-navigation are greater jamming immunity and, in the presence of high user dynamics, greater navigation accuracy. It is noteworthy that, for a user in a jam-free environment and with benign dynamics (that is, a relatively constant velocity vector), comparable navigation accuracies can be achieved with both P and C, since the 10:1 ratio in chip durations can be overcome with data smoothing.

From Table 10, it is seen that all users except Class C have stringent jamming immunity requirements, and hence will require to P-navigate. Class C, however, can make do with C-navigation.

### 4.5.3 Ionospheric Correction Technique

As is shown in Section 3, accurate navigation can only be achieved if the ionosphere is corrected by the two-frequency, L_1/L_2, technique. From Table 10, it is seen that User Classes A, B and F require 15 meter accuracy, which calls for L_1/L_2 receivers. However, User Classes C, D and E have less stringent accuracy requirements, and if the ionospheric modeling techniques prove to be as effective as anticipated, they can use a single frequency, L_1 receiver.

4.5.4 Auxiliary Sensors

The need for auxiliary sensors has been investigated by computer simulations of various equipment group configurations, in different hypothesized user dynamic scenarios. This work is fully described and reported on in Appendix 11. From these analyses, it is seen that Classes A, B and F will require an inertial measurement unit in their equipment groups, but the other classes will not. At this point, the selection of the type of IMU becomes highly conditioned by what inertial equipment is already in the user's inventory, and the choice will be made in later development phases.

4.6 CONCLUSIONS AND RECOMMENDATIONS

Based on the above tradeoffs, the optimum equipment group complements, valid at least for Phase I, can be synthesized. They are shown here in diagrammatic form in Figures 11, 12, 13 and 14.

60
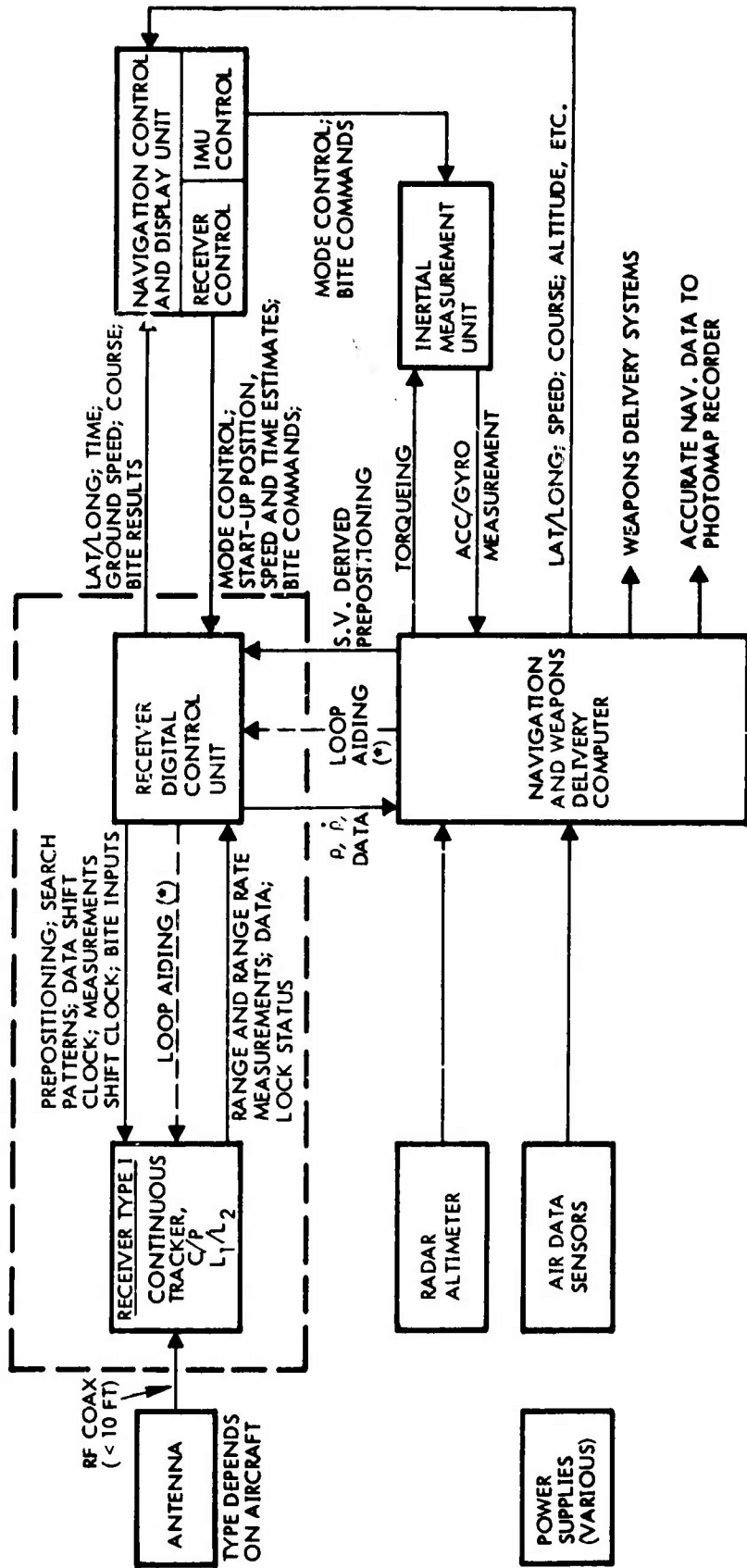
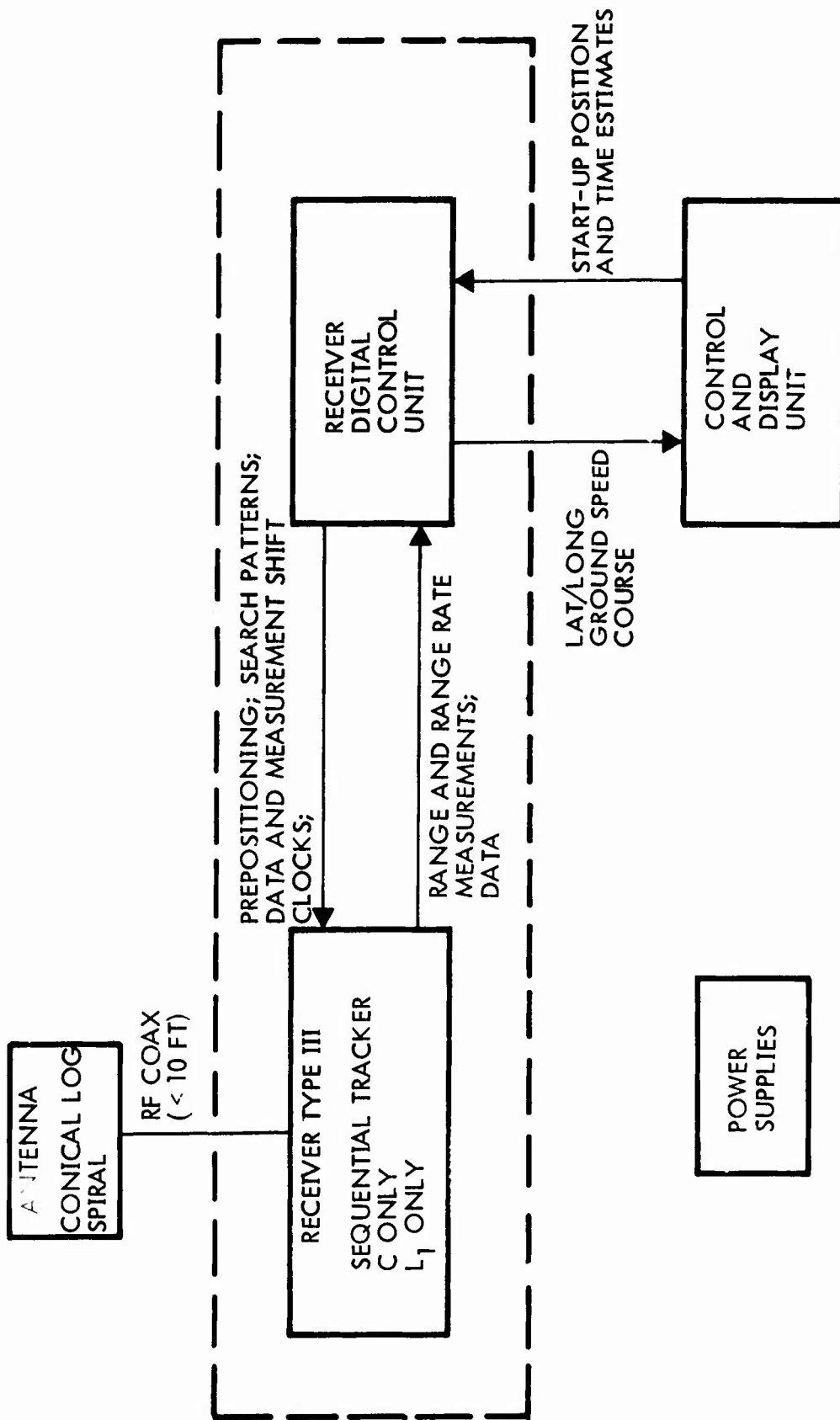Figure 11. User Equipment Group — Classes A and B

(*) CLASS A ONLY

61

Figure 12. User Equipment Group – Class C
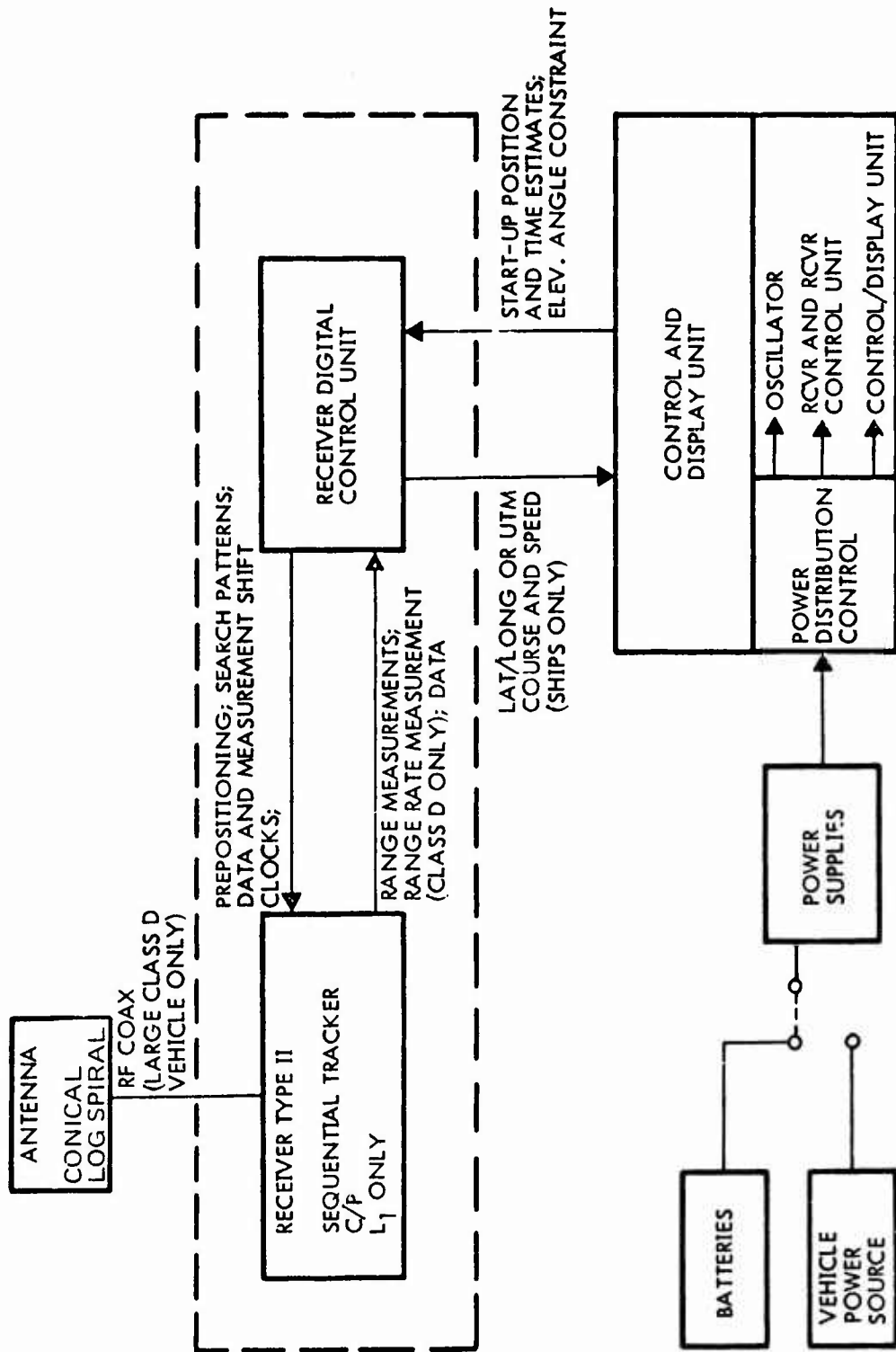
Figure 13. User Equipment Group – Classes D and E
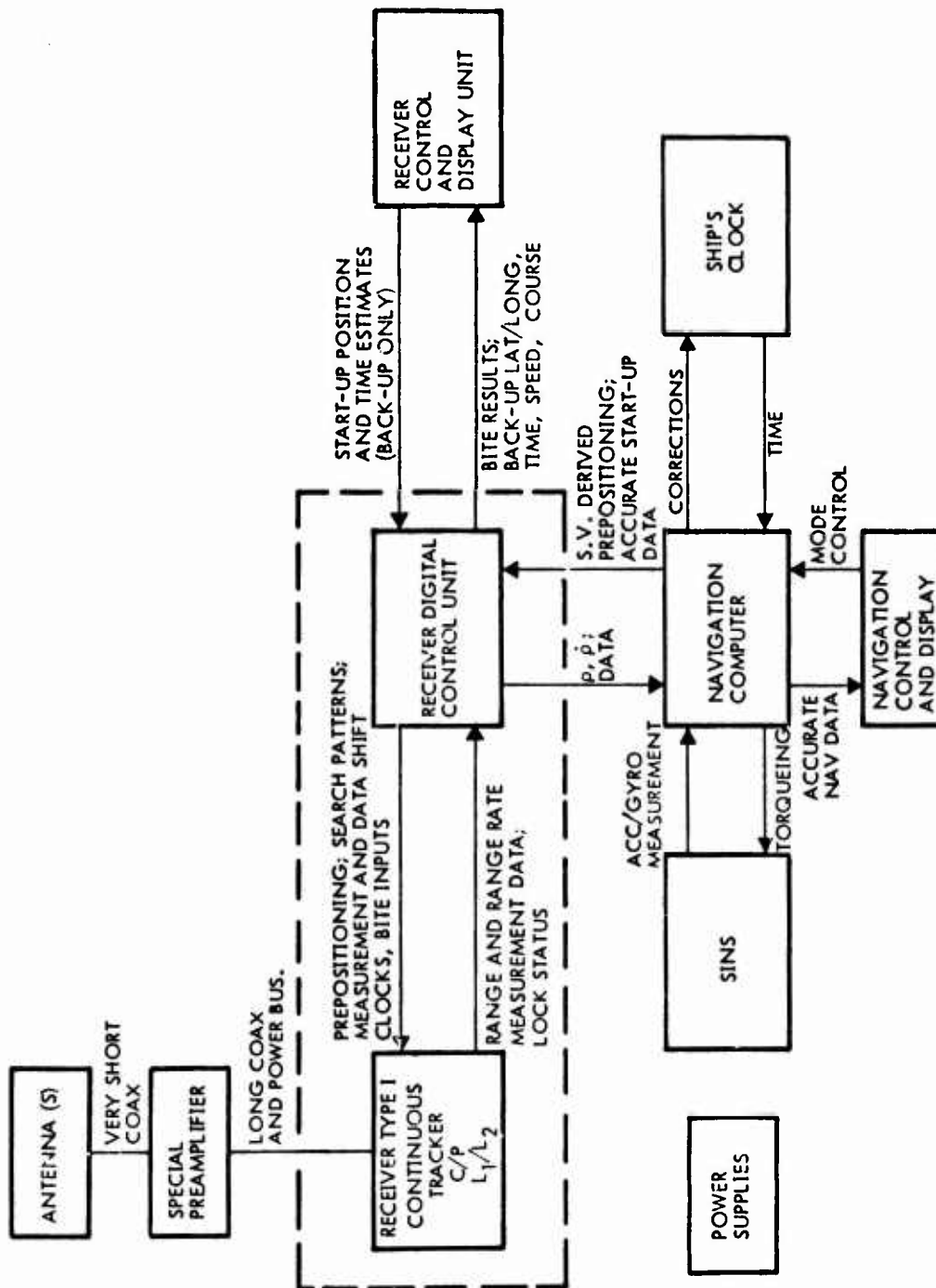
Figure 14. User Equipment Group – Class F

5. RECEIVER DESIGN TRADE STUDY

5.1 INTRODUCTION

This section presents a design for the User Receiver to be deployed in the Global Position System. The design is the outcome of a trade study effort whose goal was the overall GPS system definition. The receiver design effort supported the system definition so that items such as signal structure definition, link budget, time to first navigation fix, and position error allocations could be optimized. In this supporting role, the receiver design activity stressed feasibility of design concepts, minimization of life cycle costs, and functional operation. The result of this effort is a baseline functional receiver design which satisfies the requirements which evolved during the system definition.

5.2 RECEIVER FUNCTIONAL REQUIREMENTS

This section discusses the functional requirements for the user receiver which resulted from the definition study. Requirements for the receiver design include system requirements, cost goals, built-in test equipment requirements, packaging and manufacturing.

5.2.1 System Requirements

The receiver must perform those functions necessary for the user to compute his position and velocity. Furthermore, the receiver design must be compatible with the GPS Signal Structure. The Signal Structure assumed

in this report is contained in Appendix II of the SAMSO document, "System Specification for the Global Positioning System, Phase I, Including Appendices I and II ," SS-GPS-101A, Code ID 07868, 29 January 1974.

Receivers for each class of user must operate properly under prescribed conditions of vehicle dynamics and jamming power, which varies from class to class.

The functions which the receiver must perform are as follows:

1. Receive the L-band carrier signals L_1 and L_2 from the antenna.

2. Acquire and demodulate the C-code from each of any four satellites.

3. Obtain bit sync and demodulate satellite data from the C-code signal.

4. Handover from the C-signal to the P-signal.

5. Demodulate the P-code from each of any four satellites.

6. Demodulate satellite data from the P-code signal.

7. Accept GFE encryption devices as required to provide secure P-code operations.

8. Coherently track the reconstructed carrier from either the P or C signal from each of any four satellites.

9. Obtain pseudorange measurements from each of four satellites being tracked.

10. Obtain doppler velocity measurements from each of four satellites being tracked.

11. Transfer satellite data and tracking measurements (pseudorange and doppler) to the navigation computer.

12. Provide receiver status information to the computer.

13. Provide an indication of jamming power in the user environment to the computer.

14. Provide a measure of System Time of Day to the computer.

15. Provide a Time of Day (TOD) interrupt to the computer to synchronize computer operations to the receiver clock.

16. Accept configuration and control instructions from the computer.

17. Provide built-in test equipment (BIT) capable of detecting and indicating failures to the module level.

18. Provide power conditioning as necessary to operate from user supplied power.

Some classes of user do not require the capability to track the L_2 carrier for ionospheric calibrations. A single class of user (Class C) does not require the capability to track the P signal or the L_2 carrier. Special receiver types for these classes are considered in Section 5.5 of this report.

5.2.2 Mechanical Requirements: (Four channel GPS Receivers)

5.2.2.1 General

The packaging design of the GPS receiver was based upon certain composite physical and environmental constraints in order to minimize the impact of equipment integration into the various users parameters. Table 12 denotes the User Equipment classes and Missions as applicable thereto. Table 13 denotes the military services and equipment parameters for the various class users.

Basically, the receivers were designed to withstand the environmental and stress conditions as applicable to each user (see paragraph 5.2.2.2, Environmental Conditions).

To minimize the design risk and to achieve the aforementioned requirements, the design concept was based upon proven standard concepts with variations as suitable to achieve the required configuration and performance goals.

5.2.2.2 Environmental Conditions

The receiver sets were designed to satisfy the performance characteristic when exposed to the environments specified herein.

5.2.2.2.1 Thermal

The user receiver sets shall withstand operating and nonoperating temperatures within the following limits.

68

Table 12. User Equipment Class Missions

	Class					
	A	B	C	D	E	F
	High accuracy Medium dynamics of user	High accuracy High dynamics of user	* Medium dynamics of user	High accuracy Low dynamics	High accuracy Low dynamics	Medium accuracy Low dynamics
	High immunity to electromagnetic jamming	Medium immunity to electromagnetic jamming	Immunity to unintentional EMI	High immunity to jamming	High immunity to jamming Low weight Low power	Medium immunity to jamming
Missions	Air Force Strategic B-52, F-111	Army Helicopter USMC Close air support helicopter Navy Close support and attack aircraft	Army Mission support Navy Mission support surface vessels ASWA/C Air Force Airlift C-130, C-5, C-141, C-135	Army Wheeled and tracked land vehicles Navy Mine warfare	Army Man backpack USMC Man backpack	Navy Submarine
	Photo reconnaissance SR-71	Air Force Interdiction F-4, F-105 Close air support A-7	Search and Rescue HH-53 Mission support C-131, C-141, T-29, T-39			

Accuracy

High, 50 ft
*Acceptable accuracy as determined by cost tradeoff
Medium, 50-500 ft

69

Table 13.   User Receiver Characteristics

	Class					
	A	B	C	D	E	F
Air Force	X	X	X	X		
Army		X	X	X	X	
Navy		X	X	X		X
USMC		X			X	
Frequencies	L_1/L_2	L_1/L_2	L_1	L_1	L_1	L_1/L_2
Satellite Tracking	Continuous	Continuous	Sequential	Sequential	Sequential	Continuous
Receiving Codes	C/P	C/P	C	C/P	C/P	C/P
Input Power	115V @ 400~ 28 Vdc	115V @ 400~ 28 Vdc	115V @ 400~ 28 Vdc	115V @ 400~(Navy) 24 Vdc (Army)	24 Vdc Battery of Vehicle	115V @ 400~
Power Dissipation (W)	60	60	30	30	20	60
Weight Lbs. kg.	30.0 13.7	30 13.7	20.0 9.0	20.0 9.0	12.0 5.5	30.0 13.7
Configuration	Short-ATR	S-ATR	S-$\frac{1}{2}$ ATR	S-$\frac{1}{2}$ ATR	Back pack	S-ATR
Size Cu. in. m^3	1000 0.0168	1000 0.0168	470 0.0077	470 0.0077	1000* 0.0168	1000 0.168

*Includes power source and computer.

$\frac{1}{2}$ ATR (Short) = 4.62W x 7.62 H x 12.56 L

ATR (Short) = 10.125W x 7.62 H x 12.56 L

70

Operating

User class:	Deg C	
A	-54 to +71	(+95°C intermittent 30 min)
B	-54 to +71	(+95°C intermittent 30 min)
C	-54 to +55	(+71°C intermittent 30 min)
D	-54 to +65	
E	-40 to +52	
F	-28 to +65	

Nonoperating:

User class:	Deg C
A and B	-62 to +95
C	-62 to +85
D	-62 to +75
E	-62 to +71
F	-62 to +75

5.2.2.2.2 Solar Radiation

Class D and E equipments shall withstand solar radiation of 0 to 360 BTU/ft^2/hr for periods of up to 4 hr/day.

5.2.2.2.3 Altitude

The equipment shall withstand operating and nonoperating altitudes/pressures within the limit specified.

User Class	
A	Sea level to 21,000 m
B	Sea level to 21,000 m
C	Sea level to 15,000 m
D	Operating: Sea level to 3,000 m Nonoperating: Sea level to 15,000 m

71

E	Operating: Sea level to 4,500 m
	Nonoperating: Sea level to 15,000 m
F	Operating: TBD
	Nonoperating: Submarine pressure and to
	15,000 m transport altitude

5.2.2.2.4 Temperature/Altitude Combination

The equipment shall operate under the temperatures altitude combinations specified.

User class:

A   MIL-E-5400 P Figure 3, sheet 2, curves A and B

B   MIL-E-5400 P Figure 3, sheet 2, curves A and B

C   MIL-E-5400 P Figure 3, sheet 1, class 1, curves A and B

D   Sea level to 3,000 m full temperature limits

E   Sea level to 4,500 m

F   Sea level pressure full temperature limits.

5.2.2.2.5 Humidity

The equipments shall withstand a relative humidity of up to 100 percent, including conditions wherein condensation takes place on the equipment, applicable during both operating and nonoperating conditions per MIL-E-5400.

5.2.2.2.6 Rain, Fog, Snow, and Wind

The equipments of Classes D and E shall withstand operating and nonoperating exposure to rain, fog, ice, snow, and wind per MIL-E-4158.

5.2.2.2.7 Salt Atmosphere

The equipments shall withstand operating and nonoperating exposure to salt-sea atmosphere. Levels of exposure and conditions are TBD for each class of equipment.

5.2.2.2.8 Sand and Dust

The equipments shall withstand, in both operating and nonoperating conditions, exposure to sand and dust particles as encountered in operational areas of the world in accordance with MIL-E-5400.

5.2.2.2.9 Explosive Conditions

The equipments shall not cause ignition of an ambient, explosive, gaseous mixture with air when operating in such an atmosphere in accordance with MIL-E-5400.

5.2.2.2.10 Fungus

The equipment shall withstand, in both operating and nonoperating conditions, exposure to fungus growth as encountered in tropical climates. In no case shall overall spraying of the equipment be necessary to meet this requirement. Materials shall be fungus inert or treated in accordance with MIL-STD-454, Requirement 4.

5.2.2.2.11 Vibration

When normally mounted (with vibration isolators in place, if any) the equipment shall not suffer damage or fail to meet the specified performance when subjected to vibration within the frequency range and amplitudes specified.

User Class:

A, B	MIL-E-5400, Figure 2, Curve I
C	MIL-E-5400, Figure 2, Curve IV
D	MIL-STD-810B, Figure 514-5, Curve W
E	MIL-STD-810B, Figure 514-6, Curve AB
F	MIL-STD-167, Type I, Tables I and II

73

With isolators removed, the equipments shall not suffer damage or fail to meet the specified performance when subjected to vibration within the frequency range and amplitude specified.

Class:

A, B, C,   MIL-E-5400, Figure 2, Curve II

D   Applicable specification TBD

E   Not applicable

F   MIL-STD-167B, Paragraph 5.1.3.2.4

5.2.2.2.12 Shock

Equipment. The equipment (with isolators in place, if any) shall not suffer damage or subsequently fail to meet the specified performance when subjected to shock as specified.

User Class:

A, B, C   MIL-E-5400, 18 shocks total, 3 each axis
               each direction

               Amplitude 15 g's

               Duration 11 $\pm$ 1 msec

               Max. g point at 5-1/2 msec

               g tolerance 10 percent 0.2 to 250 Hz filter
               measurement

D   MIL-STD-810B, Method 516, Procedure I (b and d)

E   MIL-STD-810B, Method 516, Levels and conditions
               TBD

F   MIL-S-901C

5.2.2.2.13 Mounting Base (crash safety)

The mounting and attaching devices shall withstand impact shocks specified without failure (bending and distortion permitted), and the equipment shall remain in place.

Class:

A, B, C   MIL-E-5400, 12 impacts total, 2 each axis, each direction

               Amplitude 30 g's

               Duration 11 msec

               Tolerance: With 10 percent g value

               Measured with 0.2 to 250 Hz filter

               Max. value at 5-1/2 msec

D   MIL-STD-810B, Method 516, Procedure III (b and d)

E   Not applicable

F   MIL-S-901C

5.2.2.2.14 Vehicle Dynamics

The equipments shall meet the specified performance when exposed to velocities, accelerations, and jerk as described in TBD.

5.2.2.2.15 Vehicle Attitude

The host vehicle may operate in attitudes as specified for limited periods of time.

Class	Pitch (deg)	Roll (deg)	Azimuth (deg)
A	$\pm$ 30	$\pm$ 90	360
B	$\pm$ 90	$\pm$ 180	360
C	$\pm$ 30	$\pm$ 60	360
D	$\pm$ 60	$\pm$ 45	360
E	$\pm$ 30	NA	360
F	$\pm$ 45	$\pm$ 45	360

75

5.2.2.2.16 Electromagnetic Interference

Electromagnetic interference control shall be in accordance with MIL-STD-461 and as specified in the System Engineering Management Plan.

5.2.2.2.17 EMP

The equipment shall be designed to satisfy the EMP requirements specified in the GPS specification SS-GPS-101.

5.2.2.2.18 Nuclear Control Requirements

The GPS equipment shall not employ any devices/materials that will cause the equipments to be prime radiators of nuclear particles. The equipment shall not be degraded by exposure to the levels of TBD.

5.2.2.2.19 Transportability

Not applicable.

5.2.3 Cost Goals

An important consideration in the design of the user receiver is the impact of user receiver design on the total GPS program cost. Total program cost is not necessarily minimized by minimizing receiver cost. Therefore, life cycle modelling is used to assess the impact of the receiver design approach on overall life cycle costs. The cost goal considered in developing the baseline receiver design has been to minimize total life cycle costs.

5.2.4 Built-In Test Equipment

An important factor in the life cycle cost of the user equipment is maintenance, repair, and logistics. The user receiver will utilize a reasonable amount of built-in test equipment (BIT) to minimize maintenance and repair cost. The BIT will have the capability to:

a) Assess whether or not the receiver is working properly without access to the satellites.

b) Indicate on a display the existence of a fault condition.

c) Isolate faults to the module level for rapid replacement by spare modules.

The BIT will operate under computer control. It will provide both continuous monitoring capability and diagnostic testing capability.

5.3 DETAILED RECEIVER DESCRIPTION

This section presents a description of the baseline receiver design which evolved from the system definition. The design meets all the functional requirements outlined in Section 5.2 of this report. This design is for a receiver which permits navigation by continuously tracking four satellites. The design is intended to serve the needs of user classes A, B, and F. This receiver is referred to as a Type I continuous tracking receiver. Two other types of receivers have evolved from the system definition study. The Type II receiver serves the needs of user classes D and E. This receiver is referred to as a Sequential Tracking C/P receiver. The Type III receiver is a very low cost model intended to serve only the needs of Class C. It is referred to as a Sequential Tracking C receiver.

The Type I receiver is the baseline design presented in this section. The Type II and Type III receivers are described in Section 5.5 under "Alternative Design Considerations." Care was taken in the receiver definition phase to maximize the commonality of modules among the three receiver types. Therefore, the differences between receiver types are primarily in the number of modules required, the operation, and performance of the different receiver designs.

5.3.1 Key Characteristics of the Baseline Receiver

The baseline receiver is a four channel, digital processing, computer controlled, dual frequency L-Band Receiver employing phase coherent code and carrier tracking to obtain pseudorange and doppler tracking measurements continuously from four GPS satellites.

Advanced design concepts based on proven experience with the INI and INHI test programs were used to achieve the performance and Life Cycle Cost goals of the program. Modular construction and built-in test equipment are employed to eliminate the need for scheduled maintenance, obtain rapid failure detection and minimize the cost of repair and replacement.

The key design features incorporated into the baseline receiver are as follows:

1. A low noise preamp to provide maximum receiver sensitivity and jamming immunity.

2. Use of an optional line driving preamp at the antenna if required to keep rf cable transmission losses below 1 dB.

3. BIT test generator incorporated in each receiver unit.

4. Oven controlled vibration insulated crystal reference oscillator to provide stable frequency references.

5. Common code and carrier tracking loops to provide accurate code tracking in the presence of high user dynamics.

6. Tau Dither code tracking which minimizes the rf circuitry requirements, and therefore receiver costs.

7. **Dual bandwidth Costas carrier tracking loops for optimum suppressed carrier acquisition and tracking.**

79

8. Matched filter detection and digital synchronization of satellite data.

9. Direct memory access to the computer for rapid and efficient transfer of measurements to the computer.

10. Computer control of receiver configuration and operation sequences.

11. Digital receiver control and processing.

12. Maximum use of LSI technology to reduce cost, volume, weight, and power consumption of digital circuitry.

13. Maximum use of linear IC's to reduce cost, volume, weight, and power consumption of analogue circuitry.

5.3.2 Module Definition

The circuitry for the receiver will be built on plug-in modules. Faults in the receiver will be detected, and isolated to the bad module using BIT. The modules can then be quickly removed and replaced.

The baseline receiver has been partitioned into functional circuit modules using the following criteria.

1. Maximum commonality between receiver types.

2. Related functions are grouped together.

3. The number of interface signals between modules is minimized.

4. Digital logic is built exclusively on digital modules, and analogue circuitry built on analog modules wherever practical.

With these criteria in mind, the baseline receiver has been partitioned into modules as shown in Figure 15. As shown, there are twelve functional module types. These modules are listed in Table 14, along with the number

80

of modules required. In addition, there is an optional antenna line driving module included with the antenna equipment. The antenna line driving

module is used only when the transmission line losses between antenna and receiver exceed 1. dB.

The complete relationship between modules is shown more clearly in the Type I Receiver block diagram, Drawing Number Sk-100101, which is included in this report in Appendix 14.

TABLE 14. Type I Receiver Module Listing

MODULE NO.	DESCRIPTION	QUANTITY PER RECEIVER
1	RF pre-amp and first IF amp	1
2	Frequency Synthesizer	1
3	Reference Oscillator	1
4	BITE Test Generator	1
5	PN Demodulator and 2nd IF	4
6	Code and Carrier Tracking Loops	4
7	AGC and Code Search Detector	2
8	Tracking Measurements	1
9	PN Code Generators	2
10	Bit Sync and Detection	4
11	Computer I/0 and Receiver Control	1
12	Receiver Power Supply	2
	Total Modules	24
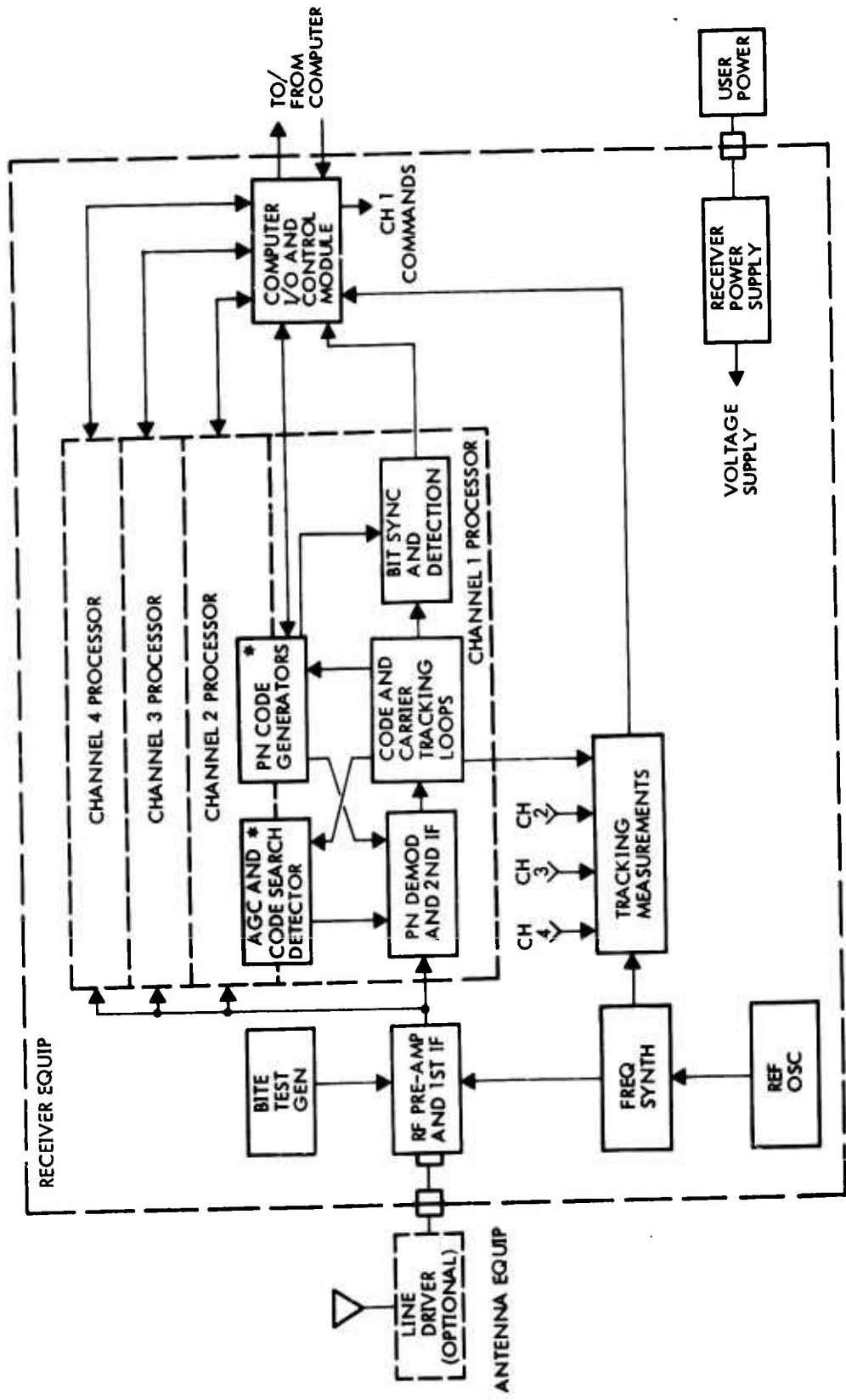
Figure 15. Module Block Diagram

83

5.3.3 Module Description

The following paragraphs describe each of the modules which make up the baseline receiver.

5.3.3.1 RF Pre-AMP and First IF

The RF Pre-Amp and First IF Module shown in Figure 16 receive L-band signals from either the antenna or the BIT test generator, filters out-of-band spurious radiation in the preselector bandpass filter, and then amplifies the signal in a low noise pre-amp. Overload protection is provided at the module input to protect against burnout from excessive in-band rf power. A postselector bandpass filter provides image rejection. Local oscillator (LO) frequencies are injected into a mixer to produce a first intermediate frequency (IF) of 55 MHz. The IF is amplified in the first IF amplifier, and the signal is distributed to the four PN Demod and 2nd IF modules.

The design of the RF Pre-amp module provides for receiving either the L_1 or L_2 carrier. This is accomplished by designing the pre- and post-selector bandpass filters as dual response filters having 30 MHz passbands about the L_1 and L_2 center frequencies. The pre-amp is a wide band device employing low noise figure transistors which passes both L_1 and L_2 signals. Discrimination between L_1 and L_2 is achieved by selecting the appropriate injection frequency to be applied to the first mixer. The desired carrier is thereby translated to 55 MHz, while the undesired carrier is rejected by the bandpass characteristics of the first IF amplifier.

84

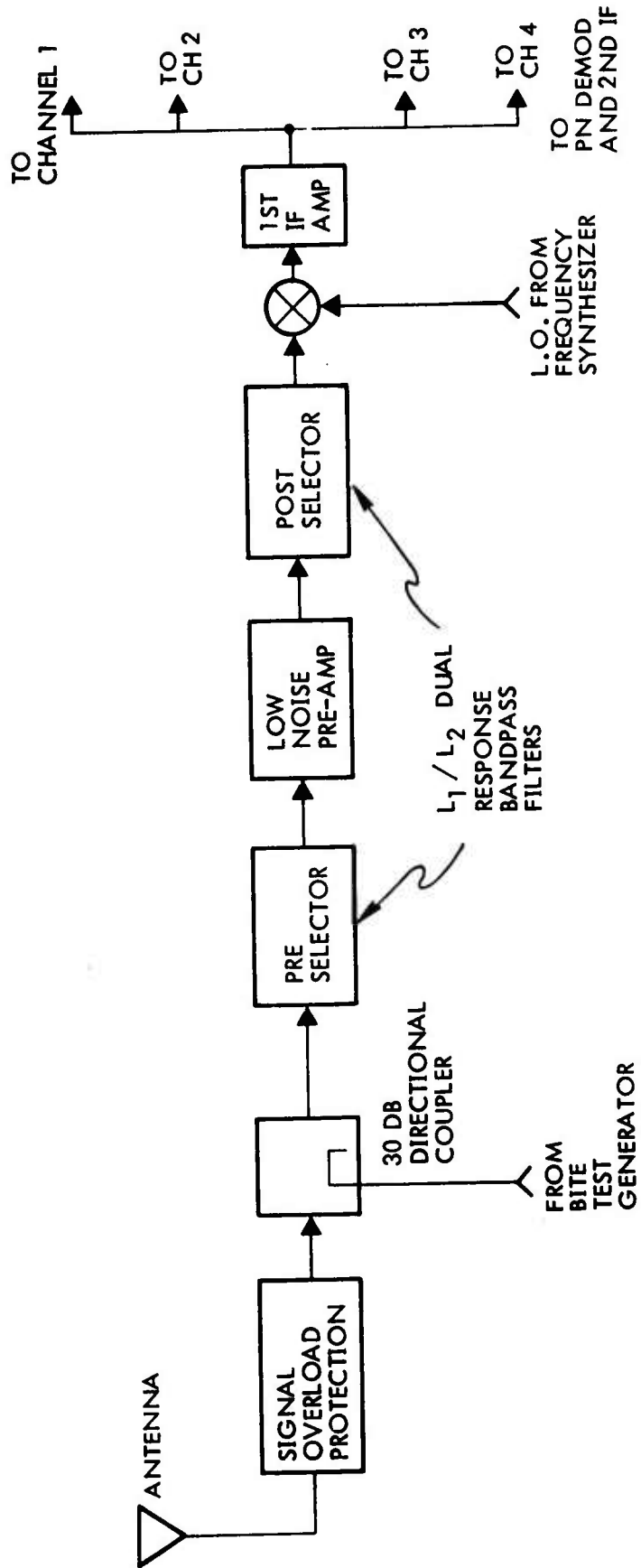Figure 16. RF Preamp and First IF Module

85

The RF Pre-Amp Module essentially determines the receiver noise figure, referenced to the input port at the receiver case. Analysis (Appendix 12) of the TRW pre-amp design concept indicates that the ambient receiver noise figure will be in the range of 3.6 dB (380°K) to 4.7 dB (576°K). The typical ambient noise figure will be 4.3 dB (494°K).

5.3.3.2 Reference Oscillator

The reference oscillator is a crystal oscillator whose frequency
is 5.115 MHz. This oscillator provides the timing reference for all
locally generated signals in the receiver, and is the source of a time-of-
day interrupt which is used to synchronize computer operations with the
receiver. The 5.115 MHz frequency drives the frequency synthesizer,
which produces and distributes all the locally generated reference signals.

5.3.3.3 Frequency Synthesizer

The frequency synthesizer module accepts a precision 5.115 MHz
reference frequency from the Reference Oscillator and generates a
number of local signals used for rf reference frequencies and for digital
timing. Figure 17 shows the frequency synthesizer details. A local
oscillator multiplier chain generates frequencies at 10.23 MHz, 15.345 MHz,
40.92 MHz, and the first IF injection frequency (referred to as L_1 LO or
L_2 LO). The 40.92 MHz clock is sent to the Tracking Measurements module,
which produces divided down versions of the clock. These signals are then
mixed as shown to produce reference frequencies at $10.23 (1 - \frac{L}{F_C})$ MHz, and
$40.92 (1 - \frac{L}{F_C})$ MHz. Here F_C is the 10.23 MHz code clock frequency, and
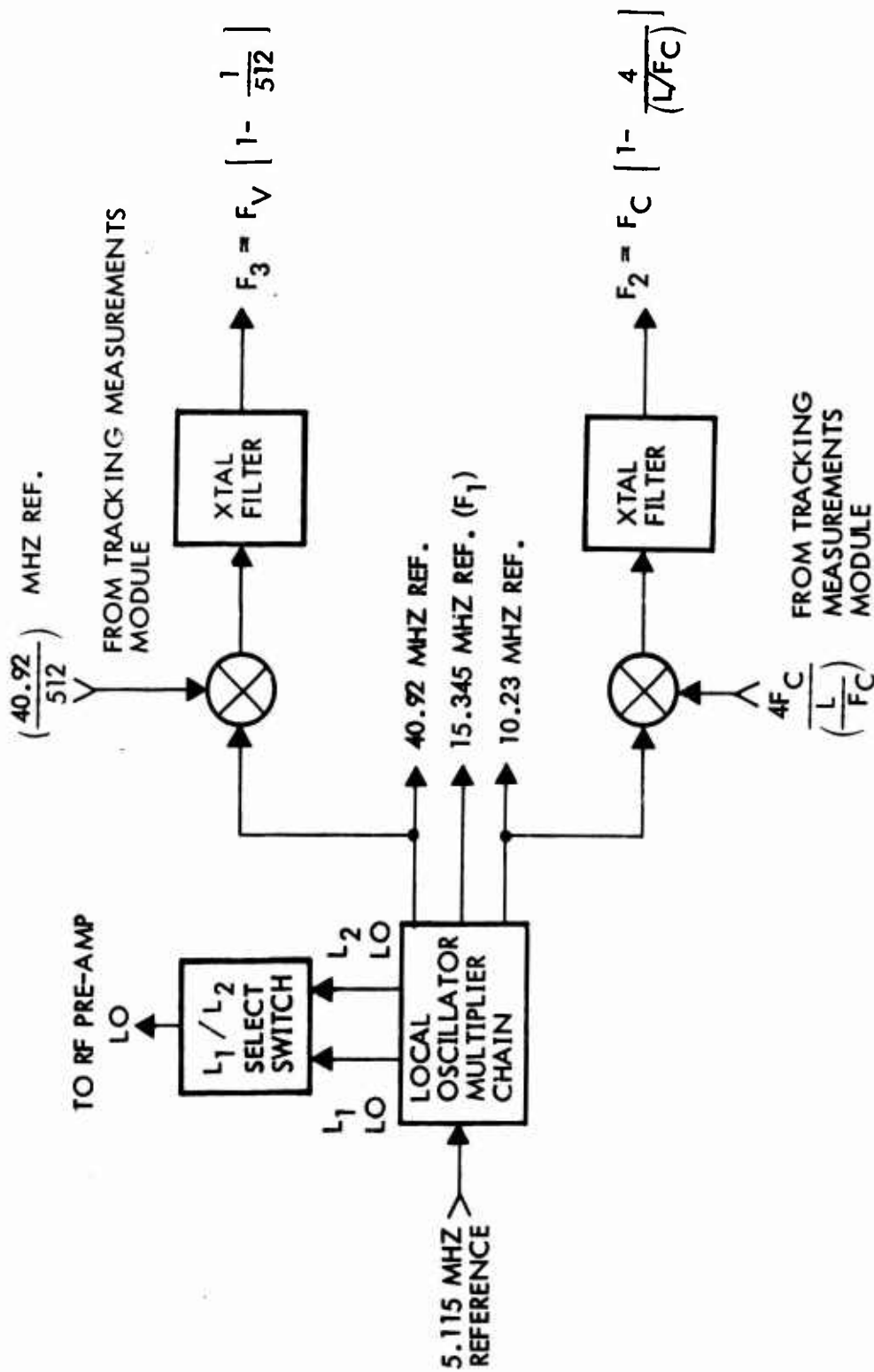L is the L_1 or L_2 carrier frequency.

Figure 17. Frequency Synthesizer Module

5.3.3.4 BIT Test Generator

The BIT Test Generator Module shown in Figure 18 is used to produce a test signal at L-band which is coupled into the receiver in the RF Pre-Amp Module with a 30 dB directional coupler. The test signal is used to evaluate the receiver under computer control thus locating failures to the module level for quick repair of the receiver by module replacement. Maximum use of computer algorithms, rather than elaborate test hardware, is used to reliably detect and isolate faults.

The test signal is a replica of a typical satellite signal, generated from reference frequencies produced by the frequency synthesizer. Test generators produce PN codes, the Manchester code, and a pseudorandom data word which is phase modulated on a test carrier which is multiplied up to L-band. A selectable attenuator provides for strong signal and threshold level checkout of the receiver.

The BIT module can be provided as an option to user receivers, since the BIT Test Generator is not required to operate the receiver. This provides flexibility in planning logistics support to minimize life cycle costs.
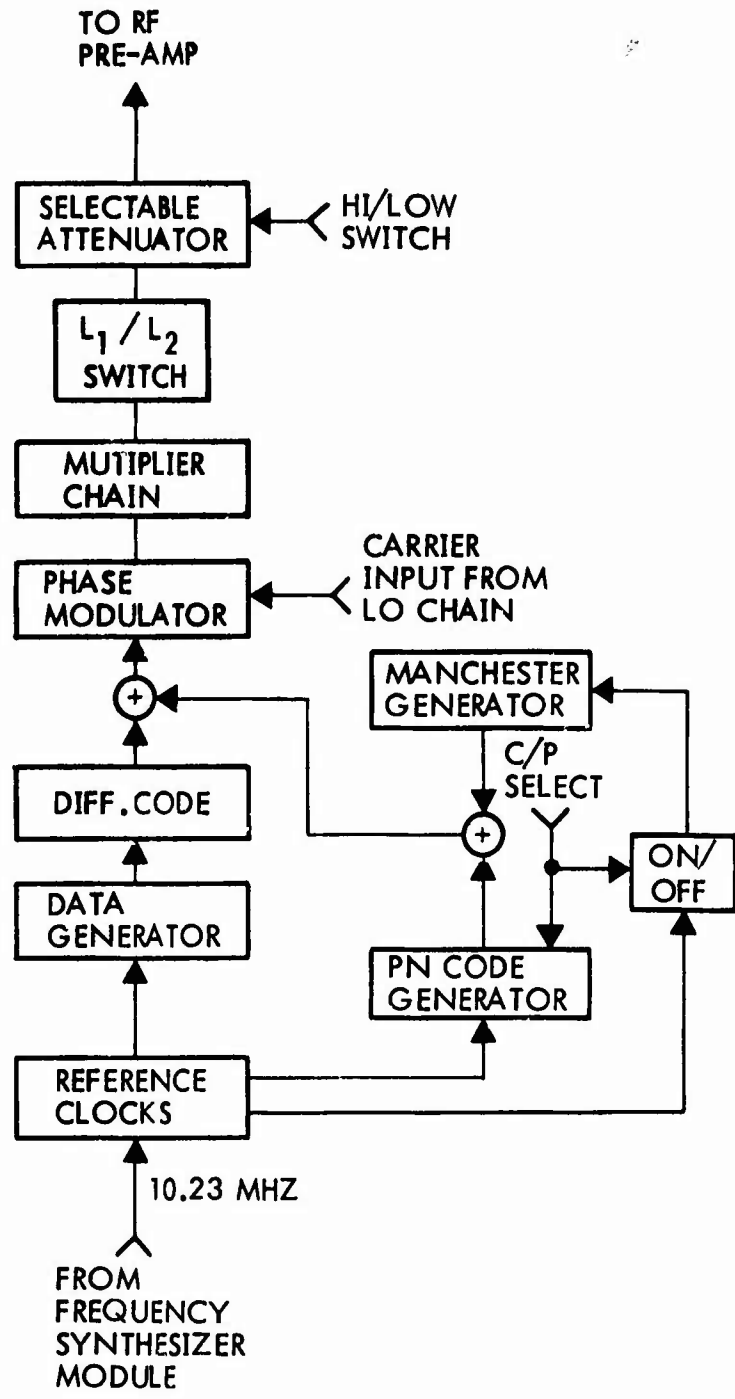
TO RF
PRE-AMP

```
          │
          ▲
   ┌──────────────┐      ┌──────────┐
   │  SELECTABLE  │◄─────│  HI/LOW  │
   │  ATTENUATOR  │      │  SWITCH  │
   └──────────────┘      └──────────┘
          ▲
   ┌──────────────┐
   │  L₁ / L₂     │
   │   SWITCH     │
   └──────────────┘
          ▲
   ┌──────────────┐
   │  MUTIPLIER   │
   │    CHAIN     │
   └──────────────┘
          ▲
   ┌──────────────┐        CARRIER
   │    PHASE     │◄───── INPUT FROM
   │  MODULATOR   │        LO CHAIN
   └──────────────┘
          ▲
         (+)◄─────────────────┐   ┌──────────────┐
          ▲                   └───│  MANCHESTER  │◄───┐
          │                       │  GENERATOR   │    │
   ┌──────────────┐               └──────────────┘    │
   │  DIFF.CODE   │                      │ C/P         │
   └──────────────┘                      │ SELECT      │
          ▲                             (+)            │
          │                              ▲             │
   ┌──────────────┐                      │ ⌐Y─┐  ┌─────────┐
   │    DATA      │                      │    ●──│  ON/    │
   │  GENERATOR   │                      │       │  OFF    │
   └──────────────┘               ┌──────────────┐└─────────┘
          ▲                       │  PN CODE     │    ▲
          │                       │  GENERATOR   │    │
   ┌──────────────┐               └──────────────┘    │
   │  REFERENCE   │──────────────────────┘            │
   │   CLOCKS     │───────────────────────────────────┘
   └──────────────┘
          ▲
          │ 10.23 MHZ
          │
```

FROM
FREQUENCY
SYNTHESIZER
MODULE

Figure 18.   BIT Test Generator Module

90

5.3.3.5 PN Demodulator and Second IF

The PN Demod and Second IF module, shown in Figure 19
accepts the amplified first IF signal, adjusts the receiver gain with
the AGC amplifier, demodulates the selected PN code, and mixes the
demodulator output with the VCO frequency to produce the second IF
frequency. The second IF signal, which is at 15.345 MHz, is amplified by
the second IF amplifier, and sent to the Code and Carrier Tracking
Loops module.

In the baseline receiver, four satellites must be tracked simultaneously.
Satellite signals are discriminated from each other by selecting a particular
C-code, or phase of the P-code. Therefore, one module is required for
each of the satellites to be tracked.

The AGC amplifier is controlled by a control voltage received from
its AGC detector. The AGC output then goes to a PN demodulator which
utilizes a locally generated code to reconstruct the carrier of a desired
satellite and generate a code tracking error signal. The PN demodulator
employs sequential balanced mixers and a locally generated coincidence
code to provide 70 dB suppression to a CW jammer. The demodulator
output is applied to a 20 KHz crystal bandpass filter which suppresses
jammer and thermal noise power by 27 dB. The filtered carrier is applied
to the second mixer and multiplied against the 40.92 MHz VCO output signal
from the carrier tracking loop. The mixer output is a signal at 15.345 MHz
which, when the carrier loop is locked, is phase coherent with the 15.345 MHz
reference produced by the local frequency generator. The mixer output
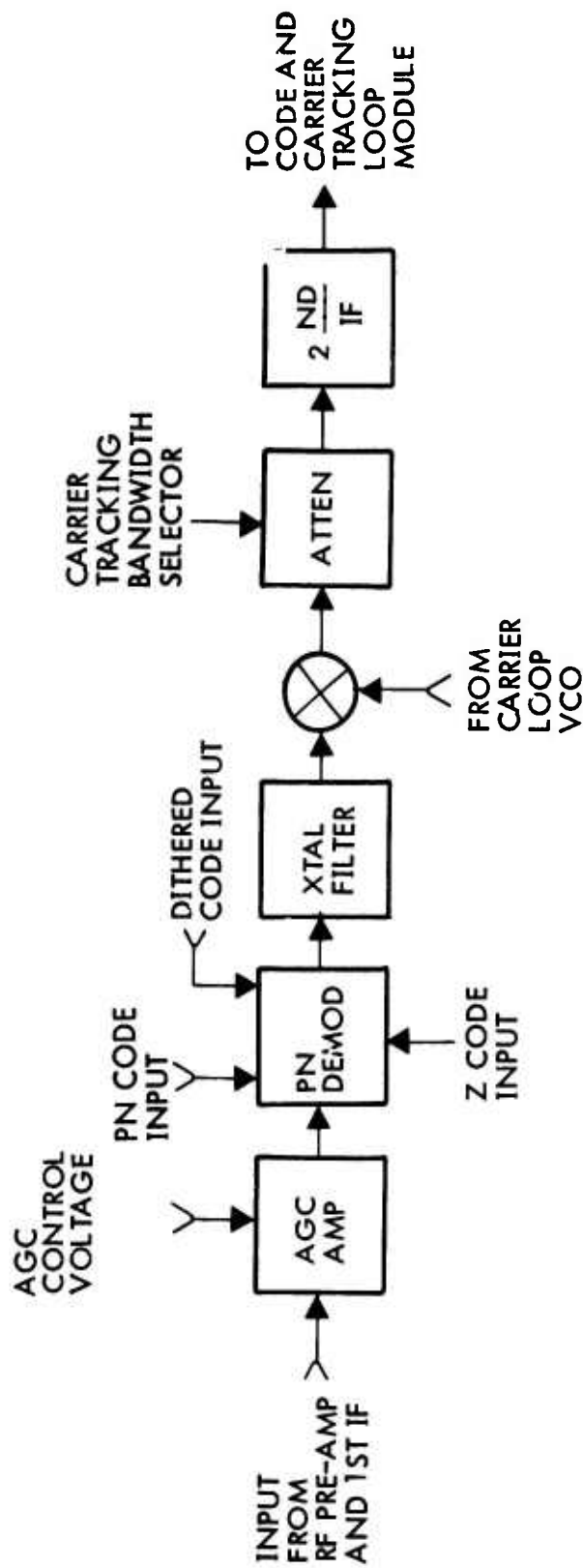is amplified by the second IF amplifier, and sent to the carrier tracking loop.

91

Figure 19. PN Demodulator and 2nd IF Module

92

5.3.3.5.1 PN Demodulator Description

The sequential balanced PN biphase demodulator is shown in Figure 20. This unit is used to reconstruct the carrier and data modulation of the received PN signal and to generate a code phasing error. A sequentially balanced modulator configuration is used to obtain approximately 70 dB of balance to a CW jamming signal. Tau-dither code error detection was selected since it offers the simplest operation and minimum hardware compared to early-minus-late or split-bit detection. The operation of the demodulator is as follows:

The 55 MHz IF signal and a locally generated replica of the satellite PN code are applied to the demodulator. To obtain the desired balance, an auxiliary PN code, referred to as the Z-code, is used to biphase modulate the signal. The Z-code is then modulo-two added to the local replica of the satellite code, referred to as the X-code, and the composite code used to biphase modulate the signal as shown. Since the Z-code is used twice, it has no effect on the reconstruction of the carrier. However, since two modulators are used sequentially, the balance is twice that obtainable with one modulator.

With local code (X-code) synchronized to the received code, the desired signal is converted to CW in the top modulator of Figure 20, while all other signals are converted to broadband noise. The amplitude of the reconstructed carrier versus code phasing is shown in Figure 21.

The $X(\tau)$ code applied to the lower modulator in Figure 20 is the X-code dithered by $\pm 1/2$ chip. This produces a tau-dithered error signal which is synchronously detected at the output of the lock detector
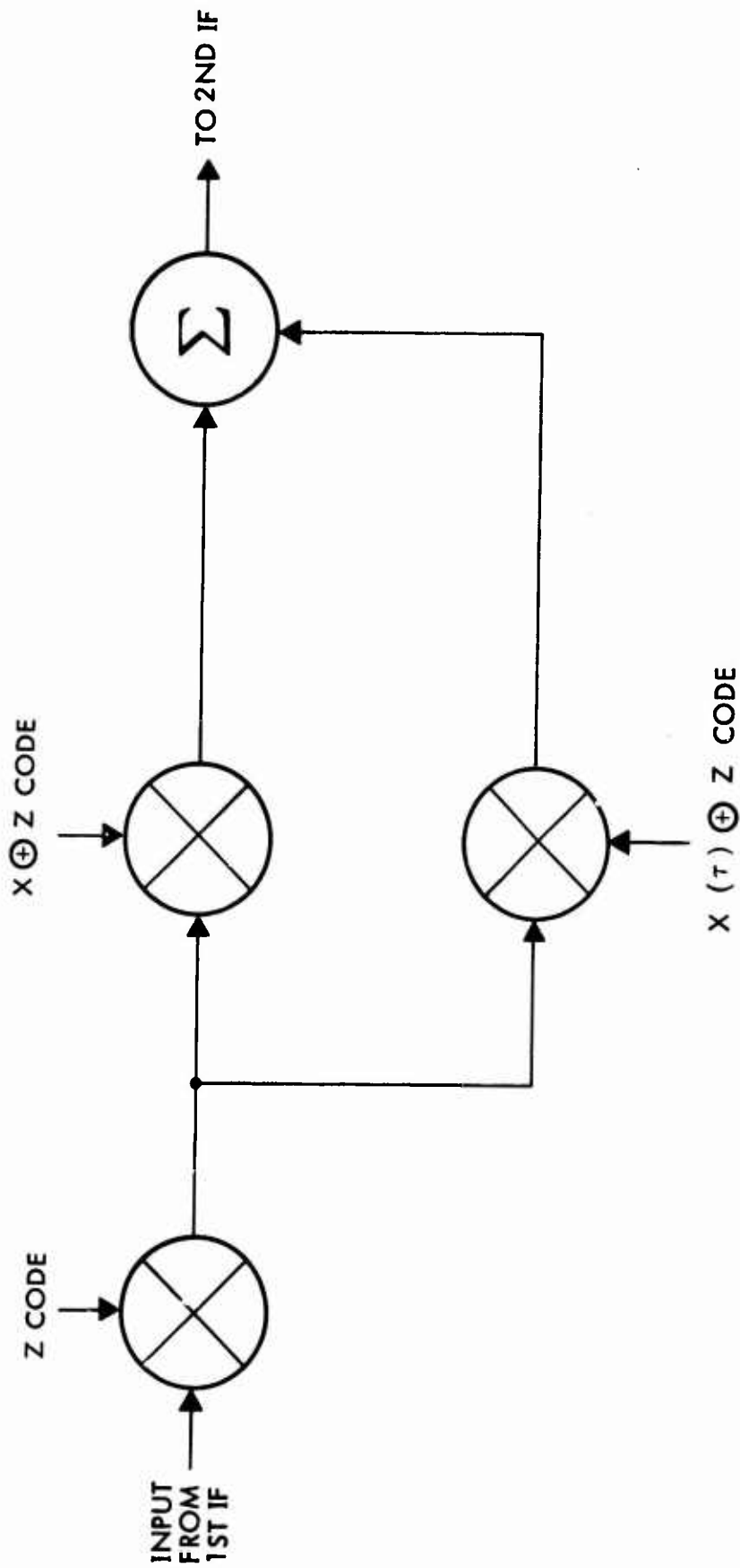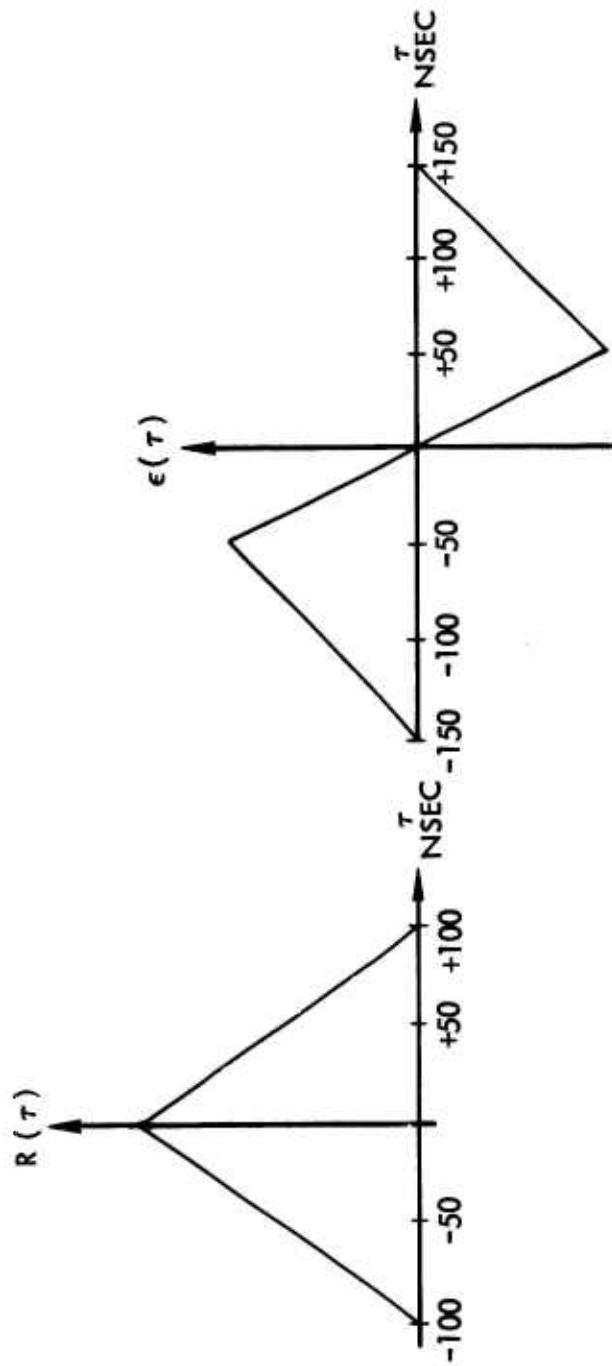
93

Figure 20. PN Demodulator

94

CARRIER AMPLITUDE CORRELATION   CODE AMPLITUDE CORRELATION

Figure 21.   Code and Carrier Amplitude Correlation

95

in Figure 22. The amplitude of this detected error signal versus code phasing is shown in Figure 21. The code tracking loop phases the local code clock to produce a null in the error signal.

The reconstructed carrier and code signal are added (in phase) for common amplification and detection. The code synchronous detector responds only to the code error signal present at the AC coupled output of the detector. The carrier loop responds to the sum of the reconstructed carrier and code error signals.

The second mixer translates the reconstructed carrier from 55 MHz to the second IF frequency of 15.345 MHz by injecting the 40.92 MHz signal obtained from the carrier tracking loop VCO. This signal is attenuated by a selectable attenuator, and amplified by the second IF amplifier. The selectable attenuator serves to aid in establishing the bandwidth of the carrier tracking loop.
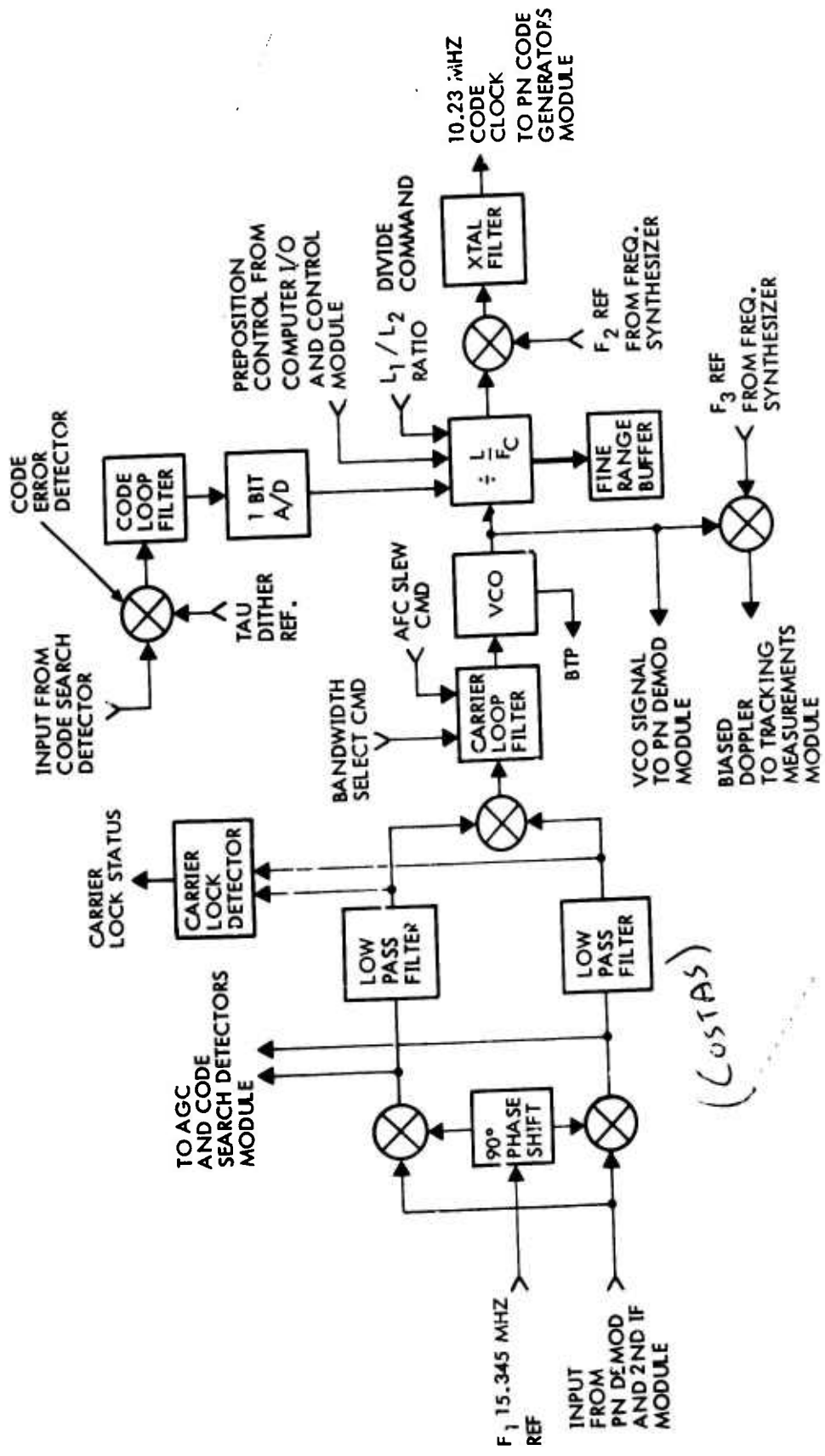
Figure 22. Code and Carrier Tracking Loops Module

97

5.3.3.6 Code and Carrier Tracking Loops Module

The code and carrier tracking loops module, Figure 22, contains the circuitry to phase lock a Voltage Controlled Oscillator (VCO) to the incoming signal obtained from the second IF amplifier, and to generate a code clock whose phase is adjusted such that a reference PN code generator is kept running in phase with the received PN code modulation.

The tracking loop is a Costas type, since the carrier is fully suppressed by the data modulation. A 15.345 MHz reference frequency is used to detect the in-phase (I) and quadrature (Q) components of the received carrier. Low pass filters follow the multipliers to establish the optimum noise bandwidth for tracking. The filtered outputs are multiplied together to produce an error signal which is proportional to the phase error between received and reference carriers. The loop filter establishes the bandwidth and tracking order of the loop. The filter time constants are selectable by command. The filter also accepts an AFC control signal which prepositions the VCO and assures rapid carrier acquisition. The loop filter output drives the VCO, whose output is used to close the tracking loop at the second mixer, and to provide a doppler signal to the Tracking Measurements Module.

An indication of carrier lock is obtained by passing the I- and Q-signals through square law detectors, and subtracting the Q from the I component. The result is a signal which oscillates about zero when the loop is out of lock and has a d.c. bias when the loop is in lock. This signal is filtered and compared against a reference voltage to obtain lock status.

5.3.3.7 AGC and Code Search Detectors Module

This module, shown in Figure 23, contains two AGC detector circuits and two code search detector circuits. Since there are two each of these circuits, one module can accommodate two processing channels.

The AGC detector serves to maintain a constant noise power at its input when signal is not present, and to maintain a constant signal to noise power when the signal is present.

The Code Search detector is a noncoherent envelope detector followed by a threshold comparison device. When signal is absent, the output of the detector is below the threshold level established for detection. The AGC circuit is designed to keep the noise power constant, even in the presence of jamming, so that the false alarm probability of the detector output is correct. When signal is present, the output of the detector is greater than the threshold level established for detection. The detector then produces an in-lock indication, which stops the code search and enables the tau dither code tracking loop.

After the PN code is acquired, and sufficient signal power is present in the receiver, the AGC circuit maintains a constant signal plus noise power at the detector input. This is necessary for the proper operation of the carrier tracking loop.

The implementation of the AGC detector is shown in Figure 24. The detector is a noncoherent detector which accepts I- and Q - input signals from the carrier tracking loop. The signals are passed through predetection low pass filters to establish the desired noise bandwidth, and then square law detected. The I and Q components are then summed and post detection low pass filtered to generate a noncoherent AGC error signal. This signal is
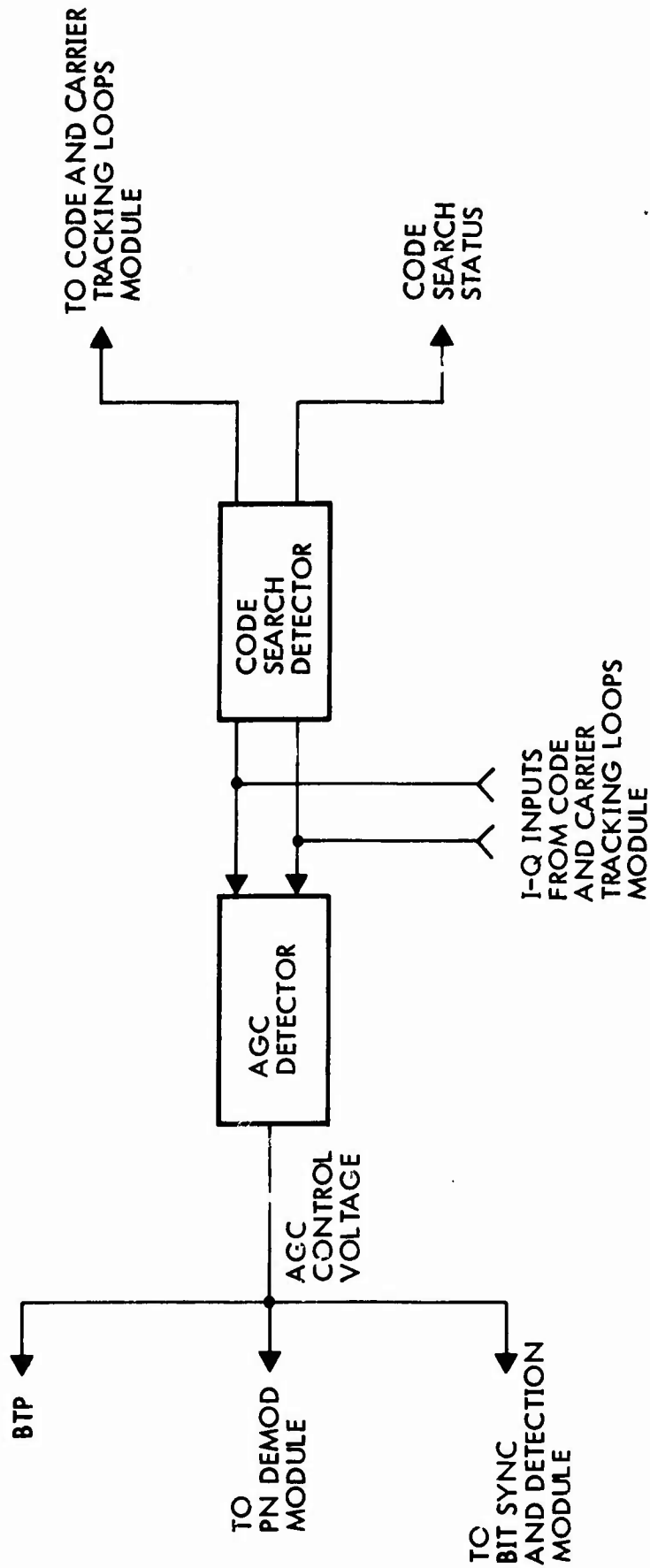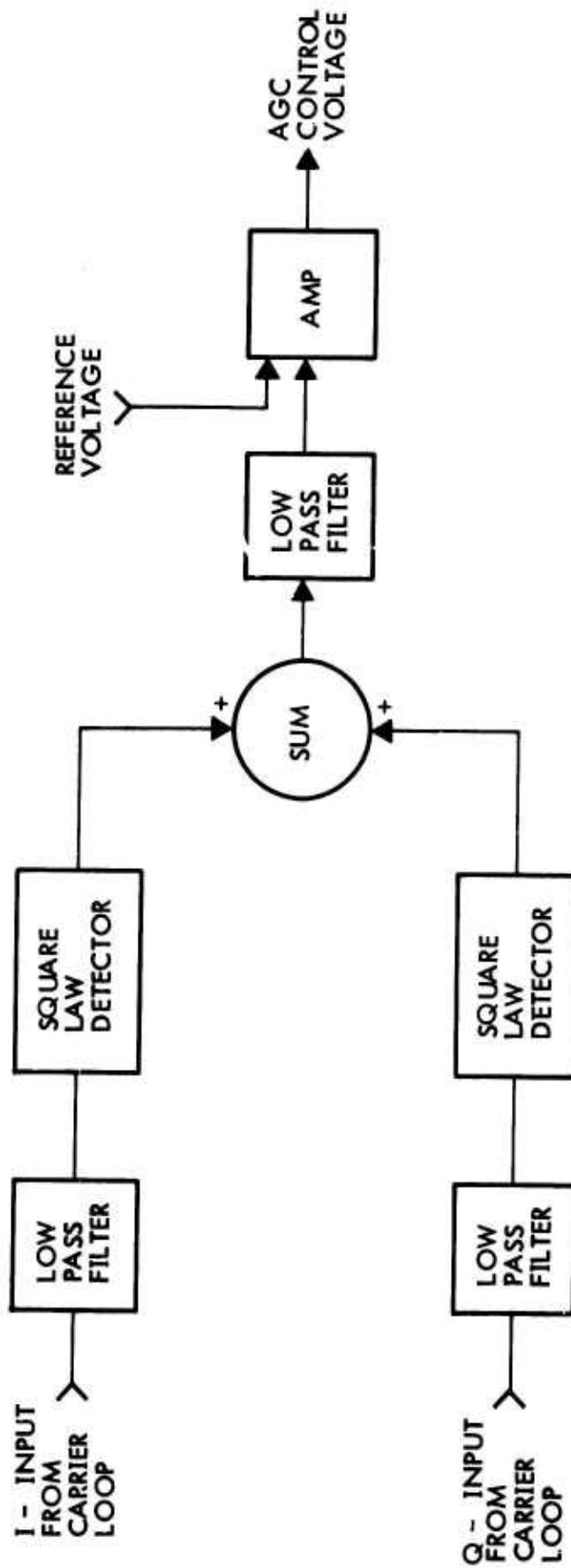
99

Figure 23. AGC and Code Search Detector Module

100

Figure 24. AGC Detector

101

added to a reference voltage and amplified to obtain the AGC control voltage. The reference voltage is used to set the minimum AGC control voltage in the presence of thermal noise alone. Jamming and/or signal power operate to increase the control voltage and thereby reduce the gain of the AGC amplifier in the IF processor.

The implementation of the noncoherent code search detector is shown in Figure 25. The code search detector functions in a similar manner to the AGC detector. The differences are that a narrower predetection filter bandwidth is used, and the signal out of the post detection low pass filter is compared against a pre-established reference voltage. This reference is set up so that when the reference code is not correlated with the received code, the signal into the voltage comparator (which is proportional to noise power) is less than the reference voltage, and the code lock indicator is out-of-lock. When the received and reference codes are correlated, the signal into the voltage comparator (which is now proportional to signal plus noise power) is greater than the reference voltage, and the code lock indicator is in-lock. Occasionally random voltage fluctuations due to noise will cause the lock detector to indicate lock when the codes are not correlated. This is a false alarm condition. Less frequently, the noise voltage fluctuations will cause the lock detector to indicate an out-of-lock condition when the codes are indeed correlated. This condition is called a missed detection.

The lock detector is used to determine the status of the code search during initial acquisition of a new satellite. The selection of bandwidths and threshold reference voltage determines the false alarm and missed detection
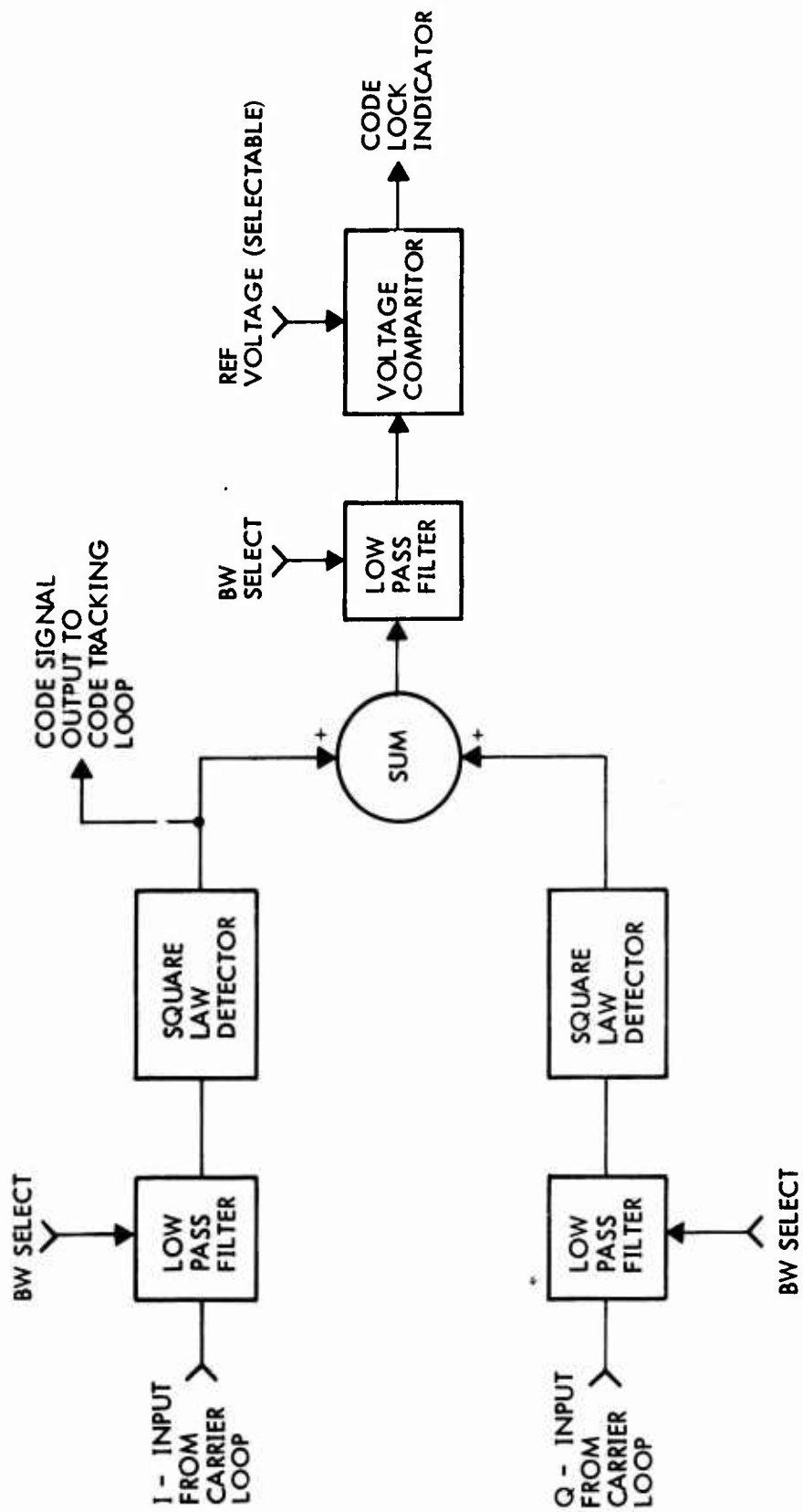
Figure 25.   Code Search Lock Detector

103

probabilities which affect the code acquisition time. The optimization of these parameters to minimize C-code acquisition time is discussed in Appendix 13.

5.3.3.8 Tracking Measurements Module

The Tracking Measurements Module, shown in Figure 26, obtains measurements of coarse velocity, fine velocity, and coarse range. It also generates two reference clocks for use by the Frequency Synthesizer module, and a receiver time-of-day (TOD) pulse which serves as a read command, and as an interrupt to the computer.

The timing references are obtained by counting down the 40.92 MHz reference signal generated in the frequency synthesizer to obtain clock rates of

$$\frac{40.92 \text{ MHz}}{(L/F_c)}$$

and

$$\frac{40.92 \text{ MHz}}{512}$$

where L/F_c is the ratio of L-band carrier frequency to code clock frequency. Since there are two L-band frequencies, L_1 and L_2 which must be implemented, a computer command selects which divide ratio is used.

A time-of-day counter, consisting of a 22 stage binary divider clocks down the 40.92 MHz reference to produce a

$$\frac{40.92 \text{ MHz}}{512}$$

clock, and a $\dfrac{40.92 \text{ MHz}}{2^{22}}$ clock pulse TOD read command which occurs every 0.102 seconds.

Velocity measurements are obtained by mixing the VCO signal from each carrier tracking loop with the locally generated F_3 reference signal. (This is done in the code and carrier tracking loop modules.)
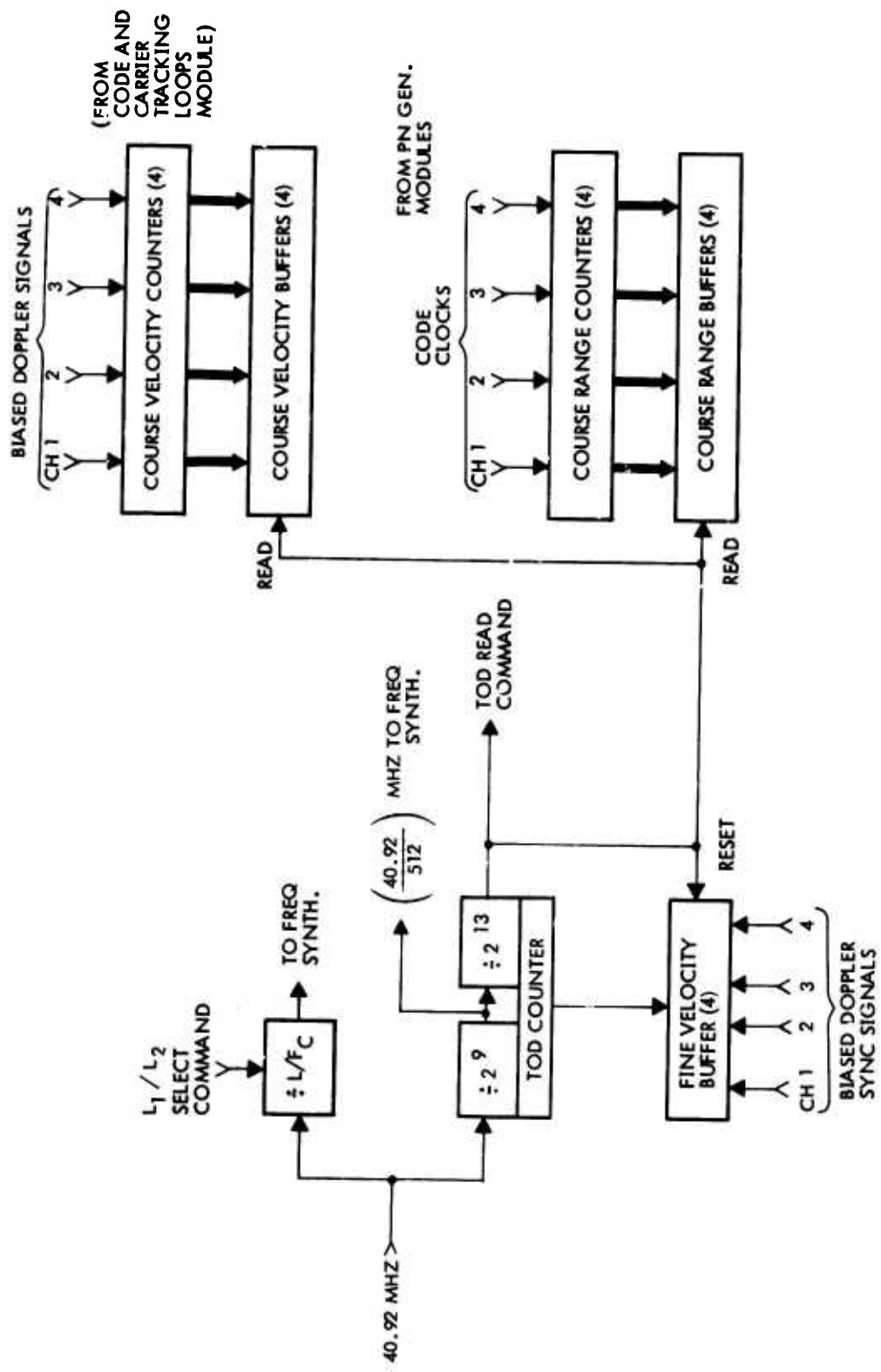
Figure 26.   Tracking Measurement Module

The output of the mixing process is a signal whose frequency is the sum of a bias frequency, $\frac{40.92}{512}$ MHz, and the difference between the local oscillator 15.345 MHz and the received carrier frequency downconverted to 15.345 MHz. This difference frequency contains the doppler shift frequency, and is called biased doppler.

Coarse velocity is measured by clocking a counter with the biased doppler signal, and reading the state of the counter at each TOD read command (each 0.102-second intervals). Fine velocity is measured by reading from the time of day (TOD) counter the time between the read command the end of the current cycle of biased doppler. Since the TOD counter is clocked at 40.92 MHz, the fine velocity count has a resolution of about 25 nanoseconds.

Coarse range measurements are made by counting cycles of each code clock in a binary counter called the Coarse Range counter. Whenever the TOD read command occurs, the counter contents are parallel shifted into the Coarse range buffer for readout to the computer. Since the code clocks are slaved to the received code clock from each satellite, the counter contents represents a measure of range. The quantization level of the count is one code chip, which represents about 100 feet for the P-Code, and 1,000 feet for the C-Code.

5.3.3.9 PN Code Generators Module

The PN Code Generators module, shown in Figure 27 accepts a 10.23 MHz code clock from the code and Carrier Tracking Loops module, generates the replica C or P code, and produces a PN Code output and a dithered PN code output which is used to demodulate the PN code from the received satellite signal.

The module provides code search control logic for initial acquisition of the C code, and provides a C-code epoch detector which provides C-code epoch pulses to the Bit Sync and Detection Module. P-Code handover logic is used to decommutate P-Code handover information obtained from the C channel data, and start the P-code PN generators running in synchronism with the received P-code. A data bit sync detector observes P-code generator epochs to derive bit sync for extracting P-channel data.

The module provides an inte ace for a security encryption device which is supplied by the government. A bypass switch is included to permit use of the receiver in either a secured or unsecured mode.

A C/P code select switch, controlled by computer command, determines whether the receiver is operated with the C-channel or P-channel. In either case, the replica code is used to generate a dithered reference, and a coincidence code (called a Z-code) is half-added to both the PN code and the dithered code. The outputs are used to obtain code sync, and to provide the necessary balance for PN demodulation, as discussed in Paragraph 5.3.3.5.
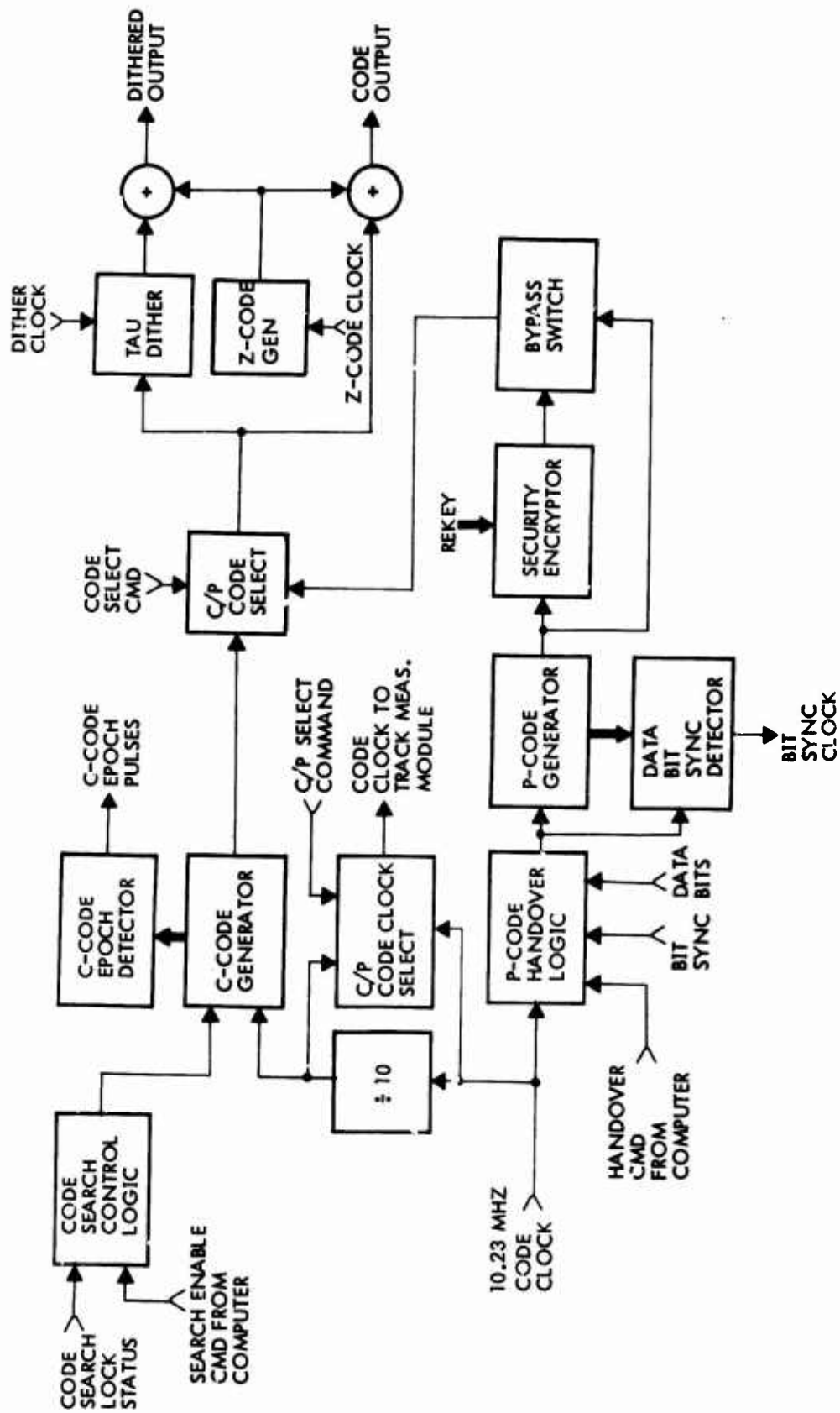
107

Figure 27. PN Code Generators

108

5.3.3.10 Bit Synchronization and Detection Module

The Bit Sync and Detection Module, shown in Figure 28, detects data bits in the received signal, obtains a bit sync pulse, decodes the differentially encoded data, and provides data bits and bit sync to the PN Code Generator module and the computer I/O and Receiver Control module.

The data signal is obtained from the coherent amplitude detector output of the Costas tracking loop (I-signal). A locally generated replica of the Manchester code square wave is multiplied with the received data signal to remove the Manchester code. The Manchester decoding circuitry is used if the data is extracted from the C channel. The Manchester decoding is bypassed using the data select switch if data is extracted from the P Code. The data signal is then detected in an integrate-and-dump type matched filter. The A/D converter samples the matched filter output just prior to dumping the filter voltage, and the digitized level is sent to the bit sync decision logic. The magnitude of the digitized signal is stored, and used to obtain correct bit sync. The sign bit of the A/D converter represents the differentially encoded data bits. The differential data decoder consists of a two bit storage register which compares each encoded bit with the preceding bit to determine whether or not a data transition occurred. This information is used to reconstruct the actual bit pattern sent from the satellite.

Bit synchronization is obtained as follows. When data is extracted from the P-Code, bit sync occurs in coincidence with a particular state of the P-Code generator. Thus, a bit sync detector circuit detects the receiver's P-Code generator state which coincides with bit sync, and generates a bit sync pulse.

When data is extracted from the C-Code, bit sync occurs in coincidence with one of the C-Code PN generator epochs. However, there are 20 epochs for every bit sync occurrence, and five epochs for every Manchester code transition. An epoch detector generates pulses coincident with the receiver C-Code generator epochs. These
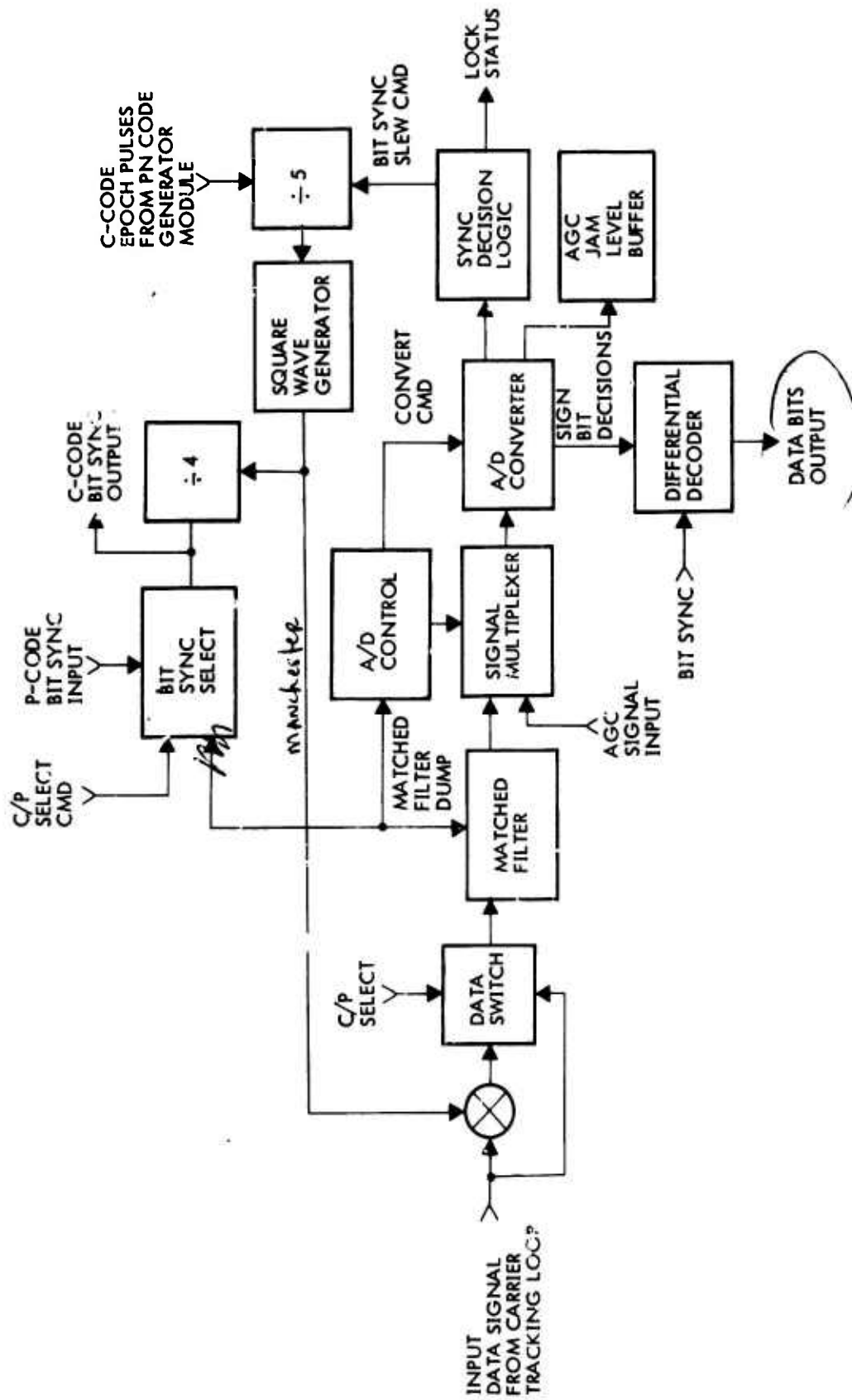
109

Figure 28. BIT Synchronizer and Detection Module

110

pulses are divided by five, and the resultant pulses drive a local Manchester code generator. The Manchester pulses are further divided by four to obtain replica bit sync pulses. The bit sync decision logic slews the divide by five counter until the digitized magnitude of the matched filter output is maximized. The sync decision logic then declares an in-lock condition, and bit sync is automatically obtained by dividing down the C-Code epoch pulses.

5.3.3.11 Computer I/O and Control Module

The Computer Input-Output (I/O) and Control Module shown in Figure 29 provide the necessary logic and control circuitry to transfer control information from the computer to the receivers, and to transfer satellite data, tracking measurements, and receiver status from the receiver to the computer. In addition, a single interrupt (the time-of-day pulse) is sent to the computer to synchronize computer instruction sequences to the receiver reference clocks.

The module also contains circuitry necessary to configure the receiver according to the configuration commanded by the computer, and to execute carrier and code pre-positioning.

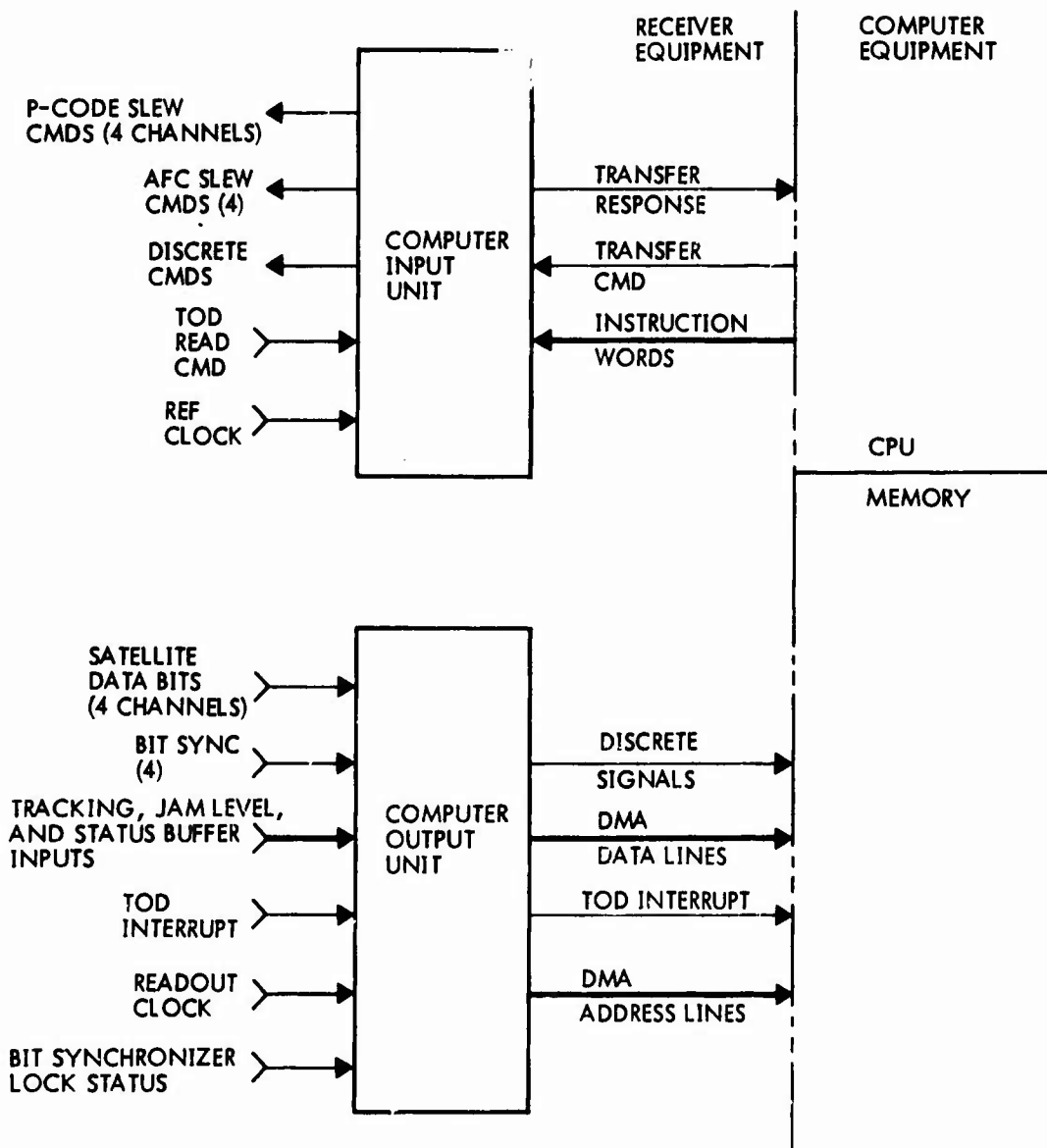A more detailed discussion of the receiver-computer interface is presented in Section 5.4.

Figure 29. Computer I/O and Control Module

112

5.3.3.12 Receiver Power Supply Module

The receiver power supply module, shown in Figure 30, accepts primary power from the user vehicle supply bus, and converts the input power to dc voltages adequate for operation of the analog and digital circuitry. The module includes a primary power on-off switch, fuse, on-off light, and elapsed running time meter. The power supply itself will provide AC to DC conversion from aircraft 400 Hz power, and provide adequate filtering and voltage regulation for proper operation of the receiver. A power-on reset flag (POR) is set each time power comes on. The flag is turned off by the computer, indicating recognition of a POR condition in the receiver. This is important, since a power glitch in the receiver will introduce timing glitches in the reference clocks which run off the reference oscillator. When a POR occurs, the receiver will remain configured in the state it was in prior to power interruption. It will be up to the computer to decide if the receiver should change its configuration in response to a power glitch.

A built-in test point (BTP) will provide voltage sensing to insure that the power supply is providing voltages in the allowable voltage range.

In the continuous receiver described in this baseline, two separate plug-ins constitute the power supply module. Each one is self-contained, and is identical to the single power supply module used in the Sequential Tracking receiver discussed in Section 5.6. The output supplies of the two plug-in supplies are tied together in parallel to provide the power capacity required for the continuous tracking receiver.
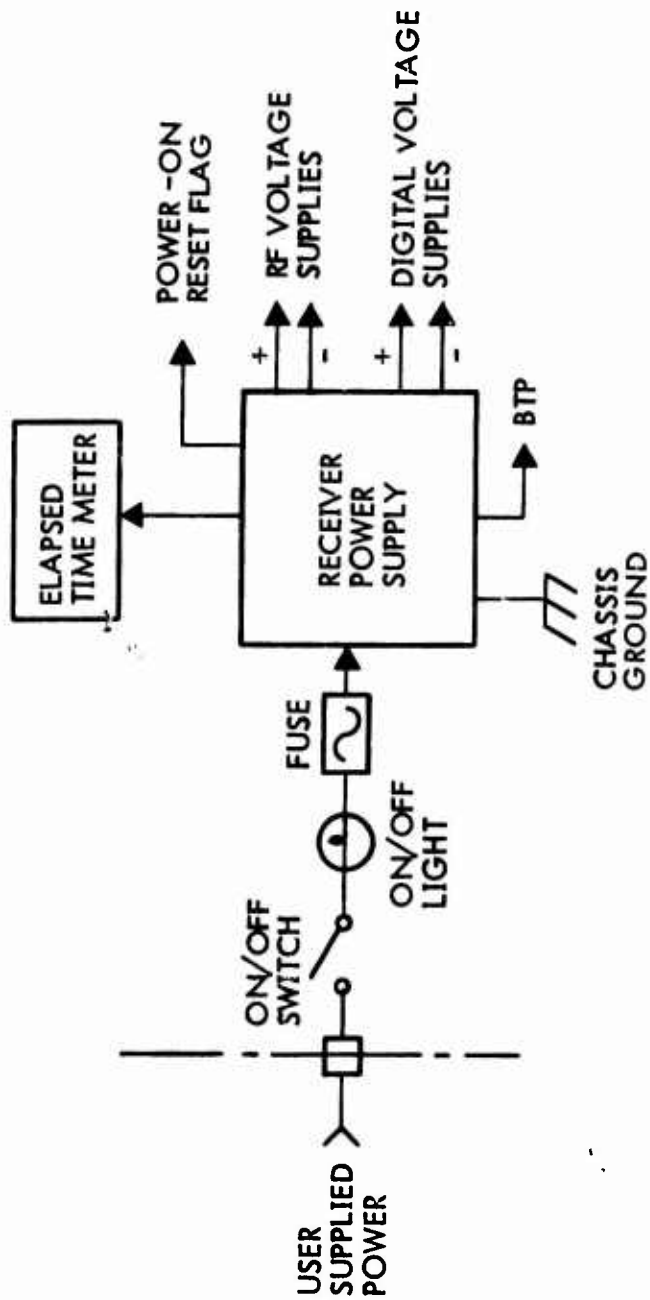
Figure 30. Receiver Power Supply Module

5.3.4 Mechanical Design and Packaging for the Baseline Continuous Tracking Receiver (User Classes A, B and F

5.3.4.1 General

The design of the GPS receiver was based upon certain physical constraints in order to minimize the impact of equipment integration into the various user parameters.

To achieve the aforementioned requirements (i.e., MIL-E-5400 Class 2) and provide for low-cost and high volume economic efficiency, the design concept was based upon proven standard concepts with variations as suitable to achieve the required configuration and performance goals.

5.3.4.2 Mechanization

5.3.4.2.1 Receiver

The basic design is in accordance with the requirements of MIL-C-172 for a MS-91403 case. As depicted in Diagram SK-100300, Sheet No. 1 (shown in Appendix 14), the unit configuration is basically a short ATR, having the parameters of 10.125 wide x 7.62 high x 12.56 long.

The construction of the receiver consists primarily of a .05" aluminum chassis fabricated in a manner to achieve minimum weight without sacrificing structural strength. A .06" panel is attached as shown to form the front face. Gussets attached to the chassis and front panel further strengthen the unit.

The rear or mounting interface utilizes DPA rack and panel connectors that accommodates power, signal, and RF connections. Connector alignment is achieved by the rear guide pin receptacles that interface with the aircraft mounting guide pins. The guide pins in conjunction with the hold-down hooks attached to the front panel serve as structural support for the receiver.

115

To achieve the maintainability goals, the plug-in modular concept is maximized throughout the design as depicted on Sheet No. 2 of diagram SK-100300 (see Appendix 14). The receiver is designed to contain up to 20 plug-in modules of similar external configuration, for RF/IF processing functions and up to 10 PC cards for digital functions that are contained in a card cage. The grouping of functions in the most efficient manner to reduce interconnects and the resolution of economics will determine the final configuration. It is significant to note that the 20 modules and 10 PC cards also represent growth possibilities since higher density of packaging is anticipated.

The XTAL oscillator and power supplies are also plug-in modules. The tentative physical location of the modules are illustrated in SK-100300 All interconnect wiring and coax-connectors are located and accessible from the bottom of the chassis.

To provide accessibility to the module back plate interconnect, the power supply modules may be removed via a disconnect plug, or pivoted outward to provide testing without the utilization of an adapter plug and harness.

To provide BIT capability, fault indicators are included adjacent to each module that isolates the fault to an SRU.

The front panel contains the following items:

a) Handle

b) Hold-down hooks

c) Fuses and holders (2)

d) Elapsed time indicators

e) Fault indicators (latch-type) isolation to LRU

116

The plug-in modules illustrate the packaging concept of the ASAs and PC boards, respectively. They are shown in Appendix 14, SK-100200, Sheet 3 and 4.

Currently the concept is based around a common modular die-cast housing having partitions separating the module into four (4) compartments, each capable of mounting a 1-1/2 x 2 ASA or PC board. Alternatives to the size may be derived by removing the separators, thus encompassing a PC board of 4 x 4 dimension.

RF input/output connections are accomplished via coax connectors, plug-in type. Signal connections are made via RF feedthroughs to a connector. Versatility of connector-module configurations is illustrated in SK-100200, Sheets 3 and 4. Two connector concepts are shown: 1) Individ insulated contacts inserted into a defined hole pattern integral with the module. 2) Conventional connector separately mounted in the module. Guide pins are also used as polarization pins to preclude any mismatch of modules.

Several concepts have been reviewed for interconnect of the modules and the input/output rack and panel interface connector. The interconnect wiring concept illustrated in Sheet 1 of drawing SK-100300 is that of wire wrap. It is significant to note that a high degree of maintainability efficiency has been designed into the unit since all modules, back plate interconnect plate, and wiring interconnect harness can be considered as independent assemblies and comply with the plug-in concept.

Interconnect options are:

1) Wire-wrap using automatic assembly

2) Mother-board (multilayered)

117

3) Flat-cable

4) Hard-wire (solder or crimped)

5) Combination.

Wire-wrap was selected as the baseline wiring method. The advantages of wire-wrap are that it provides a programmable automatic production type of technique with economic advantages, design flexibility, and ease of repairability.

5.3.4.2.2 Cover

The dust cover is fabricated from .04" aluminum having cutouts in the back face for the rack and panel connectors and guide pins. The top and bottom surfaces contain a series of 1/8" diameter punched holes for the free convection of the internal heat to the outer ambient. Two 1/2" wide strip of rubber (closed cell) and nylon of suitable thickness are bonded to the upper surface of the cover. These strips coincide with the grooves on the top surfaces of the modules to physically contain the modules, and to assure electrical continuity to their mating connectors on the back plate under the environmental physical requirement. Quick release captive fasteners contain the cover to the chassis.

5.3.4.2.3 Physical Characteristics

Size	10.125 x 7.625H x 12.563 L
Volume	1000 cubic inches/0.0168 M^3
Weight	28.5 lbs (estimated) 13.0 Kg
Dissipation	60 watts (maximum).

5.3.4.3 Thermal Considerations

Power dissipation in the receiver is less than 60 watts.

An array of 1/8" diameter holes in the top and bottom surfaces of the dust cover allows cooling air to flow through the electronics. Cooling air entering the bottom of the receiver washes the external surfaces of all the modules and exits at the top. All modules are enclosed and therefore are not subjected to contamination.

Critical devices are mounted on conductive surfaces that contribute to maintaining the devices well within their operational rating.

The watts/square inch density relative to the 540 square inch exterior surface area is approximately 0.11 watts/square inch. This heat dissipation is considered well within the art of natural cooling, convection, and radiation. External cooling other than natural convection and radiation is therefore not considered. Temperature rise in the air stream is anticipated not to exceed $20^{\circ}C$.

5.3.4.4 EMI Consideration

A high degree of RF isolation is provided by the inherent design of the modules. The module containers are partitioned to minimize local RF effects. To prevent radiated noise from entering or leaving the enclosure, the modules are RF sealed. Filters are provided on input/output power and signal lines to reduce the effects of conducted interference.

5.3.4.5 Maintainability

To achieve the maintainability goals, the plug-in modular concept is maximized throughout the design. Virtually all circuitry is packaged on printed circuit cards and contained on plug-in type modules. The dust cover utilizes quick-turn fasteners for easy removal and access to the

119

modules. Fault indicators are provided to quickly assess and isolate to an SRU. Card extractors are provided to facilitate removal of PC cards. Guide pins and polarization is provided to p eclude mismatch of modules. Modules are provided with a diagonal white strip that runs in a progressively diagonal fashion to facilitate quick visual location of each module. The modules plug into a connector backplate that is mounted onto the chassis. This connector plate is prewired and can be defined as a plug-in, since by simply removing the I/O connectors via jack-screws and the coax's connectors will enable quick replacement.

The XTAL oscillator is also modularized and plugs into its receptacle. Quick-turn fasteners are provided on these modules to maintain physical environmental integrity.

The power supplies are contained beneath the connector backplate and accessible from below. These units are contained by two quick-turn release fasteners that interface with a structural support bracket that also provides good heat-sinking to the chassis. The opposite end of the power supply is contained on a cradle that is integral with the chassis, but has the capability of enabling the power supply to pivot outward and provides complete accessibility to the connector backplate and the coax connectors thereon. Removal of the mounting screws that maintain the power supply to the cradle and disconnecting the plug-in harness connector via jack screws contained on the connector, enables the removal of each power supply.

The interconnect wiring harness has been designed to provide easy replaceability, and simply requires removal of the fasteners that contain the connectors to the chassis.

The 5. 115 MHz crystal oscillator, located at the rear section of the chassis, contains high quality components in a ruggedized construction design that is vibration compensated to assure high reliability and optimum performance.

5.4 RECEIVER-COMPUTER INTERFACE

The interface between the user receiver and the user segment computer plays an important role in defining the operational capabilities of the system, the hardware implementation of the receiver and computer, and has a significant impact on user segment and life cycle costs. The design of the interface, therefore, must be carefully evaluated, and should consider the specific goals of each phase of the GPS program. The approach taken in this report is to consider the most probable requirements and implementation for the operational system.

5.4.1 Key Characteristics

This section considers the key characteristics of the interface. These characteristics are the definition of the interface, functional requirements, requirements on receiver and computer design, and tradeoffs between hardware versus software complexity.

5.4.1.1 Interface Definition

The user equipment may be considered to include whatever hardware and software are necessary to meet the navigation requirements for a given class of user. The user equipment must do two things to meet these requirements. It must collect measurements and satellite data, and it must process these measurements to provide the user with navigation capability. Collection of measurements must clearly be done in hardware. However, control of the hardware which obtains the measurements, and processing of the measurements, can to a large extent be performed either by hardware or software.

The definition of the computer receiver interface to be used here in this report, is that the receiver consists of hardware which provides satellite data and tracking measurements to the computer, and receives control instructions from the computer which configure the receiver for a planned mode of operation. The computer consists of whatever hardware and software is necessary to plan and control

122

the operation of the receiver in its operating environment, and to utilize satellite data and tracking measurements for navigation and for receiver control.

The thrust of this definition is that the computer must do the thinking, while the receiver must carry out pre-planned sequences of operations.

5.4.1.2 Interface Functions

A number of functions can be identified which the receiver computer interface must perform. These are:

a) Provide a timing pulse from the receiver to synchronize computer timing to the receiver clock.

b) Transfer detected satellite data bits to the computer.

c) Provide tracking measurements to the computer which consist of coarse range, fine range, coarse velocity, and fine velocity.

d) Provide receiver configuration status information to the computer.

e) Provide receiver status information to the computer which indicates either proper or faulty operation of the receiver.

f) Provide receiver status information to the computer which indicates whether or not the satellite data or tracking measurements are valid.

g) Provide configuration control information to the receiver.

h) Provide P-code preposition information to the receiver.

i) Provide carrier preposition information to the receiver.

j) Provide timing information as required to the receiver for proper execution of configuration changes and prepositioning of code and carrier.

123

5.4.1.3 Requirements on Design

The receiver design must accommodate a hardware interface with
the computer which performs the functions itemized in Paragraph 5.4.1.2.
Consequently, some amount of special purpose digital logic will be required
to interface with the computer. To achieve compatibility with the computer,
the special purpose logic design must be based on the selection of a specific
computer. Such items as interface line driving requirements, types of
signals, word size, parallel versus serial I/O, interrupt capability,
timing precision, and addressing requirements will depend on the specific
computer used.

It is planned, however, that the special purpose interface logic be
packaged on a single module so that different computer installations can
be accommodated by a plug-in module change in the receiver.

The computer selected must have the capability to accept at least
one interrupt for timing synchronization. It must have sufficient computational
speed and memory capacity to plan and control operation of the receiver
in real time under a variety of missions and scenarios appropriate for a
given class of user. The computer input and output channels must be
reasonably simple, so that the design and manufacture of special purpose
digital logic for the computer interface do not become unnecessarily
complex.

5.4.1.4 Tradeoffs Between Hardware Versus Software Complexity

The selection of a specific interface between receiver and computer
can be made so as to minimize that software requirements for receiver
operation, or to minimize special purpose digital hardware necessary for
receiver operation. The selection of interface can also permit the use
of moderate amounts of hardware and software. Clearly, maximum use

124

of software results in a lower cost receiver, and greater flexibility of operation. Flexibility is desirable during the early development phase of the program, but may not be necessary for the operational system. On the other hand, minimizing software requirements by utilizing special purpose digital logic for measurement processing and receiver control will result in a higher unit cost for the receiver, but lower software development costs. These costs could be quite large during the development phase.

The best fit between hardware and software control of the receiver can best be determined by the requirements for flexibility at each program phase, and by life cycle cost modelling of alternative designs. The baseline approach described in this report utilizes a hardware implementation approach to receiver control, and a software approach to measurement processing. This is a typical implementation, thought to be representative of the operational system.

5.4.2 Approach to Implementation

This section discusses some alternative approaches to the implementation of the computer-receiver interface.

The options for defining the computer receiver interfaces can be considered in two parts. The first is the transfer of data from receiver to computer. This second is the transfer of control and preposition instructions from computer to receiver.

5.4.2.1 Data Transfer from Receiver to Computer

Four options for data transfer have been considered. These are:

   a) Bit by bit (serial) transfer

   b) Parallel word transfer under program control

   c) Direct memory access (DMA)

   d) Receiver data frame storage.

Option a) requires the minimum of special purpose logic in the receiver, and maximum software complexity. This technique requires the computer to accept each satellite data bit as it is detected by the receiver. The computer would then do all frame sync and data decommutation required. The computer would also be required to respond to a time-of-day read interrupt to access new tracking measurements. The TOD interrupt would occur about every 102 milliseconds, and would be asynchronous with the data bits which occur every 20 milliseconds for 50 BPS data.

The impact to the computer is that either the CPU must service each bit or an accumulating buffer would be required as part of the computer equipment. The assembly of satellite data by the CPU would run asynchronously with other program functions, and would be inefficient in terms of time and memory size.

Option B is similar to Option A. The use of parallel word transfer under program control would make the interface compatible with most existing computer hardware. However, the CPU would still be required to assemble the satellite data asynchronously with other program functions, and the receiver would have to provide some buffer storage.

Option C utilizes a direct access of the computer memory to insert satellite data and tracking measurements into an assembly area of memory. This method would permit the CPU to perform program functions in an orderly manner without having to service more than a single interrupt. This would provide for maximum efficiency of computer time and memory storage. The receiver, however, would have to provide buffer storage for at least one computer word full of satellite data for each satellite, would have to generate addresses for the data, and would have to provide communication signals for access with memory.

Option D is to provide storage for several computer words. A full frame of satellite data, if buffered in the receiver, could allow for a considerable amount of routine data processing in receiver hardware.

5. 4. 2. 2 Instruction Transfer from Computer to Receiver

The computer can control the receiver in one of two ways. It can issue discrete event pulses which, when received, cause a change to occur in the receiver. Or, it can send a configuration message which will be applicable at some future state of the receiver's reference clock. The first method requires no storage or decoding of data in the receiver. However, timing uncertainties in generating the pulse relative to the receiver's clock will be large. The second method requires that the receiver store and decode instruction data, but provides for timing of

127

receiver control functions whose uncertainty is limited only by how well the computer knows the receiver's time reference relative to its own.

5.4.3 Baseline Interface Description

The interface described in this section is presented as a baseline design. It is typical of what the operational system would utilize. Emphasis is on the receiver details of the interface. The description of the data transfer from receiver to computer is reasonably detailed, since the message content is quite well defined. The description of the transfer of control instructions from the computer to the receiver is more general, since the details will depend on the control strategies required to be implemented, and the degree of flexibility needed by each class of user.

5.4.3.1 Receiver to Computer Data Transfer

This function transfers tracking data and satellite data from the receiver to the computer via direct memory access (Option C). Figure 31 shows the detailed implementation in each IF processor of the four channel receiver. The following buffers are filled with tracking data each time a TOD interrupt occurs.

       1) Coarse Velocity

       2) Fine Velocity

       3) Coarse Range

       4) Fine Range

       5) Receiver Status.

In addition, data is being collected in each channel asynchronously with the TOD interrupt. Data bits are clocked into a 16 bit data buffer for transfer to memory.
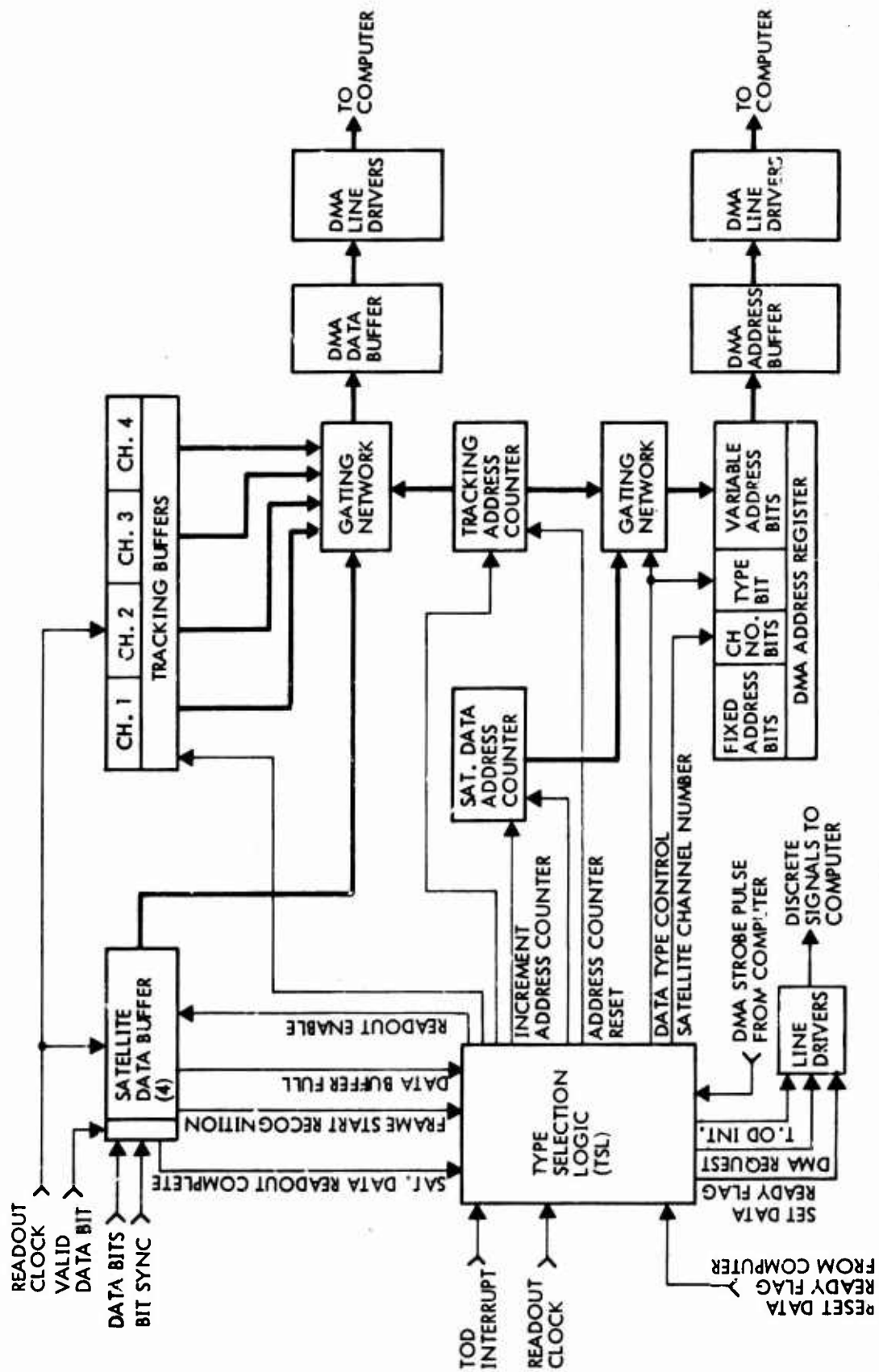
Figure 31. Computer Output Unit

The tracking buffers and data buffer contents are addressed, and transferred into computer memory via DMA lines. Transfer is controlled using the type selection logic. This logic accepts various signals to determine whether tracking buffer data type or satellite data type should be transferred to the computer.

The operation proceeds as follows. Whenever a TOD interrupt occurs, all tracking data type buffers (including receiver status) are filled with new data bits. The type selection logic (TSL) waits until the data buffer readout is complete (if it is being read out), and then gates each buffer into the DMA. A readout clock signal clocks the bits into the DMA line drivers at high speed. The buffers are selected sequentially, and a tracking address counter is incremented each time a buffer has been read out. The TSL then generates a DMA request pulse, and the computer reads the DMA data. A DMA address is generated by setting a type bit (1 for tracking, 0 for satellite data, setting ID bits indicating from which channel the data was collected [1-4]) and transferring the contents of the tracking address counter to the DMA address register. This register is read concurrently with the DMA data. After data and address have been read, the computer generates a DMA strobe pulse, indicating it has read the data. The TSL observes the DMA strobe and repeats the process, gating the next tracking buffer into the DMA and advancing the tracking address counter. Upon completion of a full readout of all tracking buffers, the TSL is in an idle mode. When in an idle mode, the TSL observes the tracking buffer to see if it has been filled. If so, the TSL checks to see if Frame Start is or has been recognized. (This is necessary to order the data. Data bits prior to the first frame start are not used.)

130

When frame start is first recognized, the TSL resets the data address counter to zero. When the data buffer is full, the TSL gates the data buffer contents into the DMA data register. The type bit is set to zero for satellite data, and the data address counter gated into the variable address of the DMA address register. The TSL then generates a DMA request pulse, the computer reads satellite data and its address, and the computer generates a DMA strobe pulse. The TSL then increments the data address counter, and returns to idle mode.

During the loading of the data buffer, the bit sync indicator in the receiver is observed. If during the clocking of data into the data buffer, the bit sync lock indicator is in lock all the time, the last bit clocked into the data buffer will be a zero, indicating the data word is valid. If at any time during the buffer fill the lock indicator is out of lock, the last bit is set to one, indicating probable bad data in that word. The data is strobed to the computer with the quality indicator bit in either event.

Four discrete commands are associated with the readout of data to the computer. These are:

1) TOD Interrupt   (to computer)

2) DMA Request   (to computer)

3) DMA Strobe   (from computer)

4) Data Ready Flag Set   (to computer)

5) Data Ready Flag Reset   (from computer).

The TOD interrupt is provided to the computer to synchronize computer timing with the receiver local oscillator clock. The DMA request   strobe have been explained.

131

The data ready flag is set by the receiver each time a full frame of satellite data has been transferred to the computer. The data ready flag is then reset by the computer after it is recognized.

5.4.3.2 Computer to Receiver Instruction Transfer

The baseline implementation for instruction transfer from computer to receiver is shown in Figure 32. Instructions from the computer are sent over the computer's program control channel from the CPU. Each word received has an identification code (ID) associated with it. There are three types of instruction words. These are:

    a) Discrete switch commands

    b) VCO Preposition words

    c) P-code Preposition words.

Parity checks are made on each word received from the computer. If parity is bad, then a parity error flag is set. If parity is good, the word is decoded, and sent to the appropriate register. Transfer commands from the computer clock the received words into the appropriate register. A transfer response is then sent back to the computer.

At each time-of-day interrupt, a read command transfers the contents of all registers into storage buffers. When transfer to storage occurs, the receiver configuration changes according to the new buffer contents. This buffering allows configuration and preposition changes to occur in synchronism with the receiver's time-of-day clock.

The Receiver Control Buffers are decoded to provide discrete switching commands to the various receiver modules.
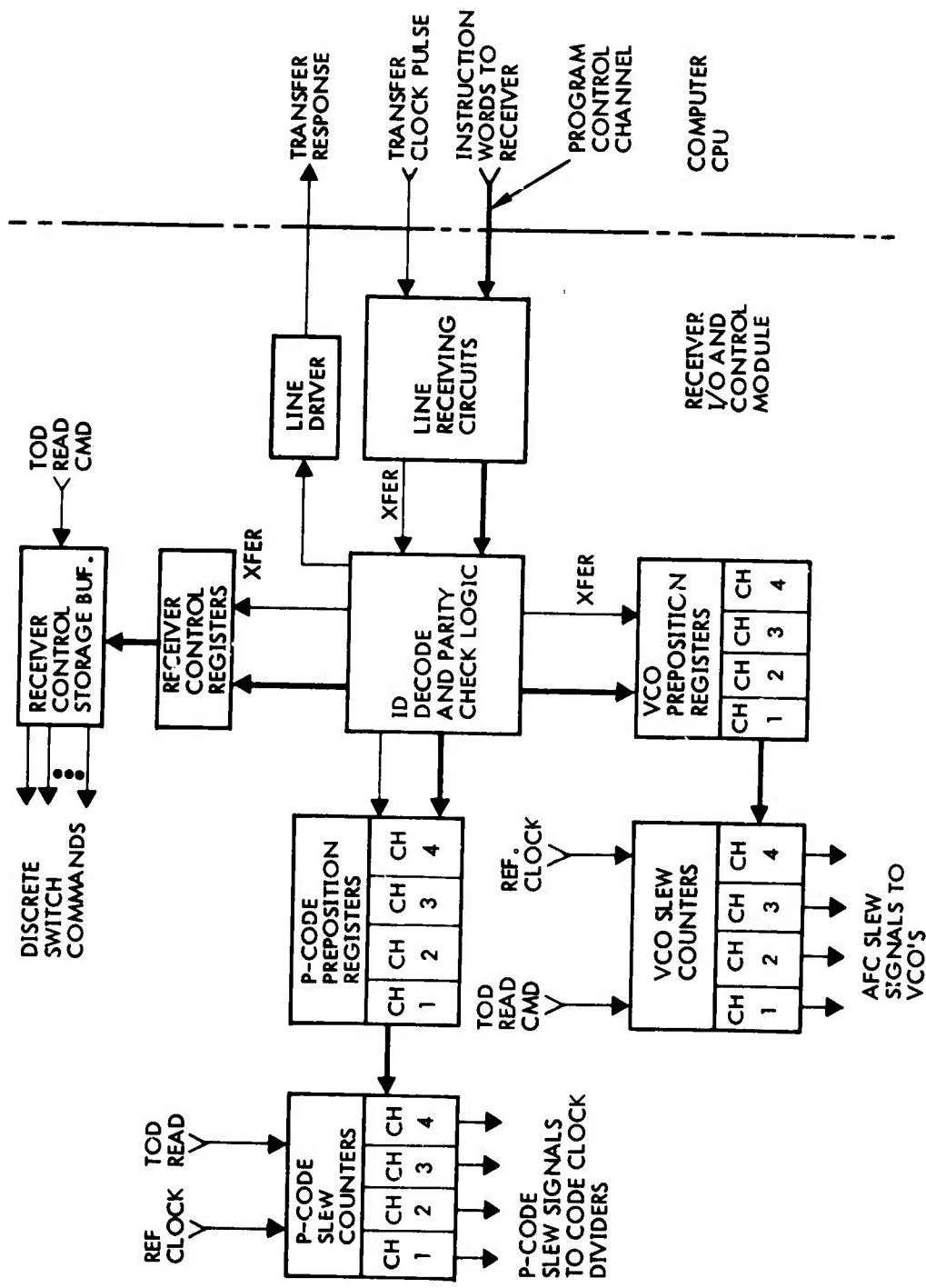
Figure 32. Computer Input Unit

133

The P-code preposition instructions are implemented for each channel by running a binary counter until its contents are the same as the word loaded into its code slew buffer. While the counter is running, a discrete slew command signal is sent to its Code and Carrier Tracking Loop module which advances and retards the P-code clock. When the counter stops running, the slew command is turned off, and preposition is completed.

The VCO preposition instructions are implemented in the same way as the P-code preposition instructions. However, a discrete AFC slew command is sent to the tracking loop VCO loop filter while the counter is running. The VCO is ramped forward or backward at a constant rate for the duration of the slew signal.

P-code preposition capability is not implemented, since in general C-code acquisition proceeds using a noncoherent code search.

5.5 ALTERNATIVE DESIGN CONSIDERATIONS

This section presents a number of alternative design concepts for the GPS user receiver. These concepts are offered as potential options to the users. A user may thereby tailor his receiver to obtain special performance or cost benefits in a sensible and cost effective manner.

The alternative design concepts discussed are a Sequential Tracking receiver which tracks both C and P channels of the L_1 carrier (Type II receiver), a Sequential Tracking receiver which tracks the C-channel only (Type III low cost receiver), the use of a parallel code correlation technique to reduce the initial C-code search time, a time-shared Bit Sync and Detection module for continuous (Type I) receivers, and the use of switched, multiple antennas.

5.5.1 Sequential Tracking Receivers (Types II and III)

This section discusses details of timeshared, sequential tracking receivers. There are two types of sequential trackers of interest. A Type II receiver tracks four satellites sequentially in either the C-channel or the P-channel. The block diagram for this type of receiver is shown in drawing number SK-100002 in Appendix 14. It uses many of the same modules as the Type I receiver (continuous tracker). The PN code generator module and the Computer I/O and Control Module are somewhat different. The Frequency Synthesizer Module does not require L_2 carrier capability and the Tracking Measurements Modules need counters for only one satellite, not four. The PN generator module must provide fly-wheel storage for the state of the PN codes of those satellites not being tracked, but which are in the user's constellation. Since the user may navigate in either C or P, flywheel storage is provided for both C and P Code PN generators.

The Sequential receiver contains two processing channels. Channel A is used for obtaining tracking measurements from each of the satellites whose code and carrier states have been acquired, and are therefore in the constellation of sequentially tracked satellites. Channel B is used to acquire new satellites for constellation revision, and for receiving satellite data from any satellite in view without interfering with the sequential tracking of the navigation constellation.

The computer I/O and Control Modules must accommodate those features of the Sequential receiver which are unique from the continuous tracking receiver. Its design is therefore somewhat different, but its principles of

operation are the same.

The Type III receiver is a sequential tracker which tracks only C-channel signals. Its construction and operation are the same as the Type II receivers, but all P-code hardware functions are removed. This receiver is the lowest cost receiver.

5.5.1.1 Mechanical Design Considerations for Sequential Receivers

The basic design is similar to that of the four channel GPS receiver
and was specifically designed for maximizing the plug-in modules utilized
in the aforementioned unit.

The basic design is also in accordance with the requirements of
MIL-C-172 for a MS-91403 case. The unit configuration is shown in
Drawing SK-100200 sheets 1 and 2 (in Appendix 14) and configures the envelope
of a 1/2 short ATR, having the physical parameters of 4.875 wide x 7.625
high x 12.562 long.

The construction of the receiver consists primarily of a .05" aluminum
chassis fabricated similar to the four channel receiver. Specific effort
was made to simplify the chassis without degradation to structural
integrity. A .06" panel is attached as shown to form the front face. Gussets
attached to the chassis and front panel further strengthen the unit. The
similarity of the sequential and 4 channel fabrication enables the usage of
identical tooling for most of the chassis fabrication of both units.

The rear or mounting interface utilizes DPA rack and panel
connector that accommodates power, signal, and RF connectors. Connector
alignment, guide pins, and hold-down hooks attached to the front panel are
similar to that of the 4 channel receiver.

The plug-in modular concept is maximized throughout the design
as depicted on sheet No. 2 of drawing SK-100200. The receiver is designed
to contain 15 plug-in modules of similar external configuration, or possible
separation into eleven (11) modules for RF/IF processing functions and 4 PC
cards for digital function that are contained in a card cage.

The grouping of functions in the most efficient manner to reduce
interconnects will determine the final configuration. Also higher density
of packaging is anticipated that will provide additional growth possibilities.

138

The pre-amp, frequency synthesizer, and the BIT r.f. generator modules are singular in quantity and are functionally common to all channels.

The XTAL oscillator is also a plug-in module. To obtain the necessary power requirements, a power supply plug-in module, identical with that of the 4 channel receiver is contained on a pivoted cradle beneath the chassis.

To provide accessibility to the module backplane interconnect, the power supply module may be removed via a disconnect plug, or pivoted outward to provide testing without the utilization of an adapter plug and harness.

To provide BIT capability, latch-type reset indicators are included adjacent to each module that isolates the fault to an SRU.

The front panel contains the following items:

a) Handle- springloaded, 90° rotation

b) Hold-down hooks

c) Fuses and holders (2) includes spare

d) Elapsed time indicator

e) Fault indicator (latch type) isolation to LRU.

It is significant to note that the modules are identical and interchangeable with the 4-channel receiver, reference sheets 3 and 4 of drawing SK-100200. The pertinent characteristics have been illustrated and explained in detail in the previous section on the 4-channel receiver and need not be repeated again.

The 5.115 MHz crystal oscillator, located at the rear section of the chassis contains high quality components in a ruggedized construction design that is vibration compensated to assure high reliability and optimum performance.

139

A mechanical mockup of this receiver was constructed simulating the features as shown on drawing SK-100200. Figures 33-36 depict some of the salient features, such as exterior cover and front panel accessories; chassis construction, module plug-in concept, both ASA and PC card; swing out power supply, etc.

5. 5. 1. 2 Cover

The dust cover is fabricated from .04" aluminum having cutouts in the back face for the rack and panel connectors and guide pins. The top and bottom surfaces contain a series of 1/8" diameter punched holes for the free convection of the internal heat to the outer ambient. A 1/2" wide strip of rubber (closed cell) and nylon of suitable thickness is bonded to the upper surface of the cover. This strip coincides with the grooves on the top surfaces of the modules to physically contain the modules, and to assure electrical continuity to their mating connectors on the back plate under the environmental physical requirements. Quick release captive fasteners contain the cover to the chassis.

5. 5. 1. 3 Physical Characteristics

Size	4.875W x 7.625H x 12.563L
Volume	470 cubic inches/.0077M^3
Weight	18/5 lbs (estimated) 8.4 Kg
Dissipation	40 watts (maximum).

5. 5. 1. 4 Thermal Considerations

Power dissipation in the receiver is less than 40 watts.

An array of 1/8" diameter holes in the top and bottom surfaces of the dust cover allows cooling air to flow through the electronics. Cooling air entering the bottom of the receiver washes the external surfaces of all the modules and exits at the top. All modules are enclosed and therefore are not subjected to contamination.
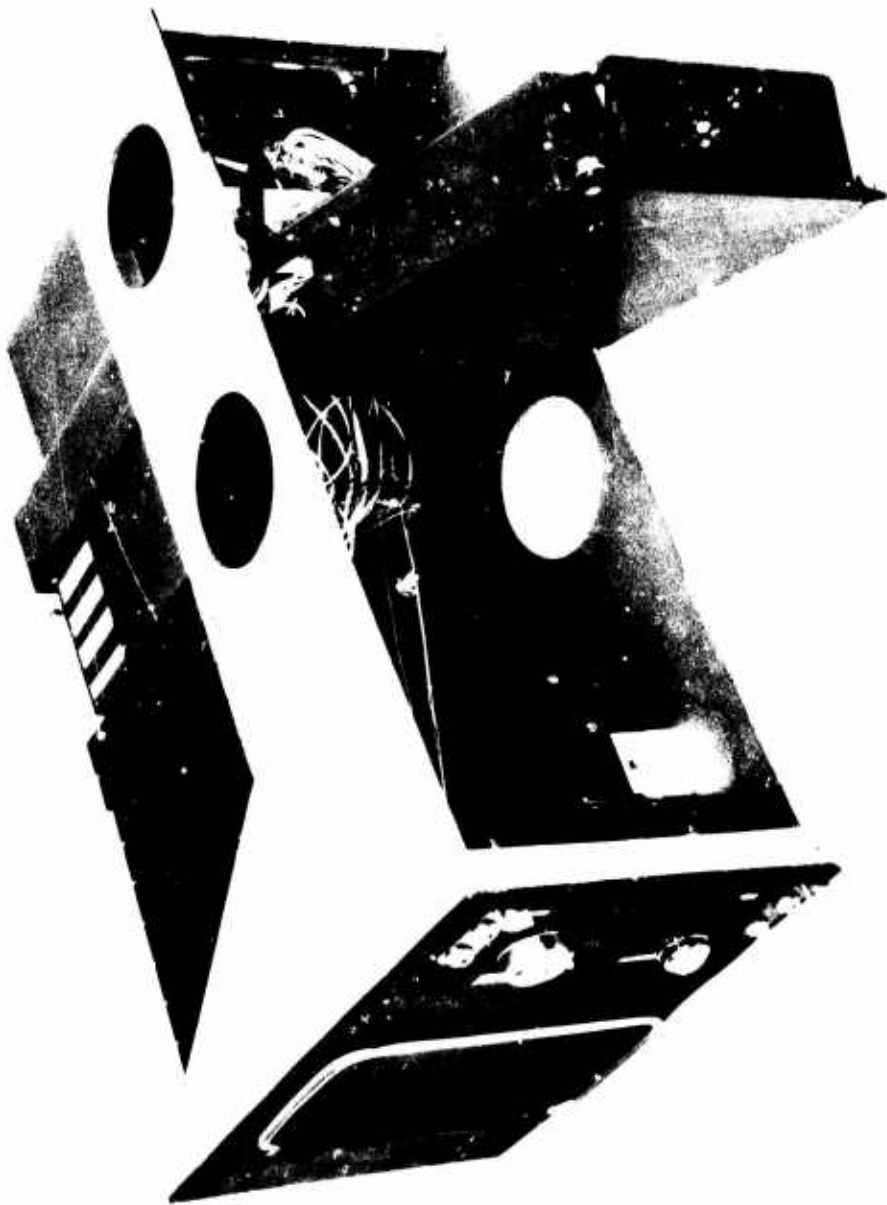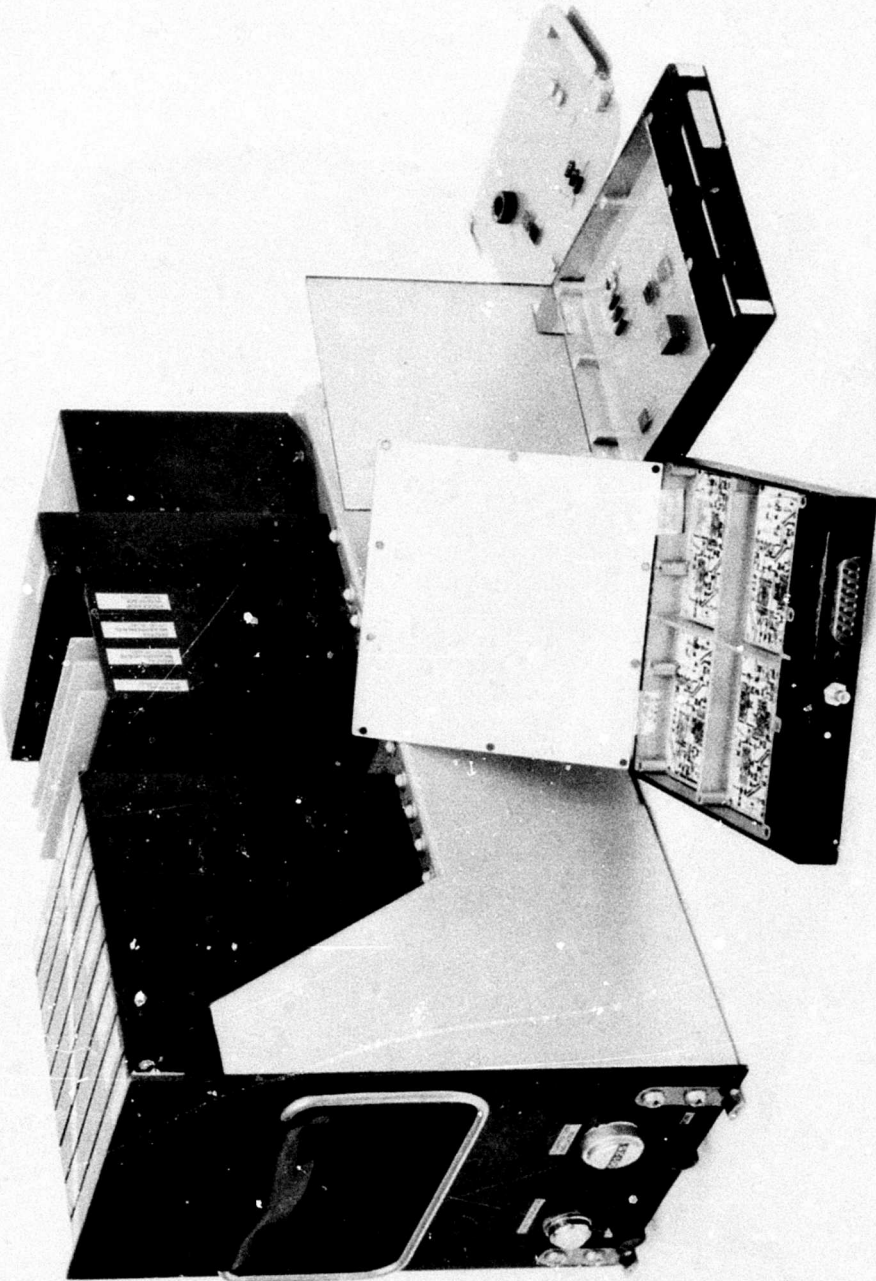
Figure 33

141
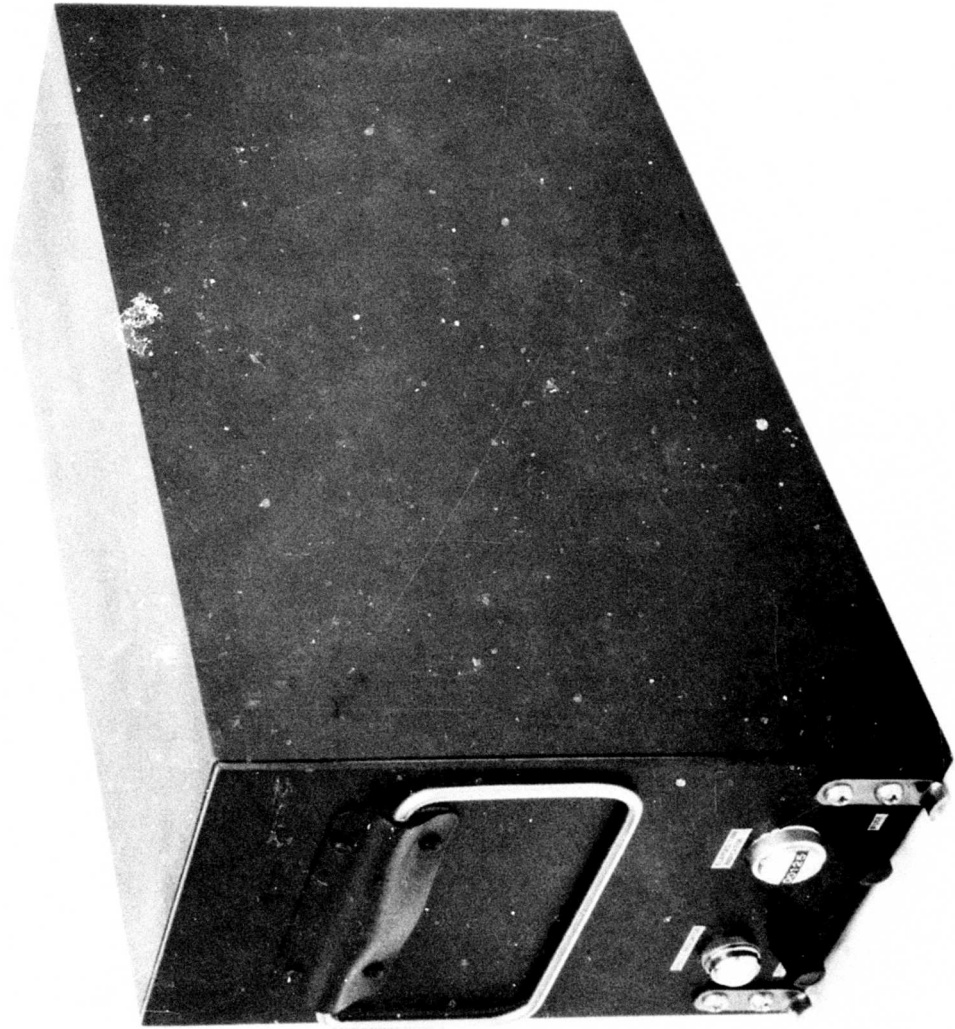
Figure 34

Figure 35

143

Figure 36

Critical devices are mounted on conductive surfaces that contribute to maintaining the devices well within their operational rating.

The watts/square inch density relative to the 400 square inch exterior surface area is approximately 0.10 watts/square inch. This heat dissipation is considered well within the art of natural cooling, convection, and radiation is therefore not considered. Temperature rise in the airstream is anticipated not to exceed $20^{\circ}C$.

5.5.1.5 EMI Consideration

A high degree of RF isolation is provided by the inherent design of the modules. The module containers are partitioned to minimize local RF effects. To prevent radiated noise from entering or leaving the enclosure, the modules are RF sealed. Filters are provided on input/output power and signal lines to reduce the effects of conducted interference.

5.5.1.6 Maintainability

To achieve the maintainability goals, the plug-in modular concept is maximized throughout the design. Virtually all circuitry is packaged on printed circuit cards and contained on plug-in type modules. The dust cover utilizes quick-turn fasteners for easy removal and access to the modules. Fault indicators are provided to quickly assess and isolate to an SRU. Card extractors are provided to facilitate removal of PC cards. Guide pins and polarization are provided to preclude mismatch of modules. Modules are provided with a diagonal white strip that runs in a progressively diagonal fashion to facilitate quick visual location of each module. The modules plug into a connector backplate that is mounted onto the chassis. This connector plate is prewired and can be defined as a plug-in, since by simply removing the I/O connectors via jack-screws and the coax's connectors will enable quick replacement.

145

The XTAL oscillator is also modularized and plugs into its receptacle. Quick-turn fasteners are provided on these modules to maintain physical environmental integrity.

The power supply is contained beneath the connector backplate and accessible from below. This unit is contained by two quick-turn release fasteners that interface with a structural support bracket that also provides good heat-sinking to the chassis. The opposite end of the power supply is contained on a cradle that is integral with the chassis, but has the capability of enabling the power supply to pivot outward and provides complete accessibility to the connector backplate and the coax connectors thereon. Removal of the mountingscrews that maintain the power supply to the cradle and disconnecting the plug-in harness connector via jack screws contained on the connector, enables the removal of the power supply.

The interconnect wiring harness has been designed to provide easy replaceability, and simply requires removal of the fasteners that contain the connectors to the chassis.

5.5.? Multiple Code Correlation for Rapid Code Search

For some users the time to initially acquire the C-code is very important. This section presents a concept for reducing the average time to acquire the C-code. The method employed is to provide multiple correlators for the C-code PN signal, and search separate regions of the possible number of one-half chip cells in which the received PN code may be found. This process is shown in Figure 37. For example, if one correlator is used, the search region for each correlator consists of 2046 half-chip cells. If two correlators are used, the search region for each correlator is only 1023 half-chip search cells. Thus, the addition of one more PN correlator and appropriate lock detection circuitry will reduce the average C-code search time by about one-half. If N correlators are used, the search time can be reduced by a factor of about $\frac{1}{N}$.

Figure 38 shows a typical implementation for two C-code correlators. In this configuration, the P-code correlator is not used, and C-code correlation is performed at the second IF frequency in order to save circuitry. Since the code search proceeds noncoherently, a single VCO is used only to translate the received signal to 15 MHz in the second mixer. Each correlator is followed by a noncoherent code search lock detector which indicates the presence or absence of code correlation after each dwell interval. One or the other of the two detectors will indicate correlation first, as the search proceeds. Once correlation is verified, that correlator is switched into the common code and carrier tracking loop, and the carrier and code loops are locked up. Receiver operation then proceeds in the usual manner.

147

CODE SEARCH
UNCERTAINTY
RANGE FOR

1 2 2046

CODE SEARCH
INTERVAL FOR
CORRELATOR
NO. 1

1 2 1023

CODE SEARCH
INTERVAL FOR
CORRELATOR
NO. 2

1024 2046
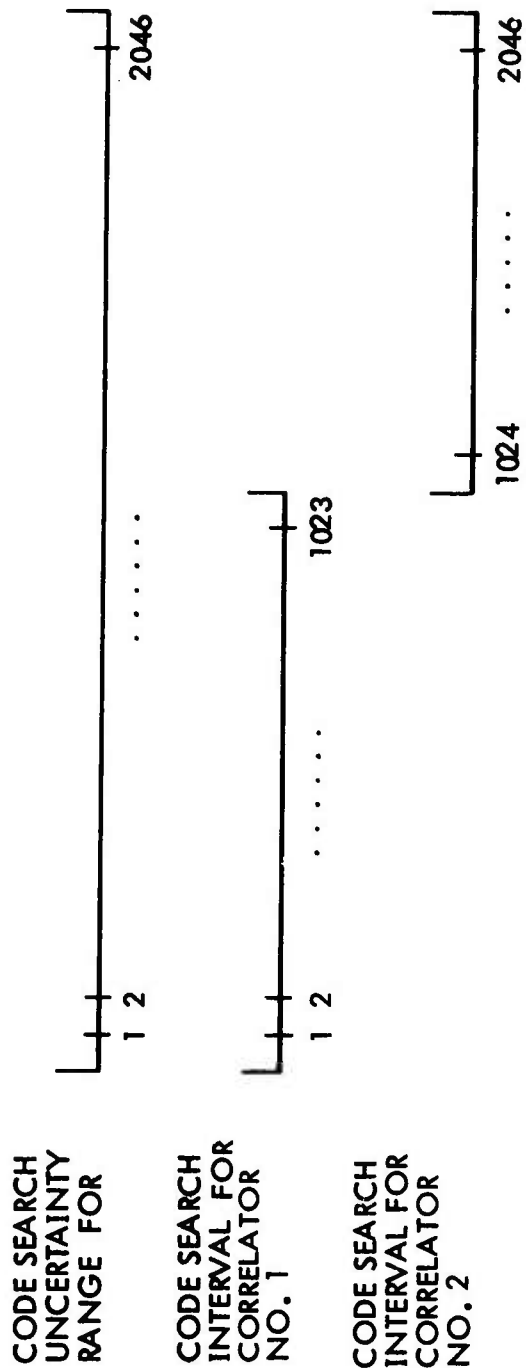
Figure 37. Multiple Correlation Code Search Region

148
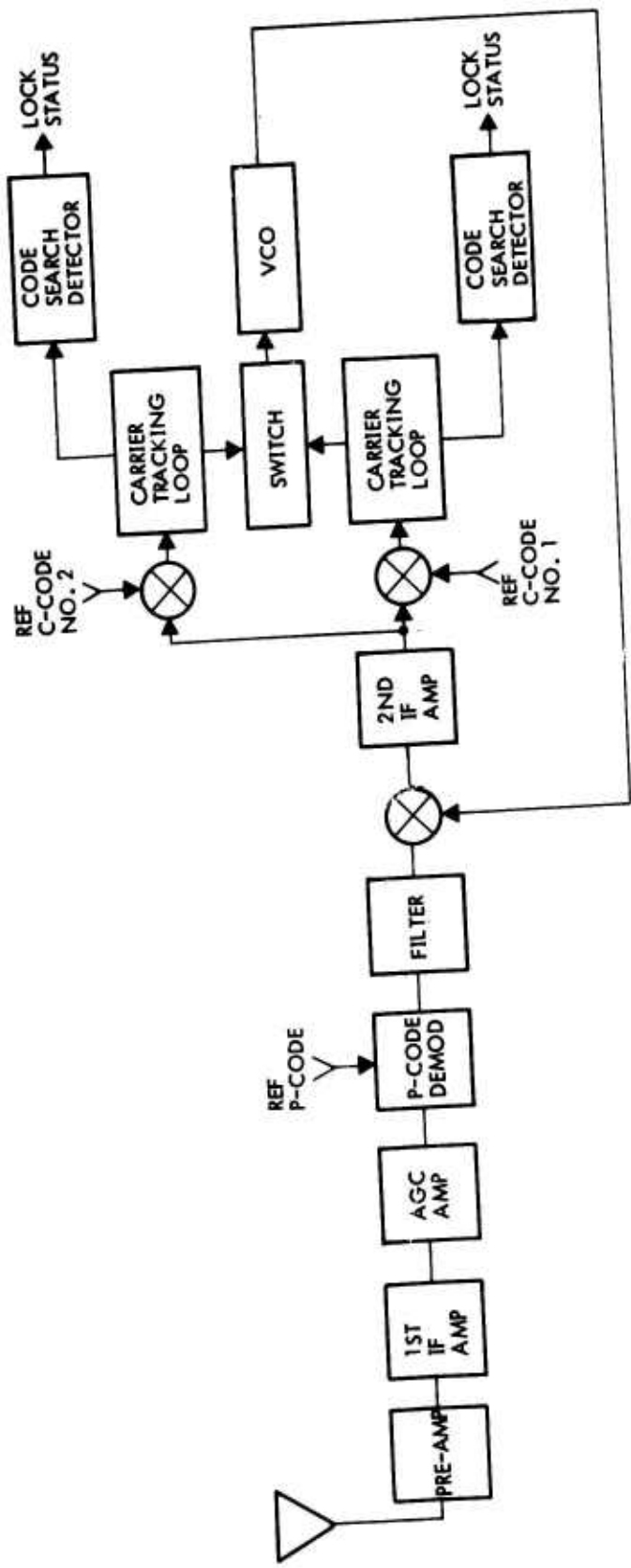
Figure 38. Multiple Correlation Code Search Receiver

149

5.5.3 Time-Shared Bit Sync and Detection Module

The baseline design of the four channel continuous receiver utilizes a Bit Sync and Detection Module in each channel. The reason for doing this is to permit simultaneous data extraction from four channels. This provides the fastest time to first fix. For some users, however, time to first fix may not need to be extremely rapid, but rather the continuous receiver is used because continuous tracking of four satellites is needed.

In the case where time to first fix may be permitted to be longer, some expense may be saved by time sharing a single Bit Sync and Detection module among the four channels. This may be accomplished by inserting a four position switch at the input to the Manchester code demodulator, and sequentially obtain a full frame of data from each satellite.

5.5.4 Switched Multiple Antennas

The baseline receiver is designed to receive satellite signals through a single antenna having hemispherical coverage. There are some types of users who could benefit from the use of two or more antennas. For instance, some highly maneuverable aircraft require navigation capability through a 360 degree roll. The baseline configuration would result in the loss of lock on all satellites through such a maneuver. In a highly jammed environment, reacquisition could be difficult. Such an aircraft would benefit from the use of a second antenna to provide auxiliary coverage during maneuvers which put the satellites out of view of the primary antenna.

A second type of user who would benefit from multiple antennas is the user who is heavily jammed. Considerable A/J margin could be obtained by the use of directional antennas, each pointed at a separate portion of the sky.

The purpose of this section is to show in principle how multiple antennas can be interfaced with the receiver. Only switched antennas are considered here, since combining signals from more than one antenna into a given channel will result in interferometry problems.

Five configurations are shown here as representative approaches. Configuration A, shown in Figure 39, utilizes a separate preamp for each antenna, and a solid state L-band switch to independently select an antenna for each channel. Configuration B, Figure 40, uses a solid state L-band switch to select the desired antenna. The input then goes to a common preamp, as in the baseline receiver.

151
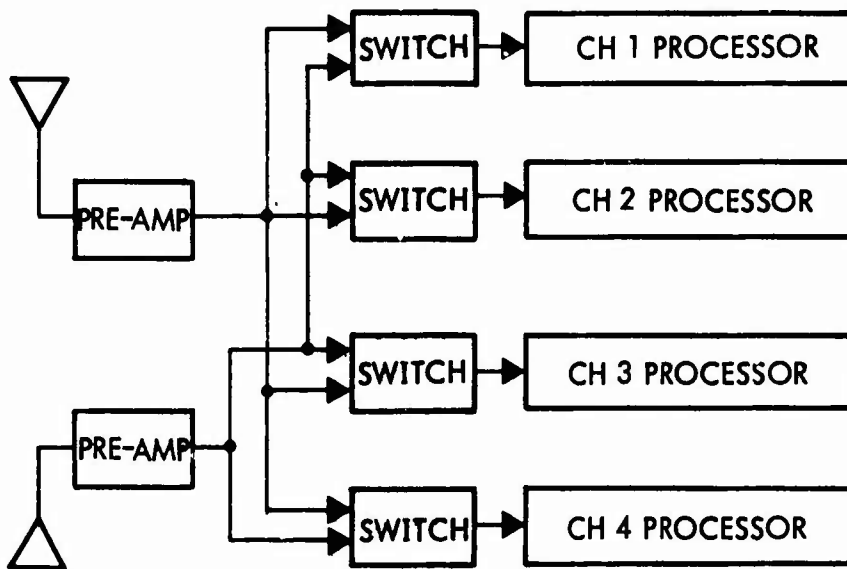
CONTINUOUS RECEIVER

2 PRE-AMP

4 SWITCHES

Figure 39. Antenna Configuration A
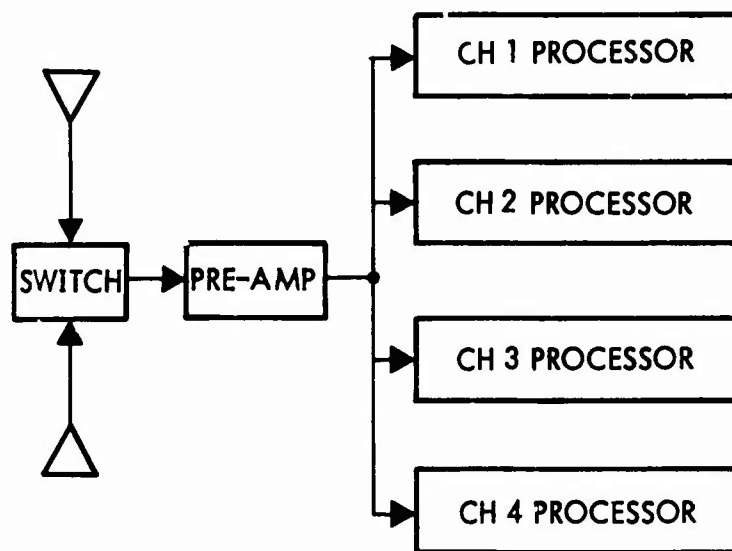
CONTINUOUS RECEIVER

1 PRE-AMP

1 SWITCH

Figure 40. Antenna Configuration B

153

Configuration C, Figure 41, is an intermediate step between A and B. Here, separate input preamps are used with each antenna, as in Configuration A, but only two switches are used. Channels 1 and 2 are committed to the same antenna, and channels 3 and 4 must use the same antenna.

For Sequential Receivers, two configurations are illustrated. Configuration D, Figure 42, uses a separate preamp after each antenna, and each of the two processing channels can select antennas independently for acquisition and tracking. Configuration E, Figure 43, is less expensive than D. It uses a single switch to select antennas, and inputs the signal into a common preamp, as is done in the Sequential Receiver which uses only one antenna.

The selection of which configuration to use would depend on tradeoffs between cost and operational requirements for each type of user who needs multiple antennas.

More than two antennas could also be accommodated if the need to do so requires it.
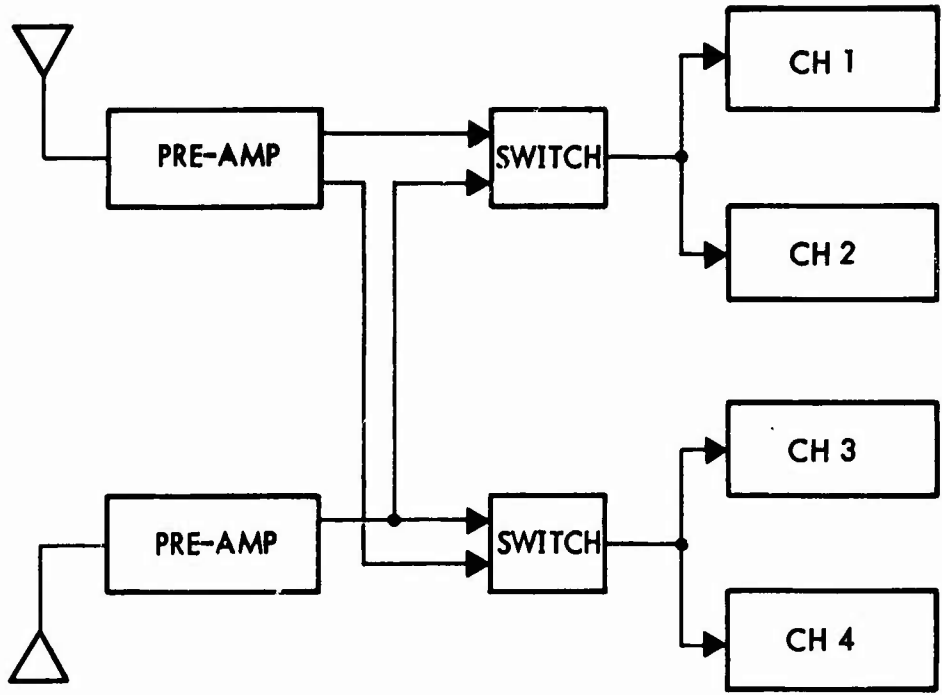
CONTINUOUS RECEIVER

2 PRE-AMPS
2 SWITCHES

Figure 41. Antenna Configuration C

155
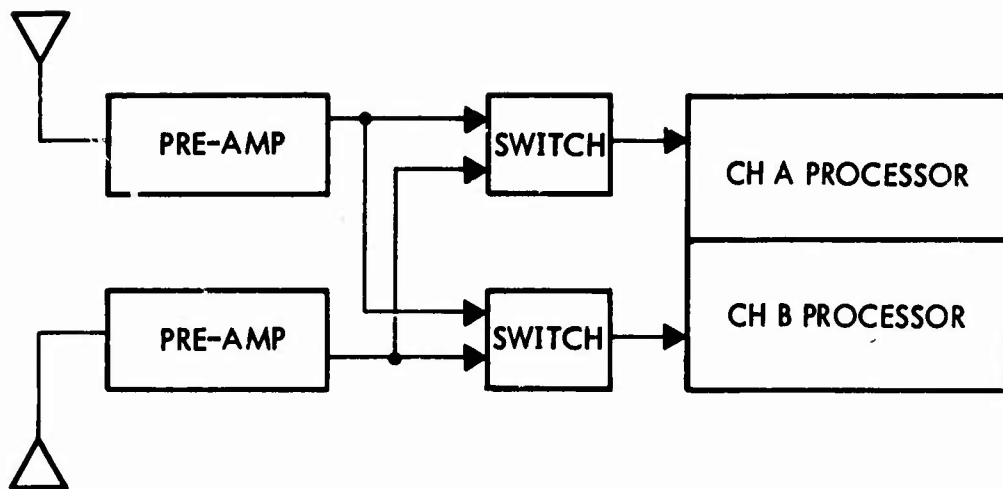
SEQUENTIAL RECEIVER

2 SWITCHES

2 PRE-AMPS

Figure 42. Sequential Receiver
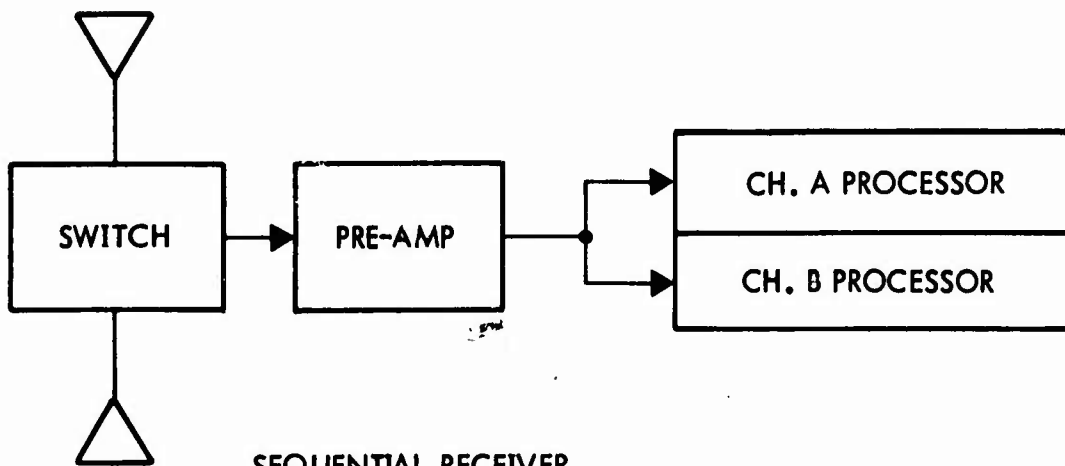
SEQUENTIAL RECEIVER

1 SWITCH

1 PRE-AMP

Figure 43. Antenna Configuration E

5.5.5 Rack Mounted 4-Channel GPS Receiver

Some types of users will utilize rack mounting of equipment. This section describes a typical rack mounting design for GPS users.

5.5.5.1 Mechanical Design

The mechanical design and packaging of the rack mounted GPS Receiver consists mainly of mounting the constituent modules of the 4-channel GPS Receiver, Mil-C-172 ATR (short) chassis, on a 19" military rack mounted drawer.

This design is therefore in accordance with the physical exterior configuration to comply with Mil-Std-189 (Racks, Electrical Equipment, 19-inch and associated Panels). The 1/8" thick front panel is 8-7 inches high x 19.0 long and is attached to an aluminum chassis .05" thick and is fabricated as noted in SK 100400 sheets 1 and 2 (in Appendix 14). The drawers can be mounted on tilt slides (now shown) capable of 90° tilt to provide accessibility to the bottom or wiring side of the chassis.

A bottom plate, or shelf is provided to receive the modules top-side, whereas the wiring harness is contained beneath the shelf. The shelf also provides the heat sink for the power supplies.

The modules that constitute the 4-channel receiver consist of modules for RF/IF processing functions, p.c. cards for digital functions that are contained in a card cage, dual power supply units, and a crystal oscillator module.

Optimum maintainability and accessibility conditions are obtained since all unit assemblies are plug-in modules and all wiring is contained beneath the shelf and accessible on rotating the drawer to a 90° tilt.

157

It is significant to note that the physical location of the RF/IF and digital card cage unit is identical to that of the ATR configuration thus providing the usage of the identical interconnect backplane of the 4-channel receiver thus optimizing tooling costs, programmable wire-wrap assembly, interchangeability, etc.

REFERENCES

1. W. L. Hjelmstad, "Second Draft of GS/US ICD", 3 October 1973, Philco-Ford, DNSDP-WLH-004.

2. W. E. Waters, "Ionospheric Predictive Models for User Equipment", 24 August 1973, Philco-Ford, DNSDP-WEW-009.

3. W. E. Waters, "Worldwide Ionospheric Prediction Model for Users", 27 November 1973, Philco-Ford, DNSDP-WEW-022.

4. R. H. Barker, 'Group Synchronizing of Binary Digital Systems", Symposium Paper Published in "Communication Theory", W. Jackson (ed.), Butterworth, London, 1953.

5. D. G. Middlebrook, 'Ionospheric Correction and Error Budget Value", 24 October 1973, Philco-Ford, DNSDP-DGM-005.

6. W. E. Waters, "DNSDP Users — Ionospheric Range Error Corrections", Philco-Ford, DNSDP-P-001-WEW, 27 July 1973.

7. W. E. Waters, "Worldwide Ionospheric Prediction Model for Users", Philco-Ford, DNSDP-WEW-022, 27 November 1973.

8. R. E. Orr, "Philco Ephemeris Data Memo", TRW, DNSDP-REO-074, 7 September 1973.

APPENDIX 1

MISCELLANEOUS ANALYSES CONCERNING THE USER RECEIVER LINK BUDGET AND THE ACQUISITION/TIME TO FIRST FIX PROCESSES

This appendix contains the detailed analyses which constituted a response to specific questions raised by SAMSO during the Definition Study. First, the questions are shown, in Attachment 1, followed by the answers in Attachment 2.

These analyses are based on the signal structure valid at 11 January 1974. In particular, it had the following characteristics:

P-Code rate	10. 23 MHz
C-Code rate	1. 023 MHz
C-Code length	1023 chips
Data rate	40 bps
Frame length	1200 bits
Handover words	5 each frame

Attachment 1

QUESTIONS

The contractor is requested to answer the following questions concerning the user equipment designs and specifications he will propose.

<u>User Receiver Link Budget</u>

1) Compute the required received signal power necessary for C/A code acquisition (including code and frequency search) within 50 seconds, and demodulation of 41 bps data at an error rate of 10^{-5}. Perform the computation for both an ideal 0 db gain antenna, and the antenna which you intend to propose. Carry out these calculations assuming no jamming.

2) Carry out the calculations in Question 1 assuming a CW jammer at -166 dbw,

3) Prepare a link budget which details a breakout of the individual losses in your user system including as a minimum:

   a) Antenna off-beam loss (your estimate at 5° elevation angles)

   b) Polarization loss (your estimate)*

   c) Receiver-antenna coupling/preselector filter losses

   d) Demodulator performance loss

   e) Correlation loss

   f) Multiple access loss

   g) Others as necessary

   Include a link margin of 6 dB. Prepare a block diagram of your user system and note the loss contributions on it at each point on the diagram.

---

*Assume that all signals will be transmitted right-hand circularly polarized with an axial ratio of 1.5 or better.

4) Prepare a detailed list of contributors to the effective receiver noise density/temperature of your user system including as a minimum:

a) Sky noise

b) Coupling and filter losses

c) Amplifier noise(s)

d) Others as necessary

Prepare a block diagram of your user system indicating the losses and noise temperature of each contributor to the effective receiver noise temperature.

5) Provide the basis for each of the estimates in Questions 1 through 4 clearly showing assumptions regarding equipment configurations and parameters which effect the calculations (parallel versus sequential frequency search, loop bandwidths, etc.).

Acquisition/Time-to-First-Fix

The contractor is requested to perform calculations for time-to-first fix for the following cases:

a) L_1 C-signal navigation

b) L_1 P-signal navigation

c) L_1 and L_2 P-signal navigation

The following assumptions may be made:

1) User knows system time to within ± 1 sec

2) User knows his position to within ± 60 n. mi. in x and y coordinates.

3) The signal structure is as specified in GPS baseline Signal Structure, first edition, November 30, 1973, JPO, SAMSO.

The contractor should specify all additional assumptions for initial signal conditions, specifically including quantitative data for signal frequency uncertainty due to:

a) satellite motion

b) user motion

c) satellite and user oscillator inaccuracy.

163

Rationale should be presented for the assumed numbers. The calculations should be performed for the continuous receiver operating without the aid of inertial devices.

6) The calculations should, as a minimum, show (as applicable) a breakout of the times to accomplish:

a) C/A code acquisition (including code and frequency search)

b) Carrier recovery for data demodulation

c) Bit synchronization

d) Barker sequence synchronization

e) C-data frame synchronization

f) P-code acquisition word recovery

g) C- to P-signal handover

h) P-signal data collection

i) L_2 signal acquisition (if applicable)

j) Computation of first fix.

The contractor should clearly show assumptions regarding equipment configuration and parameters which affect the calculations (e.g., coherent versus noncoherent techniques, parallel versus sequential frequency search, all loop bandwidths, etc.). The assumed user parameters and techniques should be consistent with the contractor's preferred approach.

The contractors should clearly show assumptions regarding data format and operating procedures that affect the calculations. These assumptions should reflect the contractor's preferred approach.

7) The contractor is requested to perform calculations for the required C/N_0 in the IF to assure expected time-to-first fix, as described in Question 6 for the following:

a) ≤3 minutes for the P-signal user (C-code should be acquired with probability 0.9 in ≤50 sec).

b) ≤5 minutes for the P-signal user (C-code should
be acquired with probability 0.9 in ≤50 sec).

8) The contractor is requested to perform calculations
for the expected time-to-first fix as defined on the
previous page given an IF C/N_0 = 34 dB-Hz (37 dB-Hz
with a 3 dB margin).

ANSWER TO QUESTION 1

The acquisition procedure for the C/A-code signal consists of the following steps:

1) **C/A-Code Selection** - The C/A-code generator in the receiver is configured to generate the Gold code corresponding to the particular satellite signal chosen to be acquired.

2) **Estimate of Frequency of Received Signal** - The computer estimates the carrier frequency of the satellite signal to be acquired.

3) **Prepositioning of the Receiver VCO Frequency** - From the frequency estimate in Step 2 and the user oscillator frequency estimate, the receiver VCO frequency is positioned so that the incoming signal will fall within the acquisition bandwidth of the receiver when the C/A-code phase is found. Thus, a frequency search for the signal is not necessary.

4) **Search All Possible Code Chip Positions** - The Gold code generator phase is stepped in one-half chip steps looking for the presence of a carrier signal in the acquisition bandwidth.

5) **Stop Search, and Allow Tracking Loops to Lock to Code and Carrier Phase When Signal is Detected in Acquisition Bandwidth** - This completes acquisition of the C/A-code.

The acquisition time is the total time required to carry out the above acquisition steps. Step 4 is by far the largest contributor to the acquisition time as the total time for the other steps is less than one sec. The following paragraphs discuss the above steps in more detail, and compute the code search time in Step 4 as a function of the carrier-to-noise density ratio C/N_o.

The first step in initial operations is constellation selection by the user's computer. For this, he uses the classical orbital elements of each satellite in the system (stored in his non-volatile memory), and he inputs his current horizontal position and the current system time. The accuracies of these inputs are given in SAMSO's questionnaire as

± 1 sec and ± 60 n. m., although ± 1 min is probably adequate. The user computer will then select the best constellation and consequently satellites to be acquired. "Best" will be determined by certain logical criteria which will probably vary from user class to user class.

The second step is the estimation by the user's computer of the frequencies of the received signals from each of the selected satellites. These estimates will be based on:

a) The nominal L_1 transmitter frequency, provided that the GPS is designed such that no satellite transmitter frequency is allowed to vary from this system nominal by more than 16 Hz ($1:10^8$). Alternatively, the estimate will be based on a value for the transmitter frequency of the particular satellite, which is determined by the Control Segment and included with the classical orbital elements for that satellite. In this latter case, the GPS must be designed such that the transmitter frequency must not drift away from this value by more than 16 Hz during the period (several weeks?) between updates of the orbital elements. The selection of which technique should be used will be based on a Satellite/Control Segment tradeoff, since it has insignificant impact on the User Segment.

b) The doppler shift induced by the motion of the satellite relative to the user's location on the rotating Earth, (that is, the total doppler shift if the user were stationary on Earth's surface). This is computed as a by-product of the calculations for constellation selection, with a maximum possible error of 40 Hz.

c) The doppler shift induced by the motion of the user. For User Classes A and B, the course and speed will be automatically, and hence very frequently, inputted to the computer from other (non-GPS) navigation sensors. The accuracy of these data will be such that the component of user velocity in the direction of the satellite will, throughout the start-up process, be known to within 30 m/sec, corresponding to a doppler shift at L_1 of 158 Hz. For User Class C, the operator will have to input course and speed at the beginning of the start-up procedure, and then fly straight and level until acquisition has been achieved. Course will

be inputted in degrees east of north to a resolution of
1 degree, and speed in Km/hr, relative to the ground,
to a resolution of 1 Km/hr. The flying constraint will
ensure that the actual course and speed will differ
from the inputted values by no more than 5 degrees
and 30 Km/hr. Additionally, we are assuming that,
for the Class C user, the maximum velocity con-
straints at start-up will be 300 m/sec horizontally
and 6 m/sec vertically. With these constraints and
inputs, the user-induced doppler shift at L_1 will, for
the Class C user, be estimable to within 141 Hz, for
any satellite above the 5 degree horizon.

For User Classes D, E, and F, course and speed
will not be inputted, and the received signal frequency
estimate will assume that the user is stationary. How-
ever, the constraints on maximum velocity for these
classes will be 30 m/sec horizontal and 6 m/sec ver-
tical, so the maximum user-induced doppler shift at
L_1 cannot exceed 160 Hz.

From the above, it can be seen that the received signal frequencies
will be estimated with a maximum possible error of 216 Hz or less (all
user classes).

The third step is the calculation, by the user's computer, of the
frequency to which the second IF VCO should be prepositioned. This
is based on the previously described received signal frequency estimate
and the nominal value of the user oscillator frequency. The user oscil-
lator must be specified such that, after warm-up, its frequency deviation
from nominal should not exceed $1:10^7$. Thus, the maximum error in
VCO prepositioning will not exceed (216 + 158), or 374 Hz.

We are configuring our receivers to have an IF acquisition band-
width of ±500 Hz, so that the signal will always lie within the passband,
even under the simultaneous occurrence of all adverse errors. From
the statistical point of view, we can assume that each error source is
independently and uniformly distributed between its maximum values,
which leads to a standard deviation of frequency error of 132 Hz, as
shown in Table 1.

168

Table 1. Acquisition Frequency Prepositioning Errors

Error Source	Maximum Frequency Error	S. D. of Frequency Error
Knowledge of transmitter frequency	$\pm$ 16 Hz	9.2 Hz
Satellite-induced doppler shift	$\pm$ 40 Hz	23.1 Hz
User-induced doppler shift	$\pm$160 Hz	92.4 Hz
User oscillator drift	$\pm$158 Hz	91.2 Hz
All	$\pm$374 Hz	132.2 Hz

In the fourth step, the receiver is prepositioned in accordance with the above described estimates. Positioning the VCO is accomplished within msec. An acquisition search is then carried out for the C/A-code. The C/A-code generator is clocked from the VCO output (after suitable translation and multiplication) A noncoherent detection processor is used, detecting the presence of reconstructed carrier, after correlation of the received signal with the replica C/A-code (with the code tracking modulation off tau-dither). The acquisition detector status is checked every t_d sec (t_d being known as the dwell time per search cell). If the check shows that the signal is not present, the Gold code generator is stepped one-half chip; if signal presence is indicated, the tau-dither modulation is activated, and the code and carrier tracking loops are enabled. At a period kt_d later, the lock status of the (coherent) carrier tracking loop is sampled. If this shows that the loop is not in lock, it is assumed that the original acquisition indication was false, and the noncoherent search is resumed.

169

A considerable amount of analysis and simulation of the acquisition process has been performed. The values of t_d, k, and also of the post-detector bandwidth, must be selected to minimize the acquisition time at signal threshold. The numerical results are shown in Table 2, and are based on the analysis in Reference 1. Where necessary, the results of that analysis have been modified to take into account the change in Gold code length from 511 to 1023.

In Table 2, we show the optimized design parameters (post-detection bandwidth, B_{pd}, dwell time per search cell, t_d, and false alarm penalty factor k) for various values of the threshold design point. The design point is shown in the second column of Table 2 as the required carrier-to-noise density ratio of the L_1-C signal at the acquisition detector input. As may be seen, it is 3.8 dB lower than the (C/N_o) ratio at the receiver input, to allow for:

a) Out of Sync Demodulation Loss - The replica and received codes can differ in phase, during dwell on the correct search cell, by as much as 1/4 chip. This would cause, at the most, a 2.5 dB correlation loss.

b) Frequency Offset of the Predetection Bandpass Filter - The 3 dB bandwidth of this filter is 500 Hz (one sided), and the standard deviation of the frequency offset will be (as was earlier shown) 132 Hz. The Barker code bit rate is 200 Hz, and hence there will be some power loss in the sidebands. This loss has been estimated to be 0.3 dB.

c) Multiple Access Loss - The effect of multiple access interference on the C/A-code acquisition has been analyzed in Reference 2. The results show that, for a 1023 bit code and an interference level which is not exceeded 95% of the time, the degradation in performance is about 1.0 dB.

The values of B_{pd}, t_d, and k are those of the optimum set, with the predetection bandwidth set at 500 Hz. F_d and P_{fa} are the resulting performance factors at threshold (the probabilities of true detection

170

Table 2. C-Code Acquisition Parameters

(C/N_o) Received	(C/N_o) at Det.	B_{pd}	t_d	k	P_d	P_{fa}	$\bar{T}$	T_{SD}	$T(90)$
dBHz	dBHz	Hz	msec				sec	sec	sec
30.8	27	12.5	24	5	.676	.097	71.4	53.8	140.3
31.8	28	10.7	28	4	.780	.051	54.0	40.7	106.1
32.8	29	13.0	23	4	.820	.055	41.3	31.1	81.2
33.8	30	14.3	20	4	.865	.056	32.9	24.8	64.7
34.8	31	-	-	-	-	-	26.7	20.1	52.5
35.8	32	18.8	17	3	.913	.021	22.0	16.6	43.2
36.8	33	-	-	-	-	-	18.3	13.8	36.0
37.8	34	25.0	12	3	.908	.020	15.7	11.8	30.9

- These values were not computed; however, the acquisition times were derived by interpolating between the adjacent values.

and false detection, respectively). $\overline{T}$, T_{SD}, and T(90) are further performance factors at threshold, namely the mean and standard deviations of the acquisition time, and the acquisition time not exceeded 90% of the time. The optimum design parameters were not computed for (C/N_o) values at the detector of 31 and 33 dBHz, but the acquisition times were interpolated for completeness in the table. The values of $\overline{T}$ were computed with the analytic expressions derived in Reference 3. Based on the Monte Carlo simulations reported in Reference 3, the standard deviation was found from the relationship

$$T_{SD} = .754 \, \overline{T}$$

Also, the 90% probability value is obtained from

$$T(90) = \overline{T} + 1.28 \, T_{SD}$$

From Table 2, the required C/N_o at the receiver input can be found which results in a 90% probability of acquiring the C/A-code within 50 sec. By interpolation from the table, the required value for C/N_o is <u>35.1 dBHz.</u> This value is based on a single acquisition circuit searching the entire 1023 bit code in one-half chip increments.

Acquisition time is very nearly directly proportional to the number of possible search cells or half-chip positions. Therefore, for the same signal levels, bandwidths, dwell times, etc., a receiver using two acquisition circuits working in parallel, each searching one-half of the code, will acquire the code in half the time needed by a single acquisition circuit receiver. Equivalently, the signal levels, bandwidths, etc., which correspond to a single circuit receiver acquiring the code in 100 sec are the same as those which correspond to a 2-circuit receiver acquiring in 50 sec. Thus, again by interpolating in Table 2, we see that the required C/N_o at the receiver input, for

172

90% probability of acquisition within 50 sec for a 2-circuit receiver, is reduced to 32. 0 dBHz.

Based on a worst case receiver noise density of -199. 6 dBw/Hz (see answer to Question 4 for derivation of this value), the required signal levels at the receiver input for 50 sec acquisition time are:

-164. 5 dBw (single acquisition circuit)

-167. 6 dBw (two parallel acquisition circuits)

The required C/N_o and signal level at the receiver input for data detection is derived in Table 3. The results are for C/A-data detection, but are the same for P-data detection except that the multiple access loss will be slightly lower with the P-code. Thus, the required signal level will be slightly less for the P-data than the C/A-data.

Since the question calls for calculations of the received signal power, the gain of the user antenna does not have to be specified. Thus, these results are valid for both the ideal 0 dB gain antenna, as well as any practical antenna.

Table 3. Signal Level Required for C/A-Data Detection

	Item	Value
	Data rate (40 bps)	16. 0 dB
(1)	E_b/N_o	9. 5 dB
(2)	Demod. loss	1. 5 dB
(3)	Multiple access loss	1. 0 dB
	C/N_o	28. 0 dBHz
(4)	Required Signal Level	-171. 6 dBw

Footnotes

(1)   Required energy per bit for 10^{-5} B. E. R. assuming coherent PSK demodulation.

(2)   Includes losses due to carrier and bit sync phase jitter plus filter detector mismatch.

(3)   The loss due to multiple access interference for 1023 bit codes with an interference level which is not exceeded 95% of the time. See Reference 2.

(4)   Assume N_o = 199. 6 dBw/Hz worst case.

ANSWER TO QUESTION 2

With a CW jammer (or unintentional interfer) power level of -166 dBw, the resulting jammer-to-signal ratios at the receiver input are as follows:

Signal Function	Required Signal Level (From Question 1)	$(J/S)_{\text{receiver input}}$
C/A-Code Acquisition - one circuit	-164. 5 dBw	-1. 5 dB
C/A-Code Acquisition - two circuits	-167. 6 dBw	+1. 6 dB
C/A-Data Detection	-171. 6 dBw	+5. 6 dB

For the 1023 bit code, the resulting J/S at the correlator output is 30 dB lower because of the processing gain of the C/A-code. Thus, the S/J (signal-to-jammer interference ratio) at the correlator output and the resulting degradation in performance is as follows using the results in Reference 2.

Signal Function	S/J (dB)	Degradation (dB)
C/A Acquisition - one circuit	31. 5 dB	~0
C/A Acquisition - two circuits	28. 4 dB	~0
C/A - Data Detection	24. 4 dB	~0. 1

Thus, the effect of the -166 dBw interference level is negligible. Only if the J/S ratio gets greater than 13 dB does an interferer or jammer begin to degrade performance.

For example, with a J/S at the receiver input of 15 dB, the following table shows the expected degradation (again the numbers are derived from Reference 2):

Signal Function	Jammer Level (dBw)	Degradation (dB)
C/A Acquisition - one circuit	-149.5	~0.2
C/A Acquisition - two circuits	-152.6	~0.1
C/A - Data Detection	-156.6	1.0

As may be seen, at this J/S ratio, the data detection performance degradation becomes significant.

ANSWER TO QUESTION 3

The L_1 RF link budget (taken from Reference 4) is given in Table 4. The results of the table show the received signal at the receiver input equals P-174.2 dBw (nominal) with a worst case additional loss of 8.7 dB where P is the satellite transmitter power in dBw. From the answer to Question 1, the most stringent requirement on signal level is C/A-code acquisition[*]. The satellite power, in the L_1-C signal, necessary for this requirement is given in Table 5.

Table 5. Satellite Power for C/A-Code Acquisition Within 50 sec

	Required Signal Level	Satellite Power[1]
One Code - acquisition circuit	-164.5 dBw	37 watts
Two Code - acquisition circuits	-167.6 dBw	18 watts

(1) Includes an added 6 dB margin to take care of worst case tolerance losses.

---

[*] But note our response to Question 7, where we point out that minimizing TTFF is a better criterion than minimizing C-code acquisition time.

Table 4. RF Link Budget at L_1

	User Elevation Angle = 10°	5°
Item	Nominal	Worst Case Tolerance
1. Satellite RF Transmit Power (dBw)	P	-1.0
2. Satellite Line Losses (dB)	-0.5	-0.4
3. Satellite Antenna Gain Toward User (dB)	12.4	-0.8
4. Satellite EIRP (dBw)	P+11.9	-2.2
5. Path Loss (f = 1575 MHz) (dB)	-184.3	-0.2
6. Propagation Loss (dB)	-0.5	-2.5
7. Received Signal Power (dBw)	P-172.9	-4.9
8. User Ant. Off-Beam Loss (dB)	0	-3.0
9. Polarization Loss (dB)	0	0
10. Rec.-Ant. Coupling/Preselector Filter Loss (dB)	-1.0	-0.5
11. Receiver Noise Power Density (dBw/Hz)	200.2	+0.6
12. Signal Correlation Loss (dB)	-0.3	-0.3
13. Signal Power at Receiver Input (dBw)	P-174.2	-8.7
14. Carrier-to-Noise Density (dB-Hz)	P+26.0	-9.3

178

Table 4. RF Link Budget at L_1 (Continued)

Comments

Line

1. Worst case over in-orbit temperature at end-of-life.

2. Design uncertainty.

3. Peak gain   = 15.4 dB

    Half-power beamwidth = 27.6 degrees

    Aperture efficiency   = 55%

    Antenna pointing error $\approx$ 0 degree nominal, 1 degree worst case.

4. Lines 1 + 2 + 3.

5. $L = 37.8 + 20 \log F \text{ MHz} + 20 \log R_{NM}$

    $F = 1575 \text{ MHz}$

    $R = 13340 \text{ NM } (10^{\circ}) \quad 13648 \text{ NM } (5^{\circ})$

6. Losses due to scintillation. Nominal value unknown; 0.5 dB assumed. 3 dB worst case from SAMSO/Aerospace.

7. Lines 4 + 5 + 6.
    Received power at output of 0 dB gain circular polarized antenna.

8. Antenna gain is measured relative to circular polarized wave. Off-angle pointing loss is caused by pattern directivity.

9. Polarization loss is included in 8 as antenna gain measured using a CP source.

10. Antenna coupling and line losses between feed and receiver pre-amp. Preselector filter insertion loss is included in receiver noise figure.

11. See answer to Question 4.

12. Due to filtering of signal in satellite to restrict RF bandwidth.

13. Lines 7 + 8 + 9 + 10 + 12.

14. Line 13 - Line 11.

ANSWER TO QUESTION 4

The effective receiver system noise temperature/noise power density referred to the receiver preamplifier input is derived as follows:

$$T_S = LT_A + (1 - L)T_L + (F - 1)T_o$$

where T_S = receiving system noise temperature

T_A = 130°K - a conservative estimate of antenna temperature of hemispheric beam looking upward with some radiation from earth coming in via sidelobes (more data needed on this)

T_L = 290°K - temperature of antenna coupling circuit and coax line connecting antenna feed and receiver input

L = -1.0 dB (0.794) nominal

-1.5 dB (0.708) worst case

Based on 25 ft of RG-type coax cable between antenna feed and receiver input or 100 ft of rigid copper coax. This value is highly user installation dependent. If cable runs become too long, receiver preamp can be located at antenna feed to minimize cable losses.

F = 4.5 dB (2.82) nominal

5.0 dB (3.16) worst case

Estimated overall receiver noise figure based on available L-band transistor devices and including preselector filter and mismatch losses.

T_o = 290°K - reference temperature.

Using the above values, the receiver system noise temperature is

$$T_S = 690.7°K \text{ nominal}$$

$$803.1°K \text{ worst case}$$

180

The corresponding receiver noise power density equals

$$N_o = K + 10 \log T_S \text{ dBw/Hz}$$

where $\quad K = -228.6 \text{ dBw/Hz-}^{\circ}\text{K Boltzmans Constant}$

Therefore,

$$N_o = -200.2 \text{ dBw/Hz nominal}$$
$$-199.6 \text{ dBw/Hz worst case}$$

Figure 1 shows the noise temperature and gain/loss contributors at various points in the user receiving system.
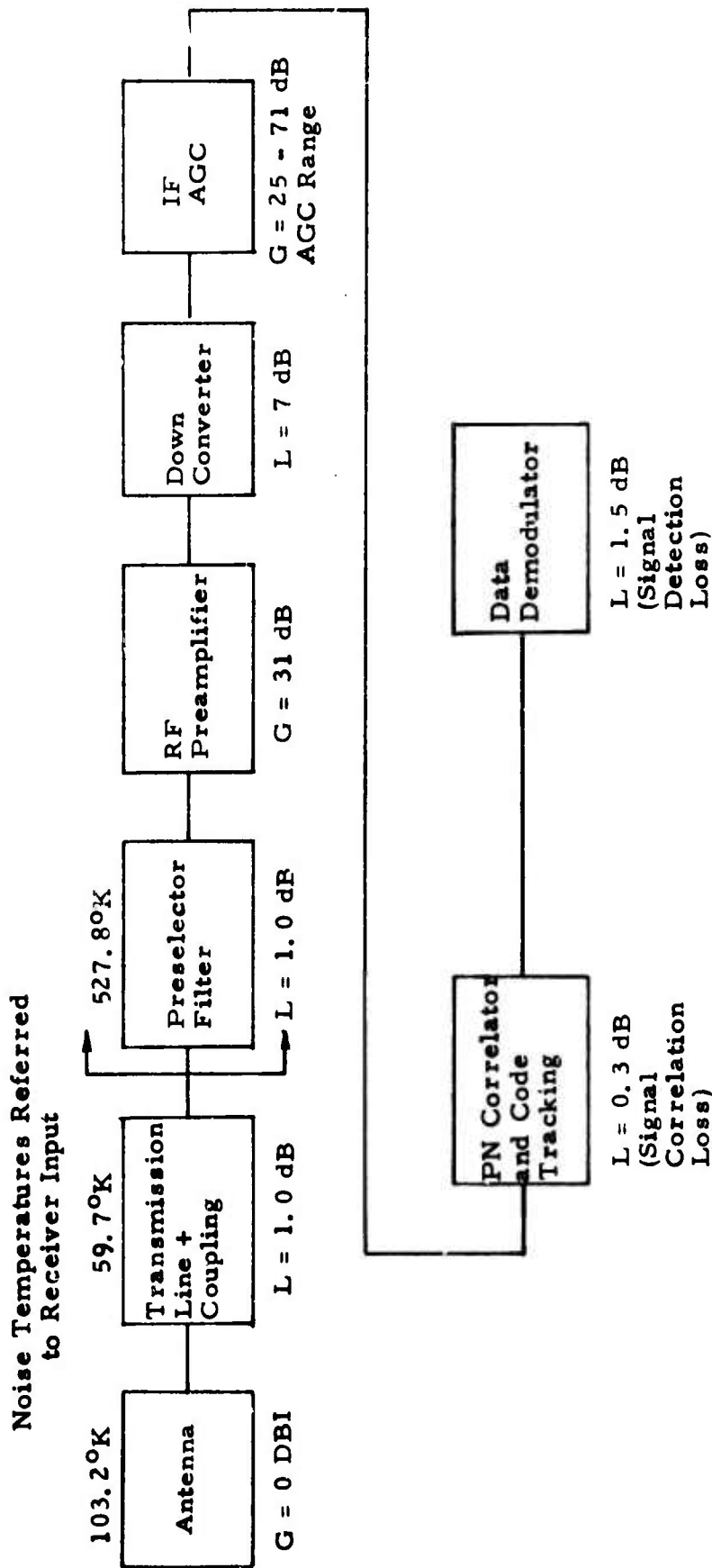
Figure 1. User Receiving Block Diagram Nominal Noise Temperature and Gain/Loss Contributions

ANSWER TO QUESTION 5

The bases for the estimates used in the preceding four answers are fully described in those answers.

ANSWER TO QUESTION 6

The time-to-first fix (TTFF) includes, in addition to the C/A-code acquisition time, discussed in the answer to Question 1, the steps discussed in the following paragraphs. The discussion assumes four channel receivers in all cases. Sequential receivers are discussed at the end of this memorandum.

When the C/A-code search is successful, the carrier and code loops are enabled and track the signal, and the Barker code and bit synchronizer lock-up. The time for loop pull-in and settling, and synchronizer lock-up, is less than 1 sec, and is an insignificant contributor to the TTFF.

The following applies only to L_1-C navigation. When the tracking loops, bit synchronizers, etc., have locked up, measurements of pseudorange and pseudorange rate are made and sent to the computer. However, they are not used there until the satellite ephemeris and clock data are received too. For this, the receiver performs a real time search for main frame sync. Since the frame duration is 30 sec, the wait time for frame sync is uniformly distributed between 0 and 30 sec. It has a mean value of 15 sec and a standard deviation of 8.7 sec.

Pending further clarification from SAMSO, on the data format, we assume that all the normal navigation data will be contained within the first 3/5 of the frame, that is, within the first 720 bits. Thus, 18 sec after the beginning of the main frame sync is received, the first fix can be made. The computation takes an insignificant amount of time.

To recapitulate, the significantly time-consuming steps in the start-up process are as shown in Table 6.

Table 6.   Start-Up for C-Navigation

Step	Mean Time (sec)	S. D. of Time (sec)
C/A-code search	See Table 2	
Wait for frame sync	15. 0	8. 7
Collect navigation data	18. 0	0

Let the mean and standard deviation of the C/A-code search be m and σ.   Then, by invoking the Central Limit Theorem, we can say that the time for any one channel to complete all its initial operations is normally distributed with a mean value of (m + 15 + 18), that is (m + 33), and with a standard deviation of $(\sigma^2 + 8.7^2)^{\frac{1}{2}}$.   These same statistics apply to each of the 4 channels, but the variates are independent.

The time to first fix is the time for the last channel to complete its initial operations.   Hence, the mean TTFF is the mean for any one channel, or (m + 33).   Of greater interest than the mean, however, is the TTFF not exceeded on some stated   percentage of start-ups. We here adopt 90% as this confidence level, and call the time, T_{90}. Then,

$$\text{Prob (all channels complete by } T_{90}) = 0.9$$

$$\text{or} \qquad [\text{Prob (any one channel complete by } T_{90})]^4 = 0.9$$

$$\text{i. e.,} \qquad \text{Prob (any one channel complete by } T_{90}) = 0.974$$

185

From any tabulation of the normal error function, it can be seen that

$$T_{90} = \text{mean} + 1.94 \text{ (standard deviation)}$$

or
$$T_{90} = (m + 33) + 1.94(\sigma^2 + 75)^{\frac{1}{2}}$$

Based on the values in Tables 2 and 6, and using the above expression, we can find the mean and 90% confidence values of the TTFF, at threshold, as a function of threshold, where threshold is given in terms of the received effective carrier-to-noise density ratio. These values are shown in Table 7.

Table 7. TTFF at Threshold, Four Channel Receiver, C-Navigation

Threshold $(C/N_o)_e$ -Received dBHz	TTFF (sec)	
	Mean	90% Confidence (T_{90})
30.8	104.4	210.1
31.8	87.0	167.7
32.8	74.3	136.9
33.8	65.9	116.9
34.8	59.7	102.2
35.8	55.0	91.3
36.8	51.3	82.9
37.8	48.7	77.1

The following applies only to four channel L_1-P navigation.

There are, conceptually, three possible techniques which follow acquisition of the C-code, as follows:

a)   Wait for C-data main frame sync, collect the navigation data from C, then handover to P.

b)   Wait for C-data main frame sync, handover to P, wait for P-data main frame sync, then collect the navigation data from P.

c)   Wait for next C-data sub-frame sync, handover to P, wait for P-data main frame sync, then collect the navigation data from P.

The requirements on the signal structure for each of these techniques are:

a)   One HOW per frame, located immediately after the navigation data. Also C- and P-data may be transmitted in phase.

b)   One HOW per frame, located immediately after the main frame sync. Also P-data delayed slightly behind C-data.

c)   Multiple HOWs in each frame, each preceded by a sync pattern. Also, P-data delayed slightly behind C-data.

It can be shown that the TTFF will be the same in each of these techniques. Accordingly, the best technique should be selected on other grounds. Clearly, technique (c), with multiple HOWs is least desirable, requiring additional complexity in both spacecraft and user equipment; indeed, the existence of multiple handover words can, itself, force an extension to the frame length, which will increase the TTFF. Technique (b) is slightly more complex, in the spacecraft, than technique (c), because it requires a phase delay between the two data signals.

187

To demonstrate the equivalence of the TTFFs, consider the following:

Let   frame duration   = T

duration from beginning of frame
to end of navigation data   = T_n

duration from beginning of sync
pattern preceding a HOW to
accomplishment of the handover   = T_h

Then, for technique (a), we have

- Wait for C-data main frame sync: uniformly distributed between zero and T

$$\text{mean} = \frac{T}{2}$$

$$\text{S. D.} = \frac{T}{\sqrt{12}}$$

- Collect navigation data

$$\text{mean} = T_n$$

$$\text{S. D.} = 0$$

- Handover to P: (HOW follows immediately behind navigation data)

$$\text{mean} = T_h$$

$$\text{S. D.} = 0$$

● And time for all above operations

$$\text{mean} = \frac{T}{2} + T_n + T_h$$

$$\text{S. D.} = T/\sqrt{12}$$

For technique (b), we have

● Wait for C-data main frame sync

$$\text{mean} = T/2$$

$$\text{S. D.} = T/\sqrt{12}$$

● Handover to P: (HOW follows immediately behind main frame sync)

$$\text{mean} = T_h$$

$$\text{S. D.} = 0$$

● Wait for P-data main frame sync: (P-data delay by T_h)

$$\text{mean} = 0$$

$$\text{S. D.} = 0$$

● Collect navigation data from P

$$\text{mean} = T_n$$

$$\text{S. D.} = 0$$

● And time for all above operations

$$\text{mean} = T/2 + T_n + T_h$$

$$\text{S. D.} = T/\sqrt{12}$$

For technique (c), we have

● Wait for C-data subframe sync: Uniformly distributed between zero and T/N

$$\text{mean} = T/(2N)$$

$$\text{S. D.} = T/(N\sqrt{12})$$

● Handover to P

$$\text{mean} = T_h$$

$$\text{S. D.} = 0$$

● Wait for P-data main frame sync: (P-data are delayed by T_h behind C-data)

If handover was made on the i-th HOW, then this wait is

$$T - (T/N)(i - 1) \quad \text{for } i > 1$$

$$\text{or} \qquad 0 \qquad\qquad \text{for } i = 1$$

Since it is equally likely that the handover is made on any HOW, the mean and S. D. of the wait for P-data main frame sync will be

190

$$\text{mean} \quad = \frac{1}{N}\sum_{i=2}^{N}\left[T - \frac{T}{N}(i-1)\right]$$

$$= \frac{T(N-1)}{2N}$$

$$(\text{S. D.})^2 = \frac{1}{N}\left\{\sum_{i=2}^{N}\left[T - \frac{T}{N}(i-1) - \frac{T(N-1)}{2N}\right]^2 + \left[\frac{T(N-1)}{2N}\right]^2\right\}$$

$$\text{or} \quad \text{S. D.} \quad = \frac{T}{N}\sqrt{\frac{N^2-1}{12}}$$

- Collect navigation data from P

$$\text{mean} \quad = T_n$$

$$\text{S. D.} \quad = 0$$

  - And time for all above operations

$$\text{mean} \quad = \frac{T}{2N} + T_h + \frac{T(N-1)}{2N} + T_n$$

$$= \frac{T}{2} + T_n + T_h$$

$$(\text{S. D.})^2 = \left(\frac{T}{N\sqrt{12}}\right)^2 + \left(\frac{T}{N}\sqrt{\frac{N^2-1}{12}}\right)^2$$

$$\text{or} \quad \text{S. D.} \quad = \frac{T}{\sqrt{12}}$$

Thus, the TTFF cannot be reduced by employing more than one HOW per frame. Recapitulating the significantly time-consuming steps in the start-up process, and assuming technique (a), we have the following table:

Table 8. Start-Up for P-Navigation

	Mean Time (sec)	S. D. of Time (sec)
C/A-code search	See Table 2	
Wait for frame sync	15.0	8.7
Collect navigation data	18.0	0
Handover to P	1.3	0

In Table 8, we have assumed, as before, a frame duration of 30 sec (T = 30) and all the navigation data in the first 3/5 of the frame (T_n = 18). Additionally, we have assumed 1.3 sec for handover time (T_h = 1.3), made up of 1 sec for reception of the HOW itself and 0.3 sec for loop pull-in and settling.

Based on the values in Tables 2 and 8, and the expressions previously derived, we can find the mean and 90% confidence values of the TTFF at threshold, as a function of threshold, where threshold is given in terms of the received effective carrier-to-noise density ratio. These values are shown in Table 9.

The following applies to L_2-P navigation:

In an earlier memorandum (Reference 5), we discussed how L_2 measurements would be made every 10 sec, with a 10 point moving arc average over a 90 sec span. Thus, in the case of L_2-P navigation, the first L_2 correction is made 10 sec after the L_1-P TTFF. This is not, in general the most accurate fix, but, of course, this comment applies to all TTFFs. This leads to the results shown in Table 10.

Table 9.   TTFF at Threshold, Four Channel
Receiver, L_1/P-Navigation

Threshold $(C/N_o)_e$-Received dBHz	TTFF (sec)	
	Mean	90% Confidence
30.8	105.7	211.4
31.8	88.3	169.0
32.8	75.6	138.3
33.8	67.2	118.2
34.8	61.0	103.5
35.8	56.3	92.6
36.8	52.6	84.2
37.8	50.0	78.3

Table 10.   TTFF at Threshold, Four Channel
Receiver, L_2/P-Navigation

Threshold $(C/N_o)_e$-Received dBHz	TTFF (sec)	
	Mean	90% Confidence
30.8	115.7	221.4
31.8	98.3	179.0
32.8	85.6	148.3
33.8	77.2	128.2
34.8	71.0	113.5
35.8	66.3	102.6
36.8	62.6	94.2
37.8	60.0	88.3

ANSWER TO QUESTION 7

By interpolation of the data shown in Table 2, it can be seen that the C/A-code can be acquired with a probability of 0.9 in less than 50 sec with a received effective carrier-to-noise density ratio of 35.1 dBHz.

With such a threshold signal level, the TTFF at threshold, for the L_1/P navigator is, from Table 9,

$$\text{mean TTFF} = 59.6 \text{ sec}$$
$$90\% \quad \text{TTFF} = 100.2 \text{ sec}$$

Thus, the expected TTFF will be 59.6 sec at the same threshold which gives a 90% acquisition time for the C/A-code of 50 sec.

Clearly, if the restriction of acquiring the C/A-code within 50 sec is removed, the expected TTFF requirements of 3 or 5 min can be met with much lower signal levels. We do not have computer calculations for such low thresholds, but as may be seen from Table 9, the expected TTFF is 105.7 sec with $(C/N_o)_e$ of 30.8 dBHz, even though, at this signal level, acquisition time of the C-code is 71.4 sec (mean value), or 140.3 sec (90% probability value).

ANSWER TO QUESTION 8

With $(C/N_o)_e$ equal to 34 dBHz, and with the receiver designed to perform optimally at this signal level, the expected TTFFs are, by interpolation of Tables 7, 9, and 10.

$$C \text{ navigator} \quad 64.7 \text{ sec}$$
$$L_1/P \text{ navigator} \quad 66.0 \text{ sec}$$
$$L_2/P \text{ navigator} \quad 76.0 \text{ sec}$$

TTFF FOR THE SEQUENTIAL RECEIVER

Although not specifically requested, the TTFF with sequential tracking receivers has also been computed, using the new (i. e., January 1974) signal structure. Also, the 2-channel sequential receiver is considered, in which one channel (known as Channel B), is used for search and acquisition of the C-code and collection of data, performing these functions in an uninterrupted manner, and the other channel (Channel A) is used to sequentially track the four signals (either C or P) and make the range and range rate measurements. Channel A is initially prepositioned by Channel B, and then routinely reacquires the signals using the flywheel method.

The initial operation steps for a sequential C-navigator which enter into the calculations for the TTFF are shown in Table 11. The TTFF is given by

$$T = \sum_{i=1}^{4} \left(t_{1i} + t_{2i} + t_{3i} \right)$$

Now, the four variates t_{1i} (i = 1, 2, 3, 4) are independent; their mean and standard deviation values (call them m and σ) are shown in Table 2.

Similarly, the four variates t_{2i} are independent; each is uniformly distributed between zero and 30 sec, and hence has a mean of 15 and a standard deviation of 8.7

The four variates t_{3i} are all fixed and equal to 18 sec.

Hence, it can easily be shown that

$$T_{mean} = 4m + 132$$

and
$$T_{SD} = (4\sigma^2 + 300)^{\frac{1}{2}}$$

Table 11. Initial Steps for Sequential C-Navigation

Channel A	Channel B	Time
	Search and acquire C1	t_{11}
	Preposition A to C1	negl.
Sequentially track C1	Wait for C1 data frame sync	t_{21}
	Collect C1 navigation data	t_{31}
	Search and acquire C2	t_{12}
	Preposition A to C2	negl.
Sequentially track C1 and C2	Wait for C2 data frame sync	t_{22}
	Collect C2 navigation data	t_{32}
	Search and acquire C3	t_{13}
	Preposition A to C3	negl.
Sequentially track C1, C2, and C3	Wait for C3 data frame sync	t_{23}
	Collect C3 navigation data	t_{33}
	Search and acquire C4	t_{14}
	Preposition A to C4	negl.
Sequentially track C1, C2, C3, and C4	Wait for C4 data frame sync	t_{24}
	Collect C4 navigation data	t_{34}

TTFF

Also, the 90% confidence value is

$$T_{90} = T_{mean} + 1.28\, T_{SD}$$

$$= 4m + 132 + 1.28(4\sigma^2 + 300)^{\frac{1}{2}}$$

Using the values of m and σ from Table 2, we have the TTFFs for Sequential C-Navigation, as shown in Table 12.

Table 12.   TTFF at Threshold, Sequential C-Navigation

Threshold $(C/N_o)_e$-Received dBHz	TTFF (min)	
	Mean	90% Confidence
30.8	6.96	9.29
31.8	5.80	7.58
32.8	4.95	6.33
33.8	4.39	5.52
34.8	3.98	4.91
35.8	3.67	4.46
36.8	3.42	4.11
37.8	3.25	3.88

The operations for the sequential L_1/P navigator are shown in Table 13.   The TTFF is given by

$$T = \sum_{i=1}^{4}\left(t_{1i} + t_{2i} + t_{3i} + t_{4i}\right)$$

Table 13.   Initial Steps for Sequential L_1/P-Navigation

	Channel A	Channel B	Time
TTFF		Search and acquire C1	t_{11}
		Wait for C1 data frame sync	t_{21}
		Collect C1 navigation data	t_{31}
		Handover C1 → P1, B → A	t_{41}
	Sequentially track P1	Search and acquire C2	t_{12}
		Wait for C2 data frame sync	t_{22}
		Collect C2 navigation data	t_{32}
		Handover C2 → P2, B → A	t_{42}
	Sequentially track P1 and P2	Search and acquire C3	t_{13}
		Wait for C3 data frame sync	t_{23}
		Collect C3 navigation data	t_{33}
		Handover C3 → P3, B → A	t_{43}
	Sequentially track P1, P2, and P3	Search and acquire C4	t_{14}
		Wait for C4 data frame sync	t_{24}
		Collect C4 navigation data	t_{34}
		Handover C4 → P4, B → A	t_{44}
	Sequentially track P1, P2, P3, and P4		

The first three sets of variates are the same as those described before. The four variates, t_{4i}, are taken as fixed values, each equal to 1.3 sec.

Hence, it can easily be shown that

$$T_{mean} = 4m + 137.2$$

$$T_{SD} = (4\sigma^2 + 300)^{\frac{1}{2}}$$

and

$$T_{90} = T_{mean} + 1.28\ T_{SD}$$

Using the values of m and σ from Table 2, we have the TTFFs for Sequential L_1/P-Navigation, as shown in Table 14.

Table 14. TTFF at Threshold, Sequential L_1/P-Navigation

Threshold $(C/N_o)_e$-Received dBHz	TTFF (min)	
	Mean	90% Confidence
30.8	7.05	9.38
31.8	5.89	7.67
32.8	5.04	6.42
33.8	4.48	5.61
34.8	4.07	5.00
35.8	3.76	4.55
36.8	3.51	4.20
37.8	3.34	3.97

REFERENCES

1) Gilder, J. R., "Optimized Acquisition Parameter for the DNSDP Receiver Code Lock Detector", TRW Memo No. DNSDP-JRG-170, 5 December 1973 (Included here as Appendix 13)

2) Philco-Ford, "Global Positioning System C-Signal Multiple Access and Jamming Performance", GPS-TM003C, 27 December 1973

3) Deckett, M., "Analysis and Simulation of the C-Code Acquisition Time", TRW Memo No. DNSDP-MD-160, 9 November 1973

4) Philco-Ford, "RF Link Analysis for Global Positioning System", GPS-TM003A, 21 December 1973

5) Deckett, M., "Description and Performance of the L_1/L_2 Ionospheric Correction Algorithm", TRW Memo No. DNSDP-MD-221, 21 December 1973 (Included here as Appendix 6)

APPENDIX 2

SIGNAL LEVEL SPECIFICATIONS

In the most recent SAMSO document describing the signal structure, it is stated that the user equipment shall be designed for the following received signal levels:

$$L_1 - C \qquad -160 \text{ dBw}$$

$$L_1 - P \qquad -163 \text{ dBw}$$

$$L_2 \qquad -166 \text{ dBw}$$

It is further stated that these are the received signal levels achievable at the output of a series-connected 0 dB antenna and 3 dB attenuator, that is to say, of an antenna which has a gain of 0 dB, relative to circular polarization.

Thus, it is possible to relate the received power levels to field strength values. This is necessary, since the antenna is part of the user equipment, and hence the signal level specification for the entire user equipment must be in terms of field strength.

The relationships for this transposition are:

$$P = FA$$

and

$$A = \frac{G\lambda^2}{4\pi}$$

where

P = received power (at output of antenna)

F = field strength

A = effective aperture of the antenna

G = antenna gain, relative to the polarization of the signal

λ = wavelength.

With these relationships, we have the values shown in the following table:

Table 1. Field Strengths

	Units	L_1-C	L_1-P	L_2
Received power, per SAMSO spec	dBw	-160	-163	-166
Antenna gain (SAMSO antenna)	dB	0	0	0
Wavelength	m	.19	.19	.24
Effective aperture (SAMSO antenna)	m^2	.00287	.00287	.00458
Field strength	dBw/m^2	-134.6	-137.6	-142.6

Thus, the starting point for all signal level specifications for the user equipment can be expressed as follows:

"The user equipment shall be designed to operate with right hand circular polarized signals emanating from satellites whose elevation angles are 5 degrees or greater, and whose field strengths are equal to, or greater than,

$$-134.6 \quad dBw/m^2 \quad \text{for } L_1\text{-C}$$

$$-137.6 \quad dBw/m^2 \quad \text{for } L_1\text{-P}$$

$$-142.6 \quad dBw/m^2 \quad \text{for } L_2 \quad \text{"}$$

202

Now, for the purposes of specifying the minimum received power at the receiver input with which the receiver must operate, we will assume that, under worst conditions, the user antenna gain, relative to CP, is -4 dB, and that there are 1 dB of line losses between the antenna and the receiver. This is equivalent to specifying the receiver such that the antenna gain, relative to CP, and referenced to the receiver input, can be as low as -5 dB. This is not unreasonably large allowance, or an overly stringent receiver specification, when one considers the difficulties faced by the antenna designer.

Thus, using $G = -5$ dB, and the specified field strengths, we have the minimum powers at the receiver input, as

$$-165.0 \quad \text{dBw} \quad \text{for } L_1\text{-C}$$

$$-168.0 \quad \text{dBw} \quad \text{for } L_1\text{-P}$$

$$-171.0 \quad \text{dBw} \quad \text{for } L_2$$

These values serve as both the minimum received power, at the receiver, and also as the "threshold" level.

APPENDIX 3

USER SOFTWARE EPHEMERIS ALGORITHM
AND EPHEMERIS DATA FORMAT

INTRODUCTION

This analysis expands upon one suggested method (Reference 1) of computing the current satellite ephemeris in the user software. The associated satellite data format requirement is also discussed, as well as the computational accuracy of this method. Although there are many other ways of implementing these computations, the conclusions here about accuracy and data requirements should remain approximately true.

Gregory-Newton Formula

The discrete counterpart of the Taylor Series is the Gregory Newton formula:

(1)
$$y(t) = y_0 + k \Delta y_c + \frac{k(k-1)}{2!} \Delta^2 y_0 + \frac{k(k-1)(k-2)}{3!} \Delta^3 y_0 + \cdots$$

Which is computed from a difference table formed from the function $y = f(t)$ as follows ($k = t/\Delta t$):

t	k	y	Δy	$\Delta^2 y$	$\Delta^3 y$	$\Delta^4 y$
0	0	y_0				
			Δy_0			
Δt	1	y_1		$\Delta^2 y_0$		
			Δy_1		$\Delta^3 y_0$	
$2\Delta t$	2	y_2		$\Delta^2 y_1$		$\Delta^4 y_0$
			Δy_2		$\Delta^3 y_1$	
$3\Delta t$	3	y_3		$\Delta^2 y_0$		
			Δy_3			
$4\Delta t$	4	y_4				

205

A simple example would be $y = t^3$; for $\Delta t = 2$:

t	k	y	Δy	$\Delta^2 y$	$\Delta^3 y$	$\Delta^4 y$
0	0	0				
			8			
2	1	8		48		
			56		48	
4	2	64		96		0
			152		48	
6	3	216		144		
			296			
8	4	512				

$$y(5) = 0 + 2.5(8) + \frac{2.5(1.5)}{2}(48) + \frac{2.5(1.5)0.5}{6}(48)$$

$$= \quad 20 + 90 + 15 = 125$$

If the satellite data channel transmitted the coefficients y_o, Δy_o, $\Delta^2 y_o$, etc. for each component X, Y, Z, of the satellites predicted orbit, the user software could compute the position at any time using the Gregory-Newton formula.

The ground tracking station would compute these coefficients periodically by forming such difference tables from values y_o, y_1, y_2, etc. taken from estimates of the predicted orbits.

The satellite velocity can also be computed from the same coefficients by differentiating the Gregory-Newton formula with respect to k:

$$(2) \quad y^1(t) = \frac{1}{\Delta t} \left[\Delta y_0 + \frac{k+(k-1)}{2!} \Delta^2 y_0 + \frac{k(k-1)+k(k-2)+(k-1)(k-2)}{3!} \Delta^3 y_0 + \cdots \right]$$

In Reference 1, it was suggested that y_o, y_1, y_2, etc., be transmitted and the difference table be computed by the user. This is less desirable because it increases both the data transmitted and the user computations.

206

OTHER FORMULAS

There are several other interpolation/extrapolation formulas which may be used with difference coefficients, including Gauss, Stirling's, Bessel's, Lagrange's and Everett's. Everett's formula in particular is mentioned in Reference 2. To a cursory examination, these formulas appear slightly more complicated than the Newton-Gregory and offer minor accuracy advantages, at best. Considerable numerical analysis would be required to qualify the above statement.

Everett's formula uses only the even-order differences $\Delta^2 y$, $\Delta^4 y$, etc. It is possible that a comparative study would show that, for the same user ephemeris computation accuracy, fewer coefficients would have to be transmitted to the user for Everett's formula. If at a future time the data channel capacity becomes a problem, such a study would determine if a more complex user algorithm would save a few bits in the data channel. At present, minimizing user computations seems more significant.

COMPUTATIONAL ASSUMPTIONS

The accuracy of the computed position is greatest near the center of the table, and is also affected by truncation of the transmitted coefficients and the smallest term carried in the Gregory-Newton formula.

In order to evaluate the computational accuracy of this approach, the following assumptions were made.

The worst case satellite orbit conditions were represented by approximating a segment near perigee by a circular orbit with a geocentric radius of 9×10^7 ft and an earth-relative velocity of 7854 ft/sec. This gives an angular rate of one degree per 200 seconds, so that

$$(3) \qquad x(t) = 9 \times 10^7 \sin (.005\ t\ \deg)$$

$$(4) \qquad y(t) = 9 \times 10^7 \cos (.005\ t\ \deg)$$

and tables could be constructed with $\Delta t = 200$ sec corresponding to one degree intervals.

207

The coefficients y_0, Δy_0, $\Delta^2 y_0$, etc., are transmitted periodically to the user. In order to give the greatest time of applicability of a set of coefficients, it was assumed that they will be transmitted in advance, that is, transmitted before the time corresponding to y_0.

The transmitted coefficient truncation was then determined by requiring truncation errors at $k = -9$ ($t = -30$ minutes) to be less than 0.5 feet. The results are:

QUANTITY	MAXIMUM MAGNITUDE	LEAST INCREMENT	BITS INCLUDING SIGN
y_0	1.8×10^8 ft	0.5 ft	30
Δy_0	1.6×10^6	0.05	27
$\Delta^2 y_0$	3×10^4	0.01	23
$\Delta^3 y_0$	500.	0.0025	19
$\Delta^4 y_0$	10.	0.00075	16
$\Delta^5 y_0$	0.15	0.000275	11
$\Delta^6 y_0$	0.003	0.000125	6

The magnitude of y_0 has been increased to allow for apogee. Remember that the differences are over 200 second time increments, so that

$$\dot{y} \simeq \frac{\Delta y_0}{200}$$

$$\ddot{y} \simeq \frac{\Delta^2 y_0}{(200)^2}$$

etc.

COMPUTATIONAL ACCURACY

The error in computing equations (3) and (4), using coefficients truncated as described, was evaluated as a function of time. The results are shown in Figure 1. The three curves show the error for terminating the Gregory-Newton formula at the fourth, fifth, and sixth differences, respectively.
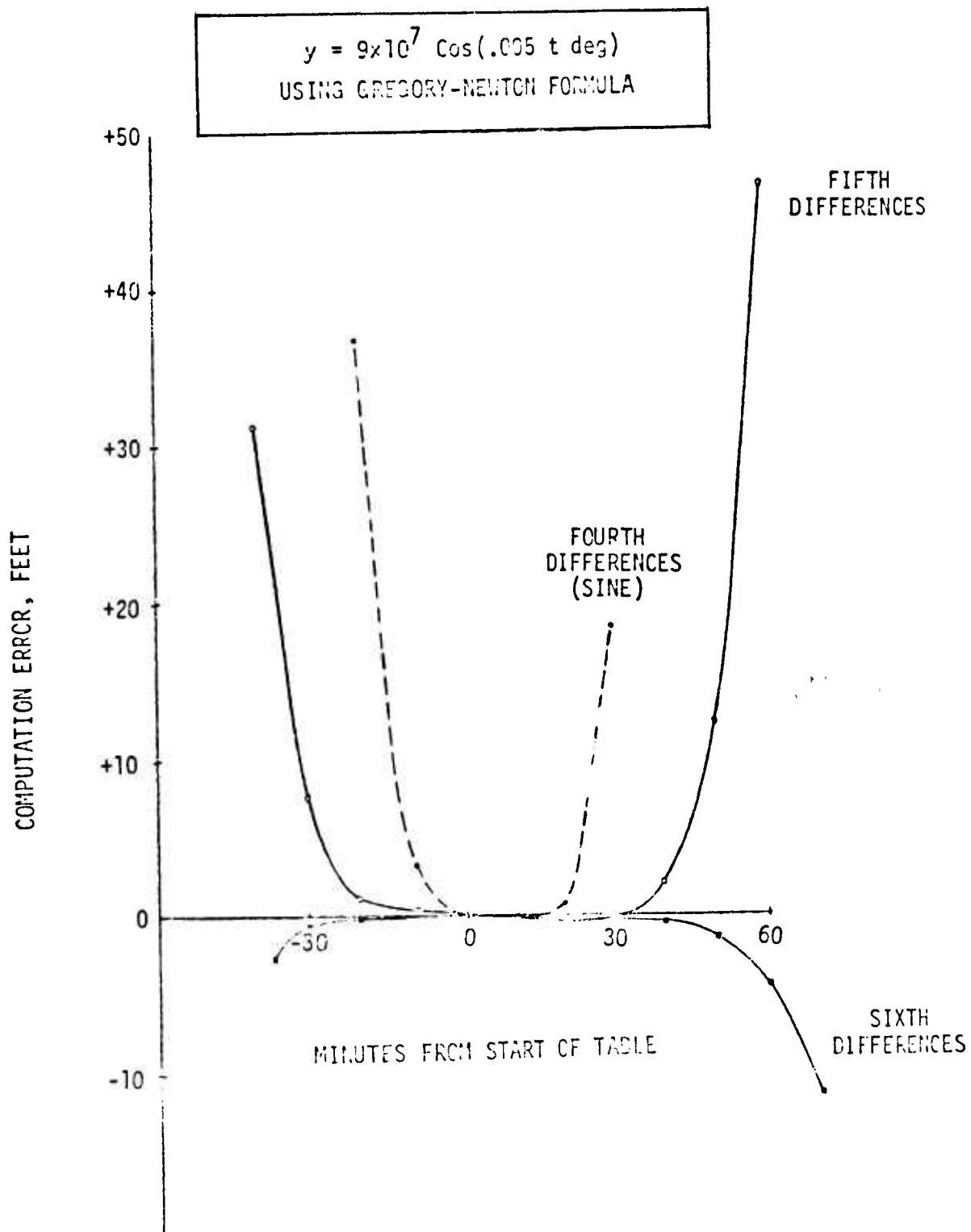
Figure 1. Error in Computation of Position

209

If the computational accuracy requirement were set at one foot, for example, the fourth difference solution would be adequate for 21 minutes, the fifth difference for 57 minutes, and the sixth difference for 80 minutes.

The error in computing the derivatives of equations (3) and (4), using formula (2), was also evaluated. The same truncated coefficients were used as for position. The results are shown in Figure 2. The fourth difference solution is better than the fifth difference solution before the table start time. The reason for this is not apparent at the present time.

For maximum error of 0.01 ft/sec, the fourth difference is good for 80 minutes, fifth difference for 67 minutes, and sixth difference for >100 minutes.

These accuracy statements refer only to the computational error made by the user, and are additional to any error made by the ground station in predicting the satellite ephemerides or the values y_o, y_1, y_2, etc. from which the difference table is formed. The ground station must also carry more bits of significance than indicated above for the transmitted data, in order to avoid computational errors in forming the difference table.

EPHEMERIS DATA BIT REQUIREMENT

If fifth differences were required but not sixth, the number of bits required for ephemeris data per satellite would be

$$3(126) = 378$$

plus a time word. If the time word had a maximum magnitude of 24 hours and a least increment of 10^{-4} sec (0.8 ft at 8000 fps) 30 bits would be required, for a total of

$$\boxed{408 \text{ bits}}$$

$$\frac{dy}{dt} = -\left(\frac{\pi}{180}\right)\left(\frac{2 \times 10^7}{200}\right)\sin (.005 \; t \; deg)$$

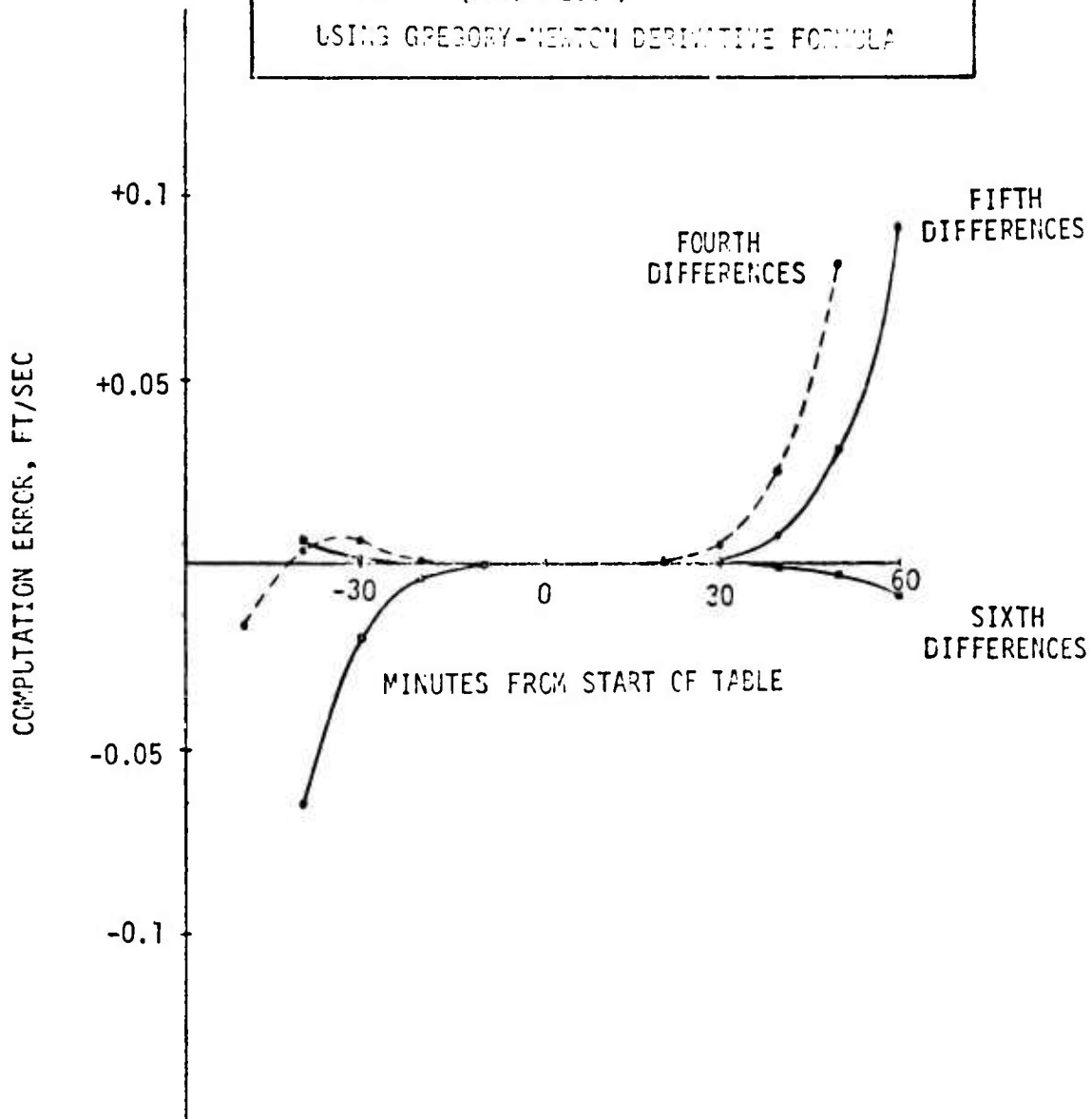USING GREGORY-NEWTON DERIVATIVE FORMULA

Figure 2. Error in Computation of Velocity

211

In Reference 2, 522 bits were allotted to ephemeris data. Some of the 114 bit surplus may be used for parity checks, addressing, less compact format, etc., for which requirements remain to be determined.

SATELLITE OSCILLATOR DATA

Although not part of the ephemeris data, it is convenient to specify here the data format for the satellite oscillator phase and frequency corrections for which no specific provision was made in Reference 3.

At a frequency of 1.6×10^9 Hz, a doppler of 1.6 Hz corresponds to 1 ft/sec.

If the maximum relative frequency error from nominal is

$$10^{-6} (1.6 \times 10^9) = 1600 \text{ Hz}$$

and the desired smallest correction is 0.0016 Hz, corresponding to 0.001 ft/sec, the range of correction is $10^6:1$, requiring 20 bits plus sign.

If the relative phase error is considered to be reset to zero every 24 hours, the maximum error is

$$24(3600)1600 = 1.3824 \times 10^8 \text{ cycles}$$

One cycle is 0.625 foot. If the desired smallest phase correction is 0.1 ft, corresponding to 0.16 cycles, the range of correction is $8.64 \times 10^8 = 1$, requiring 30 bits plus sign.

Then with the above assumptions, the frequency and phase correction word requirements are:

Frequency word	21 bits
Phase word	31 bits

212

REFERENCES

1. 08260-6086-R3-00, "Satellite System for Precise Navigation, System 621B (U)," Volume 3, dated 1969 January 31.

2. SAMSO TR72-247, "System 621B Signal Definition Study (U)," Final Report, dated October 1972.

3. WDL-TP4420, "Definition of Ground and User Segments of the Defense Navigation Satellite Development Program (DNSDP) (U)," Volume 1, dated 23 April 1973.

APPENDIX 4

EPHEMERIS DATA FORMAT FOR 12 HOUR ORBITS

INTRODUCTION

The numerical results in Reference (1)[*] have been made obsolete by the change to 12 hour circular orbits. In addition, Reference (2) is no longer valid since the requirement to limit C-signal user navigation accuracy has been eliminated. This analysis updates the numerical results of Reference (1) for the new orbits. The results presented here are applicable to both the P and C signal users. Reference (1) should be read as an introduction to this analysis.

DISCUSSION

Following the same method as in Reference (1), the satellite position coordinates were approximated as

$$(1) \quad X(t) = 8.7 \times 10^7 \sin (.00886t) \text{ deg}$$

$$(2) \quad Y(t) = 8.7 \times 10^7 \cos (.00886t) \text{ deg}$$

for a circular orbit with geocentric radius of 8.7×10^7 feet and an earth-relative velocity of 13460 ft/sec. The angular rate is 1.77 degrees per 200 seconds.

The table of difference coefficients was constructed using the same time interval (200 seconds) as before. The errors in computing the Gregory-Newton formula (Reference 1) were determined to be not very sensitive to the time interval chosen.

For the new orbit, the transmitted coefficient bit requirements were determined to be as follows.

---

[*] Reference 1 is included in this report as Appendix 3.

QUANTITY	MAXIMUM MAGNITUDE (feet)	LEASE INCREMENT (feet)	BITS INCLUDING SIGN
y_o	10^8	0.5	29
Δy_o	3×10^6	0.05	27
$\Delta^2 y_o$	10^5	0.01	25
$\Delta^3 y_o$	3000	0.0025	22
$\Delta^4 y_o$	100	0.00075	18
$\Delta^5 y_o$	3	0.000275	15
$\Delta^6 y_o$	0.1	0.000125	11

The least increments (quantization) remain the same, but the magnitude of the higher order terms is increased for the new orbit.

The errors in computing position and velocity using Gregory-Newton formulas truncated at the fifth and sixth difference terms are shown in Figures 1 and 2. The worst errors are shown in each case, that is, fifth order position and velocity errors are worst for Equation (2) and its derivative, and sixth order position and velocity errors are worst for Equation (1) and its derivative. For position, the 1σ errors due to the coefficient quantization indicated above, are shown separately. The quantization errors are additional to the formula truncation errors.

EPHEMERIS DATA BIT REQUIREMENT

The formula truncation error is less than one foot for about 31 minutes for fifth differences, and for about 55 minutes for sixth differences. About 1/2 foot 1σ of coefficient quantization error is additional to the truncation error.

It is emphasized that these computational errors are independent of ground station errors in predicting the satellite ephemeris.
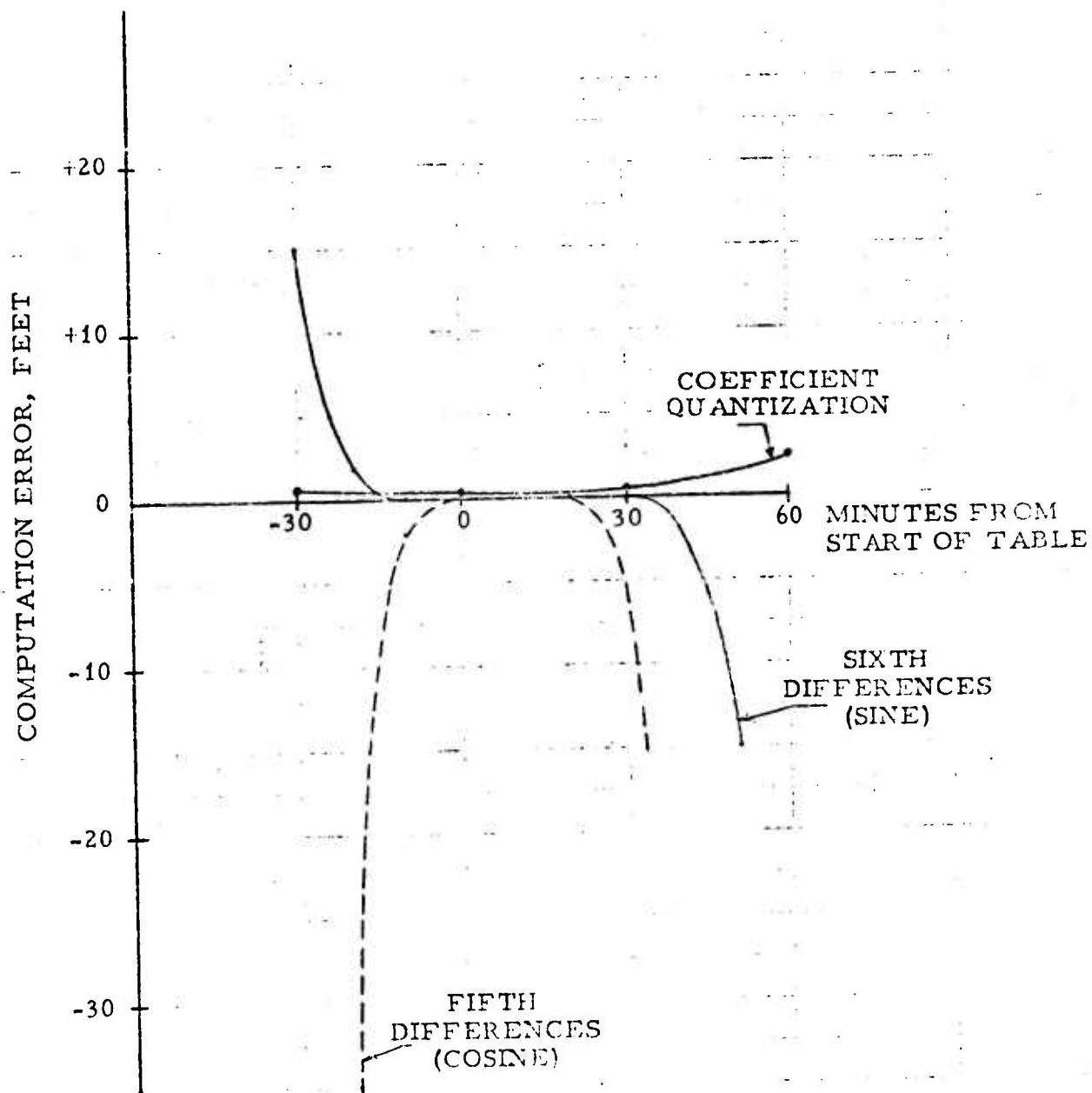
Figure 1. Error in Computation of Position Using
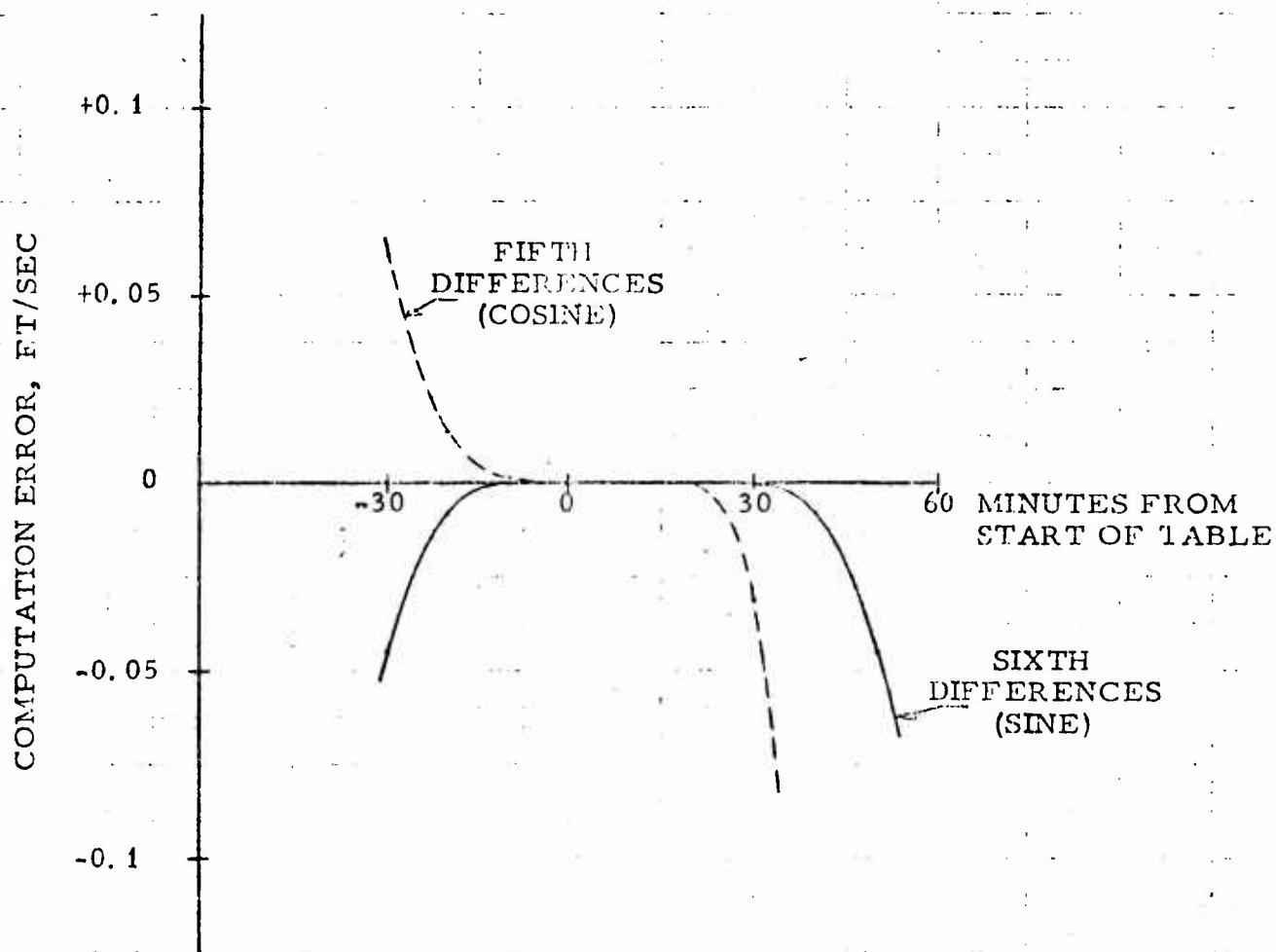Gregory-Newton Formua for 12 Hour
Orbits

217

Figure 2. Error in Computation of Velocity
Using Gregory-Newton Formula
for 12 Hour Orbits

218

If 31 minute validity for the ephemeris data is adequate the ephemeris/oscillator message bit requirement is:

Difference coefficients	136 x 3	408
Time word		30
Oscillator corrections		56
Total		494

If 55 minutes data validity is required, the result is:

Difference coefficients	147 x 3	441
Time word		30
Oscillator corrections		56
Total		527

CONCLUSIONS

The previous 24 hour orbits required transmission of fifth order difference coefficients to achieve data validity periods of about one hour. The new 12 hour orbits require sixth order terms to achieve approximately the same validity period.

The ephemeris data message requirement is increased by 63 bits over that of Reference (1).

219

REFERENCES

(1) DNSDP-REO-027, "DNSDP User Software Ephemeris Algorithm and Ephemeris Data Format," by R. E. Orr, dated 6 August 1973 (included here as Appendix 3).

(2) DNSDP-REO-051, "Ephemeris Data Format for C-Signal User," by R. E. Orr, dated 17 August 1973.

APPENDIX 5

## ANALYTIC ORBIT PROPAGATION FOR DNSDP

INTRODUCTION

In order for the DNSDP user navigation to "get started," it is necessary for the user software to predict the current satellite positions and velocities before any signals have been acquired. This is because, in order to minimize time to first fix, the receiver needs to be told which satellites to acquire and their approximate dopplers.

To accomplish this, the software must be able to propagate the satellite positions and velocities over long periods of time, in order to minimize the frequency of initial constant updates. These initial constants must be stored in the computer memory from the time they were last received over the data link on a previous mission. If the constants are not present or are too old, they will have to be supplied by other means.

ACCURACY REQUIREMENTS

The satellite range rate geometry for a 12 hour circular orbit is as follows for a user in the plane of satellite motion:
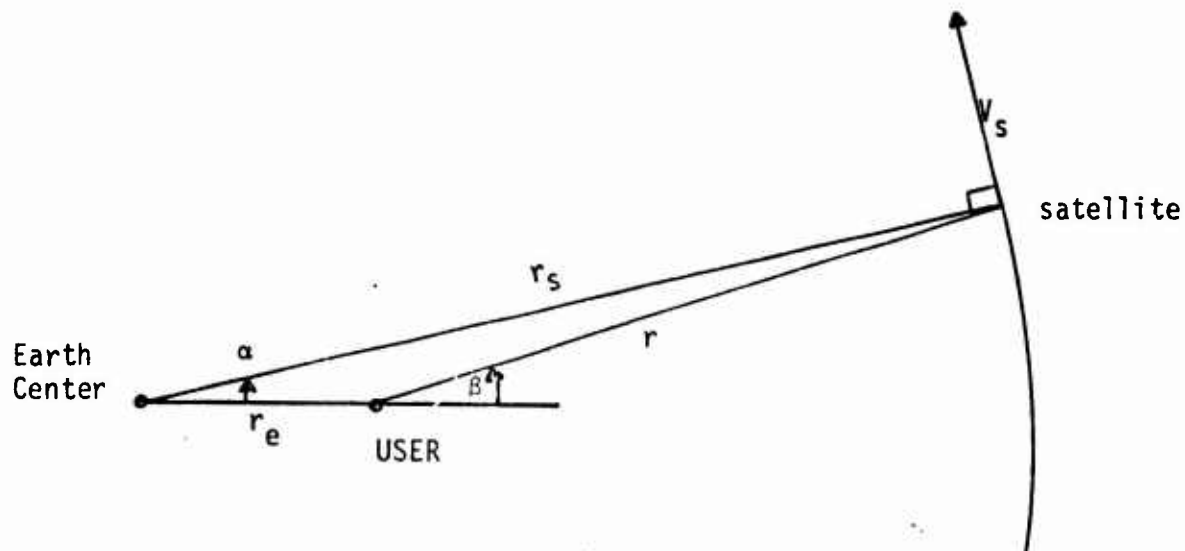
V_s is the satellite velocity, 12,700 fps

r_s is the satellite geocentric radius, 87.2×10^6 ft

r_e is the earth's radius, 20.9×10^6 ft

r is the range from user to satellite

Ignoring the rotation of the earth, the range rate is:

$$\dot{r} = V_s \frac{r_e}{r_s} \sin \beta = V_s \frac{r_e}{r} \sin \alpha$$

since V_s is normal to r_s.

A variation in satellite position ΔP along the direction of motion is:

$$\Delta P = r_s \, \Delta \alpha$$

and the change in range rate $\Delta \dot{r}$ is:

$$\Delta \dot{r} = V_s \frac{r_e}{r} \cos \alpha \, \Delta \alpha$$

so that

$$\frac{\Delta \dot{r}}{\Delta P} = \frac{V_s \, r_e}{r_s \, r} \cos \alpha$$

From the low of cosines,

$$r = (r_e^2 + r_s^2 - 2 r_e r_s \cos \alpha)^{1/2}$$

Substituting in numerical values,

$$r = (8.04 \times 10^{15} - 3.64 \times 10^{15} \cos \alpha)^{1/2}$$

$$\dot{r} = (2.65 \times 10^{11}) \frac{\sin \alpha}{r}$$

$$\frac{\Delta \dot{r}}{\Delta P} = (3044) \frac{\cos \alpha}{r}$$

α	r	$\dot{r}$	$\frac{\Delta \dot{r}}{\Delta P}$
0	66.3×10^6 ft	0 fps	4.59×10^{-5} fps/ft
30°	69.9×10^0 ft	1896 fps	3.77×10^{-5} fps/ft
60°	78.9×10^6 ft	2909 fps	1.93×10^{-5} fps/ft
80°	86.1×10^6 ft	3031 fps	6.14×10^{-6} fps/ft

The problem is symmetrical about $\alpha = 0$ and values of $(\alpha) > 80^\circ$ represent lines of sight below the horizon.

The worst case is for a satellite directly overhead ($\alpha = 0$). A satellite position error of 100, 000 feet will produce an error in predicted range rate of 4.6 ft/sec. The total doppler error requirement is understood to be 500 fps.

For satellite selection purposes, the line of sight vectors must be known within a few degrees. Taking $\Delta \beta$ as a measure of the line of sight error, which is maximum for $\alpha = 0$, $\Delta \beta = \Delta P/r = 1.51 \times 10^{-8}$ rad/ft. A satellite position error of 100, 000 ft produces a line of sight error of 1.51×10^{-3} radians = 0.09 degree.

It would appear that satellite along track position errors of the order of 10^6 feet would be acceptable for initial satellite selection and acquisition purposes.

APPROACH

Orbit integration schemes use a very large amount of computing time to propagate 24 satellites over many days. This would increase the time to first fix. Therefore, an analytic solution was investigated. The method solves the Kepler two-body equations with corrections added for the earth's J2 gravity term (Reference 1, page 369).

The inputs to the analytic algorithm are the orbital elements listed below.

ORBITAL ELEMENT		NOMINAL VALUE
a,	semi-major axis	87,297,171. ft.
e,	eccentricity	0.0099236
i,	inclination	62.49886 deg.
Ω,	node	-0.0007463 deg.
ω,	argument of perigee	-0.0566 deg.
MA,	mean anomaly	45.09174 deg.
t_0,	initial time	0 sec

The values of the orbital elements chosen represent average values over a 30 day period taken from an integrated trajectory produced by a large program which models the earth's gravitational field in detail as well as the gravity of the sun and moon.

The satellite position as a function of time generated by the analytic routine was compared with the integrated reference trajectory. The magnitude of the difference vector was plotted versus time.

Note that any error in the ground station's prediction of the future average orbital elements is not considered here.

ACCURACY RESULTS

Figure 1 shows the satellite position errors at 2400 hours each day versus days from initialization. The error is not zero at time zero when average values of the orbital elements are used instead of initial values. However, when initial values are used, the error increases to 2.8×10^6 feet at 30 days.
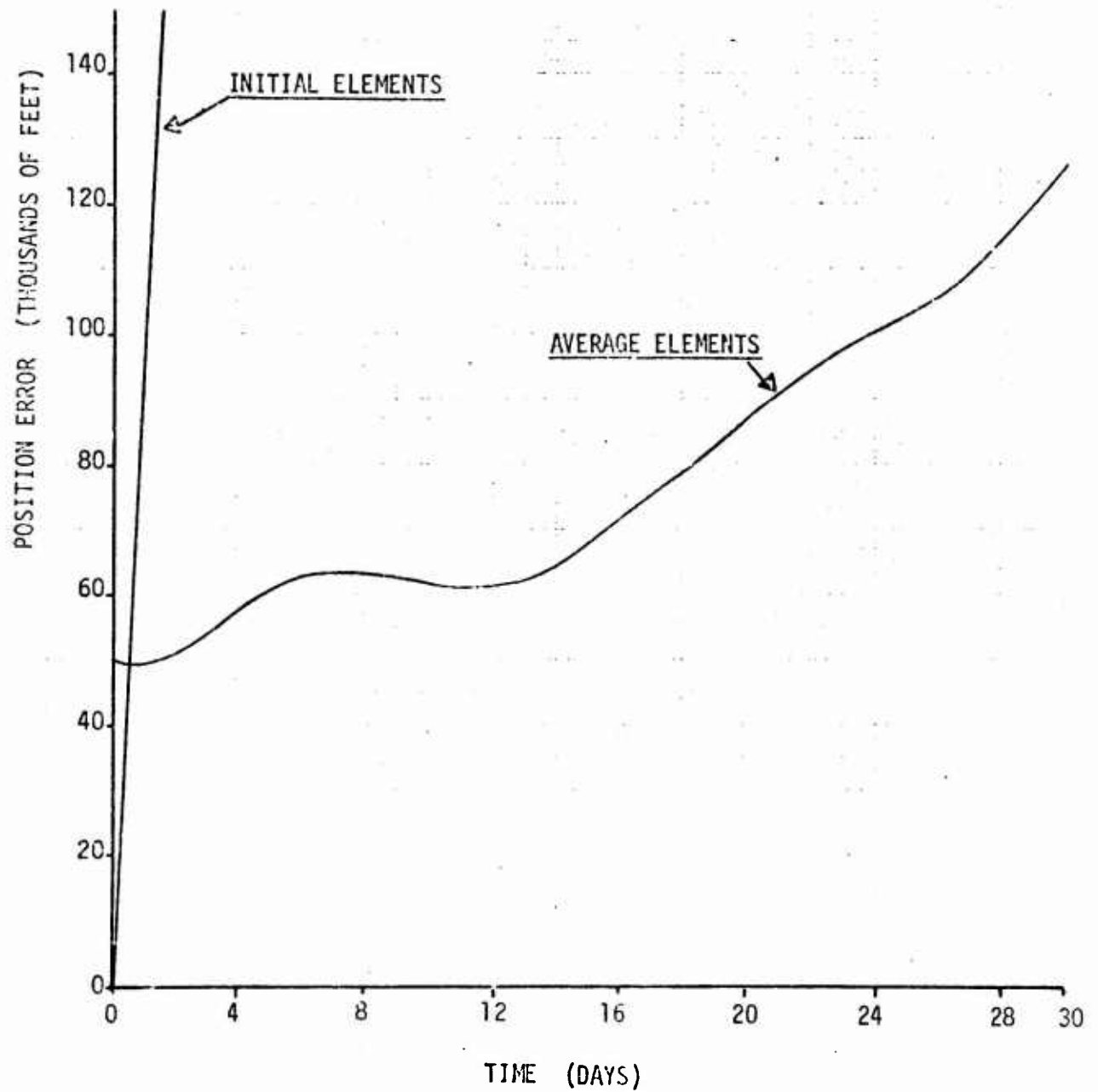
Figure 1. Computational Position Error at 2400 Hours Versus
Days Since Constants Update

Figure 2 shows the hourly variations of the satellite position errors during the first and 60th orbits.

The velocity errors (not plotted) reached a maximum value of 18.8 fps at the 30th day.

ORBIT ELEMENT SENSITIVITIES

In order to determine the sensitivity of the analytic solution to orbit element variations, runs were made perturbing each element individually. The results were as follows.

ELEMENT	PERTURBATION	ORBIT CHANGE AT 30 DAYS
a	100. ft	99. ft
e	0.001	150,000. ft
i	0.5^{o}	750,000. ft
Ω	0.5^{o}	750,000. ft
ω	0.02^{o}	30,000. ft
MA	0.01^{o}	15,000. ft
t_o	1.0 sec	13,000. ft

ORBIT ELEMENT SCALING

The number of bits required to specify the orbit element data to the user was estimated by assuming a permissible error at 30 days due to quantization of ± 5000 feet for each element. Using the sensitivities already determined, the quanta were computed and compared with the assumed maximum values for orbits of interest. Constant biases were assumed to be removed from the data before scaling for transmission to the user.
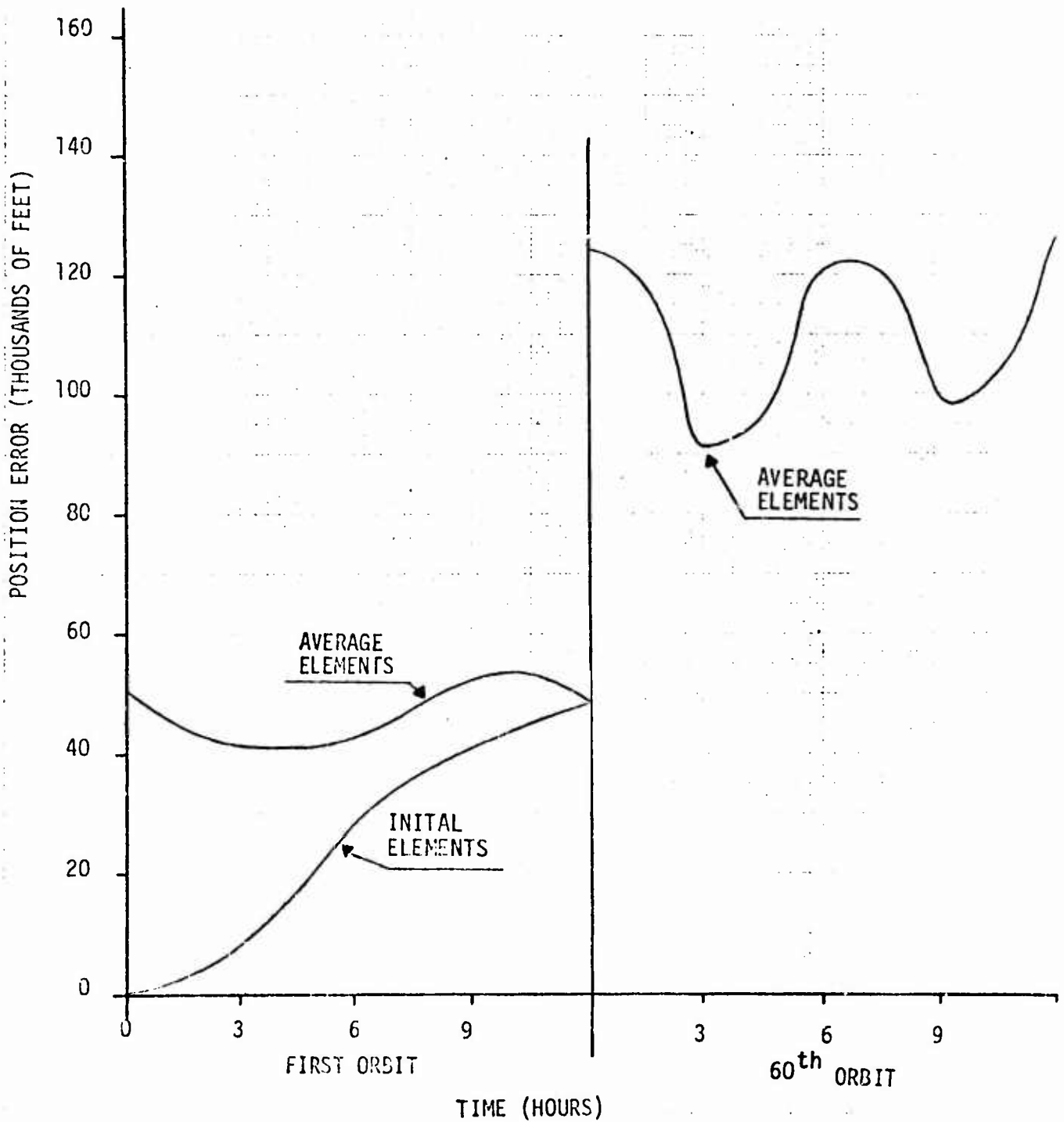
Figure 2. Computational Position Error Versus Time for First Orbit and 60th Orbit Since Constants Update

ELEMENT	MAXIMUM VARIATION	QUANTUM	RANGE	BITS
a	$9 \times 10^7 \pm 10^7$ ft	10^4 ft	2000	11
e	0.1 ± 0.1	6.7×10^{-5}	3000	12
i	$62.5^\circ \pm 10^\circ$	6.7×10^{-3} deg	3000	12
Ω	$\pm 180^\circ$	6.7×10^{-3} deg	54,000	16
ω	$\pm 180^\circ$	6.7×10^{-3} deg	54,000	16
MA	$\pm 180^\circ$	6.7×10^{-3} deg	54,000	16
t_0	0 to 365 days (3×10^7 sec)	0.77 sec	4.1×10^7	26

An orbital error of ± 5000 feet due to each of seven quantities should give a total one sigma quantization error of

$$\sigma_Q = \sqrt{\frac{7}{3}(Q)^2} = 7638. \text{ feet at 30 days}$$

DATA LINK REQUIREMENTS

In a system with 24 satellites, 24 values of a, e, i, Ω, ω, and MA will need to be periodically transmitted to the user. If all these values are for the same time span, only one value of t_0 need be transmitted.

The total number of bits for data is then

$$11+12+12+16+16+16 = 83(24) = 1992 + 26 = 2018.$$

The requirements for ID bits and parity bits remain to be determined. A substantial number of spare bits should also be provided for future contingencies. This data need not be transmitted very frequently. Once or twice a day should be adequate, since the data is applicable for such a long period of time.

EMERGENCY NAVIGATION

In addition to the orbit element data discussed here, the satellites, once acquired, transmit to the users more accurate ephemeris data for precision navigation use. This data is good only for one-half to one hour and is frequently recomputed by the ground station for transmission to the satellite.

In the event of ground station malfunction or destruction, the user could navigate using the orbit element data. Navigation accuracy would be greatly degraded in this case.

CONCLUSIONS

1) An analytic orbit propagation algorithm can provide satellite position accuracies adequate for constellation selection and signal acquisition for periods considerably longer than 30 days. At 30 days, the predicted range rate error is of the order of 6 fps (exclusive of errors in ground station orbit prediction).

2) In the event of ground station outage, users should be able to navigate using the analytic orbit data with approximate 10 n. mi. accuracy for periods up to two weeks. These figures can probably be improved somewhat by further study and algorithm development.

3) The number of bits required for transmission of orbit element data for 24 satellites is estimated as 2018 bits, plus I/O, parity, and spare bits. This data should be transmitted by all satellites, once or twice a day.

REFERENCE

P. R. Escobal, "Methods of Orbit Determination," John Wiley
& Sons, 1965.

230

APPENDIX 6

DESCRIPTION AND PERFORMANCE OF THE L_1 / L_2 IONOSPHERIC CORRECTION ALGORITHM

1. INTRODUCTION

In this analysis, a reasonably simple algorithm is described which might be used for correction of the ionospheric errors in range measurements made against the L_1 signals. This algorithm makes use of similar measurements made against the L_2 signal.

The expected performance of the algorithm is also given. In this context, performance is measured by the standard deviation of residual error after correction.

Whereas, it can be expected that the actual algorithm ultimately used will differ, in detail, from the one proposed here, the performance will most probably remain the same.

2. THE IONOSPHERIC MODEL

It is here assumed that the ionospheric effect on measurements of pseudorange can be simply modelled as

$$\rho_T = \rho_i + \frac{K}{f_i^2}$$

where

ρ_T = true pseudorange

ρ_i = measured pseudorange

f_i = carrier frequency

K = a factor which depends upon the integrated electron density along the radio path when the measurement is taken.

We further assume that K is invariant between the user and a specific satellite during any 2 minute period.

It is believed, that the errors caused by the invalidity of these assumptions are very small ($\ll$ 1 foot).

231

3. DESCRIPTION OF THE ALGORITHM

At regular intervals of time T, each channel of the receiver will make measurements of pseudorange against the L_2 signal $(\tilde{\rho}_2)$. These will be compared with the last measurement made against L_1 signal $(\tilde{\rho}_1)$. The time interval between making these 2 measurements (τ) will be small (approximately 100 msec), but the geometric range between user and satellite will change significantly during that time, and will have to be taken into account. Thus,

$$\tilde{\rho}_2' = \tilde{\rho}_2 - \dot{R}\tau - 1/2\ \ddot{R}\ \tau^2$$

where $\tilde{\rho}_2$ is the L_2 pseudorange applicable at the same time that $\tilde{\rho}_1$ was measured, and $\dot{R}$ and $\ddot{R}$ are the navigation filter estimates of the geometric range rate and range acceleration. The error incurred in using this simple extrapolation is

$$\tau\ \Delta\dot{R} + \frac{\tau^2}{2}\ \Delta\ddot{R}$$

where $\Delta\dot{R}$ is the error in the estimate of $\dot{R}$, etc.

In practice, $\tau < 0.1$ seconds, $\Delta\dot{R} < 1$ fps and $\Delta\ddot{R} < 10$ ft/sec^2, so that the extrapolation error is insignificant.

The difference measurement, $\Delta\rho$, is then formed,

$$\Delta\rho = \tilde{\rho}_2' - \tilde{\rho}_1$$

Then, n such difference measurements will be averaged

$$\overline{\Delta\rho} = \frac{1}{n} \sum^{n} \Delta\rho$$

This term is linearly related to the estimate of K applicable at this time,

$$K = (\overline{\Delta\rho}) / \left(\frac{1}{f_2^2} - \frac{1}{f_1^2} \right)$$

232

Thus, the ionospheric correction term, R_I, is

$$R_I = \frac{K}{f_1^2}$$

$$= \omega \, \overline{\Delta\rho}$$

where

$$\frac{1}{\omega} = \left(\frac{f_1}{f_2}\right)^2 - 1$$

This term, R_I, will be added to every measurement ρ_1 in the following period T. At the end of that period, a new ρ_2 measurement will be made, which will be extrapolated to $\tilde{\rho}_2'$ and will generate a new $\Delta\rho$ value. The average will then be computed again.

To reiterate, the equations of the algorithm are,

$$\tilde{\rho}_2' = \tilde{\rho}_2 - \dot{R}\tau - 1/2 \, \ddot{R} \, \tau^2$$

$$\Delta\rho = \tilde{\rho}_2' - \tilde{\rho}_1$$

$$\overline{\Delta\rho} = \frac{1}{n} \sum^n \Delta\rho$$

$$R_I = \omega\overline{\Delta\rho}$$

$$\rho = \tilde{\rho}_1 + R_I$$

4. PERFORMANCE OF THE ALGORITHM

As previously stated, errors caused by the invalidity of the model are assumed to be negligible ($\ll$ 1 foot). Also, with the expected time interval between ρ_1 and ρ_2 measurements, it was shown that the extrapolation process will not cause significant error.

The term ω will be a program constant, based on the nominal values of f_1 and f_2. It can be easily shown that variations in f_1 and f_2 from their nominal values will cause only insignificant errors in the ionospheric correction.

233

The only significant error sources are the measurement noise errors. These are uncorrelated with each other, and uncorrelated serially.

Thus

$$\sigma^2(\Delta \rho) = \sigma^2(\tilde{\rho}_1) + \sigma^2(\tilde{\rho}_2)$$

and

$$\sigma^2(\overline{\Delta \rho}) = \frac{1}{n}\sigma^2(\Delta \rho)$$

$$\sigma^2(R_I) = \frac{\omega^2}{n}\left[\sigma^2(\rho_1) + \sigma^2(\rho_2)\right]$$

Typically,

$$\sigma(\tilde{\rho}_1) = \sigma(\tilde{\rho}_2) \qquad \text{and } n = 10$$

Thus,

$$\sigma(R_I) = .73\ \sigma(\tilde{\rho})$$

Such a result would, for example, be obtained with an equipment group which made L_2 measurements every 10 seconds, and averaged 10 pseudorange differences each time. This is not an excessive load on the computer, and does not interrupt the L_1 measurement process so often as to degrade the navigation filter performance. At the same time, the assumption of constant ionospheric error is made only for 100 seconds.

234

RECEIVER RANGE AND RANGE RATE
MEASUREMENT ERRORS

This appendix computes the user receiver range and range rate measurement errors due to receiver noise, quantization, instrumentation, and due to user accelerations. The receiver noise, quantization, and instrumentation errors are random and uncorrelated from measurement to measurement. The acceleration errors are bias errors.

The errors attributable to the user oscillator are not included here.

RANGE ERRORS

The total random range error is the rms sum of the noise, quantization, and instrumentation errors, as follows:

$$\sigma_T(P) = \left[\sigma_n^2(R) + \sigma_q^2(R) + \sigma_I^2(R)\right]^{\frac{1}{2}} \tag{1}$$

The noise error in turn has two sources: phase jitter in the carrier (Costas) tracking loop and phase jitter in the delay lock loop (DLL). Phase jitter in the Costas tracking loop is equal to[1]

$$\sigma_{\phi 1} = \left[\frac{B_1}{(C/N_o)_{L1}}\left(1 + \frac{W}{2(C/N_o)_{L1}}\right)\right]^{\frac{1}{2}} \tag{2}$$

where $\sigma_{\phi 1}$ = rms phase jitter in carrier loop

B_1 = one-sided loop bandwidth

W = noise bandwidth of RC data filter in the loop

$(C/N_o)_{L1}$ = signal-to-noise density ratio in loop

Phase jitter in the DLL is equal to[2]

$$\sigma_{\phi 2} = 2\pi \left[\frac{B_2}{(C/N_o)_{L2}} \left(1 + \frac{2B_{IF}}{(C/N_o)_{L2}} \right) \right]^{\frac{1}{2}} \tag{3}$$

where $\sigma_{\phi 2}$ = rms phase jitter in DLL

B_2 = one-sided loop bandwidth

B_{IF} = predetection IF bandwidth

$(C/N_o)_{L2}$ = signal-to-noise density ratio in DLL

Range error is related to the phase jitter as follows:

$$\sigma(R) = \frac{\lambda_c}{2\pi} \sigma_\phi$$

where λ_c = code wavelength

The total rms range error due to phase jitter in the two loops equals

$$\sigma_n(R) = \frac{\lambda_c}{2\pi} \left[\sigma_{\phi 2}^2 + \left(\frac{\sigma_{\phi 1}}{N} \right)^2 + 2 \frac{\sigma_{\phi 1}}{N} \sigma_{\phi 2} \rho_{12}(0) \right] \tag{4}$$

where   N = carrier-to-code frequency ratio

$\rho_{12}(0)$ = cross-correlation between Costas loop and DLL noise

The function $\rho_{12}(0)$ can be neglected since it is close to zero[3]. Therefore, Equation 4 reduces to

$$\sigma_n(R) = \frac{\lambda_c}{2\pi}\left[\sigma_{\phi2}^2 + \left(\frac{\sigma_{\phi1}}{N}\right)^2\right]^{\frac{1}{2}} \qquad (5)$$

The rms quantization errors for the coarse and fine range measurements are as follows:

$$\sigma_{qc}(R) = \frac{\lambda_c}{\sqrt{12}} \qquad (6)$$

$$\sigma_{qf}(R) = \frac{\lambda_c}{\sqrt{12}\,N} \qquad (7)$$

When the delay lock loop is locked and tracking, the tracking error oscillates in a random manner about the true range with a rms error of one carrier wavelength in range. This is because the loop is always adding or deleting one count of the N divider between the carrier and code loops. This results in an instrumentation error equal to the carrier wavelength. Thus

$$\sigma_I(R) = \lambda_c/N \qquad (8)$$

237

A range bias error occurs from receiver accelerations due to an additional phase tracking error in the receiver carrier loop. For an acceleration step, the peak phase error in the carrier loop is

$$\Delta\phi \;=\; \frac{1.845}{B_1^2}\left(\frac{A}{\lambda_s}\right) \tag{9}$$

where A = acceleration (fps^2)

λ_s = carrier wavelength = λ_c/N

The resulting error in the code loop is $1/N$ as big, and so the resulting bias error is

$$\Delta R \;=\; \frac{\lambda_c}{2\pi}\frac{\Delta\phi}{N} \tag{10}$$

Combining Equations 9 and 10

$$\Delta R \;=\; \frac{1.845}{2\pi B_1^2}\, A \tag{11}$$

RANGE RATE ERRORS

The total random range rate error is the rms sum of the noise and quantization errors as follows:

$$\sigma_T(\dot{R}) \;=\; \left[\sigma_n^2(\dot{R}) + \sigma_q^2(\dot{R})\right]^{\frac{1}{2}} \tag{12}$$

The range rate noise error results from the phase noise in the carrier tracking loop. The receiver range rate counter averages the carrier frequency for T sec. Thus, the range rate measurement equals

238

$$\dot{R} = \frac{\lambda_s}{2\pi T}\left[\phi(t + T) - \phi(t)\right] \tag{13}$$

where $\phi(t)$ = carrier loop VCO phase

T = averaging time for doppler count

The rms range rate error is then

$$\sigma_n(\dot{R}) = \frac{\lambda_s\sqrt{1-\rho_{11}(T)}}{2\pi T}\left(\sqrt{2}\ \sigma_{\phi 1}\right) \tag{14}$$

where $\rho_{11}(T)$ = autocorrelation of carrier loop noise

$\sigma_{\phi 1}$ = carrier loop phase noise [Equation (2)]

The autocorrelation function $\rho_{11}(T)$ is negligibly small[3], and can be assumed to be zero. Thus

$$\sigma_n(\dot{R}) = \frac{\lambda_s}{2\pi T}\left[\frac{2B_1}{(C/N_o)_{L1}}\left(1 + \frac{W}{2(C/N_o)_{L1}}\right)\right]^{\frac{1}{2}} \tag{15}$$

The rms quantization errors for the coarse and fine range rate measurements are as follows:

$$\sigma_{qc}(\dot{R}) = \frac{\lambda_s}{T\sqrt{12}} \tag{16}$$

$$\sigma_{qf}(\dot{R}) = \frac{\lambda_s}{2NT\sqrt{12}} \tag{17}$$

239

The range rate bias error due to receiver accelerations is equal to

$$\Delta \dot{R} = \frac{\lambda_s}{2\pi} \left(\frac{\Delta \dot{\phi}}{T} \right) \tag{18}$$

Where $\Delta \phi$ is the phase tracking error in the carrier loop as given by Equation 9.

RESULTS

Table 1 gives a tabulation of the random range and range rate errors as a function of effective received carrier-to-noise density ratio[*] for both a P-code and C/A-code receiver. These are single measurement errors and apply to both sequential and continuous tracking receiver types. Table 2 is a tabulation of the range and range rate bias errors due to receiver acceleration.

Assuming a τ-dither DLL implementation, the signal-to-noise density ratio in the two tracking loops (carrier and code) are related to the effective carrier-to-noise density ratio as follows[3]:

$$(C/N_o)_{L1} = (C/N_o)_e - 1.25 \text{ dB} \tag{19}$$

$$(C/N_o)_{L2} = (C/N_o)_e - 4.77 \text{ dB} \tag{20}$$

---

[*] Effective carrier-to-noise density ratio includes jammer noise and is related to the unjammed carrier-to-noise density ratio as follows (for the P-signal):

$$(C/N_o)_e = \frac{(C/N_o)_{signal}}{1 + \left(\frac{10^{-7}}{1.023} \right) (J/S)(C/N_o)_{signal}}$$

Table 3 shows the receiver parameter values which were assumed in computing the results of Tables 1 and 2.

The total coarse range and range rate random errors $[\sigma_T(R_C)$ and $\sigma_T(\dot{R}_C)]$ apply only when a receiver does not contain fine range and range rate extraction circuits. It is planned at present to provide fine measurement circuits for all receivers so the coarse measurement errors do not apply.

P-Code Receiver

Table 1. Random Range and Range Rate Errors

Quantity		Eq	(C/N$_0$)$_e$ dBHz						
			24	26	28	30	32	34	36
$\sigma_n(R)$	ft	(5)	12.7	8.8	6.2	4.5	3.4	2.6	2.0
$\sigma_{qc}(R)$	ft	(6)	27.8	→	→	→	→	→	→
$\sigma_{qf}(R)$	ft	(7)	0.18	→	→	→	→	→	→
$\sigma_I(R)$	ft	(8)	0.625	→	→	→	→	→	→
$\sigma_T(R_c)$	ft	(1)	30.6	29.2	28.5	28.2	28.0	27.9	27.9
$\sigma_T(R_i)$	ft	(1)	12.7	9.8	6.2	4.5	3.5	2.7	2.1
$\sigma_n(\dot{R})$	fps	(15)	0.17	0.13	0.10	0.08	0.07	0.05	0.04
$\sigma_{qc}(\dot{R})$	fps	(16)	0.90	→	→	→	→	→	→
$\sigma_{qf}(\dot{R})$	fps	(17)	0.003	→	→	→	→	→	→
$\sigma_T(\dot{R}_c)$	fps	(12)	0.92	0.91	0.91	0.90	0.90	0.90	0.90
$\sigma_T(\dot{R}_f)$	fps	(12)	0.17	0.13	0.10	0.08	0.07	0.05	0.04

C/A-Code Receiver

Table 1. Random Range and Range Rate Errors (Continued)

Quantity		Eq	$(\overline{C/N_o})_c$, dBHz						
			24	26	28	30	32	34	36
$\sigma_n(R)$	ft	(5)	241.8	156.7	102.9	68.7	47.0	32.9	23.7
$\sigma_{qc}(R)$	ft	(6)	277.8	→					
$\sigma_{qf}(R)$	ft	(7)	0.18	→					
$\sigma_I(R)$	ft	(8)	0.625	→					
$\sigma_T(R_c)$	ft	(1)	368.3	318.9	296.2	286.2	281.7	279.7	278.8
$\sigma_T(R_f)$	ft	(1)	241.8	156.7	102.9	68.7	47.0	32.9	23.7
$\sigma_n(\dot{R})$	fps								
$\sigma_{qc}(\dot{R})$	fps								
$\sigma_{qf}(\dot{R})$	fps				These errors are the same as the P-Code Receiver				
$\sigma_T(\dot{R}_c)$	fps								
$\sigma_T(\dot{R}_f)$	fps								

243

Table 2. Range and Range Rate Acceleration
Bias Errors

P- and C/A-Code Receivers

Quantity	Equation	Accelerations (g's)			
		1	2	4	7
$\triangle R$ (ft)	(11)	0.095	0.19	0.38	0.66
$\triangle \dot{R}$ (fps)	(18)	0.47	0.94	1.89	3.3

Table 3. Assumed Receiver Parameter Values

Parameter	Value	
	P-Code	C/A-Code
B_1	10 Hz	10 Hz
B_2	0.5 Hz	0.5 Hz
W	40 Hz	200 Hz
B_{IF}	80 Hz	400 Hz
λ_c	96.25 ft	962.5 ft
N	154	1540
$\lambda_s = \lambda_c/N$	.625 ft	.625 ft
T	0.2	0.2

REFERENCES

(1)   TRW Memo DNSDP-JKH-154, "Performance and Stability
       Considerations of the DNSS Receiver I-Q Loop", By J. K.
       Holmes, 3 December 1973

(2)   Gill, W. J., "A Comparison of Binary Delay-Lock Track-
       ing Loop Implementations", IEEE Transactions AES Vol.
       AES2, No. 4, July 1966

(3)   TRW Systems Group, "System 621B Timeshared User
       Equipment Study", Vol II, Appendix 11, SAMSO TR 72-
       202, Vol II, January 1973

APPENDIX 8

NAV-SAT RECEIVER DUAL
FREQUENCY TRADE STUDY

DUAL-FREQUENCY IMPLEMENTATION

Front End

Since operation is required on either 1575 MHz or 1240 MHz, the pre-
selector must either be of sufficiently broadband to pass both frequencies
or else have a separate passband at each frequency. The former approach,
although of lower loss and simpler design, has an unnecessarily large band
of acceptance for extraneous signals, added constraints on the selection
of LO frequencies, and increased difficulty of spurious response rejection.

A filter is required both before and after the preamplifier. The
former is needed to prevent overloading of the preamplifier by very strong
out-of-band signals, with resultant intermodulation products. Additionally,
it (as a diplexer) serves as a channel separator where separate preamplifiers
are used for each channel. The latter is used to remove preamplifier output
noise from the first mixer image band, and may also, as a diplexer, be used
to combine the two channels. Since insertion loss is critical only on the
input filter, its selectivity requirements should be minimized. If dual-
amplifiers are used, there are three feasible configurations, shown in
Figure 1. In each, a diplexer provides separate channels for each pre-
amplifier. In configuration (a), the preamplifier outputs are combined
in another diplexer and fed to the first mixer, which has selectable
LO frequencies to provide a fixed first IF. Both channels may be active
simultaneously without significant spurious responses from the undesired
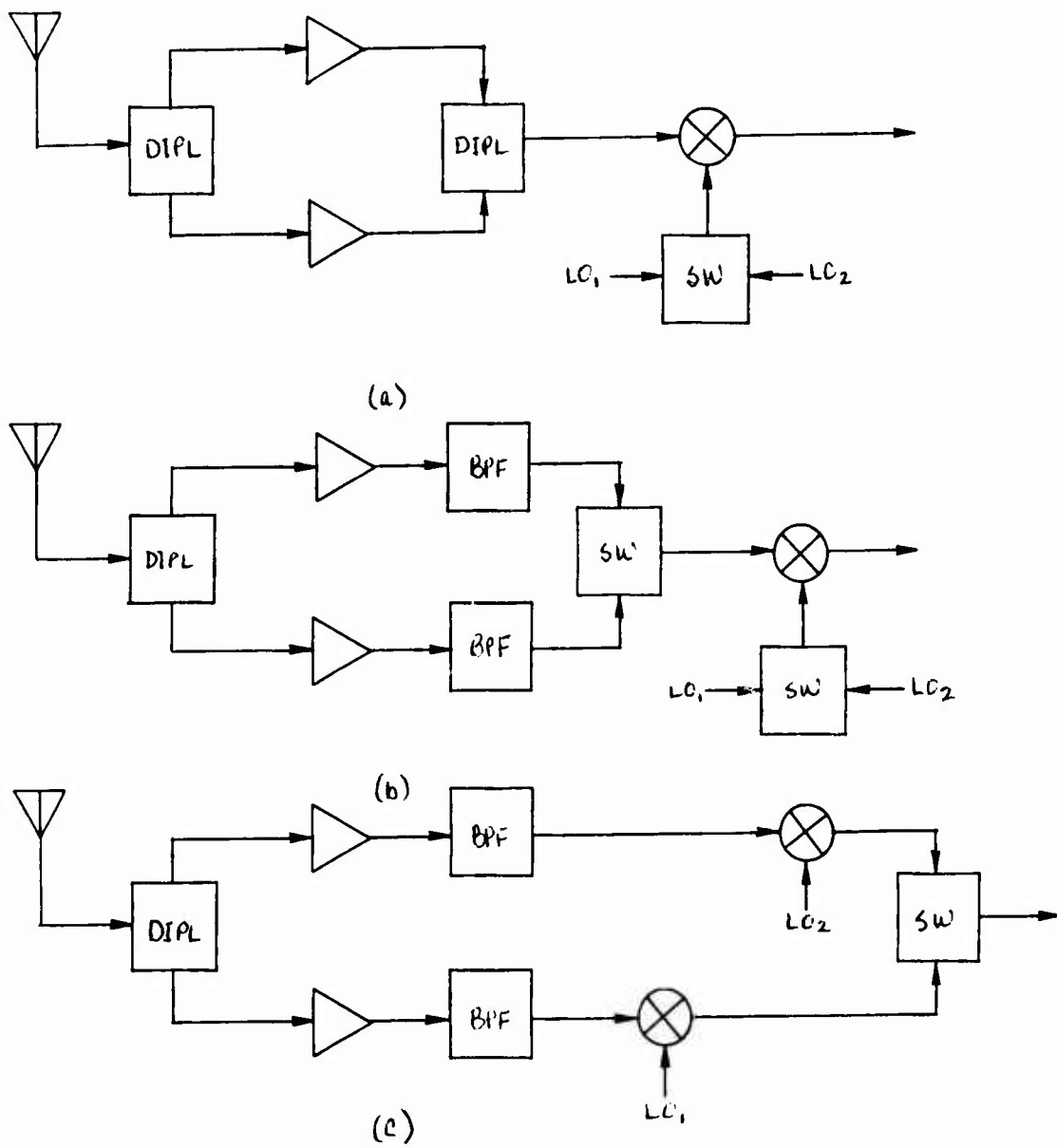channel (see Figures 2 and 3). However, the unused channel may be given

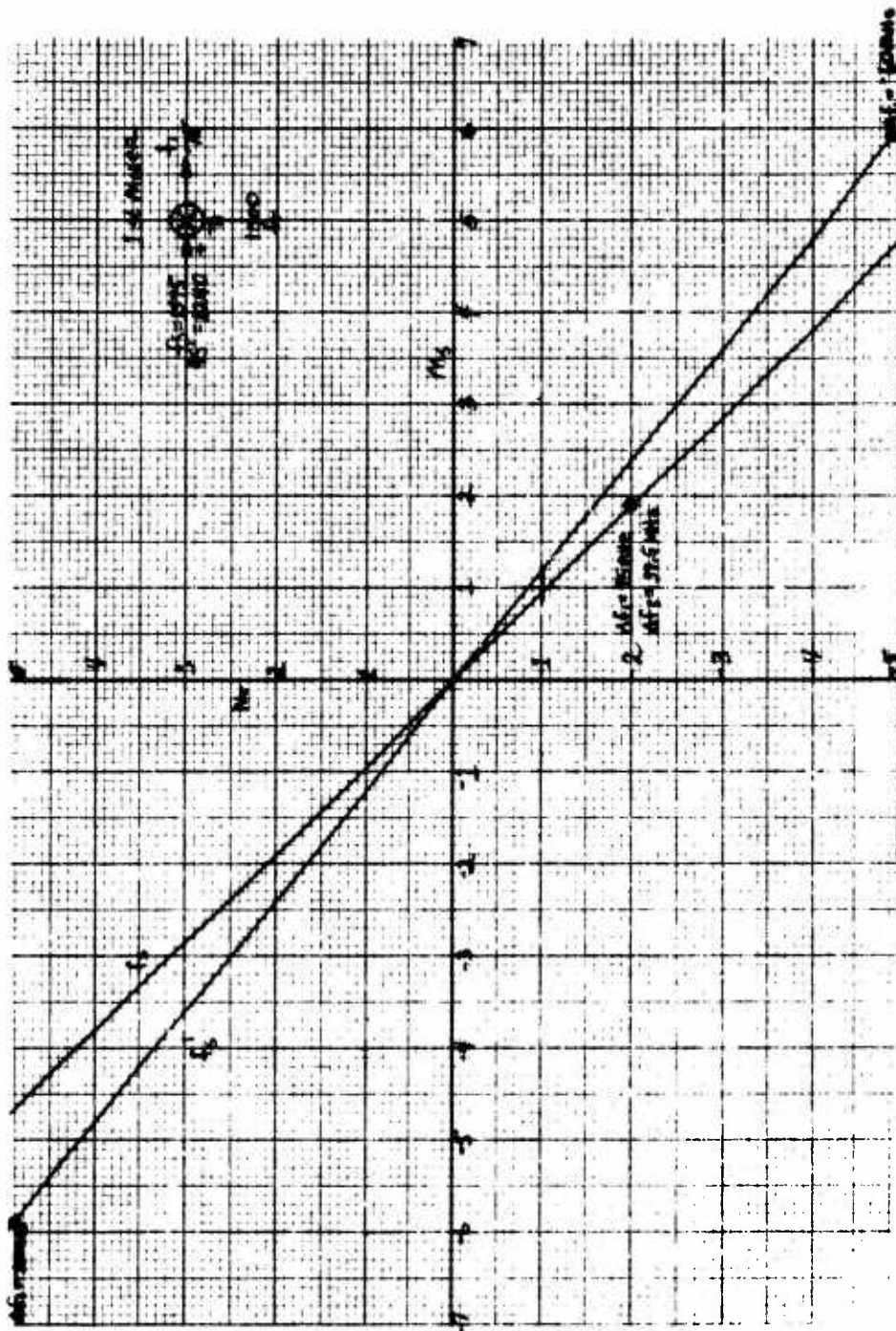Figure 1. Dual Preamp Configurations
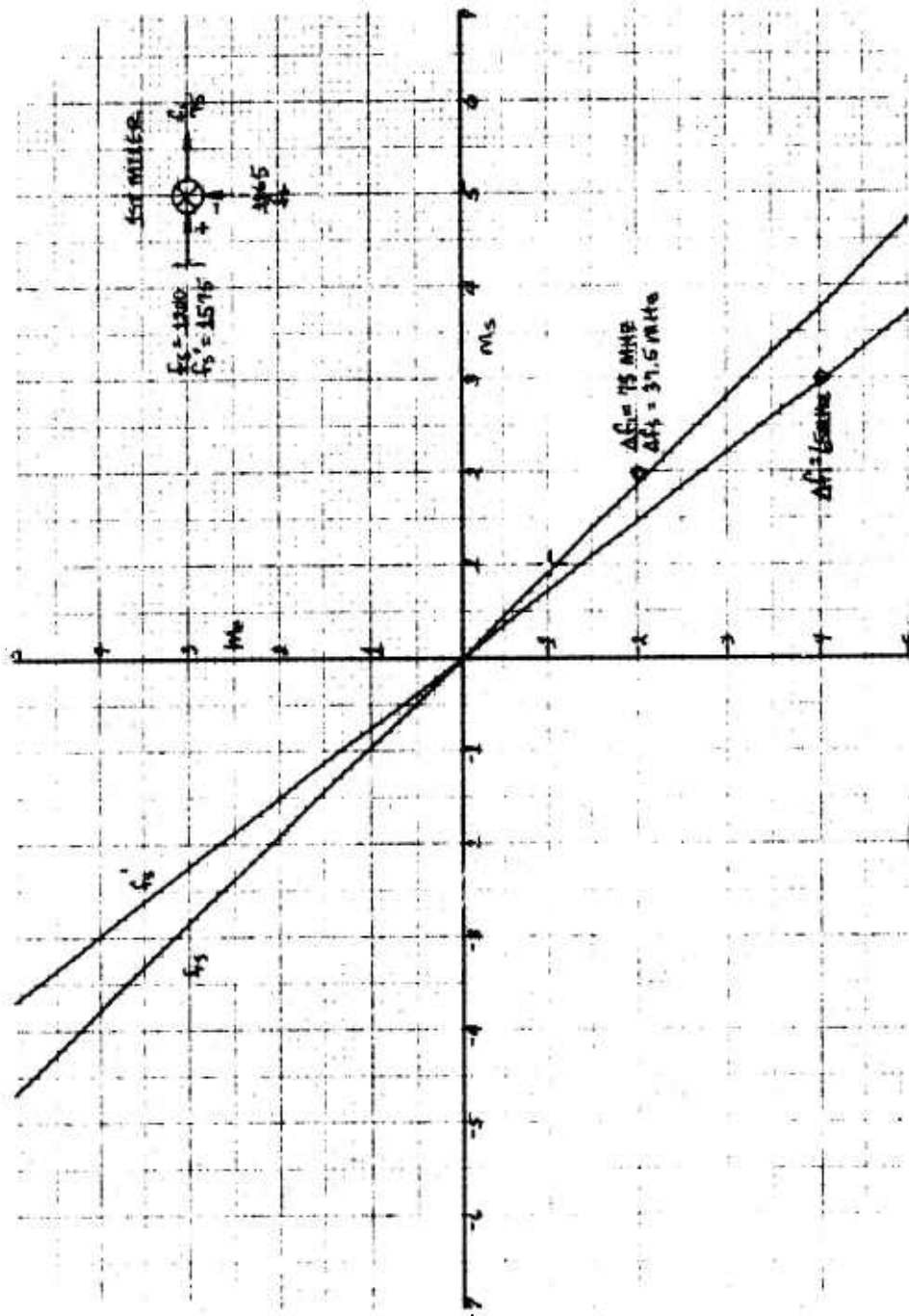
Figure 2. Spurious Response Chart

Figure 3. Spurious Response Chart

appreciable isolation by removing prime power from its amplifier, provided amplifier input/output impedance changes do not affect the diplexer response unacceptably.

Configuration (b) differs only in that the second diplexer is replaced by a pair of bandpass filters selected by a switch. While this provides much greater isolation of the undesired channel, it is more complex and the added isolation is unnecessary.

In configuration (c), separate first mixers are used, eliminating R-F switching of the LO's, and the channel switching is done at IF rather than R-F. While this affords a maximum of isolation and is slightly superior to configuration (b), it is more complex than (a) and the additional isolation is not required. Thus, (a) is the preferred two-amplifier configuration.

In the single-preamplifier approach of Figure 4, the amplifier input may be filtered either by a dual-response filter (two diplexers back-to-back) or by a broad-band filter passing both channels. While the broad-band filter has the lower loss and is of simpler design, it subjects the preamplifier input to a much wider spectrum of extraneous signals. Either is appropriate for either configuration (a) or (b), and the selection depends on the definition of expected signal environment.

In configuration (a) the post-amplification filter may again be a pair of back-to-back diplexers feeding a first mixer having selectable LO's. Alternatively, a diplexer whose outputs are switch-selected may be used for rejection of the undesired channel.

In configuration (b) a separate mixer is used for each channel, switching the mixer outputs in lieu of the LO, with elimination of the combining diplexer or switch. This appears to be a preferable arrangement, since it trades the diplexer or switch for an added mixer, saving in weight, size, or cost and giving some measure of redundancy. Additionally, the two mixers can now be optimized, since each operates at fixed frequencies. Isolation is also improved, particularly if a diplexer is used in lieu of a switch in configuration (a).

251
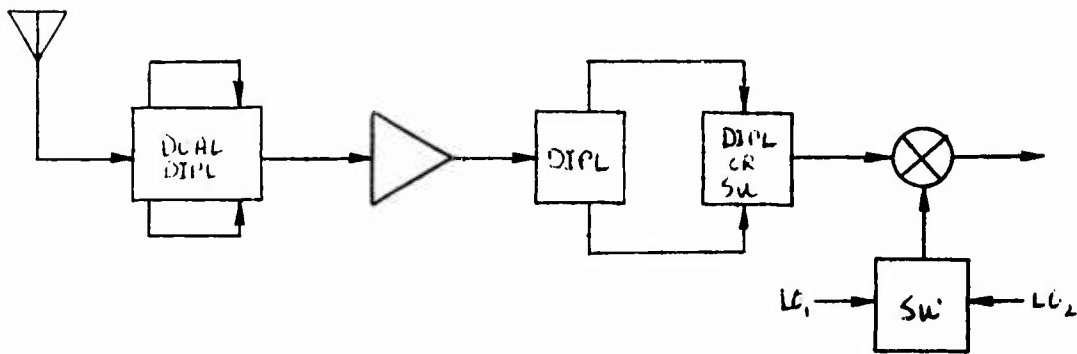
(a)
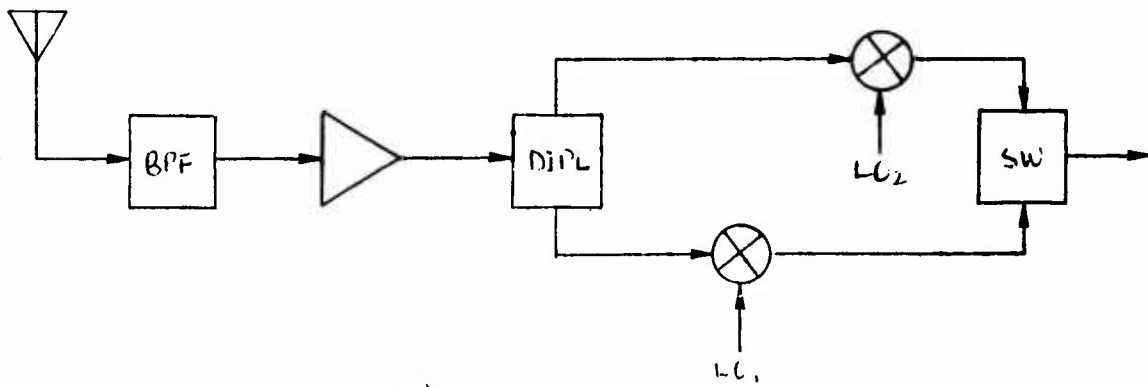
(b)

Figure 4.   Single Preamp Configurations

Comparing the approaches of Figure 1(a) and Figure 4(b), there is perhaps an even trade between the quasi-redundancy of the dual mixers and dual preamps, although cost-wise, the dual mixers are preferable. The two optimized, single-frequency mixers of Figure 4(b) are also preferred over the single, dual-frequency mixer. Although not critical, undesired channel isolation is superior in the single-amplifier, dual mixer approach. Input filter losses for the Figure 1(a) configuration would rank between those for the configurations shown in Figures 4(a) and 4(b), and none would probably exceed 0.5 dB.

It is concluded that the single preamplifier configuration of Figure 4(b) is preferable, with the decision of input filter configuration to be determined.

Frequency Plans

In providing a capability for operation on an alternate frequency of 1240 MHz in addition to the prime frequency of 1575 MHz, the following constraints are imposed:

1. All LO signals are integral multiples of the 5 MHz master oscillator frequency (f_0).

2. The phase-lock VCO operates at 60 MHz (Case 1) or 40 MHz (Case 2).

3. Inversion of the signal spectrum is not permitted.

4. All multipliers are to have prime factors of 7 or less.

5. Minimum circuit complexity is desired.

Additionally, these are practical constraints on the choice of intermediate frequencies. The second IF is desirably limited to not more than about 30 MHz in order to permit use of integrated circuitry.

The higher the first IF, the easier LO and image rejection become. However, if the first IF is much over 100 MHz, crystal filters become unfeasible. If spectrum compression and subsequent narrow-band filtering are done following the second mixer, then the second mixer must operate at the full spread-spectrum bandwidth with accompanying more severe spurious-response problems.

A further desirable constraint is that the first IF not be harmonically related to the second IF. Since the phase-detector reference signal is coherent with the second IF, any harmonic coincident with the first IF

253

which leaks into the first mixer is amplified by the full receiver IF gain, less the leakage of the spectrum-compression modulators. Were it not for the spectrum-compression circuitry, this would be considered a mandatory constraint.

CASE 1. (60 MHz VCU)

The minimum-impact on the receiver configuration is to provide an alternate first LO signal of 1165 MHz (low-side injection) or 1315 MHz (high-side injection). Since these are derived from the master oscillator at 5 MHz, the required multiplier factors are 233 or 263. However, these are both prime numbers and such multiplication and subsequent filtering is unfeasible. While it is possible to count down a VCO from such an LO frequency for phase locking, this approach is not treated here.

The alternative for generation of the alternate LO is to mix the outputs of two multiplier chains each having low prime factors. Candidate multiplier factors are 225+8, 224+9, and 125+108 (low-side injection), and 256+7, 245+18, 243+20, and 135+128 (high-side injection). Since mixing two frequencies having a very large ratio results in close-in low-order spurious responses, the latter number pair in each case if favored. Low-side injection for the 1st mixer is preferable since the required LO frequency is somewhat lower. The LO mixer is free of low-order spurious responses, and the received spectrum remains uninverted, as with the prime frequency. The configuration is shown in Figure 5, and the LO mixer spur chart is Figure 6.

An alternative to this scheme, shown in Figure 7, in effect moves the LO mixer to the signal path, resulting in a triple-conversion receiver. The required LO multiplier factors, for conversion to 75 MHz are 300 and 233 for the prime and alternate signals, respectively (with low-side injection for each). These can each be expressed as the sum of two numbers having low prime factors with one of these numbers being common. Eliminating sets with obvious spur problems results in the following sets having prime factors of 7 or less:
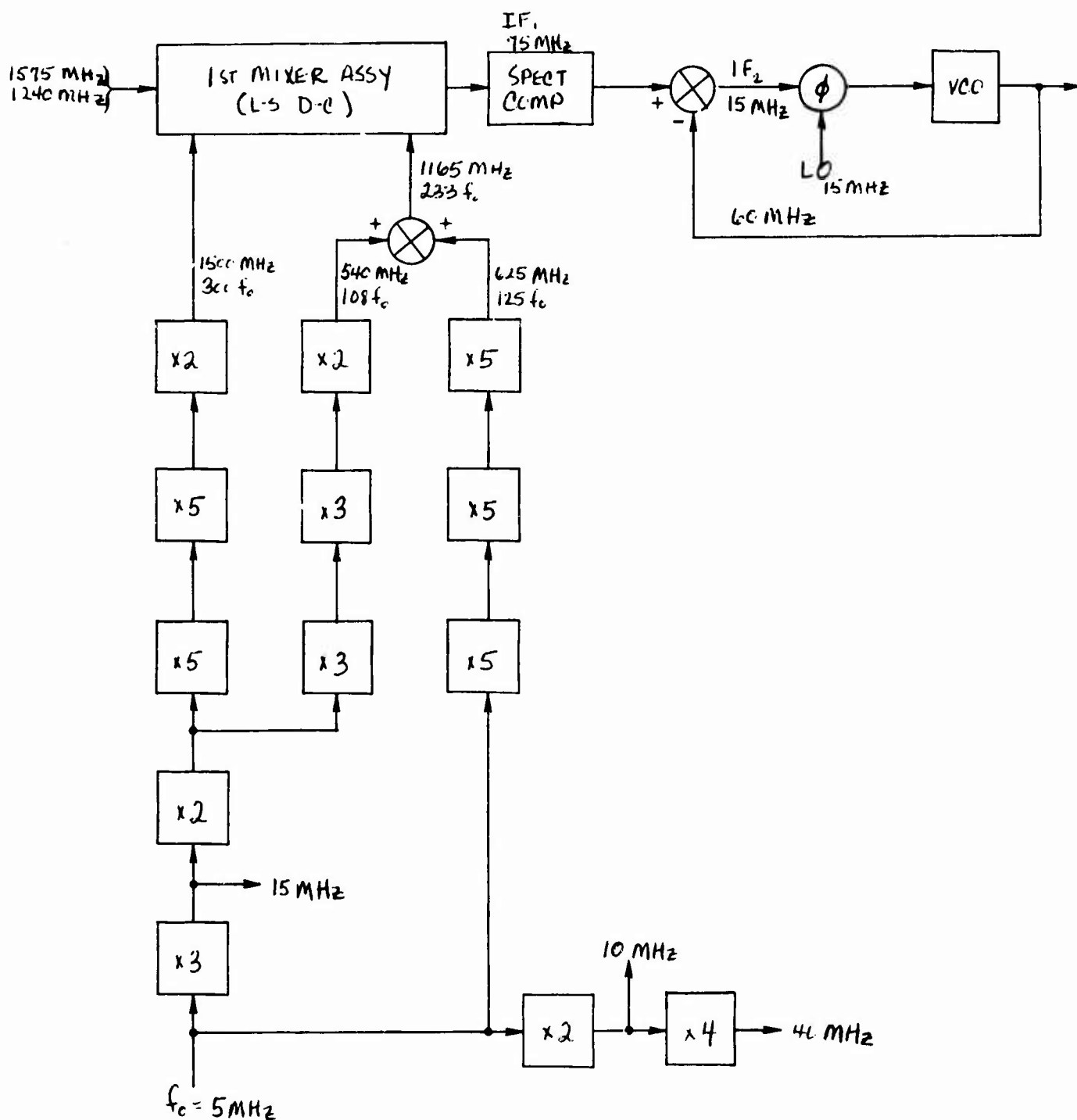
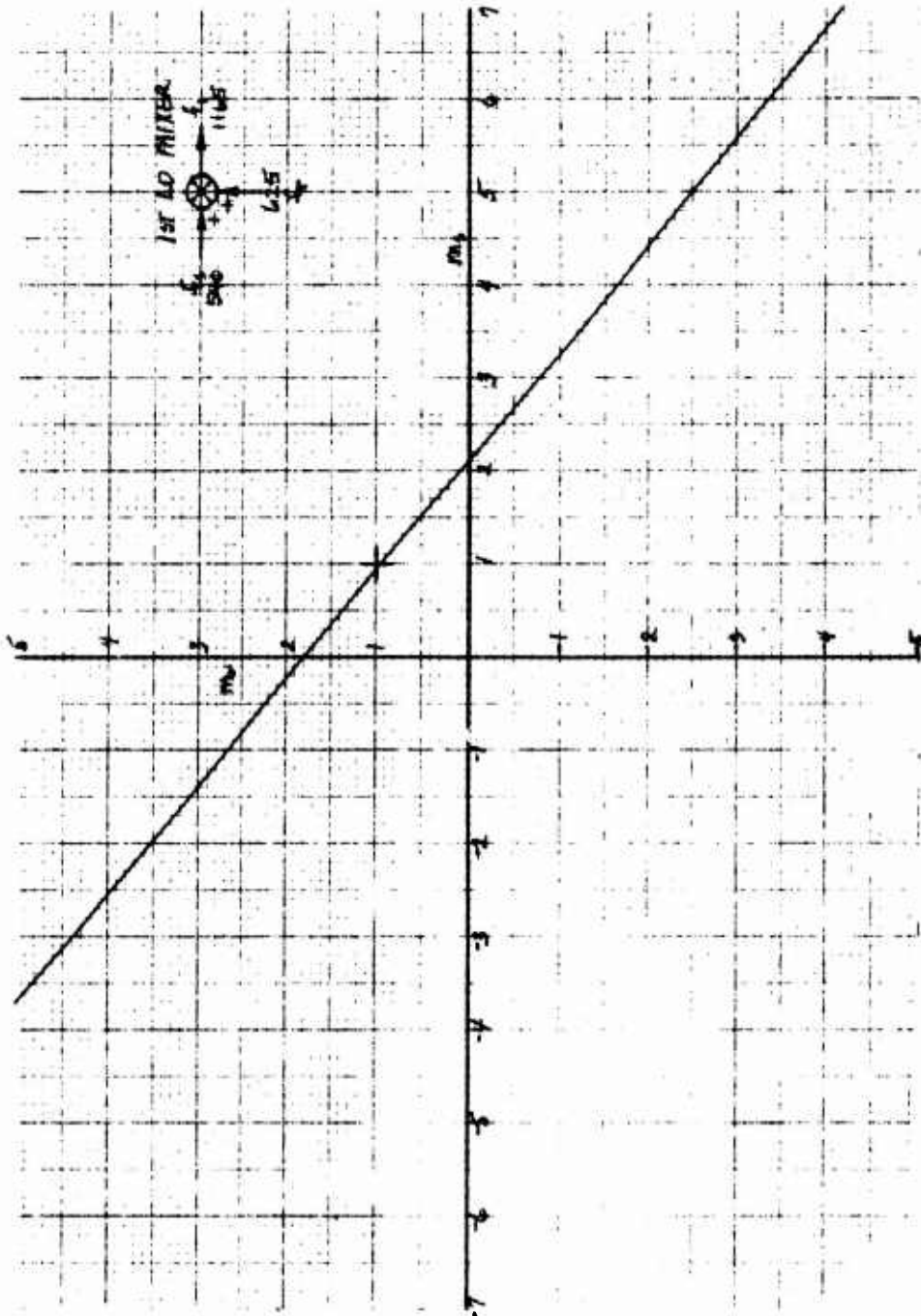Figure 5. 1st LO Chains, Dual-Conversion
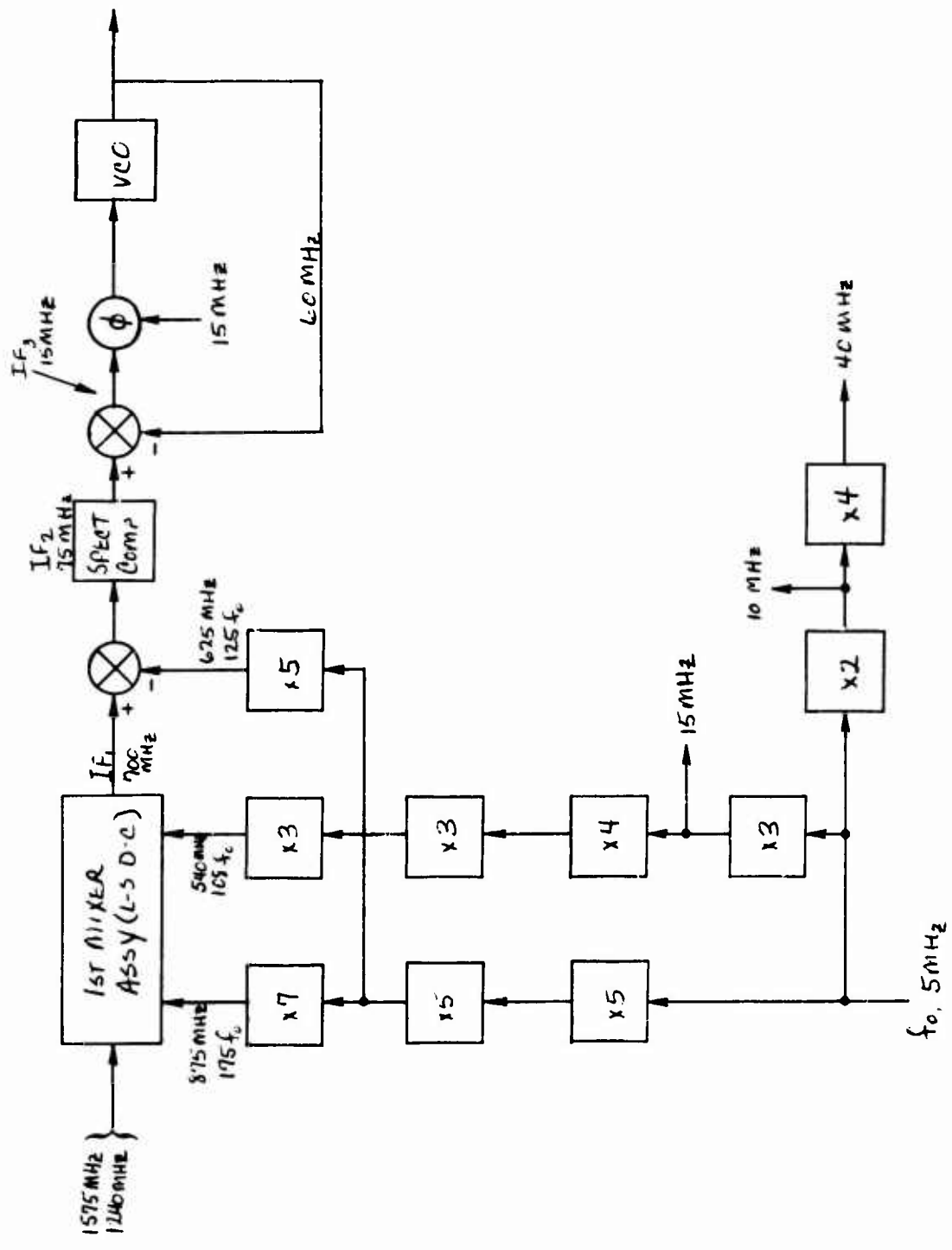
255

Figure 6.   LO Spurious Response Chart

Figure 7. 1st LO Chains, Triple-Conversion

257

$$300 = 108+192, \quad 223 = 108+125$$
$$300 = 125+175, \quad 233, = 125+108.$$

The first set of numbers results in unacceptably poor spurious responses in the first mixer at the alternate frequency, as shown in Figure 8. The second set has acceptable responses, as shown in Figures 9 and 10. These multiplier factors are used in the plan of Figure 7, with the common term being the multiplier factor for the second LO.

Figure 11 shows an alternate dual-conversion scheme in which mixing is not required for generation of LO signals. In this plan, using low-side injection for both mixers, a short phase-lock loop is used, and the IF's are changed to 700 MHz and 60 MHz. The first mixer LO's and first IF are the same as in Figure 7, for which the spurious response charts of Figures 9 and 10 are applicable. The second mixer has a down-conversion ratio of about 10 to 1; hence its principal spur is half the IF above the LO - a 4th-order product at 670 MHz.

There is no loss of loop gain in closing the phase-lock loop around the phase detector instead of the 2nd mixer, and 60 MHz is a tractable frequency for gain, selectivity, and operation of the spectrum-processing circuitry. The first IF, at 700 MHz, is not unreasonable from the standpoint of stage gain and noise figure, and permits much improved image and LO rejection over the previously considered lower frequencies. Equivalently, the preselector requirements can be relaxed, permitting a simpler design. This scheme, combined with the preamplifier arrangement of Figure 4(b), is the recommended Case 1 configuration, summarized in Figure 12.

CASE 2. (40 MHz VCO)

The circuit configuration primarily considered is that of Figure 13, in which the phase-lock loop is closed around the second mixer. The second IF's considered are 15, 25 and 30 MHz. Since the second mixer LO (multiplied VCO) signal is a multiple of eight times the master-oscillator frequency, if the phase-detector reference signal multiplier is a submultiple of eight, the first IF will necessarily be a harmonic of the second IF. The phase-detector reference multipliers considered are therefore 3, 5, and 6.
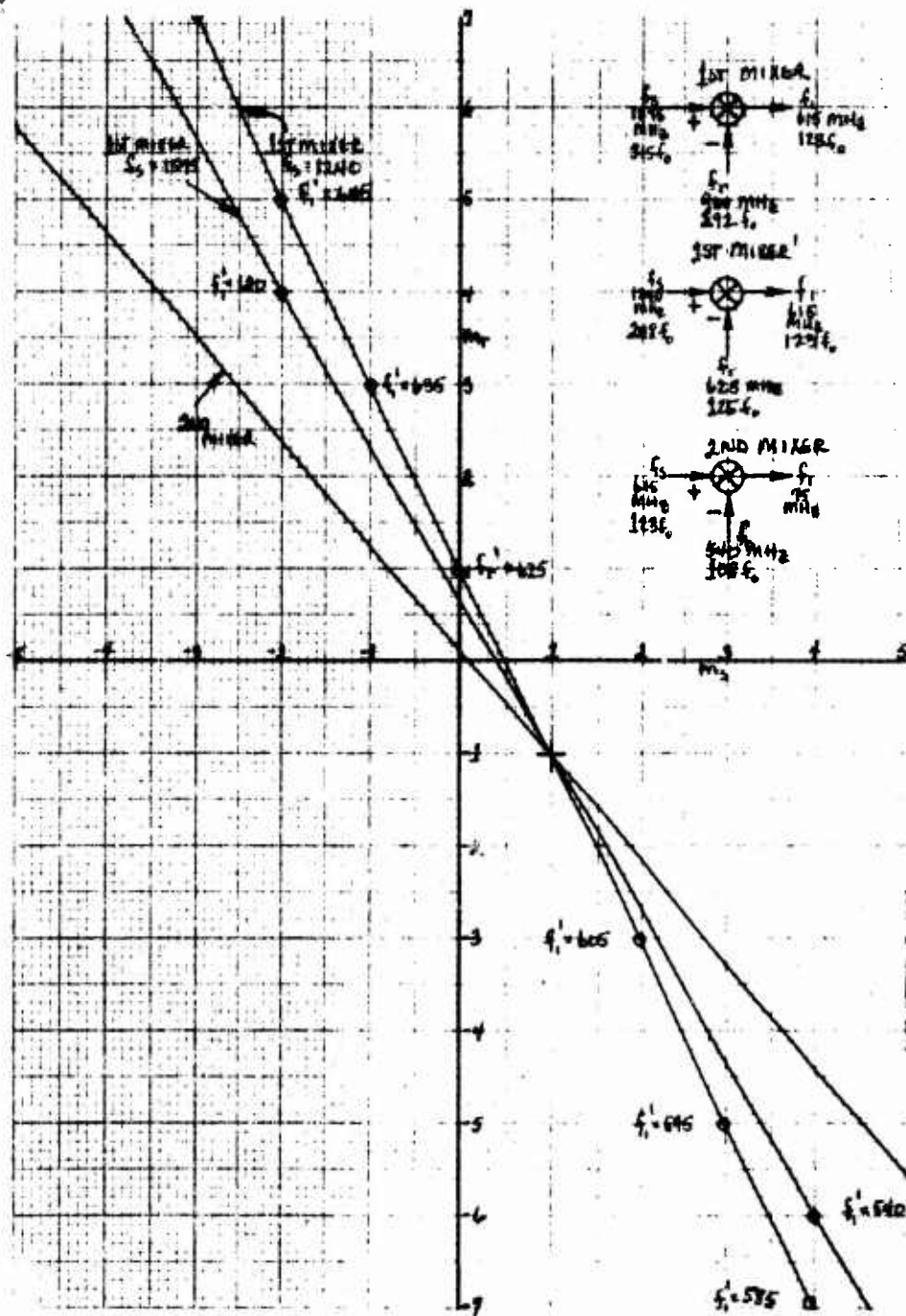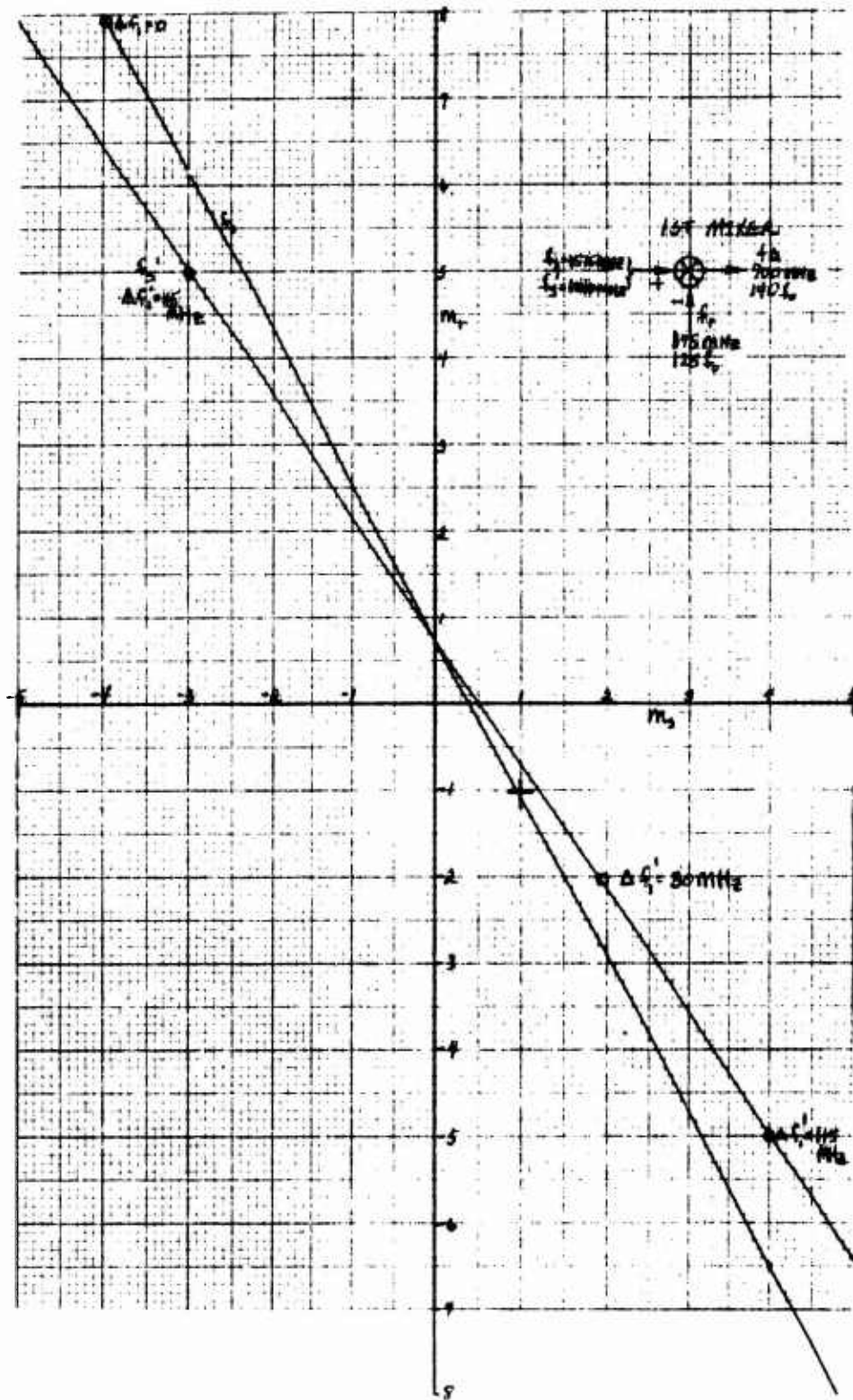
Figure 8.   Spurious Response Chart
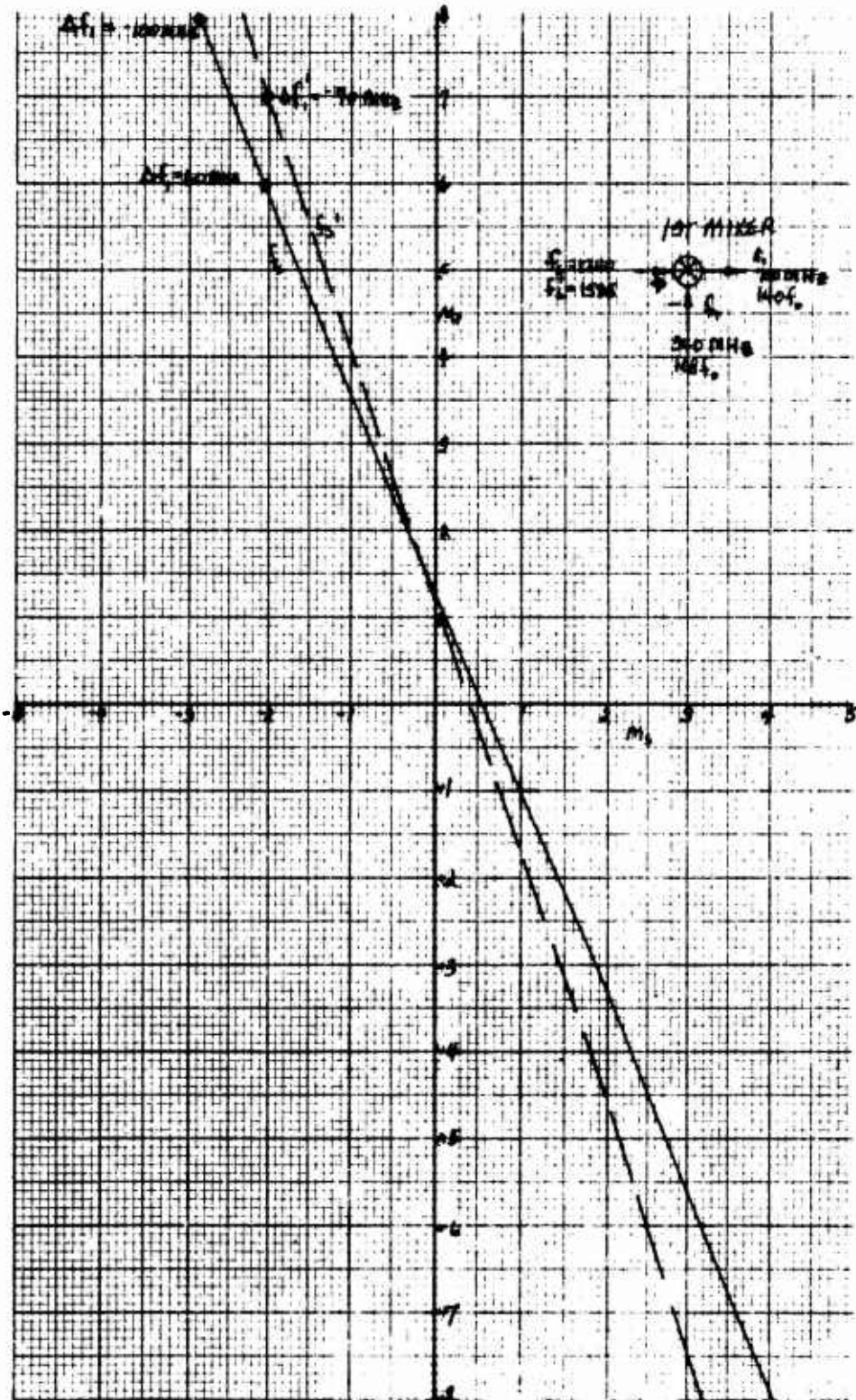
259

Figure 9. Spurious Response Chart

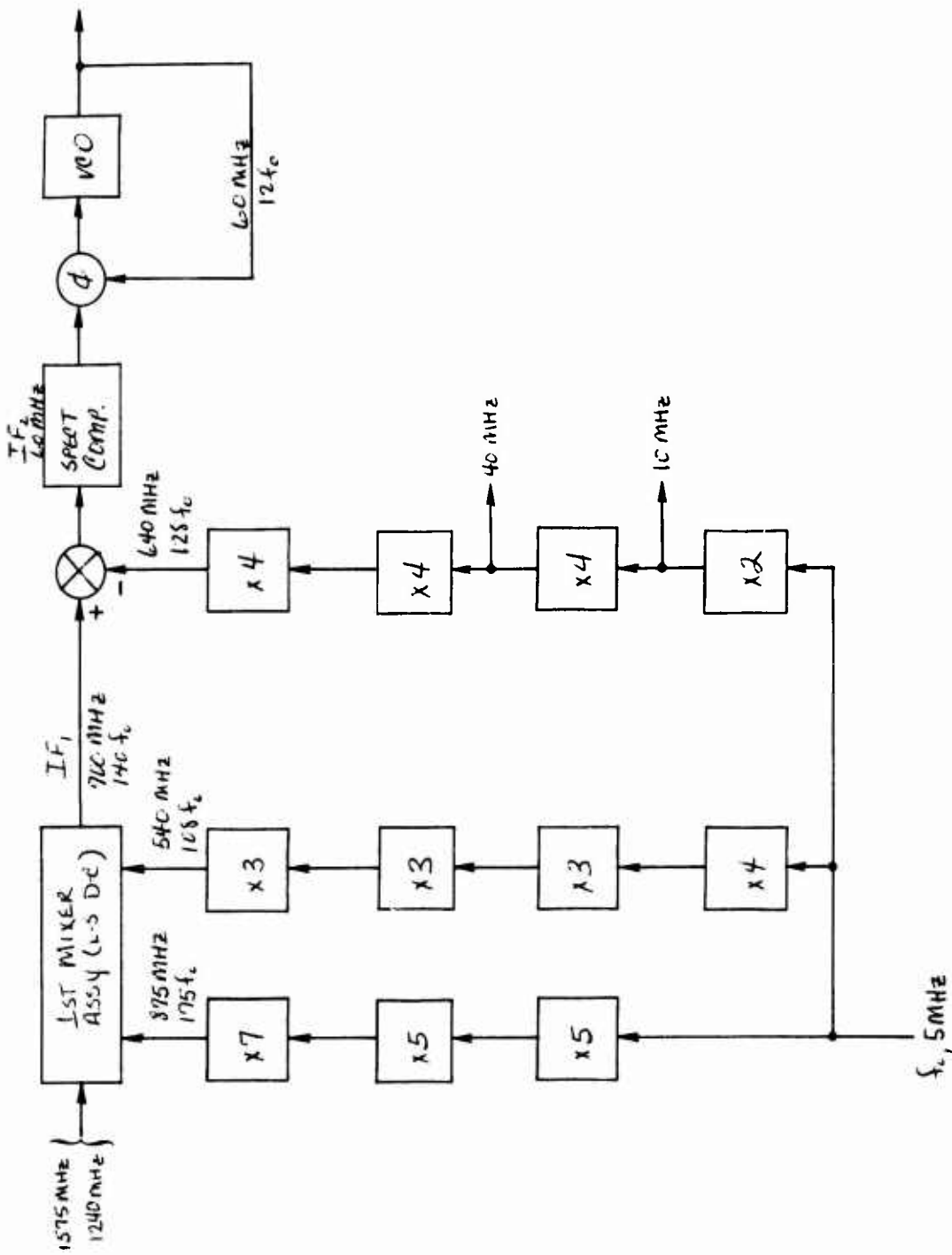Figure 10. Spurious Response Chart

261

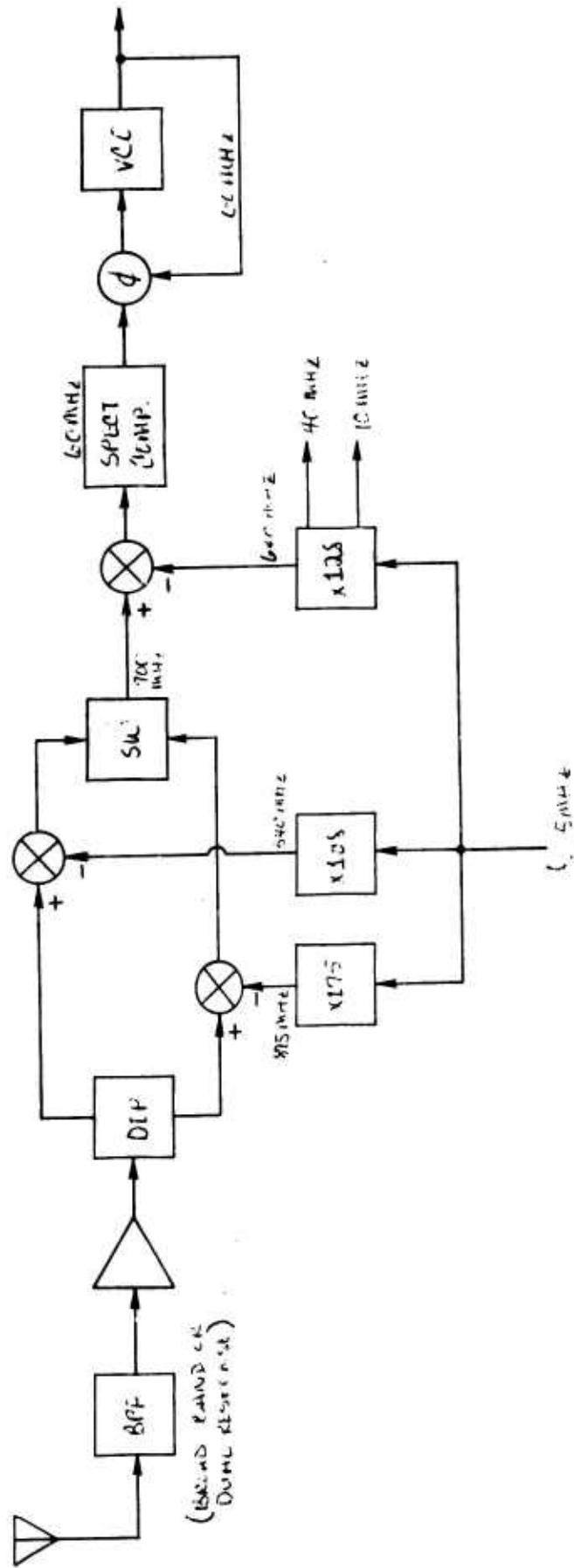Figure 11. 1st LO Chains, Alternate Dual-Conversion Configuration

Figure 72. Recommended Configuration (Case 1)

263
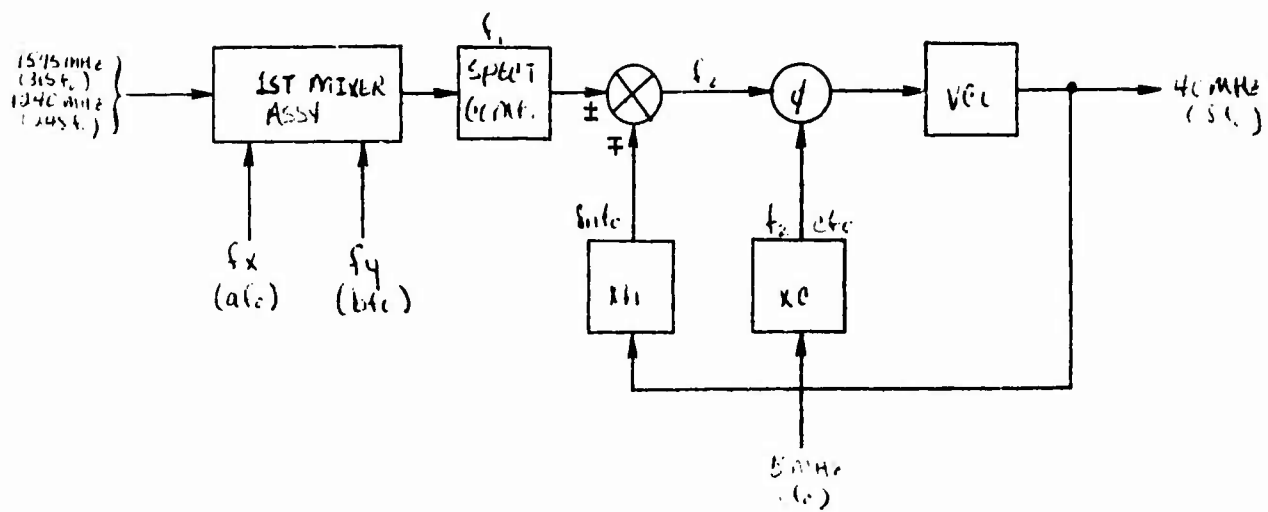
Inj	a	b	c	n	fx	fy	f_1	f_2	Set
LS	304	237	3	1	1520	1185	55	15	1
LS	296	229	3	2	1480	1145	95	15	2
LS	302	235	5	1	1510	1175	65	25	3
LS	294	227	5	2	1470	1135	105	25	4
LS	301	234	6	1	1505	1170	70	30	5
LS	293	226	6	2	1465	1130	110	30	6
HS	328	261	3	2	1640	1305	65	15	7
HS	336	269	3	3	1680	1345	105	15	8
HS	334	267	5	3	1670	1335	95	25	9
HS	333	266	6	3	1665	1330	90	30	10

Figure 13. Long-Loop Configuration

264

With these constraints, the choices of receiver frequencies and multiplier factors, giving a first IF between 55 and 110 MHz, are tabulated in Figure 13. Sets 8 and 10 are eliminated from further consideration because they result in a harmonic relation between first and second IF's. The remaining sets are tabulated in Figure 14 in order of first IF.

None of the required first LO multiplier factors can be factored into prime numbers of seven or less except for the 294 multiplier of set 4. This requires the LO frequencies to be generated by multiplication and mixing, rather than by multiplication alone. To achieve circuit simplicity, it is desirable that there be a common frequency between the two sets that are summed or differenced to provide the required first LO multiplication for each of the two received frequencies. This permits use of only three multiplier chains instead of four. One chain is then common to both frequency generators, as shown in the block diagram of Figure 14. This requirement eliminates sets 3, 6, and 9, which have no such common term. The spur charts for the signal second mixer and for the first LO mixers, for each of the remaining frequency sets, are shown in Figures 15-29. In the latter set, multiplier factors are used in lieu of frequencies.

Evaluation of sets 1, 2, 4, 5, and 7 is made on the basis of image/LO rejection capability, second mixer and LO mixer spurious responses, and overall circuit simplicity. The resulting ranking, in order of preference, is largely subjective because of the comparison of unlike things in many cases, and is shown in Table 1. The ranking in terms of second-mixer spurs is given minimum weight, since by use of a narrow-band crystal pre-mixer filter, no significant spur problems should exist for any of these sets. The most attractive frequency plan, considering the above factors, appears to be that of set 4, with set 2 being second choice. The overall multiplier/mixer configuration for set 4 is shown in Figure 30. Low-side injection is used in both first and second mixers. Figure 31 illustrates the relative complexity of the other LO generation schemes.

It is possible to find a frequency combination such that no mixing is required to generate the first LO frequencies. That is, the two first LO signals may each be generated by multipliers having prime factors of seven or less. However, this entails a very high first
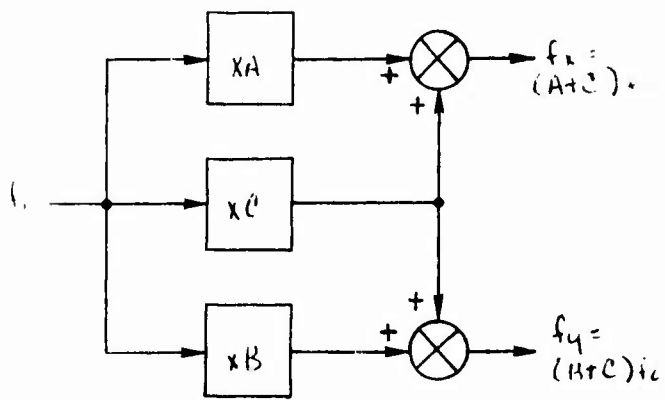
Sets 1,2,5,7
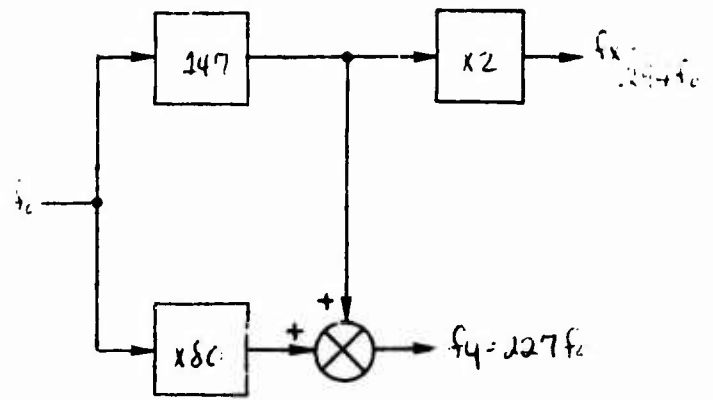
Set 4

Set	Inj	f_1	f_2	a	b	A	B	C
1	LS	55	15	304	237	2^8	$3^3.7$	$2^4.3$
						$2^6.3$	5^3	$2^4.7$
						$2^4.7$	$3^2.5$	$2^6.3$
7	HS	65	15	328	261	2^8	$3^3.7$	$2^3.3^2$
						$2^4.7$	$3^2.5$	$2^3.3^2$
3	LS	65	25	302	235	-	-	-
5	LS	70	30	301	234	2^8	$3^3.7$	$3^2.5$
						$5^2.7$	$2^2.3^3$	$2.3^2.7$
						$2^4.7$	$3^2.5$	$3^3.7$
2	LS	95	15	296	229	2^8	$3^3.7$	$2^3.5$
9	HS	95	25	334	267	-	-	-
4	LS	105	25	294	227	3.7^2	$2^2.5$	3.7^2
6	LS	110	30	293	226	-	-	-

Figure 14. LO Generator Configuration
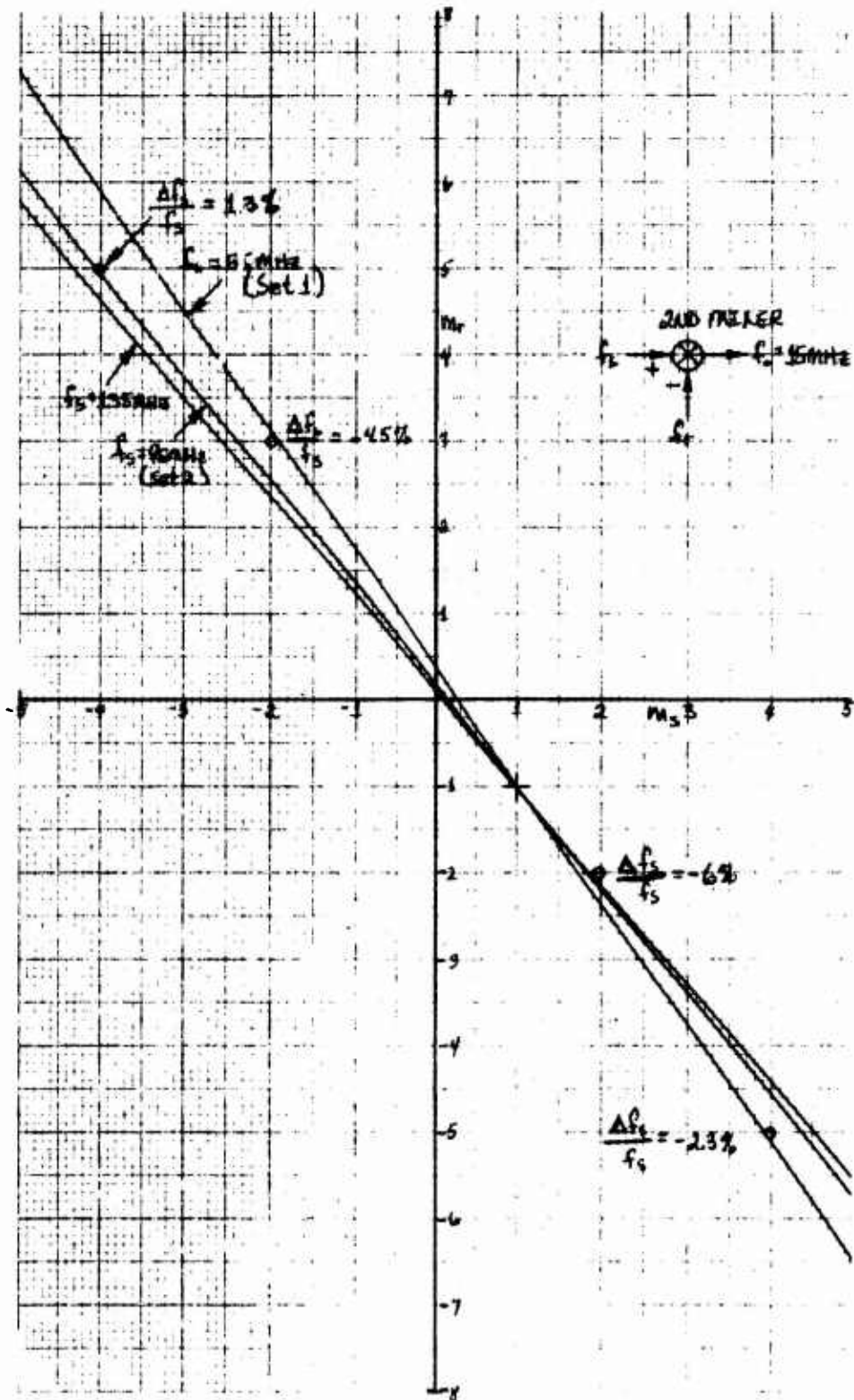
Figure 15. Spurious Response Chart

267
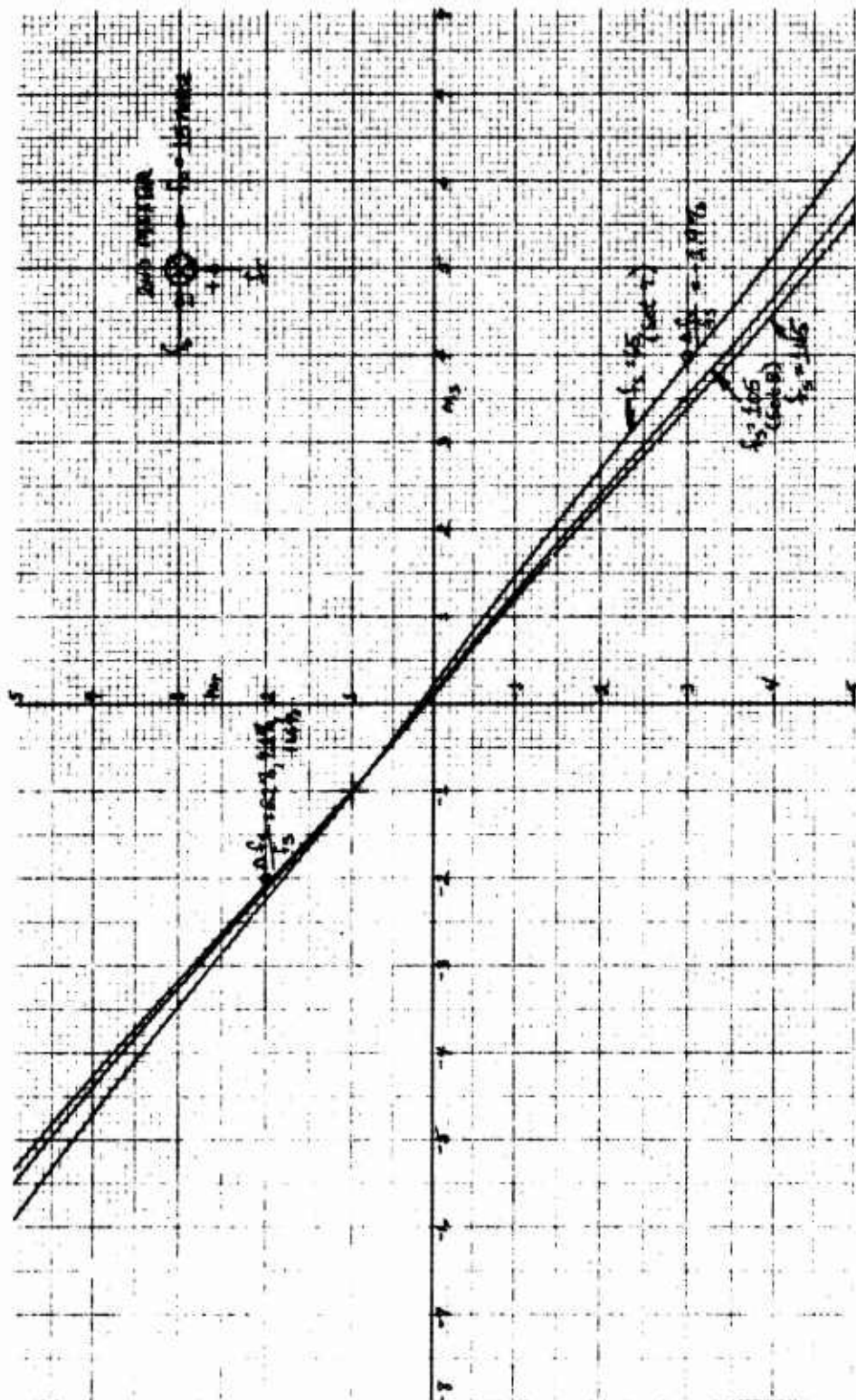
Figure 16.   Spurious Response Chart

268
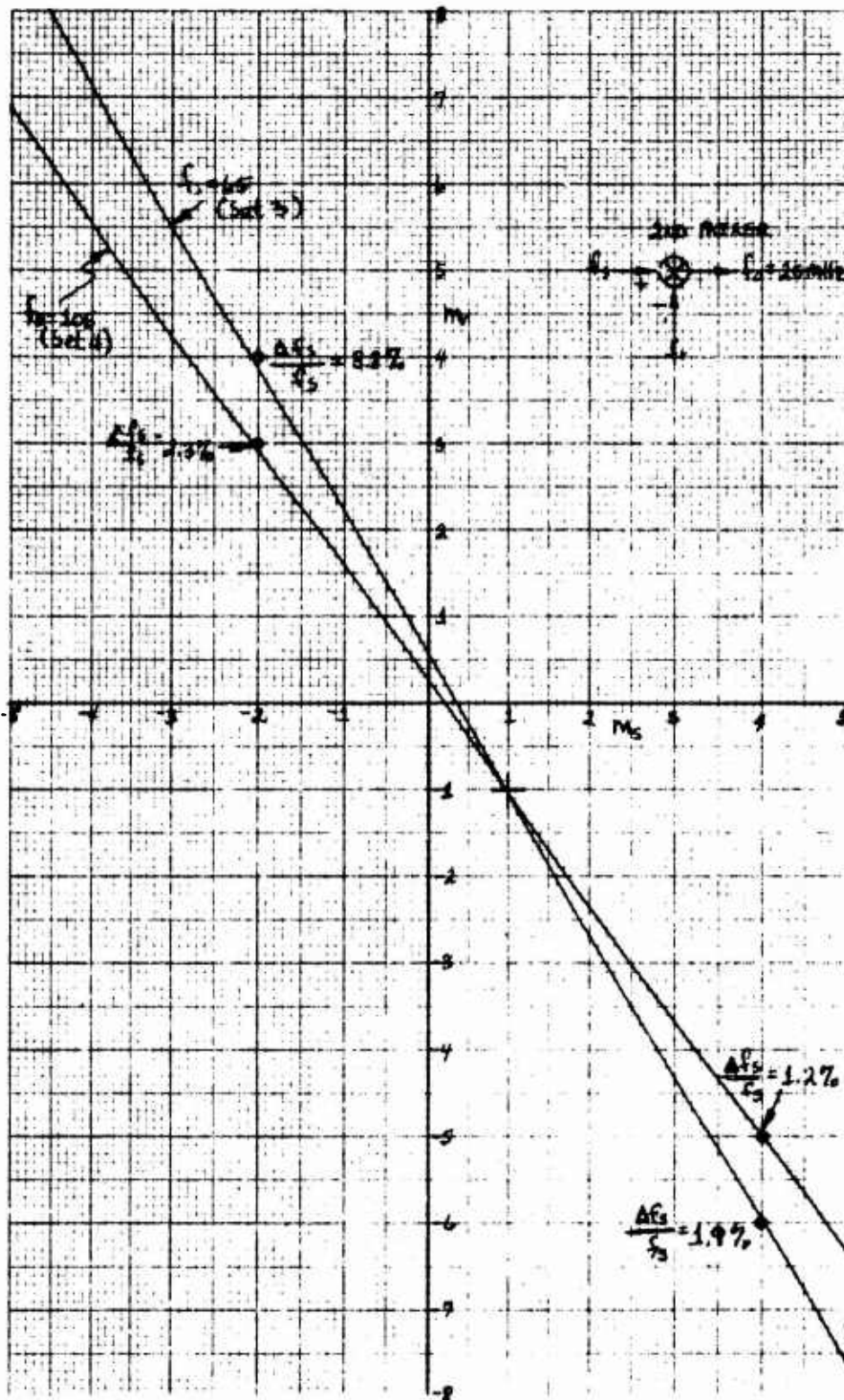
Figure 17.   Spurious Response Chart

269
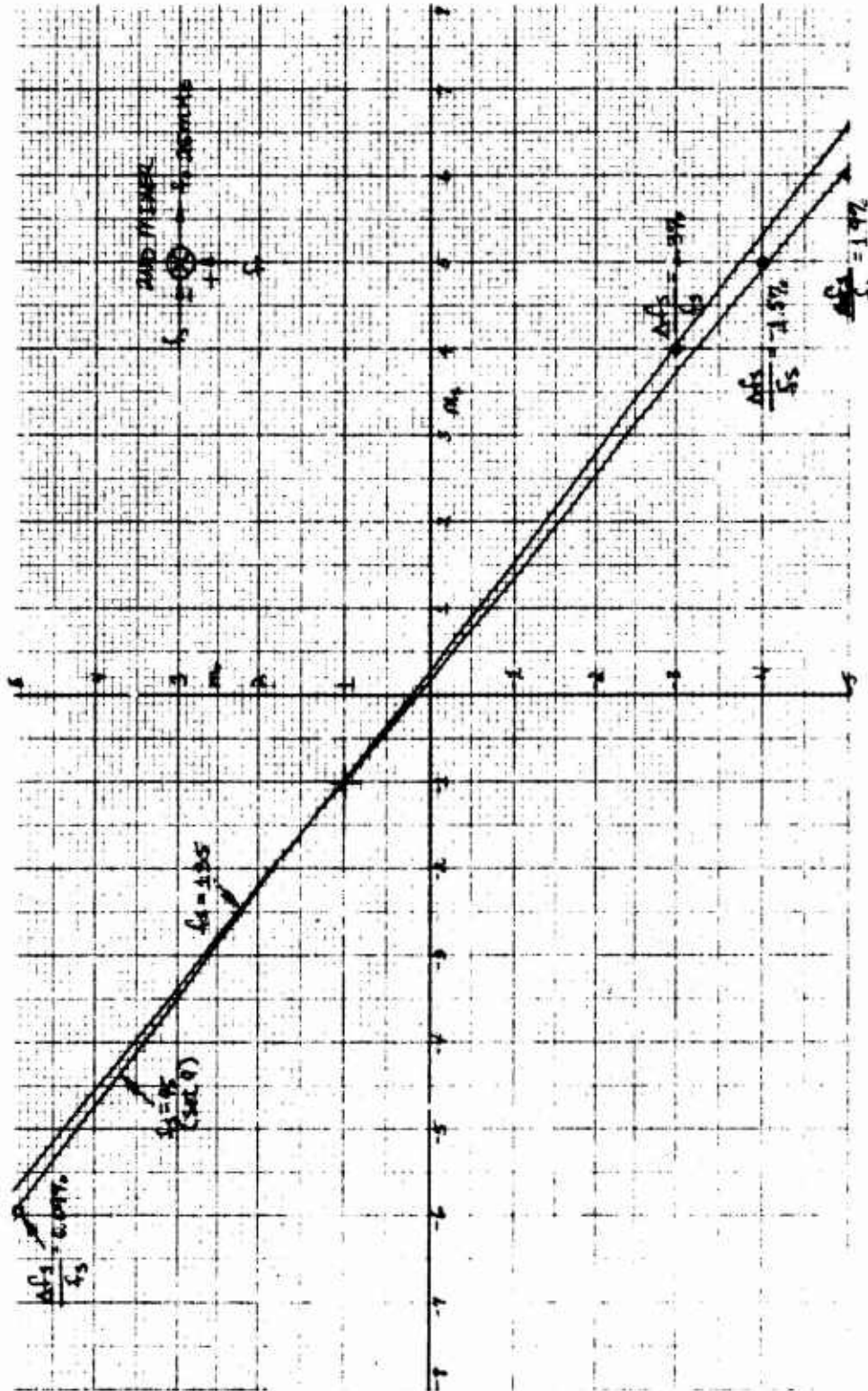
Figure 18. Spurious Response Chart

270
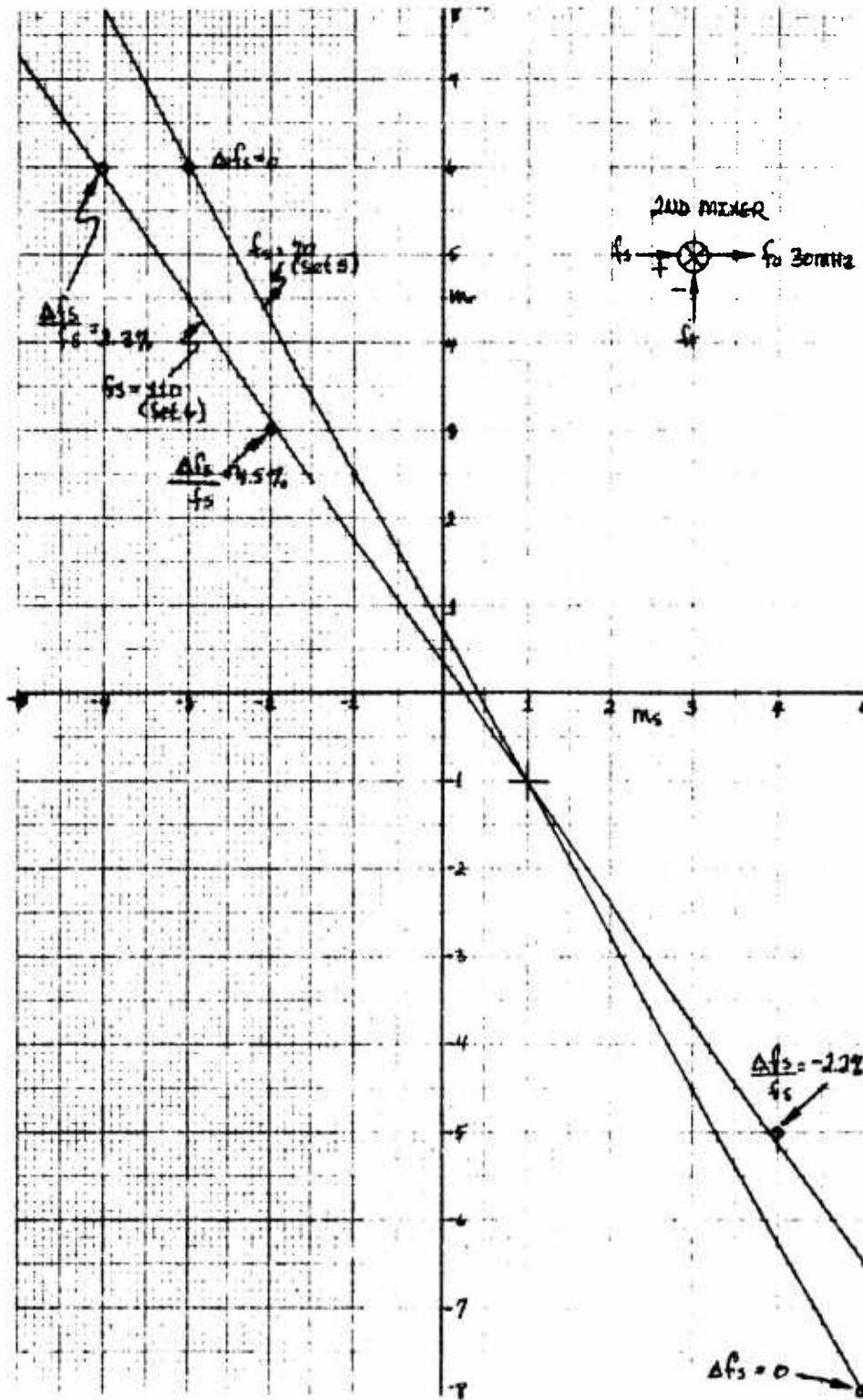
Figure 19. Spurious Response Chart

271
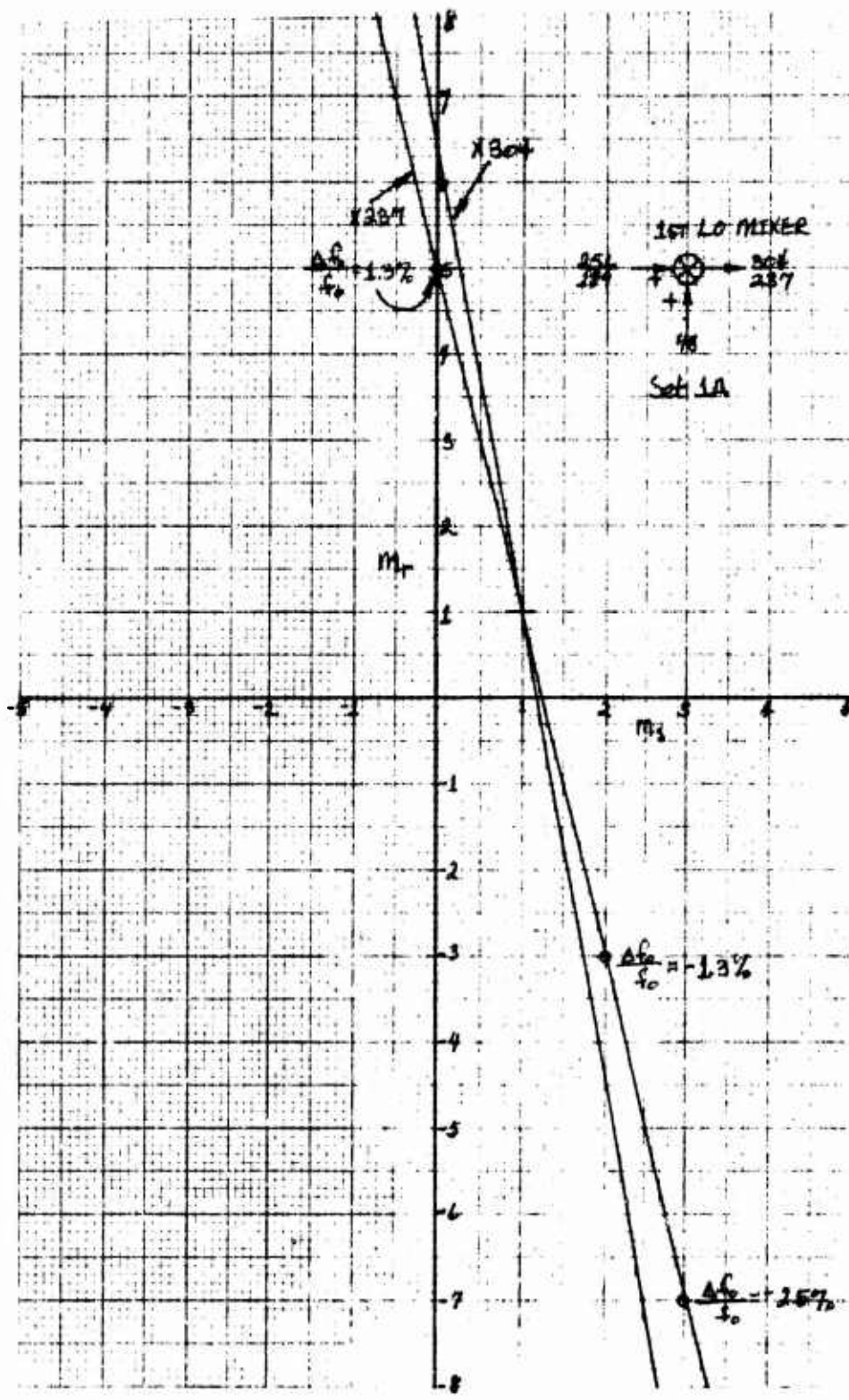
Figure 20.   Spurious Response Chart

272
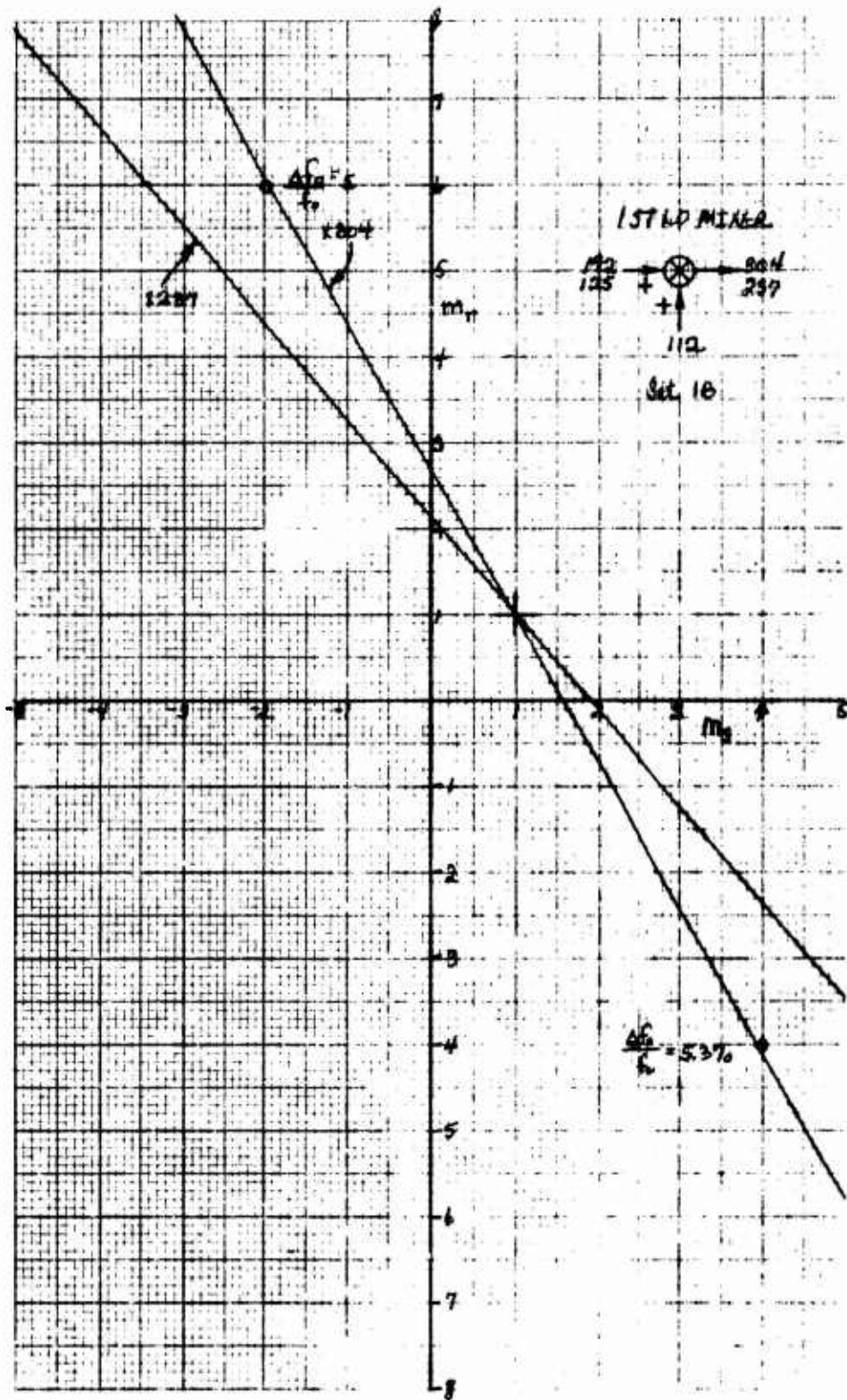
Figure 21.   Spurious Response Chart
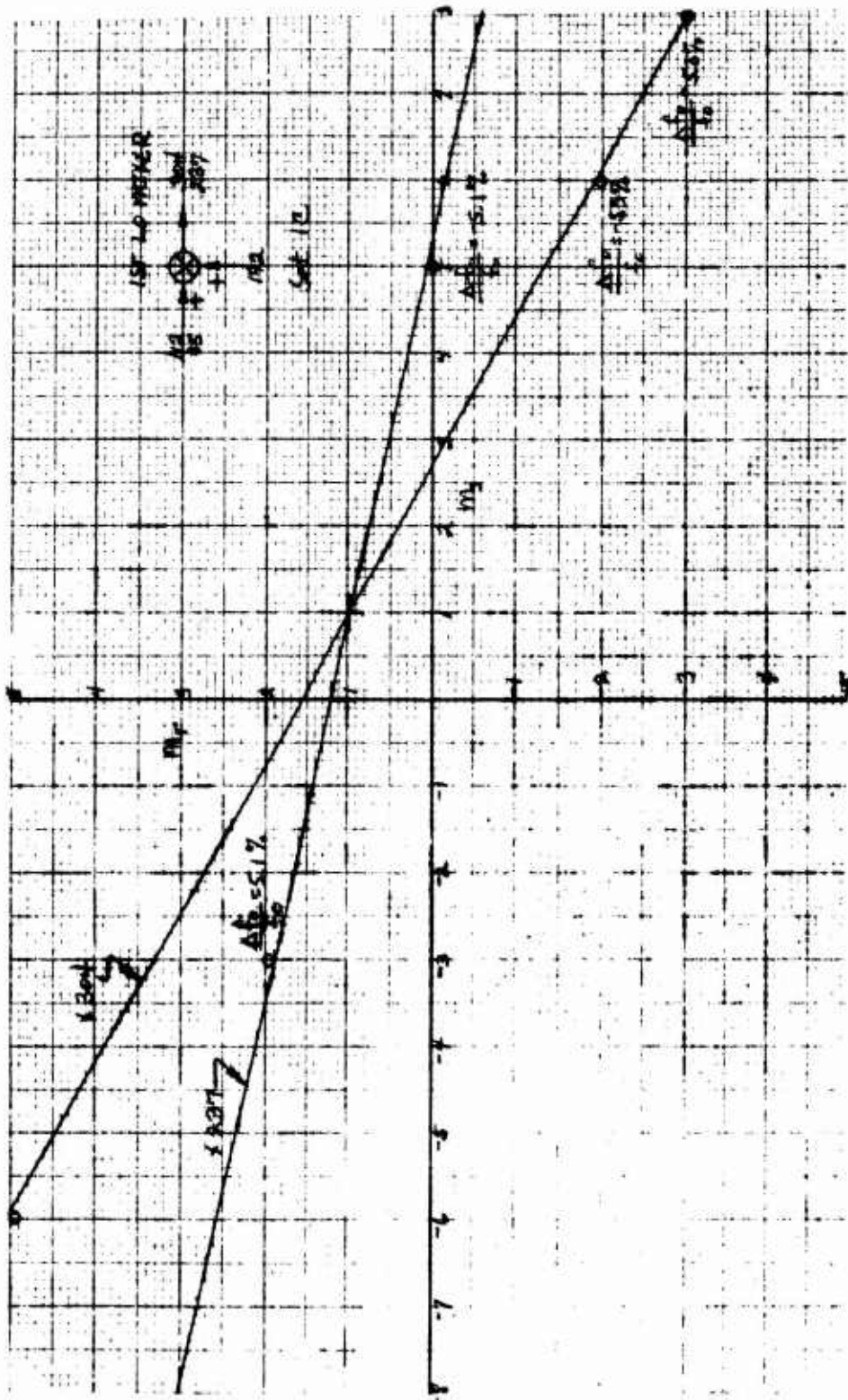
Figure 22. Spurious Response Chart

274
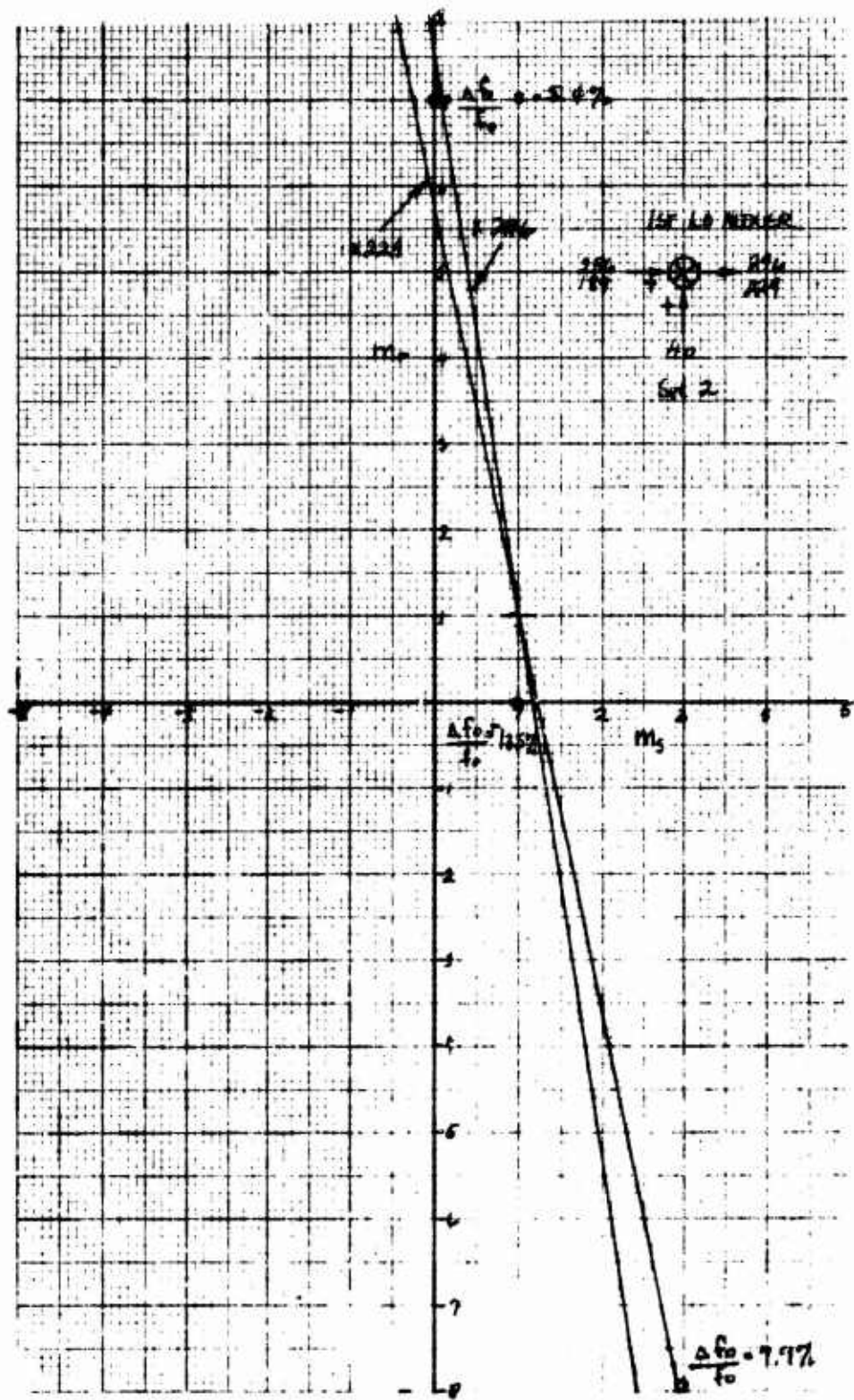
Figure 23.   Spurious Response Chart

275
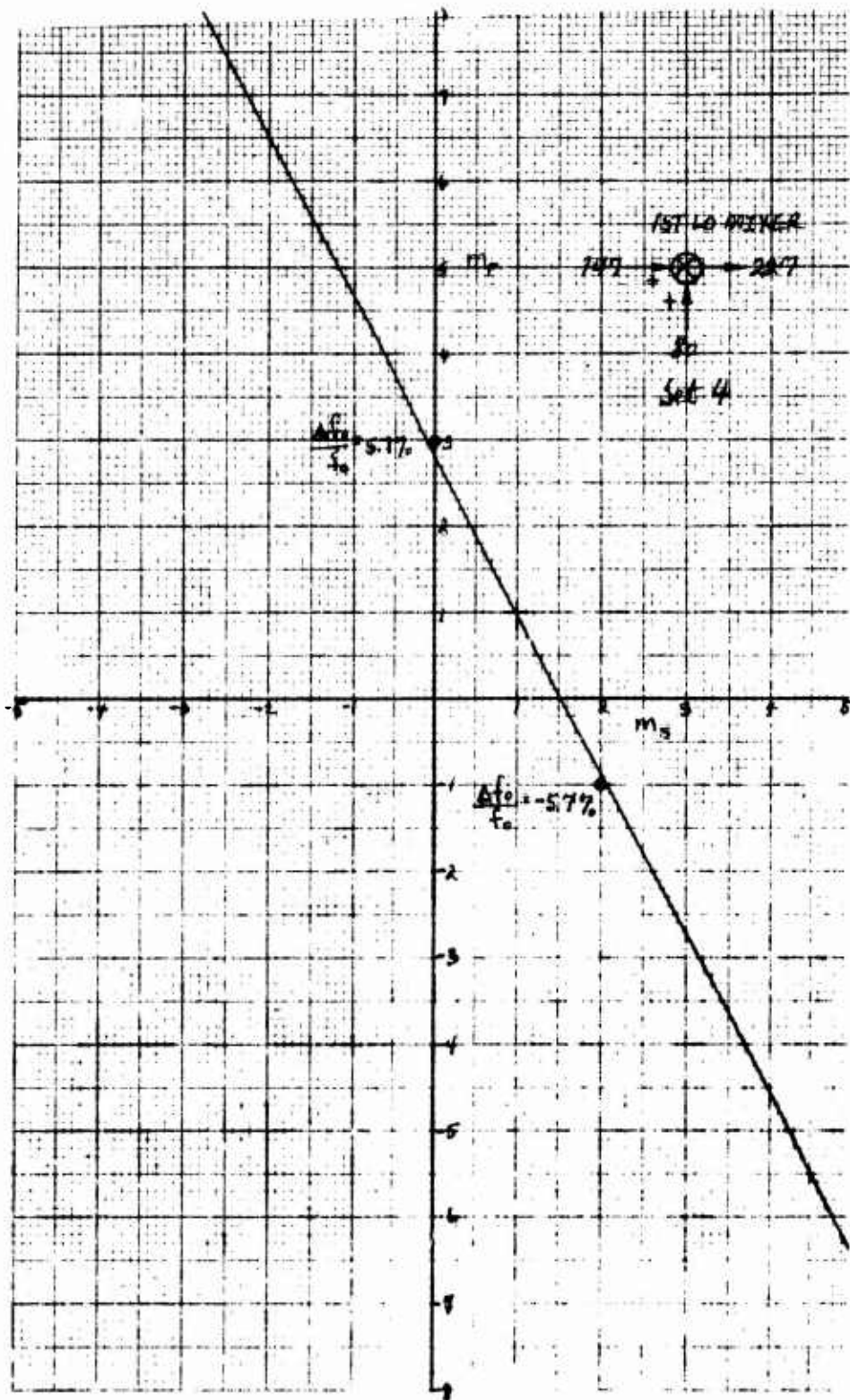
Figure 24.   Spurious Response Chart
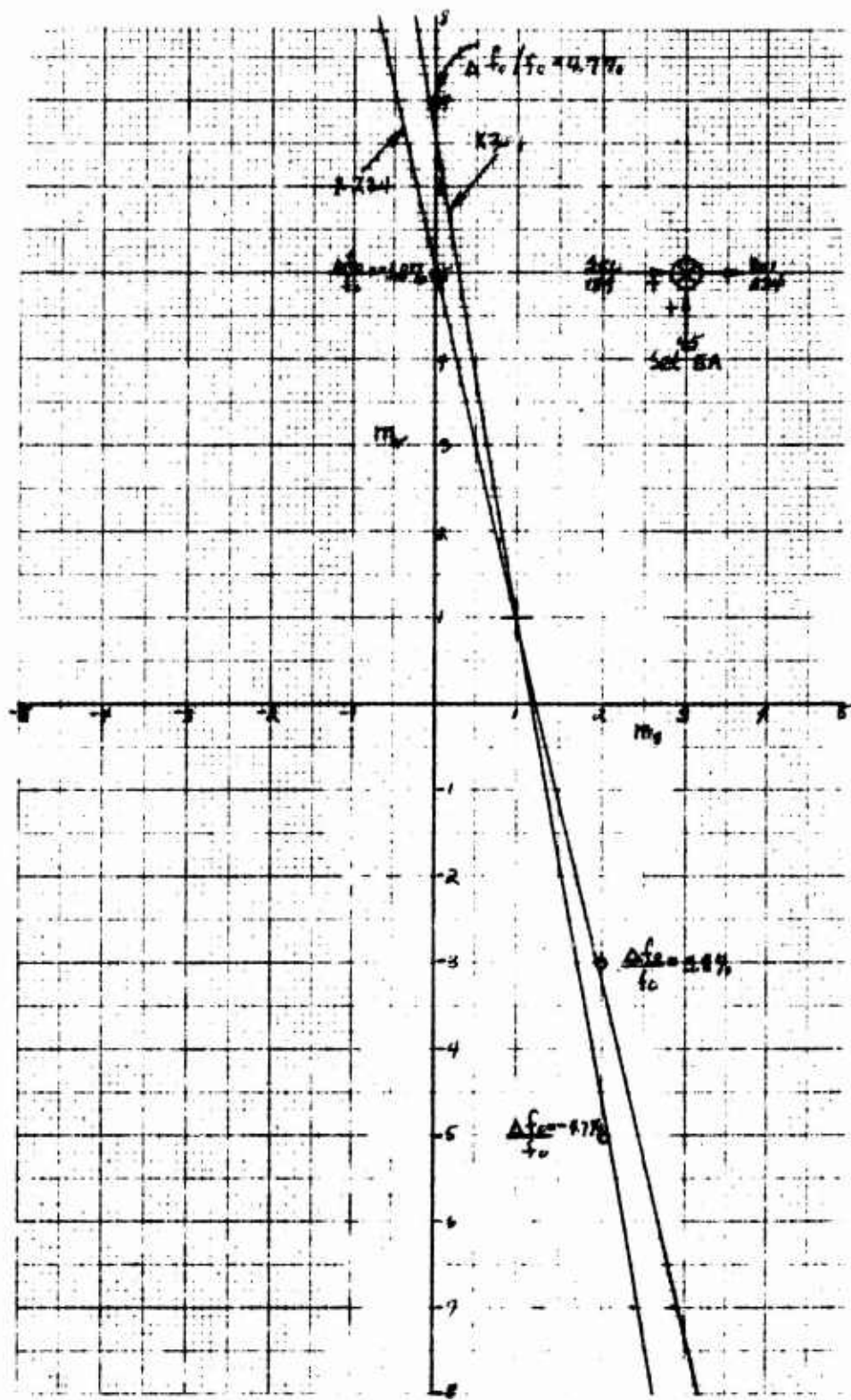
Figure 25.   Spurious Response Chart

277
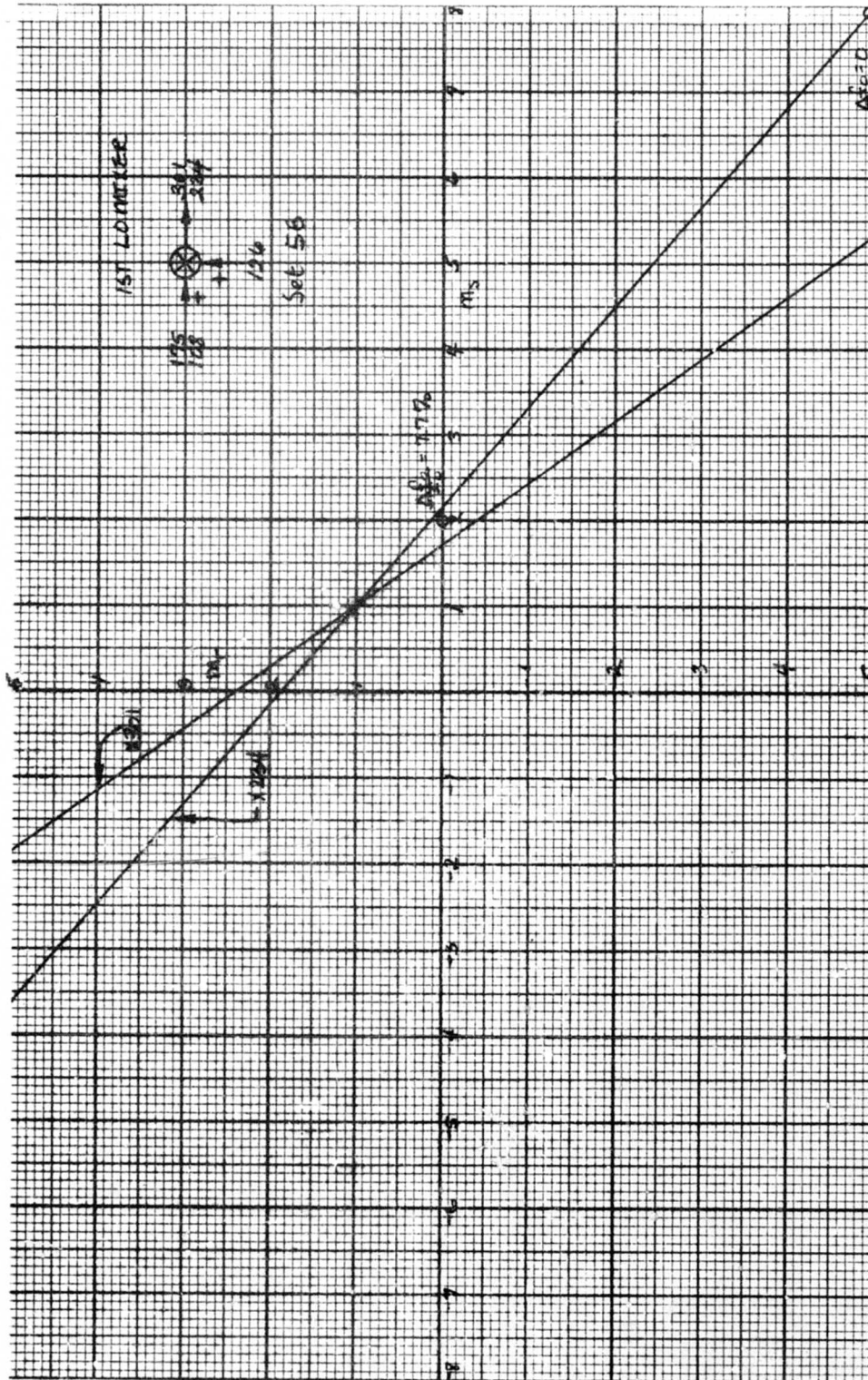
Figure 26. Spurious Response Chart

278
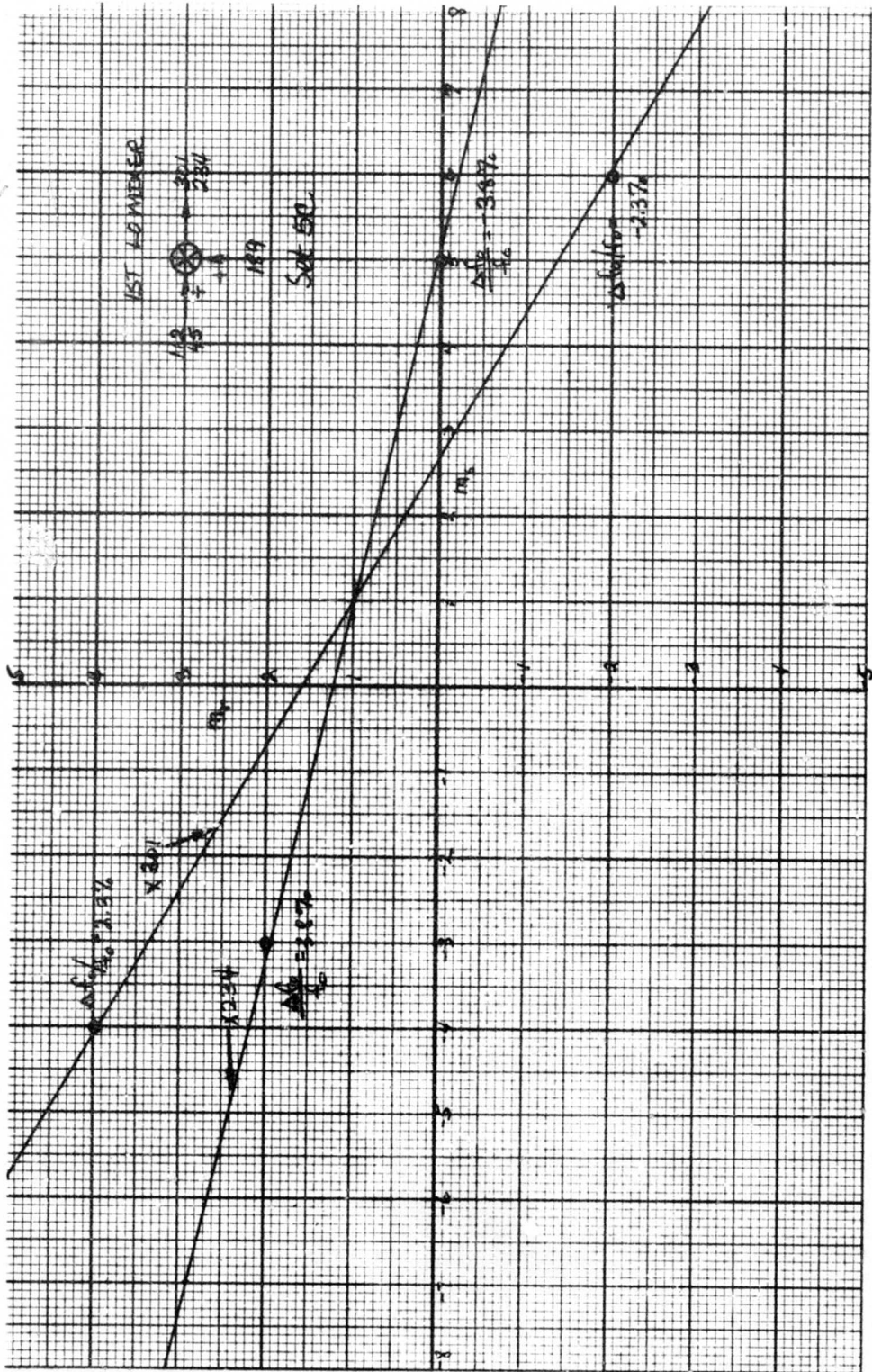
Figure 27. Spurious Response Chart

Figure 28. Spurious Response Chart

Figure 29.   Spurious Response Chart
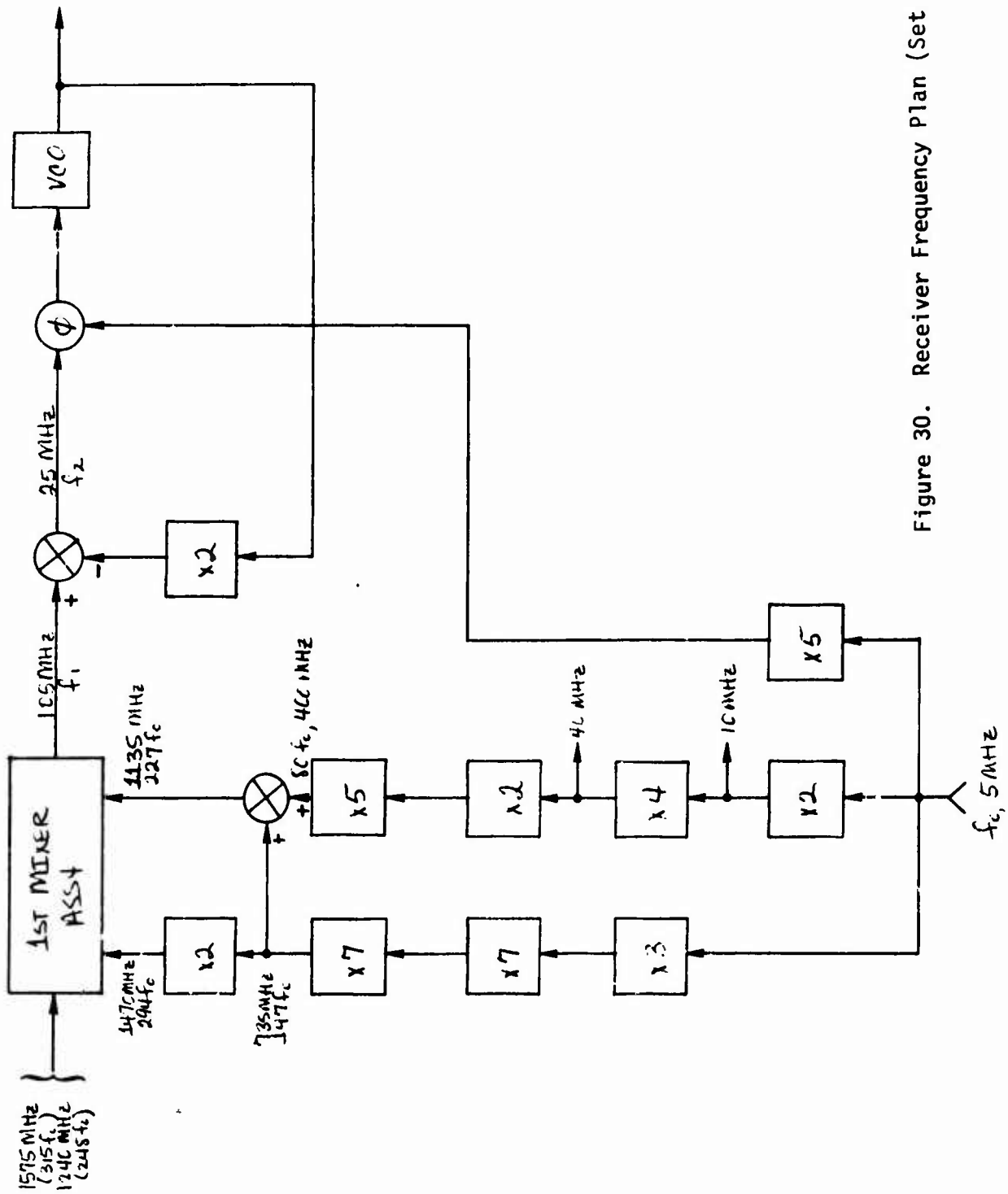
Figure 30. Receiver Frequency Plan (Set 4)

282
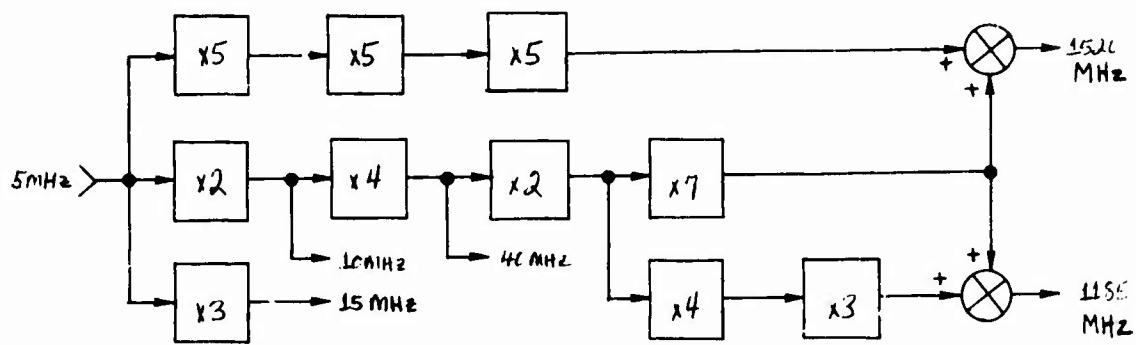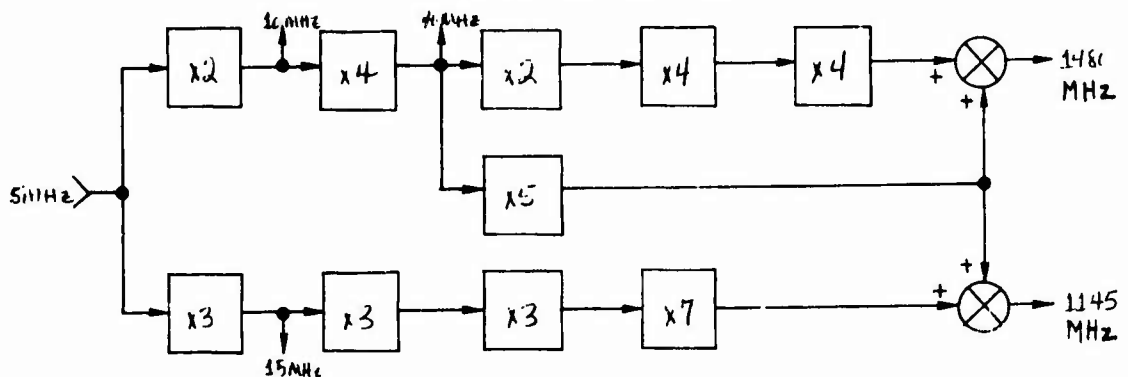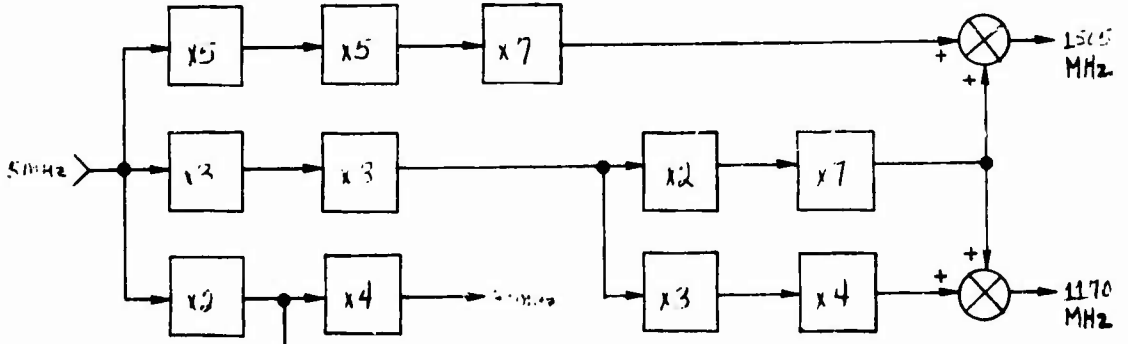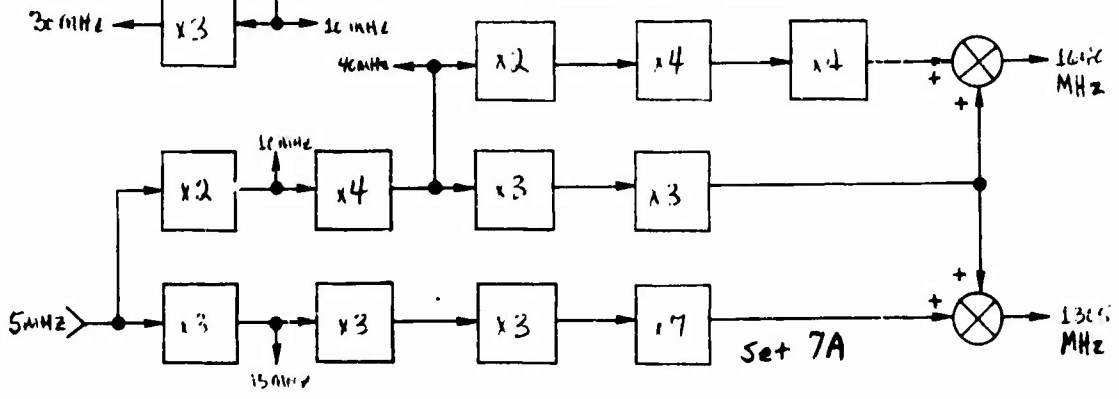
Figure 31. LO Generator Schemes

283

TABLE 1.   RANKING OF FREQUENCY PLAN SETS (CASE 2)

Simplicity	LO Mixer Spurs	2nd Mixer Spurs	Image/LO Rejection
4	1B	5	4
1B	2	1	2
2	4,5B	7	5
5B,7A	7A	2	7
		4	1

IF, precluding narrow-band filtering prior to the second mixer since crystal filters are not feasible at frequencies much above 100 MHz.

No frequency combination satisfying the problem constraints was found for a second IF of 25 or 30 MHz. For a 15 MHz second IF, the most favorable appearing combination consists of first LO multipliers of 192 and 125 and a second LO (VCO) multiplier of 15. This combination, shown in Figure 32, results in a 615 MHz first IF. While this gives excellent image and LO suppression, IF noise figure is somewhat higher and stage gain is lower than for the much-lower first IF's previously considered.

The use of a high first IF is made feasible if spectrum compression is done at the first IF and narrow-band filtering at the second IF. An additional, wider-band filter between the modulation and second mixer is then needed to suppress excitation frequencies leading to spurious responses in the second mixer. The rejection bands include those frequencies of half the second IF or greater removed from the carrier. With such filters, there are no second-mixer spur problems. However, the first-mixer spur chart, Figure 33, shows close-in, low-order spurs, particularly for the 1240 MHz input frequency. This particular set of frequencies is therefore undesirable.

An alternate frequency set for this configuration, shown in Figure 34, has first LO multipliers of 112 and 45 and a second LO multiplier of 25. This results in first and second IF's of 1015 and 15 MHz, respectively. The first IF is undesirably high. IF rejection is now more significant than image or LO rejection; and IF noise figure and stage gain are more of a problem. However, the first mixer spurious responses, shown in Figure 35, are entirely acceptable, and the configuration, shown in Figure 34, is slightly simpler than that of the previous set (Figure 32). The relative bandwidth required of the filter immediately proceeding the second mixer is now little more than half that of the previous case - a severe constraint, considering that the second-mixer image is only 30 MHz from the center of the passband.

A modification of this scheme, shown in Figure 36, closes the phase-lock loop around the phase detector instead of the second mixer. It is even simpler in configuration, but requires a first IF of 840 MHz

285

Figure 32. High First IF, Configuration A₁
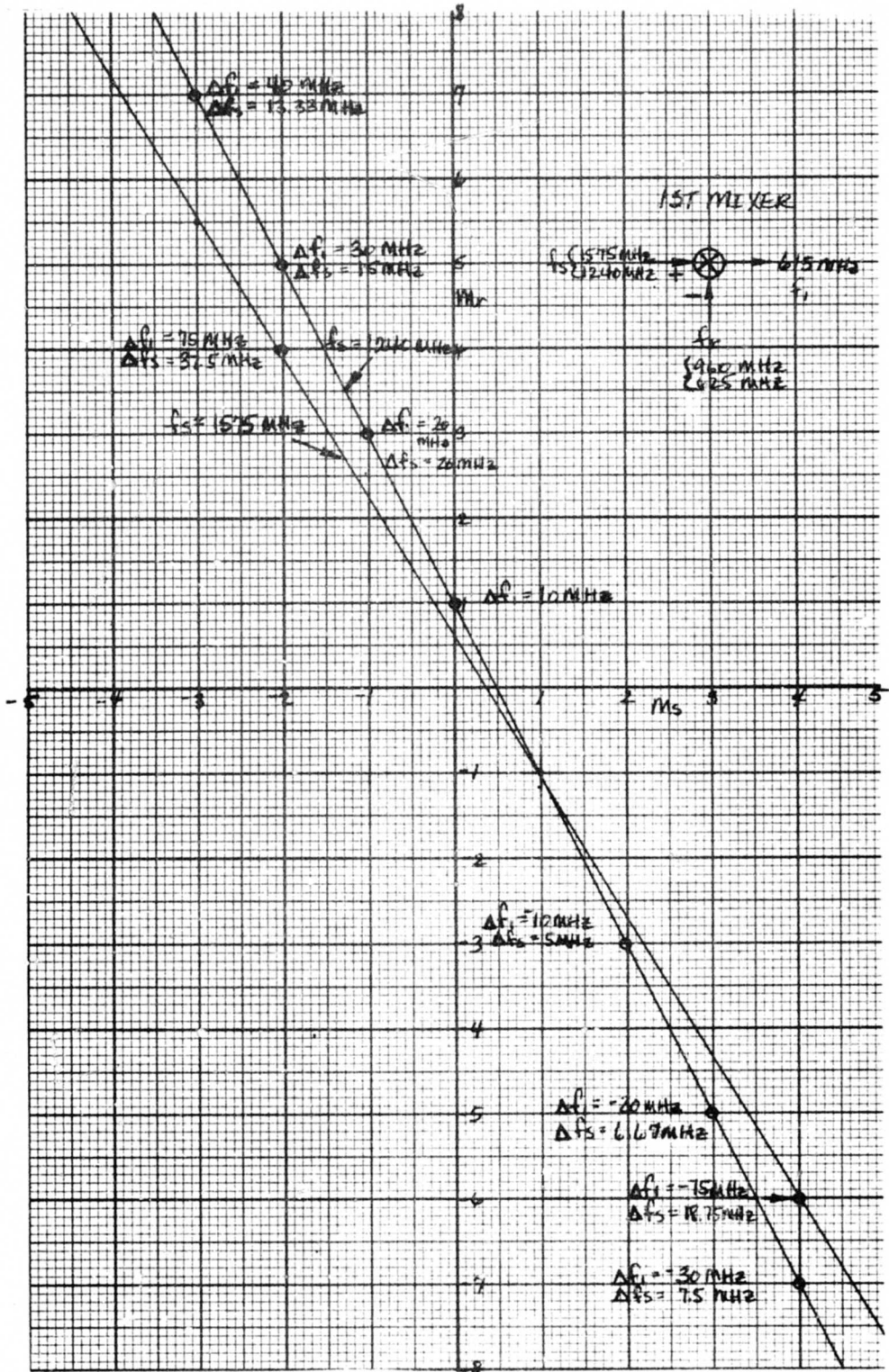
Figure 33. Spurious Response Chart
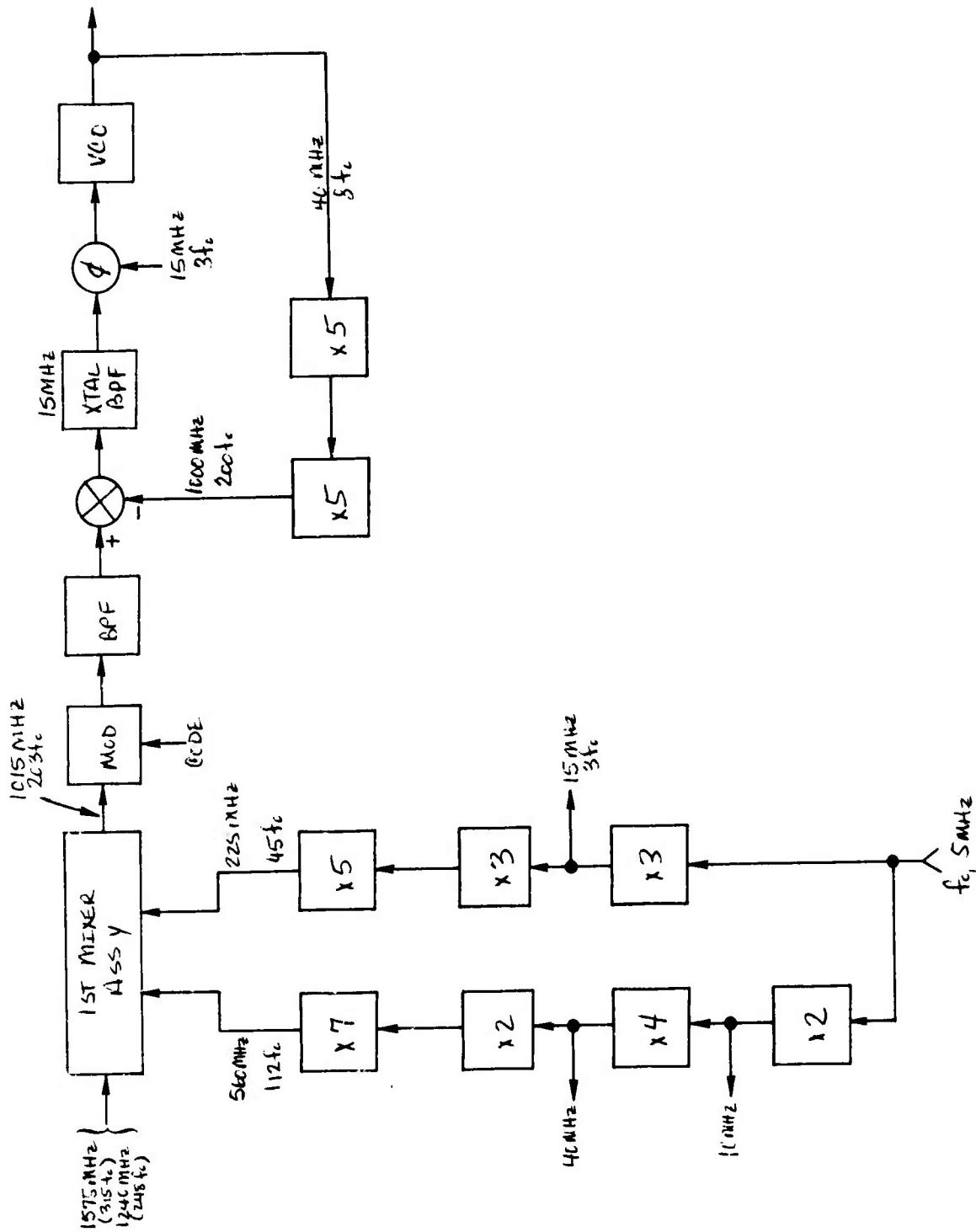
Figure 34. High First IF, Configuration A_2
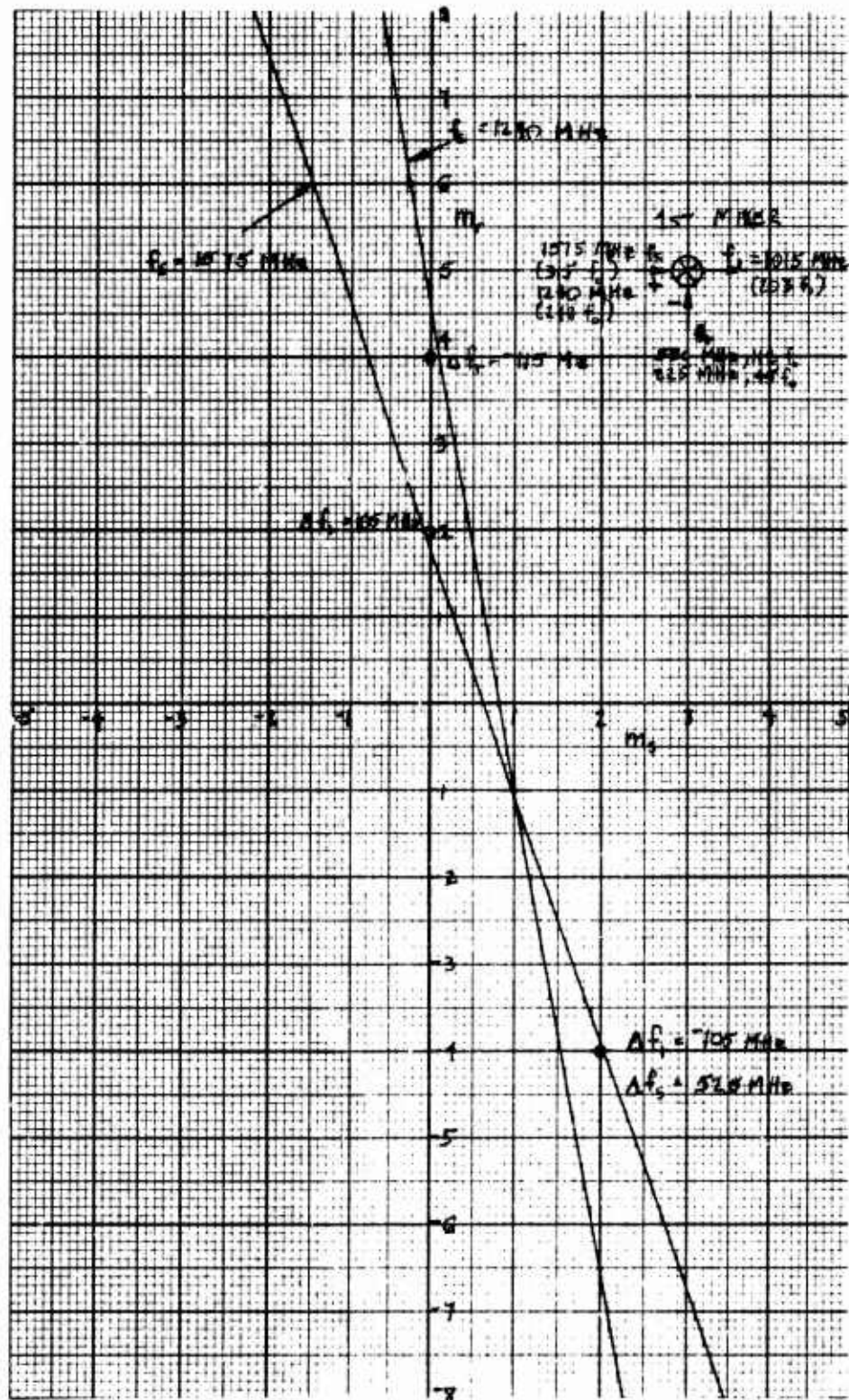
Figure 35.   Spurious Response Chart

289
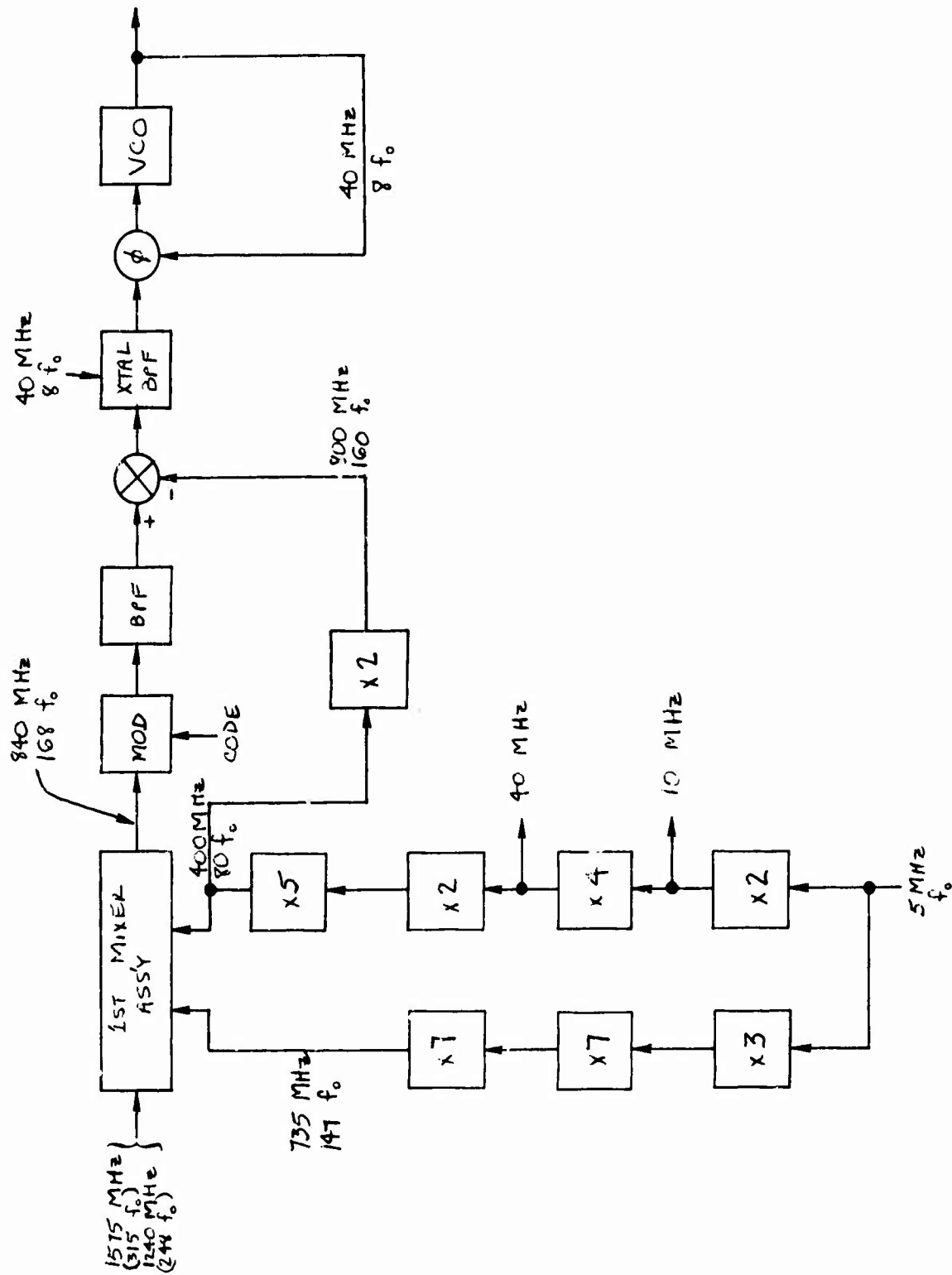
Figure 36. High First IF Configuration B

290

and a second IF of 40 MHz. Its first-mixer spur chart, Figure 37, shows the worst-case spur to be for the 1240 MHz input. It is of 6th order and is excited by an input 20 MHz below the carrier. It is most likely acceptable, particularly since being of even order in both signal and LO it is amenable to considerable suppression by use of a doubly-balanced mixer.

The conclusion for Case 2 is that the most likely candidate schemes are those of Figures 30, 34, or 36. There is no clearly outstanding choice among these, and the selection is necessarily subjective, based largely on compatibility with the overall receiver design philosophy.
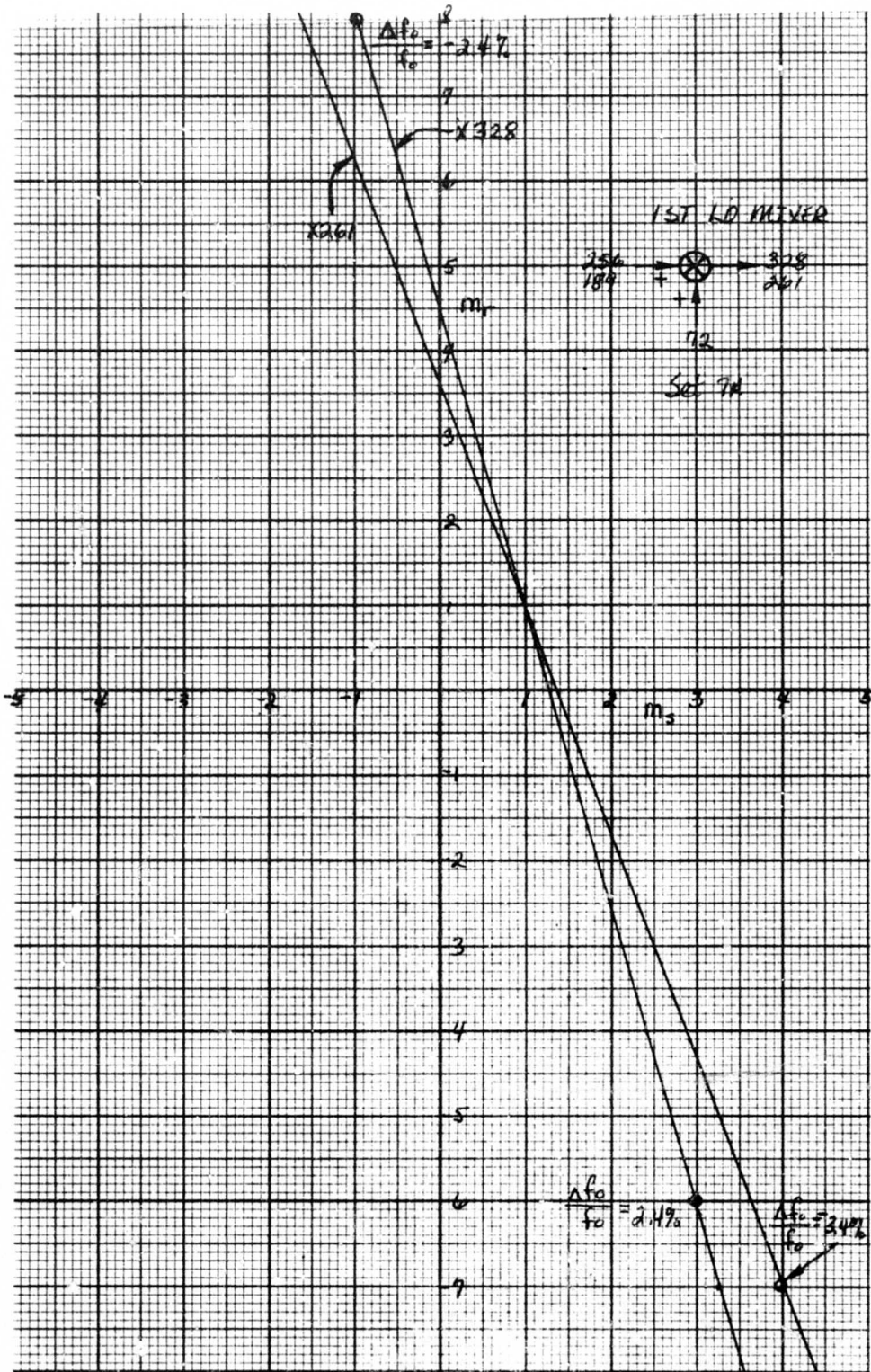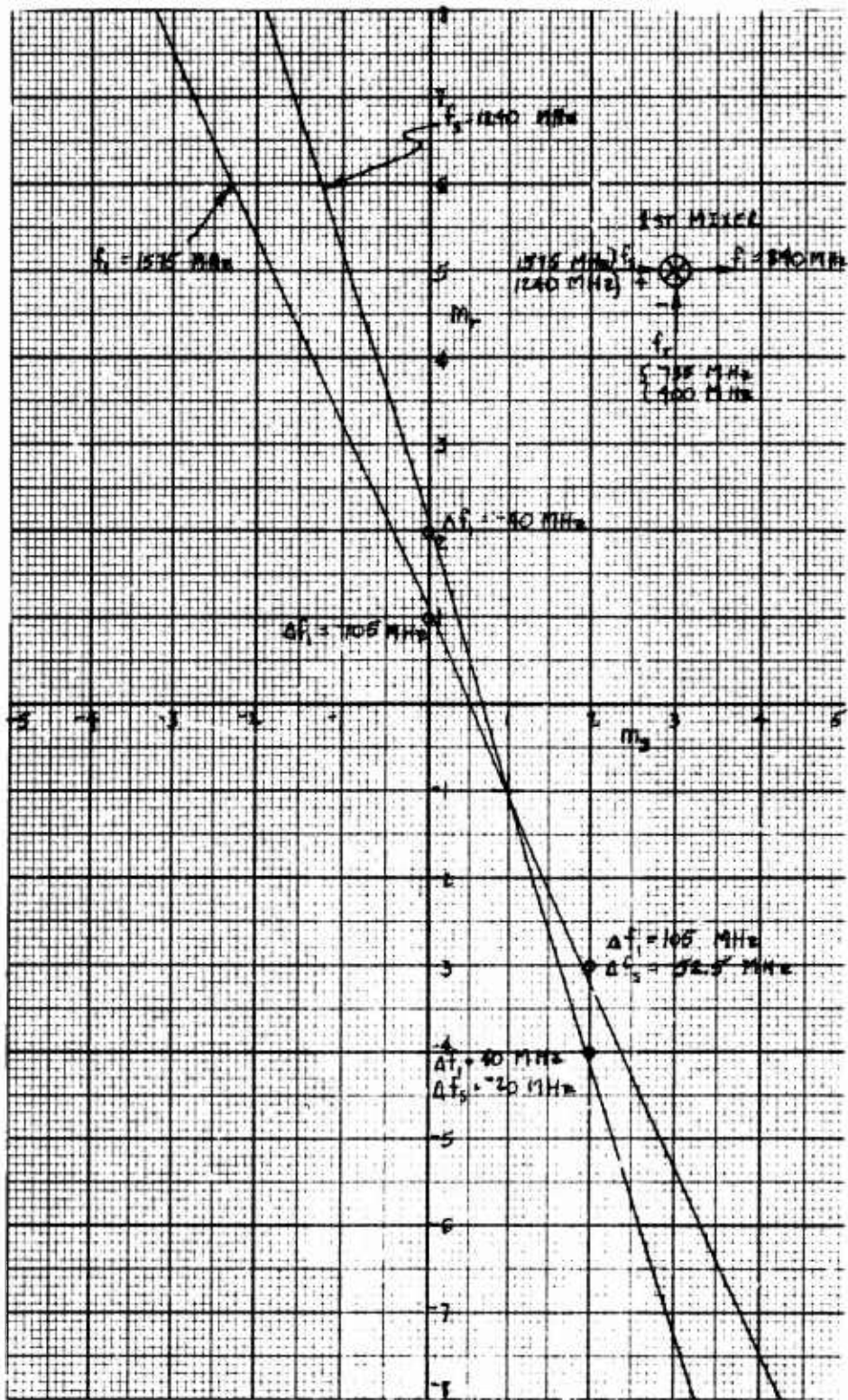
Figure 37.   Spurious Response Chart

APPENDIX 9

DERIVATION OF MAXIMUM
L_1/L_2 RANGE DIFFERENCE

In a memo from W. E. Waters (Philco-Ford), entitled "DNSDP Users - Ionospheric Range Error Corrections", and dated 27 July 1973, the equation for ionospheric range error is given as

$$R_e = 1.32 \left(1 + \frac{H}{R}\right)\left(\frac{I_v}{f^2}\right) \bigg/ \left\{ \sin^2 E + \frac{2H}{R} + \left(\frac{H}{R}\right)^2 \right\}^{1/2}$$

where R_e = ionospheric range error, feet

   H = scale height of the ionosphere

   R = Earth's radius (= 6378 Km)

   Iv = vertical integrated electron content, hexams

   f = radio frequency, GHz

   E = elevation angle, user to satellite

Waters also gives a range of values for H (350-400 Km), and a maximum vertical integrated electron content of 260 hexams.

For a worst case analysis, we will use

   H = 400 Km

   Iv = 260 hexams

   E = 10 degrees

Then,

   R_e (f = 1.575 GHz)   368 ft

   R_e (f = 1.24 GHz)   594 ft

Thus, the maximum difference in ionospheric range error is (594-368) or 226 ft.

APPENDIX 10

CORRELATIONS OF TROPOSPHERIC CORRECTION ERRORS

In the referenced memo errors were derived for the various methods of correcting for the tropospheric delay in the user software. The method likely to be employed by the great majority of users is a predetermined function of line of sight elevation and user altitude:

$$\Delta R = \csc E \, K_T \, e^{-\left(\frac{h}{K_H}\right)}$$

h = user altitude above sea level

E = line of sight elevation

K_T and K_H are predetermined constants

K_T and K_H are actually functions of the atmospheric conditions along the line of sight. The 1σ error in this expression was estimated as 2.0 feet at $E = 10^{\circ}$, or

$$\sigma_{\Delta R} = 0.35 \csc E \text{ feet}$$

If the atmosphere about the user is assumed to be homogeneous in azimuth the covariance matrix of tropospheric correction errors for four satellites is:

$$(0.35)^2 \begin{bmatrix} \csc^2 E_1 & \csc E_1 \csc E_2 & \csc E_1 \csc E_3 & \csc E_1 \csc E_4 \\ \csc E_2 \csc E_1 & \csc^2 E_2 & \csc E_2 \csc E_3 & \csc E_2 \csc E_4 \\ \csc E_3 \csc E_1 & \csc E_3 \csc E_2 & \csc^2 E_3 & \csc E_3 \csc E_4 \\ \csc E_4 \csc E_1 & \csc E_4 \csc E_2 & \csc E_4 \csc E_3 & \csc^2 E_4 \end{bmatrix}$$

Since $\sigma_{\Delta R_{ij}} = \sqrt{\sigma^2_{\Delta R_i} \, \sigma^2_{\Delta R_j}}$, the correlations are all unity.

295

REFERENCE

DNSDP-REO-039, "Accuracy of Various Tropospheric Delay Correction Methods," dated 13 August 1973

APPENDIX 11

PERFORMANCE ANALYSIS RESULTS FOR NONSYNCHRONOUS ORBIT SATELLITES

SUMMARY

A set of 7 ATOP runs were made to determine the performance of IMU-Navsat and Navsat-only navigation systems for different missions and with the latest P-code and C-code range-range rate error models. At the end of each of the IMU-Navsat runs, the position errors are almost the same, independent of IMU quality and A/C maneuvers, provided 3 minutes of settling time after the maneuvers is allowed. In the case of Navsat only navigation, the position errors show a dependence on dynamics. In addition to tabulated data at the end of the runs, a complete set of plots of the one-sigma state errors are also included.

General Description of Performance Analysis Runs

The following is a verbal description of Runs 1 through 7 to help provide a rapid understanding of the type of missions that were considered and error models used.

Run #1   Class A, IMU-Navsat (P-code), high performance aircraft flies due north (600 kts at 30 K ft altitude) for 1 minute. Executes a 4g (resultant) turn through 90° due west and flies for another 3 minutes. Last 3 minute period is run with only 3 satellites. Random satellite dropouts (PLOCK = .95) also occur.

Run #2   Class A, repeat of Run #1 with medium quality IMU (run was not made since Run #1 and Run #3 showed little difference in performance).

Run #3   Class A, repeat of Run #1 with poor quality IMU (IMU errors assumed to be ten times larger than in Run #1).

Run #4   Class B, repeat of Run #1 with 7g resultant in the turn. Use 4-satellite navigation throughout.

Run #5   Class C, Navsat only (C-code), medium performance aircraft flies due north (400 kts at 30 K ft altitude) for 1 minute. Executes a 1/2 g (lateral component) turn through 90° due west and flies for another 3 minutes. Single channel. Random satellite dropouts (PLOCK = .95).

Run #6   Class D, similar to Run #5 except straight path with
          low dynamics and small measurement errors, simu-
          lating P-navigation.

Run #7   Class E, similar to Run #6 except stationary user
          (no acceleration Markov noise).

Initial Satellite and User State Vector Data

Satellite Locations

Number	Latitude	Longitude
#1	$0°$	$-90°$
#2	$-13°$	$-142.4°$
#3	$56.8°$	-148.2
#4	$13.0°$	$-37.6°$

$60°$ inclined orbits

Radius = 14,346 n. miles

User Location

   $30°$ N Latitude $-100°$ Longitude

Satellite Azimuth (Heading Relative to North)

   #1 $30°$
   #2 $30.867°$
   #3 $65.934°$
   #4 $30.867°$

Satellite ECI Position Vectors (feet)

$$XSAT(1) = 0.0$$
$$= -1.96209668E7$$
$$= 7.29852864E7$$
$$= 1.96209668E7$$

$$YSAT(1) = 8.722368E7$$
$$= 6.733521E7$$
$$= 4.05909148E7$$
$$= 5.18555118E7$$

$$ZSAT(1) = 0.0$$
$$= -5.18555118E7$$
$$= -2.516771405E7$$
$$= 6.733525112E7$$

298

Measurement Noise and Markov Noise

The range and range rate measurement errors are shown below as one-sigma values for the P-code and C-code error models.

P-Code (One-Sigma)

        Range   =   8.026 ft

        Range Rate =   .102 ft/sec

C-Code (One-Sigma)

        Range   = 33.4 ft

        Range Rate =   .05 ft/sec

The IMU acceleration measurement error is taken as .001 ft/sec^2 for the accurate system in Run #1 and altimeter data error is 100 ft (one sigma). Several of the states are also subject to Markov noise processes as shown in Table 1.

Navigation Performance

The filter performance for Runs #1 through #7 at the end of the run are shown in Table 3 for each state variable estimate. The units are defined in the column for Run #1 and are not repeated in the other columns. Time histories of the errors are shown in Figures 1 through 45. Position errors are given in units of feet, velocity in units of ft/sec, and attitude errors ϕ_x, ϕ_y, ϕ_z in units of arc seconds. For the Navsat only cases (Runs #5, #6, #7) the IMU attitude errors are obviously not given.

Table 1. A-Priori Errors

State Component		One-Sigma Error Class A, B	One-Sigma Error Class C, D, E
Position	x	6561ft(2km)	32808ft(10km)
	y	6561ft	32808ft(10km)
	z	160ft	160ft
Velocity	$\dot{x}$	3.28ft/sec(1m/sec)	32.8ft/sec(10m/sec)
	$\dot{y}$	3.28ft/sec	32.8ft/sec(10m/sec)
	$\dot{z}$	3.28ft/sec	32.8ft/sec(10m/sec)
Acceleration	a_x	$3.28 \cdot 10^{-3}$ft/sec^2(10^{-3}m/sec^2)	
	a_y	$3.28 \cdot 10^{-3}$ft/sec^2	
	a_z	$3.28 \cdot 10^{-3}$ft/sec^2	
Phase	User	1.E12ft(∞)	1.E12
	Sat.#1	9.84ft(3m)	
	Sat.#2	9.84ft(3m)	
	Sat.#3	9.84ft(3m)	
	Sat.#4		
User Frequency		100ft/sec	100ft/sec
Gimbal Angle	ϕ_x	.005deg	
	ϕ_y	.005deg	
	ϕ_z	.005deg	
Gimbal Rates	$\dot{\phi}_x$	.01deg/hr	
	$\dot{\phi}_y$	.01deg/hr	Note: Missing States are not included in Filter
	$\dot{\phi}_z$	.01deg/hr	
Accelerometer Scale Factor	K_x	10^{-4}	
	K_y	10^{-4}	
	K_z	10^{-4}	
Accelerometer Bias	b_x	$2 \cdot 10^{-4}$g	
	b_y	$2 \cdot 10^{-4}$g	
	b_z	$2 \cdot 10^{-4}$g	
Altimeter	h	100ft	

Run #1 IMU

300

Table 2. Markov Sigmas and Correlation Times

State Component	Class A, B		Class C	
	Sigma	Tau	Sigma	Tau
a_x	3.280 ft/sec^2	3 sec	1.0936 ft/sec^2	3 sec
a_y	3.280 ft/sec^2	3 sec	1.0936 ft/sec^2	3 sec
a_z	9.842 ft/sec^2	7.5 sec	3.2808 ft/sec^2	7.5 sec
User Frequency	1 ft/sec	1 sec	1 ft/sec	1 sec
Altimeter Noise	100 ft	25 sec	——	——

Table 3. Filter Errors at End of Run (One Sigma)

State Variable		Run #1	Run #3	Run #4	Run #5	Run #6	Run #7
Position	x	19.95 ft	19.95	19.89	37.55	27.03	25.92
	y	16.58 ft	16.58	16.54	37.62	30.62	29.97
	z	41.60 ft	41.61	41.39	134.60	131.00	130.41
Velocity	$\dot{x}$	.0348 ft/sec	.0549	.0355	6.54	1.62	.111
	$\dot{y}$	.0399 ft/sec	.0572	.0398	6.42	1.20	.0875
	$\dot{z}$	.167 ft/sec	.197	.1655	2.06	.854	.190
Acceleration	$\ddot{x}$	.00106 ft/sec^2	.0109	.00106	2.58	.315	.000903
	$\ddot{y}$	.00106 ft/sec^2	.0109	.00106	2.34	.283	.000690
	$\ddot{z}$	.00106 ft/sec^2	.0102	.00106	1.65	.248	.00141
Phase	User	38.41 ft	38.42	38.27	123.50	120.2	119.57
	Sat.#1	9.38 ft	9.39	9.38	9.56	9.53	9.52
	Sat.#2	7.76 ft	7.76	7.75	8.60	8.46	8.44
	Sat.#3	9.34 ft	9.34	9.33	9.53	9.49	9.49
	Sat.#4	7.63 ft	7.63	7.62	8.53	8.38	8.37
Frequency User		.161 ft/sec	.181	.16	.987	.800	.207
Gimbal Angle	ϕ_x	16.03 sec	110.52	15.9			
	ϕ_y	16.00 sec	112.32	16.00			
	ϕ_z	11.81 sec	56.85	11.97			
Rate	$\dot{\phi}_x$	.00965 deg/hr.	.0597	.00966			
	$\dot{\phi}_y$	.00978 deg/hr.	.0633	.00979			
	$\dot{\phi}_z$	.00995 deg/hr.	.0999	.00995			
Acceleration S.F.	K_x	$6.55 \cdot 10^{-5}$	$2.81 \cdot 10^{-4}$	$6.68 \cdot 10^{-5}$			
	K_y	$6.05 \cdot 10^{-5}$	$2.56 \cdot 10^{-4}$	$6.04 \cdot 10^{-5}$			
	K_z	$8.97 \cdot 10^{-5}$	$8.94 \cdot 10^{-4}$	$8.97 \cdot 10^{-5}$			
Acceleration Bias	D_x	.00246 ft/sec^2	.0173	.00246			
	D_y	.00244 ft/sec^2	.0171	.00243			
	D_z	.00305 ft/sec^2	.0288	.00305			
Altimeter		59.09 ft	59.09	59.98			

t = 250 sec

302

REFERENCE

TRW 10C 6451.17-31, Performance Analysis Results for
Non-Synchronous Orbit Satellites, By D. F. McAllister,
Dated 14 January 1974.

303

X POSITION ERROR

RUN 1: FIGURE 1

```
2.44CE+C1 !
2.36CE+C1 I
2.28CE+C1 I
2.20CE+C1 I        *
2.20CE+C1 *       **
2.12CE+C1 I      ***
2.C4CE+01 I    ****** **
1.96CE+C1 I   ************ ***
           ***************** ****
          * ****************************** **
         ************************************** *******
                                    ************* *****
1.88CE+C1 I
1.80CE+C1 I
1.72CE+C1 I
1.64CE+C1 I
1.56CE+C1 I
1.48CE+C1 I
1.4CCE+C1 I
1.32CE+01 I
1.24CE+01 I
1.16CE+C1 I
1.C8CE+C1 I
1.CCCE+C1 I
          6.0CCF+C0      6.6CCE+C1      1.26C5+C2      1.36C5+C2      2.46C6+C2    TIME
```

Y POSITION ERROR

RUN 1: FIGURE 2

305

Z POSITION ERROR
RUN 1: FIGURE 3

```
1.12CE+C2 I
          I
1.08CE+C2 I
          I
1.04CE+C2 I
          I
1.00CE+C2 I
          I
9.60CE+C1 I
          I
9.20CE+C1 I
          I
8.80CE+C1 I
          I
8.40CE+C1 I
          I
8.00CE+C1 I
          I
7.60CE+C1 I
          I
7.20CE+C1 I
          I
6.80CE+C1 I
          I
6.40CE+C1 I
          I
6.00CE+C1 I
          I
5.60CE+C1 I
          I
5.20CE+C1 I
          I
4.80CE+C1 I
          I
4.40CE+C1 I
          I
4.00CE+C1 I

          6.00CE+CO    6.60CCE+C1    1.260E+C2    1.80JE+C2    2.46CT+02
                                                  TIME
```

X VELOCITY ERROR
RUN 1: FIGURE 4

1.28CE-C1 I
1.22CE-C1 I
1.26CE-C1 I
1.2CCE-C1 I
1.14CE-C1 I
1.C8CE-C1 I
1.C2CE-C1 I
5.6CCE-C2 I
5.CCCE-C2 I
8.4CCE-C2 I
7.8CCE-C2 I
7.2CCE-C2 I
6.6CCE-C2 I
6.CCCE-C2 I
5.4CCE-C2 I
4.8CCE-C2 I
4.2CCE-C2 I
3.6CCE-C2 I
3.CCCE-C2 I

6.00CE+C0   6.6CCE+01   1.260E+C2   1.8CCE+C2   2.46CE+02
                          TIME

307

Y VELCCITY ERROR

RUN 1: FIGURE 5

1.38CE-C1 I
1.32CE-C1 I
1.26CE-C1 I
1.2CCE-C1 I *
1.14CE-C1 I
1.C8CE-C1 I *
1.C2CE-C1 I *
9.6CCE-C2 I *
9.CCCE-C2 I **
8.4CCE-C2 I **
7.8CCE-C2 I *
7.2CCE-C2 I
6.6CCE-C2 I
6.CCCE-C2 I
5.4CCE-C2 I
4.8CCE-C2 I
4.2CCE-C2 I
3.6CCE-C2 I
3.CCCE-C2 I

6.0CCE+00   6.6CCE+C1   1.26CE+C2   1.86CE+C2   2.46CE+02   TIME

308

Z VELOCITY ERROR

RUN 1: FIGURE 6

PHIX

RUN 1: FIGURE 7

```
2.08CE+C1 I
          I
2.02CE+C1 I
          I
1.96CE+C1 I
          I
1.9CCE+C1 I
          I
1.84CE+C1 I
          I
1.78CE+C1 I  **
          I  **
1.72CE+C1 I  ** *
          I   ***
1.66CE+C1 I    ** ******** *
          I          ** ***** ***
1.6CCE+C1 I                   **** ****** ******** **** ***** ***** **** ***** ****
1.54CE+C1 I
          I
1.48CE+C1 I
          I
1.42CE+C1 I
          I
1.36CE+C1 I
          I
1.3CCE+C1 I
          I
1.24CE+C1 I
          I
1.18CE+C1 I
          I
1.12CE+C1 I
          I
1.C6CE+C1 I
          I
1.CCCE+C1 I
         6.0CCE+00    6.6CCE+C1    1.26CE+C2    1.86CE+C2    2.46CE+02
                                     TIME
```

310

PHIY

RUN 1: FIGURE 8

2.080E+01 I
          I
2.020E+01 I
          I
1.960E+01 I
          I
1.900E+01 I
          I
1.840E+01 I
          I
1.780E+01 **
          I
1.720E+01 **
          I
1.660E+01 I
          I
1.600E+01 I
          I
1.540E+01 I
          I
1.480E+01 I
          I
1.420E+01 I
          I
1.360E+01 I
          I
1.300E+01 I
          I
1.240E+01 I
          I
1.180E+01 I
          I
1.120E+01 I
          I
1.060E+01 I
          I
1.000E+01 I

6.000E+00   6.600E+01   1.260E+02   1.860E+02   2.460E+02   TIME

311

PHIZ

RUN 1: FIGURE 9

2.08CE+C1
2.C2CE+C1
1.96CE+C1
1.9CCE+C1
1.84CE+C1
1.78CE+C1
1.72CE+C1
1.66CE+C1
1.6CCE+C1
1.54CE+C1
1.48CE+C1
1.42CE+C1
1.36CE+C1
1.3CCE+C1
1.24CE+C1
1.18CE+C1
1.12CE+C1
1.C6CE+C1
1.CCCE+C1

6.0CCE+C0   6.6CCE+C1   1.260E+C2   1.8C0E+C2   TIME   2.46CE+02

X POSITION ERROR

RUN 3: FIGURE 10

```
2.440E+01 I
2.360E+01 I
2.280E+01 I
2.200E+01 I
2.120E+01 I
2.040E+01 I
1.960E+01 I
1.880E+01 I
1.800E+01 I
1.720E+01 I
1.640E+01 I
1.560E+01 I
1.480E+01 I
1.400E+01 I
1.320E+01 I
1.240E+01 I
1.160E+01 I
1.080E+01 I
1.000E+00 I
```

5.000E+00   5.000E+01   1.000E+02   1.500E+02   TIME   2.000E+02

313

Y POSITION ERROR

RUN 3: FIGURE 11

2.440E+01 I
2.360E+01 I
2.280E+01 I
2.200E+01 I
2.120E+01 I
2.040E+01 I
1.960E+01 I
1.880E+01 I
1.800E+01 I
1.720E+01 I
1.640E+01 I
1.560E+01 I
1.480E+01 I
1.400E+01 I
1.320E+01 I
1.240E+01 I
1.160E+01 I
1.080E+01 I
1.000E+01 I

0.000E+00   6.000E+01   1.200E+02   1.800E+02
                        TIME   2.400E+02

POSITION ...?

RUN 3: FIGURE 12

1.120E+02 I
1.080E+02 I
1.040E+02 I
1.000E+02 I
9.600E+01 I
9.200E+01 I
8.800E+01 I
8.400E+01 I
8.000E+01 I
7.600E+01 I
7.200E+01 I
6.800E+01 I
6.400E+01 I
6.000E+01 I
5.600E+01 I
5.200E+01 I
4.800E+01 I
4.400E+01 I
4.000E+01 I

TIME

315

X VELOCITY ERROR

RUN 3: FIGURE 13

Y VELOCITY ERROR

RUN 3: FIGURE 14

317

Z VELOCITY ERROR

RUN 3: FIGURE 15

8.200E-01 I
7.800E-01 I
7.400E-01 I
7.000E-01 I
6.600E-01 I
6.200E-01 I
5.800E-01 I
5.400E-01 I
5.000E-01 I
4.600E-01 I
4.200E-01 I
3.800E-01 I
3.400E-01 I
3.000E-01 I
2.600E-01 I
2.200E-01 I
1.800E-01 I
1.400E-01 I
1.000E-01 I

6.000E+00   6.600E+01   1.260E+02   1.860E+02   TIME   2.460+02

318

PHIX

RUN 3: FIGURE 16

```
1.720E+02 I
1.680E+02 I  **
          I  **
1.640E+02 I ****************
1.600E+02 I
          I
1.560E+02 I                                          *
          I
1.520E+02 I                                          **
          I
1.480E+02 I                                          **
          I
1.440E+02 I                                       *
          I
1.400E+02 I                                       *
          I
1.360E+02 I                                     **
          I
1.320E+02 I                                   **
          I
1.280E+02 I                                 *
          I                                 *
1.240E+02 I                               *
          I
1.200E+02 I                          ***********
          I                       *********
1.160E+02 I                     *********
          I                   *******
1.120E+02 I                 *******
          I              ******************
1.080E+02 I
          I
1.040E+02 I
          I
1.000E+02 I
          0.000E+00      6.000E+01      1.200E+02      1.800E+02      2.400E+02   TIME
```

319

PHIY

RUN 3: FIGURE 17

1.720E+02 I
1.680E+02 I
1.640E+02 I
1.600E+02 I
1.560E+02 I
1.520E+02 I
1.480E+02 I
1.440E+02 I
1.400E+02 I
1.360E+02 I
1.320E+02 I
1.280E+02 I
1.240E+02 I
1.200E+02 I
1.160E+02 I
1.120E+02 I
1.080E+02 I
1.040E+02 I

6.000E+00   6.605E+01   1.320E+02   1.980E+02   2.640E+02   TIME

320

PHIZ

RUN 3: FIGURE 18

1.940E+02
1.860E+02
1.780E+02
1.700E+02
1.620E+02
1.540E+02
1.460E+02
1.380E+02
1.300E+02
1.220E+02
1.140E+02
1.060E+02
9.800E+01
9.000E+01
8.200E+01
7.400E+01
6.600E+01
5.800E+01
5.000E+01

6.000E+00   3.600E+01   1.260E+02   1.860E+02   2.460E+02   TIME

X POSITION ERROR

RUN 4: FIGURE 19

2.044CE+C1 I
2.36CE+C1 I
2.28CE+C1 I
2.20CCE+C1 I
2.12CE+C1 I
2.C4CE+C1 I
1.56CE+C1 I
1.88CE+C1 I
1.8CCE+C1 I
1.72CE+C1 I
1.64CE+C1 I
1.56CE+C1 I
1.48CE+C1 I
1.4CCE+C1 I
1.32CE+C1 I
1.24CE+C1 I
1.16CE+C1 I
1.C8CE+C1 I
1.CCCE+C1 I

6.0CCE+CC   6.6CCF+C1   1.26CE+C2   1.86CE+C2   2.46C7+C2   TIME

322

Y POSITION ERROR
RUN 4: FIGURE 20

2.44CE+C1
2.36CE+C1
2.28CE+C1
2.2CCE+C1
2.12CE+C1
2.C4CE+C1
1.96CE+C1
1.88CE+C1
1.8CCE+C1
1.72CE+C1
1.64CE+C1
1.56CE+C1
1.48CE+C1
1.4CCE+C1
1.32CE+C1
1.24CE+C1
1.16CE+C1
1.C8CE+C1
1.CCCE+C1

6.0CCE+C0   6.6C0E+C1   1.2C0E+C2   1.86CE+C2   TIME   2.46CE+02

323

Z POSITION ERROR
RUN 4: FIGURE 21

```
1.12CE+C2 I
1.C8CE+C2 I
1.C4CE+C2 I
1.CCCE+C2 I
9.6CCE+C1 I
9.2CCE+C1 I
8.8CCE+C1 I
8.4CCE+C1 I
8.CCCE+C1 I                                                                              *
7.6CCE+C1 I                                                                            **
7.2CCE+C1 I                                                                          **
6.8CCE+C1 I                                                                        ***
6.4CCE+C1 I                                                                      ****
6.CCCE+C1 I                                                                    ****
5.6CCE+C1 I                                                                  *****
5.2CCE+C1 I                                                                *****
4.8CCE+C1 I                                                              ******
4.4CCE+C1 I                                                            ********
4.CCCE+C1 I . . . . . . . . . . . . . . . . . . . . . . . . . . . . . . . . . . . . .
           6.CCCE+00      6.6C0F+C1      1.26CE+C2      1.80CE+C2      2.46CE+C2   TIME
```

324

X VELOCITY ERROR
RUN 4: FIGURE 22

325

VELOCITY ERROR
RUN 4: FIGURE 23

```
1.38CE-C1 I
          I
1.32CE-C1 I
          I
1.26CE-C1 I
          I
1.2CCE-C1 I              *
          I
1.14CE-C1 I          *
          I
1.C8CE-C1 I        *
          I
1.C2CE-C1 I      *
          I
9.6CCE-C2 I    *
          I  *
9.CCCE-C2 I **
          I *
8.4CCE-C2 I **
          I
7.8CCE-C2 I *
          I *
7.2CCE-C2 I *
          I
6.6CCE-C2 I
          I
6.CCCE-C2 I
          I
5.4CCE-C2 I
          I
4.8CCE-C2 I
          I
4.2CCE-C2 I
          I
3.6CCE-C2 I
          I
3.CCCE-C2 I
          .
        6.0CCE+C0        6.6CCE+C1        1.26CE+C2        1.8SCE+C2        2.4CCE+C2   TIME
```
326

Z VELOCITY ERROR
RUN 4: FIGURE 24

```
8.2CCE-C1 I
7.8CCE-C1 I
7.4CCE-C1 I
7.CCCE-C1 I
6.6CCE-C1 I
6.2CCE-C1 I
5.8CCE-C1 I
5.4CCE-C1 I      *
5.CCCE-C1 I      *
4.6CCE-C1 I      *
4.2CCE-C1 I     **
           I    **
3.8CCE-C1 I    **
3.4CCE-C1 I    **
3.CCCE-C1 I    **
2.6CCE-C1 I    ***
2.2CCE-C1 I     **  ***
1.8CCE-C1 I        ***
1.4CCE-C1 I
1.CCCE-C1 I
```

6.0CCE+CC   6.6CCE+C1   1.26CE+C2   1.86CE+C2   TIME   2.46CE+C2

327

PHIX

RUN 4: FIGURE 25

TIME

6.0CCF+C0   6.6CCF+C1   1.26CE+C2   1.86CF+C2   2.4cCF+C2

2.C8CE+C1
2.C2CE+C1
1.96CE+C1
1.9CCE+C1
1.84CE+C1
1.78CE+C1
1.72CE+C1
1.66CE+C1
1.6CCE+C1
1.54CE+C1
1.48CE+C1
1.42CE+C1
1.36CE+C1
1.3CCE+C1
1.24CE+C1
1.18CE+C1
1.12CE+C1
1.C6CE+C1
1.CCCE+C1

328

PHIY

RUN 4: FIGURE 26

2.08CE+01

2.02CE+01

1.96CE+01

1.90CE+01

1.84CE+01

1.78CE+01

1.72CE+01

1.66CE+01

1.60CE+01

1.54CE+01

1.48CE+01

1.42CE+01

1.36CE+01

1.30CE+01

1.24CE+01

1.18CE+01

1.12CE+01

1.06CE+01

1.00CE+01

6.00CE+00   6.60CE+01   1.26CE+02   1.86CE+02   2.46CE+02   TIME

329

PHIZ

RUN 4: FIGURE 27

```
2.08CE+C1 I
2.02CE+C1 I
1.96CE+C1 I
1.90CE+C1 I
1.84CE+C1 I
1.78CE+C1 I
1.72CE+C1 I
1.66CE+C1 I
1.60CE+C1 I
1.54CE+C1 I
1.48CE+C1 I
1.42CE+C1 I
1.36CE+C1 I
1.30CE+C1 I
1.24CE+C1 I
1.18CE+C1 I
1.12CE+C1 I
1.06CE+C1 I
1.00CE+C1 I
         6.0CCE+C0    6.6CCE+C1    1.26CE+C2    1.86CE+C2    2.46CE+02   TIME
```

X POSITION ERROR

RUN 5: FIGURE 28

```
1.020E+02 I
9.800E+01 I
9.400E+01 I
9.000E+01 I
8.600E+01 I
8.200E+01 I
7.800E+01 I
7.400E+01 I
7.000E+01 I           *
6.600E+01 I*          
6.200E+01 I**
5.800E+01 I*
5.400E+01 I
5.000E+01 I **
4.600E+01 I **
4.200E+01 I **
3.800E+01 I **
3.400E+01 I
3.000E+01 I
          6.00E+00      6.600E+01      1.200E+02      1.800E+02      2.400E+02   TIME
```

331

Y POSITION ERROR

RUN 5: FIGURE 29

```
5.520E+01 I
5.380E+01 I
5.240E+01 I                    *
5.100E+01 I
4.960E+01 I
4.820E+01 I
4.680E+01 I **
4.540E+01 I                *
4.400E+01 I             *
4.260E+01 I          ***
4.120E+01 I        **
3.980E+01 I      *
3.840E+01 I    **
3.700E+01 I  **                                                          *
3.560E+01 I ***                             *                          **
3.420E+01 I ******* *          *** ***** *** ***  *****
3.280E+01 I  **  *             **  ********* ** ****
3.140E+01 I
3.000E+01 I

          6.000E+00      6.600E+01      1.260E+02      1.860E+02      2.460E+02
                                                   TIME
```

332

Z POSITION ERROR

RUN 5: FIGURE 30

1.720E+02 I
1.680E+02 I
1.640E+02 I
1.600E+02 I
1.560E+02 I
1.520E+02 I
1.480E+02 I
1.440E+02 I
1.400E+02 I
1.360E+02 I
1.320E+02 I
1.280E+02 I
1.240E+02 I
1.200E+02 I
1.160E+02 I
1.120E+02 I
1.080E+02 I
1.040E+02 I
1.000E+02 I

6.000E+00   6.600E+01   1.260E+02   1.860E+02   2.460E+02

TIME

333

X VELOCITY ERROR

RUN 5: FIGURE 31

```
1.640E+01 I
1.560E+01 I
1.480E+01 I
1.400E+01 I
1.320E+01 I
1.240E+01 I
1.160E+01 I
1.080E+01 I
1.000E+01 I
9.200E+00 I
8.400E+00 I
7.600E+00 I
6.800E+00 I
6.000E+00 I
5.200E+00 I
4.400E+00 I
3.600E+00 I
2.800E+00 I
2.000E+00 I
```

6.000E+00   6.600E+01   1.260E+02   1.800E+02   2.460E+02   TIME

334

Y VELOCITY ERROR

RUN 5: FIGURE 32

335

Z VELOCITY ERROR

RUN 5: FIGURE 33

X POSITION ERROR

RUN 6: FIGURE 34

TIME

Y POSITION ERROR

RUN 6: FIGURE 35

```
3.080E+01 I
          *
3.020E+01 I                                                                              ****#*%####*
         **
2.960E+01 I*                                    ***#**##*#*#*#**####*### **
         I*****                        ***#**#**##****##**#*## *
2.900E+01 I                   * ***#*#*#######*####*#### **
         I*********#*##****## **** *
2.840E+01 I
         I                  *
2.780E+01 I
         I
2.720E+01 I
         I
2.660E+01 I
         I
2.600E+01 I
         I
2.540E+01 I
         I
2.480E+01 I
         I
2.420E+01 I
         I
2.360E+01 I
         I
2.300E+01 I
         I
2.240E+01 I
         I
2.180E+01 I
         I
2.120E+01 I
         I
2.060E+01 I
         I
2.000E+01 I
          6.000E+00        6.500E+01        1.260E+02        1.860E+02    TIME    2.460E+02
```

Z POSITION ERROR

RUN 6: FIGURE 36

1.720E+02 I
1.680E+02 I
1.640E+02 I
1.600E+02 I
1.560E+02 I
1.520E+02 I
1.480E+02 I
1.440E+02 I
1.400E+02 I
1.360E+02 I
1.320E+02 I
1.280E+02 I
1.240E+02 I
1.200E+02 I
1.160E+02 I
1.120E+02 I
1.080E+02 I
1.040E+02 I
1.000E+02 I

6.000E+00   6.600E+01   1.260E+02   1.860E+02   2.460E+02   TIME

339

Y VELOCITY ERROR

RUN 6: FIGURE 36

1.620E+00 I
1.580E+00 I
1.540E+00 I
1.500E+00 I
1.460E+00 I
1.420E+00 I
1.380E+00 I
1.340E+00 I
1.300E+00 I
1.260E+00 I
1.220E+00 I
1.180E+00 I
1.140E+00 I
1.100E+00 I
1.060E+00 I
1.020E+00 I
9.800E-01 I
9.400E-01 I
9.000E-01 I

6.000E+00   6.500E+01   1.260E+02   1.960E+02   2.450E+02   TIME

X VELOCITY ERROR

RUN 6: FIGURE 37

```
2.440E+00 I
          I
2.360E+00 I
          I
2.280E+00 I
          I
2.200E+00 I
          I
2.120E+00 I
          I
2.040E+00 I
          I
1.960E+00 I
          I
1.880E+00 I
          I
1.800E+00 I
          I
1.720E+00 I
          I
1.640E+00 I
          I
1.560E+00 I
          I
1.480E+00 I
          I
1.400E+00 I
          I
1.320E+00 I
          I
1.240E+00 I
          I
1.160E+00 I
          I
1.080E+00 I
          I
1.000E+00 I
          6.000E+00     5.600E+01     1.260E+02     1.860E+02     2.460E+02   TIME
```

341

Z VELOCITY ERROR

RUN 6: FIGURE 39

X POSITION ERROR

RUN 7: FIGURE 40

```
3.080E+01 I
3.020E+01 I
2.960E+01 I
2.900E+01 I **
2.840E+01 I **
2.780E+01 I *
2.720E+01 I
2.660E+01 I *
           *
2.600E+01 I *
           ***
2.540E+01 I *
           *****
           ****************   **************** *
           ****************  ********************
2.480E+01 I                  **************
                             *********
2.420E+01 I
2.360E+01 I
2.300E+01 I
2.240E+01 I
2.180E+01 I
2.120E+01 I
2.060E+01 I
2.000E+01 I
          6.000E+00        5.600E+01        1.340E+02        1.850E+02        2.450E+02   TIME
```

343

Y POSITION ERROR

RUN 7: FIGURE 41

3.080E+01 I
3.020E+01 I
2.960E+01 I
2.900E+01 I
2.840E+01 I
2.780E+01 I
2.720E+01 I
2.660E+01 I
2.600E+01 I
2.540E+01 I
2.480E+01 I
2.420E+01 I
2.360E+01 I
2.300E+01 I
2.240E+01 I
2.190E+01 I
2.120E+01 I
2.060E+01 I
2.000E+01 I

6.000E+00   6.500E+01   1.260E+02   1.860E+02   2.460E+02   TIME

344

Z POSITION ERROR

RUN 7: FIGURE 42

1.720E+02
1.680E+02
1.640E+02
1.600E+02
1.560E+02
1.520E+02
1.480E+02
1.440E+02
1.400E+02
1.360E+02
1.320E+02
1.280E+02
1.240E+02
1.200E+02
1.160E+02
1.120E+02
1.080E+02
1.040E+02
1.000E+02

6.000E+00   6.500E+01   1.240E+02   1.860E+02   2.460E+02   TIME

345

X VELOCITY ERROR

RUN 7: FIGURE 43

Y VELOCITY ERROR

RUN 7: FIGURE 44

Z VELOCITY ERROR
RUN 7: FIGURE 45

348
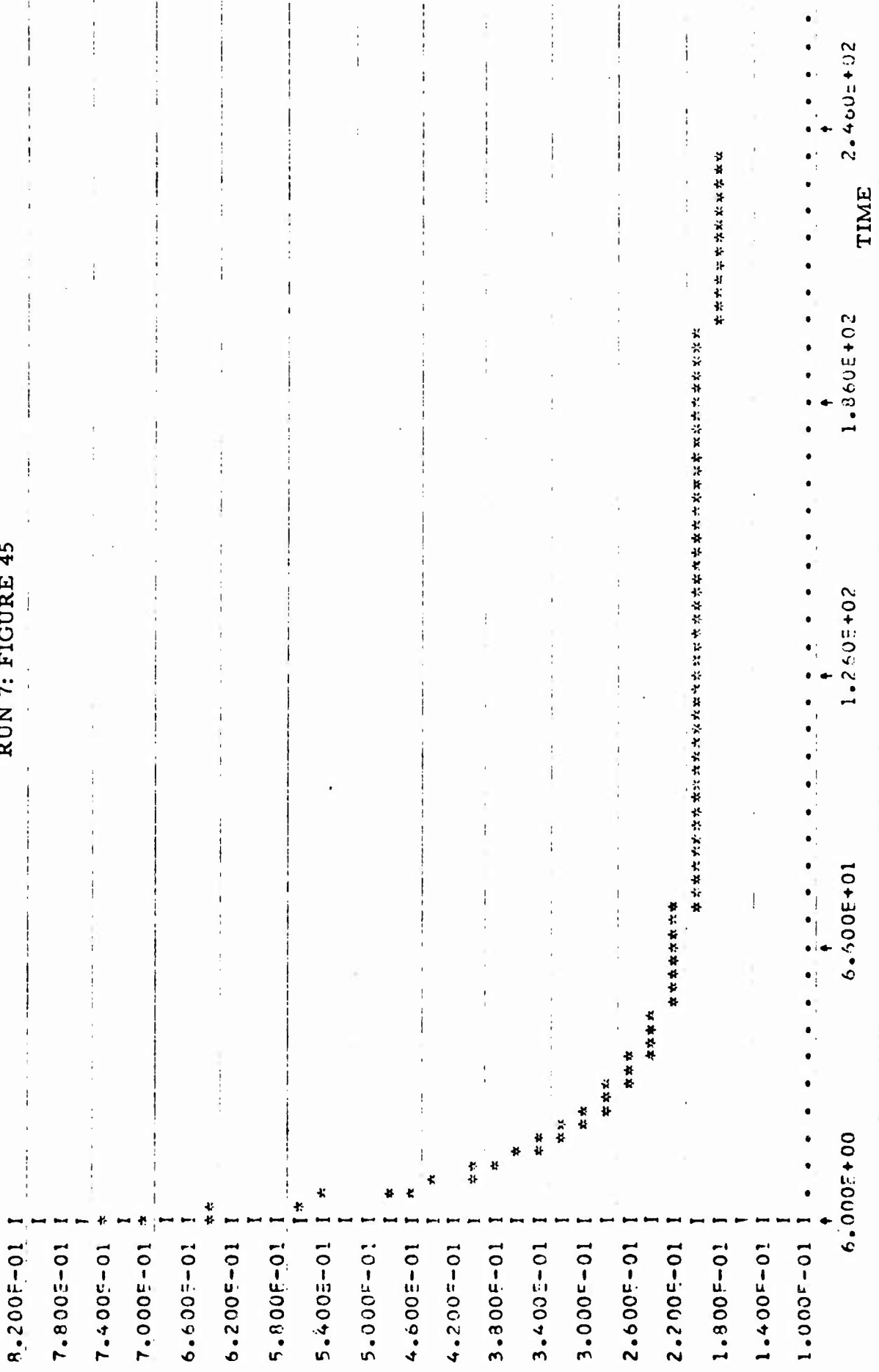
APPENDIX 12

GPS RECEIVER NOISE TEMPERATURE

The Philco Document RF Link Analysis for Global Position System GPS-TM003A, December 21, 1973 describes on page 10 the system noise as $T = LT_A + (1 - L) T_L + T_R$. The value of T_R is the total Noise Temperature of the DNSS Receiver referred to its input and a value of 4.0 dB ($438^{\circ}K$) nominal is assumed. An expression has been written for this overall receiver noise temperature to determine the noise performance versus cost. The receiver preamp is taken as shown in Figure 1 and the expression derived is somewhat different than that usually seen because the Loss L is defined as P_{out}/P_{in} in the Philco report.

Figure 1. Receiver Preamplifier
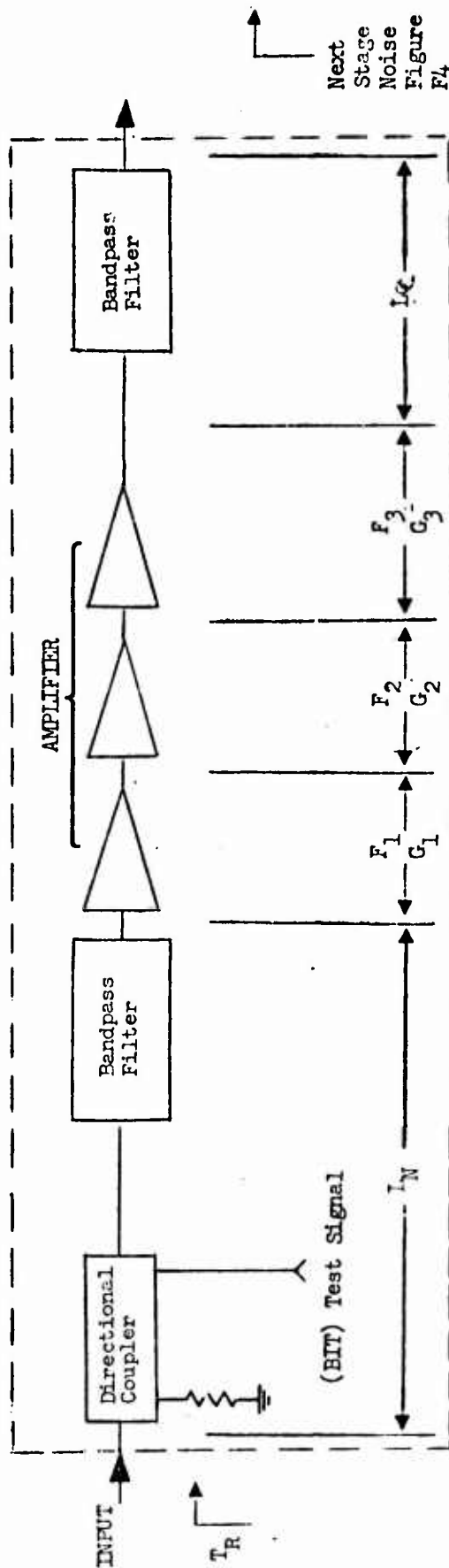
NOTES:

- L_N Total insertion loss due to cables, coupler and filter P_{out}/P_{in}

- L_C Total insertion loss due to cables and filter

- F_1, F_2, F_3 Noise figure of each stage

- F_4 Total two solid Noise Figure of Mixer

- G_1, G_2, G_3 Power Gain of each stage

- T_1, T_2, T_3 Effective noise temperature of each stage

350

$$T_R = \left(\frac{1 - L_N}{L_N} \right) T_N + \frac{1}{L_N} \left(T_1 + \frac{T_2}{G_1} + \frac{T_3}{G_1 G_2} + \frac{T_4}{G_1 G_2 G_3 L_C} \right)$$

The excess noise temperature can be related to the Noise Figure

$$T = (F - 1)T_0 \quad \text{where } T_0 = 290°K$$

We can express the total receiver noise temperature in terms of the individual transistor stage Noise Figures and Power Gains.

$$T_R = \left(\frac{1 - L_N}{L_N} \right) T_N + \frac{1}{L_N} \left[\left(F_1 - 1 \right) T_0 + \frac{\left(F_2 - 1 \right) T_0}{G_1} + \frac{\left(F_3 - 1 \right) T_0}{G_1 G_2} \right.$$

$$\left. + \frac{\left(F_4 - 1 \right) T_0}{G_1 G_2 G_3 L_C} \right]$$

Since $T_0 = 290°K$

$$T_R = 290 \left\{ \frac{\left(1 - L_N \right)}{L_N} + \frac{1}{L_N} \left[\left(F_1 - 1 \right) + \frac{\left(F_2 - 1 \right)}{G_1} + \frac{\left(F_3 - 1 \right)}{G_1 G_2} + \frac{\left(F_4 - 1 \right)}{G_1 G_2 G_3 L_C} \right] \right\}$$

EXAMPLES

    (1)   Example of low noise "L" Band preamplifier using high

          gain transistors

                $F_1 =$ 2.5 db (1.78)

                $F_2, F_3 =$ 3 db (2)

                $F_4 =$ 12 db (15.8)

$$L_N = \quad\quad\quad -1.0 \text{ db } (.8)$$

$$G_1 = \quad\quad\quad 12 \text{ db } (15.8)$$

$$G_2, G_3 = \quad\quad\quad 12 \text{ db } (15.8)$$

$$T_R = 290 \left[.25 + 1.25 \left(.78 + \frac{1}{15.8} + \frac{1}{(15.8)^2} + \frac{1}{(15.8)^3 \; .8} \right) \right]$$

$$T_R = 290 \left[.25 + 1.25 \; (.78 + .063 + .004 + .0003) \right]$$

$$T_R = 290 \; (.25 + 1.06) = (1.31)$$

$$T_R = 380°K$$

$$F_R = 3.64 \text{ db}$$

(2) Example of low noise "L" Band preamplifier using low gain
transistors

$$F_1 = \quad\quad\quad 2.5 \text{ db } (1.78)$$

$$F_2, F_3 = \quad\quad\quad 3 \text{ db } (2)$$

$$F_4 = \quad\quad\quad 12 \text{ db } (15.8)$$

$$L_N = \quad\quad\quad -1 \text{ db } (.8)$$

$$G_1 = \quad\quad\quad 6 \text{ db } (3.97)$$

$$G_2, G_3 = \quad\quad\quad 6 \text{ db } (3.97)$$

$$T_R = 290 \left[.25 + 1.25 \left[\left(.78 + \frac{1}{3.97} + \frac{1}{(3.97)^2} + \frac{1}{(3.97)^3} .8 \right) \right] \right]$$

$$T_R = 290 \left[.25 + 1.25 \; (.78 + .25 + .0635 + .296) \right]$$

$$T_R = 290 \left[.25 + 1.25 \; (1.39) \right] = 290 \; (1.99)$$

$$T_R = 576\,^\circ K \; (4.75 \; db)$$

(3) Example of low noise "L" Band preamplifier using a more typical mix of various gain transistors

$$F_1 = \quad 2.5 \; (1.78)$$

$$F_2 = \quad 3 \; db \; (2)$$

$$F_3 = \quad 4 \; db \; (2.51)$$

$$F_4 = \quad 12 \; db \; (15.8)$$

$$L_N = \quad -1 \; db \; (.8)$$

$$G_1 = \quad 6 \; db \; (3.97)$$

$$G_2 = \quad 8 \; db \; (6.3)$$

$$G_3 = \quad 10 \; db \; (10)$$

$$T_R = 290 \left[.25 + 1.25 \left(.78 + \frac{1}{3.97} + \frac{1}{(3.97)(6.3)} + \frac{1}{(3.97)(6.3)(10)(.8)} \right) \right]$$

$$T_R = 290 \left[.25 + 1.25 \; (.78 + .25 + .060 + .074) \right]$$

$$T_R = 290 \left[.25 + 1.25 \; (1.16) \right] = 290 \; (.25 + 1.45)$$

$$T_R = 494\,^\circ K \; (4.32 \; db)$$

The total Noise Figure of a cascaded amplifier can be shown to be equal to[1] (1).

$$(1) \quad F_t = F_1 + \frac{F_2 - 1}{G_1} + \frac{F_3 - 1}{G_1 \, G_2} + \ldots\ldots + \frac{F_n - 1}{G_1 \, G_2 \ldots (G_{n-1})}$$

Where F_1, F_2, F_3 or the Noise Figure of each cascade stage and G_1, G_2, G_3 or the power gains of each stage.

If we also give the noise temperature relationship to Noise Figure as

$$F = 1 + \frac{Te}{To} \qquad\qquad Te = (F - 1)\ To$$

Where Te is the effective excess noise temperature and To is standard room temperature defined as 290°K.

One can express the total system noise in terms of temperature or Noise Figure (2) (5)

$$(2) \quad 1 + \frac{T_t}{To} = 1 + \frac{T_1}{To} + \frac{T_2}{To\ G_1} + \frac{T_3}{To\ G_1\ G_2} + \ldots$$

$$+ \frac{T_n}{To\ G_1\ G_2 \ldots (G_{n-1})}$$

$$(3) \quad T_t = T_1 + \frac{T_2}{G_1} + \frac{T_3}{G_1\ G_2} + \ldots + \frac{T_n}{G_1\ G_2 \ldots (G_{n-1})}$$

$$(4) \quad 1 + \frac{T_t}{T_o} = F_1 + \frac{F_2 - 1}{G_1} + \frac{F_3 - 1}{G_1\ G_2} + \ldots + \frac{F_n - 1}{G_1\ G_2 \ldots (G_{n-1})}$$

---

(1) Skolnik., Merrill I. Introduction to Radar Systems pp 363-366,

McGraw Hill, 1962.

$$(5) \quad T_t = T_o\left(F_1 - 1 + \frac{F_2 - 1}{G_1} + \frac{F_3 - 1}{G_1 G_2} + \dots \frac{F_n - 1}{G_1 G_2 \dots (G_{n-1})}\right)$$

If the amplifier is preceded by an attenuator (loss due to cables, filter, etc.) the total loss can be treated as you would a typical stage of gain but it's gain would be less than one and its Noise Figure or excess temperature would be $Te_{(loss)} = \frac{1-L}{L}$ To $\quad$ G = 1 when defined as $L = P_{out}/P_{in}$.

It is more common to treat the loss as an additional source of noise and then add it to the overall cascade amplifier where the gain of the total amplifier is multiplied by the gain (loss) of the attenuator. This gives the total temperature of a cascade amplifier preceded be an attenuator as (6).

$$(6) \quad T_R = \left(\frac{1-L}{L}\right) T_o + \frac{1}{L}\left(T_1 + \frac{T_2}{G_1} + \frac{T_3}{G_1 G_2} + \dots \quad \dots \right.$$
$$\left. + \frac{T_n}{G_1 G_2 (G_{n-1})}\right)$$

Expressing the noise temperature of each stage of the amplifier in the more common way as noise figure we get from $Te = (F - 1)$ To

$$(7) \quad T_R = \left(\frac{1-L_N}{L_N}\right) + T_N + \frac{1}{L}\left(\left(F_1 - 1\right) T_o + \frac{\left(F_2 - 1\right) T_o}{G_1}\right.$$
$$\left. + \frac{\left(F_3 - 1\right) T_o}{G_1 G_2} + \dots\dots + \frac{\left(F_n - 1\right) T_o}{G_1 G_2 \dots (G_{n-1})}\right)$$

Where T_N is the equivalent of the attenuator typically close to 290°K.

APPENDIX 13
OPTIMIZED ACQUISITION PARAMETERS FOR THE
DNSDP RECEIVER CODE LOCK DETECTOR

SUMMARY:

This appendix presents an analytic model for the performance of
the noncoherent lock detector. From this model, optimized design
parameters were selected which minimize the average acquisition
time. In particular, it was found that for a $C/N_0 = 30.dB$-Hz and
a $\pm$ 500 Hz predetection noise bandwidth, the mean time to acquisi-
tion would be 16.4 seconds if the half-code chip dwell time is
set at 21 milliseconds. The reader is cautioned that the analytic
methods used here are approximate, and that breadboard confirma-
tion of these results will be necessary during the receiver
development phase of the program.

1. INTRODUCTION

The NAVSAT satellite program uses several earth-orbiting satellites
to transmit signals to users around the world. Each satellite transmits
an L-band carrier biphase modulated by a very long secure PN code (P-code)
and by a 511 chip nonsecure PN code (C-code) in quadrature with the
P-code. The P-code provides high resolution range data to the user,
but cannot be easily acquired without advanced knowledge of the state
of the P-code being transmitted by each satellite. The shorter C-code
is therefore used for initial acquisition of the receiver.

The C-code for each satellite is unique, and therefore permits the
user receiver to select the satellite to be tracked. Furthermore, biphase
data is transmitted with the C-code to provide data to the user.

The signal is demodulated by correlating either the P or C code
with a replica generated by the receiver. In the initial acquisition
of the C-code, the receiver steps the replica code in half-chip increments
until correlation is obtained. It is the purpose of the lock detector
to tell when code correlation has been achieved. Once code correlation
is obtained, the lock detector signals the receiver to stop its code
search, and permits the tracking loop to lock to the carrier. Data may
then be extracted, and velocity and range measurements made using the
received doppler and PN code information. It is important, particularly
in the single channel sequential receiver concept, to lock the receiver
as rapidly as possible. Therefore, this report presents an optimization
of the lock detector design which permits the receiver to acquire C-code
lock in the minimum possible time.

2. LOCK DETECTOR DESCRIPTION

Figure 1 is a functional block diagram of the lock detector. The rf
processor receives the L-band signals from the antenna, amplifies the signal,
and mixes the signal down to the first IF frequency. An AGC amplifier works
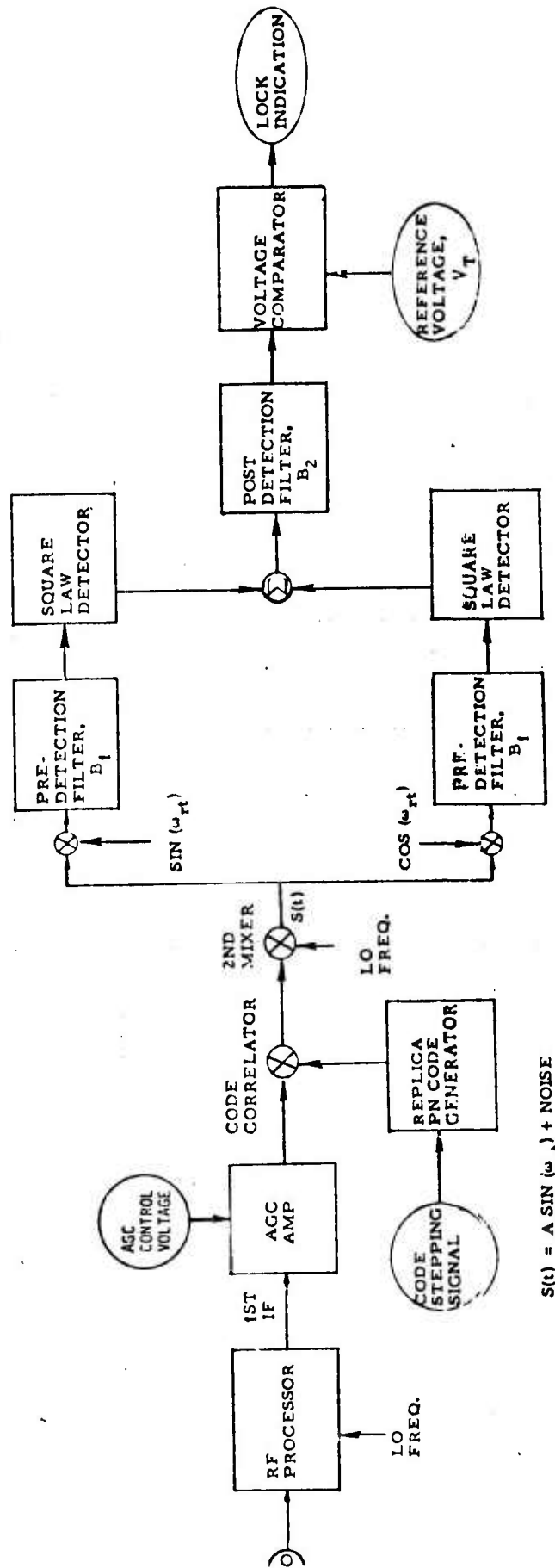
Figure 1. Lock Detector Functional Block Diagram

$S(t) = A \sin(\omega_{st}) + \text{NOISE}$

359

to hold the total noise power constant. The receiver generates the replica code for the proper satellite, and multiplies it with the incoming signal for a predetermined dwell time, t_D. At the end of each dwell time, the lock indicator is observed. If the lock indication is out of lock, the code generator is stepped by one-half code chip. If the lock indication is in-lock, the code generator remaining in its existing state for another dwell time, when the lock indicator is again observed to determine.whether or not to continue the search.

A second mixer is used to bring the signal down to the second IF frequency, where the signal is split into two paths. In-phase and quadrature reference frequencies are used to obtain a baseband representation of the signal. Since the lock detector must operate in a noncoherent mode, the reference frequency, W_r, will in general be different from the received signal frequency, W_c. The predetection filters are used to establish the noise bandwidth of the lock detector. They must be wide enough to accommodate the uncertainty in knowledge of the received carrier frequency plus the modulation spectrum of the data (approximately ± 200 Hz bandwidth). The square law detector then rectifies the signal. The in-phase and quadrature signals are summed to produce a detector output. This output will have some positive average voltage in the presence of noise only, and a larger positive average voltage in the presence of signal plus noise. An analysis of this output is found in reference 1.

The received power expected to be present at the DNSDP receiver input results in a signal to noise ratio too low for reliable operation of the lock detector without some further filtering of the noise. Therefore, a post detection low pass filter is used to improve the signal to noise ratio prior to making the lock decision. Lock indication is obtained with a voltage comparator, which compares the output of the post detection filter with a preset reference voltage. If the output of the post detection filter is greater than the reference voltage, then in-lock indication is produced. Otherwise, an out-of-lock indication occurs.

3. LOCK DETECTION PEPFORMANCE MODEL

To understand the operation of the lock detector and its effect on receiver cperation, one would like to know at each decision time the probability that an in-lock indication occurs when no signal is present (false alarm), and the probability that an out-of-lock indication occurs when signal is, indeed, present (missed detection). To calculate these probabilities, we must know the probability density function of the voltage at the output of the post-detection filter with and without signal present. The probability of false alarm, P_{FA}, is

$$1) \qquad P_{FA} = \int_{V_T}^{\infty} p_N(V)dV$$

and the probability of missed detection, P_{MD}, is

$$2) \qquad P_{MD} = 1 - \int_{V_T}^{\infty} p_{SN}(V)dV$$

Here, V_T = the threshold voltage used by the voltage comparator

V = the port detection filter output voltage

$p_N(V)$ = probability density of V when noise only is present

$p_{SN}(V)$ = probability density of V when signal plus noise is present

However, determining the probability density functions $p_N(V)$ and $p_{SN}(V)$ when the lock detector uses a post detection filter is a difficult theoretical problem in detection theory.

Several theories have been published in the open literature, but little experimental verification is available. Kac and Siegert, (reference 2) presented an analysis many years ago which is mathematically rigorous, but requires the solution of an integral equation in order to

361

obtain the density functions in closed form. Emerson (reference 3) provides a closed form solution which is also rigorous, and provides expressions for the density functions when both the predetection and post detection filters are Gaussian shaped filters. Marcum (reference 4) uses a sampling theory approach to the problem. Skolnik (reference 5) uses the work of Marcum to obtain his post detection integration improvement factors which have been used in earlier analyses of the lock detector problem for the NAVSAT program. Bussgang, Nesbeda, and Safran (reference 6) use an approach somewhat similar to Marcum's, and present density functions for the case when the post detection filter is a single pole low pass filter.

Since our low cost application uses a single pole low pass filter for the post detection filter, the method of Bussgang has been utilized extensively in this analysis.

The probability density function described by Bussgang for the post detection filter output voltage, V, is given by:

$$3) \qquad p(V)dV = \frac{\lambda_1}{\lambda_2}\frac{1}{\Gamma\left(\frac{\lambda_1^2}{\lambda_2}\right)}\left(\frac{\lambda_1}{\lambda_2}V\right)^{\lambda_1^2/\lambda_2 - 1}\exp\left[-\left(\frac{\lambda_1 V}{\lambda_2}\right)\right]dV$$

Here, λ_1 = mean output voltage, normalized to unity with noise only present

λ_2 = normalized standard deviation of the output voltage

$\Gamma(\bullet)$ = gamma function

The quantities λ_1 and λ_2 are functions of time, signal to noise power ratio, and the amount of post detection filtering used. They are given by:

362

4) $\qquad \lambda_1(t) = 1 + \overline{X}(t)\left\{1 - e^{-4B_2 t}\right\}$

5) $\qquad \lambda_2(t) = \phi\left[1 + 2\,\underline{X}(t)\left\{1 - e^{-8B_2 t}\right\}\right]$

where:

6) $\qquad \phi = \dfrac{1 - \exp(-2B_2/B_1)}{1 + \exp(-2B_2/B_1)}$

$\mathbf{t}$ = time from application of signal

$X(t)$ = signal-to-noise power **ratio**

B_1 = single-sided noise bandwidth of the predetection filter

B_2 = single-sided noise bandwidth of the post detection filter

The signal to noise power ratio, $X(t)$, depends on the carrier to noise density ratio, C/N_0, at the front end of the receiver, the predetection noise bandwidth, B_1, and the predetection filter response as a function of the difference, β, between the received and reference frequencies. Furthermore, the SNR, X, increase with time from the application of signal until the steady state output of the predetection filter is reached. For a single pole low pass predetection filter, $X(t)$ is shown in Attachment 1 to be

7) $\qquad X(t) = \left(\dfrac{C}{2B_1 N_0}\right)\left[\dfrac{1}{1 + \left(\frac{\beta}{4B_1}\right)^2}\right]\left[1 - 2\,\exp\left(-\dfrac{B_1 t}{4}\right)\cos(\beta t) + \exp\left(-\dfrac{B_1 t}{2}\right)\right]$

The probabilities of missed detection and false alarm may be obtained now by substituting equations 4,5,6 and 7 into equation 3, and then solving the integrals in equations 1 and 2. The integrals 1 and 2 are more easily evaluated using the Incomplete Gamma Function. Numerical

evaluation of P_{FA} and P_{MD} using incomplete gamma functions is presented in reference 7. There it is shown that:

8)
$$P_{MD} = I(u,p)$$

and

9)
$$P_{FA} = 1-I(u,p)$$

where

10)
$$U = \frac{V_T}{\sqrt{\lambda_2}}$$

11)
$$p = \frac{\lambda_1^2}{\lambda_2} - 1$$

$$I(u,p) = \text{Incomplete Gamma Function}$$

Now the incomplete gamma function serves quite well when the ratio

of $B_1/2B_2$ is in the range $0 \le \frac{B_1}{2B_2} \le 50$. When the ratio gets much larger than 50, the TRW timeshare computer can no longer handle the enormous numbers generated by the gamma function in the denominator of equation 3. Fortunately, it is a well-known principle in the theory of noise processes that when noise is passed through a sufficiently narrow bandpass filter, its amplitude distribution tends toward gaussian. Therefore, we may approximate the density function of equation 3 by a gaussian density when $B_1/2B_2$ is sufficiently large (e.g., ≥ 20). Reference 7 presents numerical methods for evaluating the false alarm and missed detection probabilities using a gaussian density function. There it is shown that:

12)
$$P_{FA} = \frac{1}{2} \text{erfc}\left(\frac{S_N}{\sqrt{2}}\right)$$

13)
$$P_{MD} = \frac{1}{2} \text{erfc}\left(\frac{S_{SN}}{\sqrt{2}}\right)$$

364

where

$$\text{erfc}(\bullet) = \text{complementary error function}$$

14) $$S_N = \frac{(V_T)^{1/3} - (1 - \frac{\lambda_2}{9})}{\sqrt{\frac{\lambda_2}{9}}}$$

with λ_2 evaluated for noise only

15) $$S_{SN} = \frac{\left(\frac{V_T}{\lambda_1}\right)^{1/3} - \left(1 - \frac{\lambda_2}{9\lambda_1^2}\right)}{\sqrt{\frac{\lambda_2}{9\lambda_1^2}}}$$

with λ_1 and λ_2 evaluated for signal plus noise.

The false alarm and missed detection probabilities are evaluated in reference 7 as a function of normalized threshold, V_T, and steady state SNR, X_S, for various values of the ratio $B_1/2B_2$.

5. ACQUISITION TIME MODEL FOR C-CODE

In order to understand the impact of a lock detector design on the receiver performance, it is necessary to develop a model for the time to acquire the C-code. Deckett, reference 8, describes the code search process and presents an analytic model for the mean time to acquire code lock.

The C-code consists of a 511 chip PN sequence. The received signal is correlated with a locally generated reference for a dwell time t_D seconds. At the end of this dwell time interval the lock detector is observed. If an out-of-lock indication is obtained, the local reference code state is shifted one-half chip. If an in-lock indication occurs, the search is stopped, and the lock detector is observed k more dwell intervals. If at the end of k intervals one or more out-of-lock indications occur,

365

it is concluded that the signal is not present, and that only false alarm indications were received. If, however, all observations of the lock detector indicate an in-lock condition, the signal is judged to be present, and the carrier tracking loop is then enabled. The time to correctly acquire the code is given by (reference 8).

16) $$Tacq = t_D (i+1) + A(M+N_i-i-1)$$

where $Tacq$ = acquisition time (sec.)

       t_D = dwell time (sec.)

        i = number of missed detections

       N = total possible search cells, (i.e., half-chip states)

       M = cell number where signal actually exists

       A = time spent in cells where signal does not exist

Here i, A, and M are random variables. An expression for the mean time to acquisition, $<Tacq>$, was derived in reference 8.

17) $$< Tacq> = t_D (< i> +1) + < A> (< M> + N < i > - < i> - 1)$$

Here, $< \bullet >$ denotes expected value

18) $$< i> = \frac{P_{MD}}{1-P_{MD}}$$

19) $$< M> = \frac{N+1}{2}$$

20) $$< A> = t_D (1 + k \, P_{FA})$$

where P_{MD} = probability of missed detection

       P_{FA} = probability of false alarm

        k = false alarm penalty in dwell intervals

6. OPTIMIZATION OF RECEIVER PARAMETERS

In the preceding pages, it was shown how a number of receiver parameters affect the false alarm and missed detection probabilities, and therefore affect the code acquisition time. Since it is highly desirable to minimize the time necessary to acquire the C-code, the receiver design parameters were traded off to obtain an optimum set of receiver parameters which minimizes acquisition time.

The parameters subject to optimization are:

a) Predetection filter bandwidth, B_1

b) Post detection filter bandwidth, B_2

c) Code cell dwell time, t_D

d) False alarm penalty, k

e) Threshold reference voltage, V_T

These parameters may be uniquely determined so as to minimize $< Tacq >$ once we know C/N_0 and the allowable probability that k successive false alarms follow an in-lock indication. (Should this happen, the code search would not resume until the computer recognizes such a condition and re-starts the code search.)

Figure 2 shows the minimized average acquisition times vs. C/N_0 for a family of predetection bandwidths. Figure 3 shows the dwell times required to achieve the acquisition times in Figure 2. Figure 4 shows the sensitivity of average acquisition time to changes in the predetection filter noise bandwidth. Figures 5, 6 and 7 show the sensitivity of average acquisition time to changes in the threshold reference voltage, V_T.

The probabilities of false alarm and missed detection, and the false alarm penalty, k, are listed in Table 1 for some typical minimized acquisition times.

367
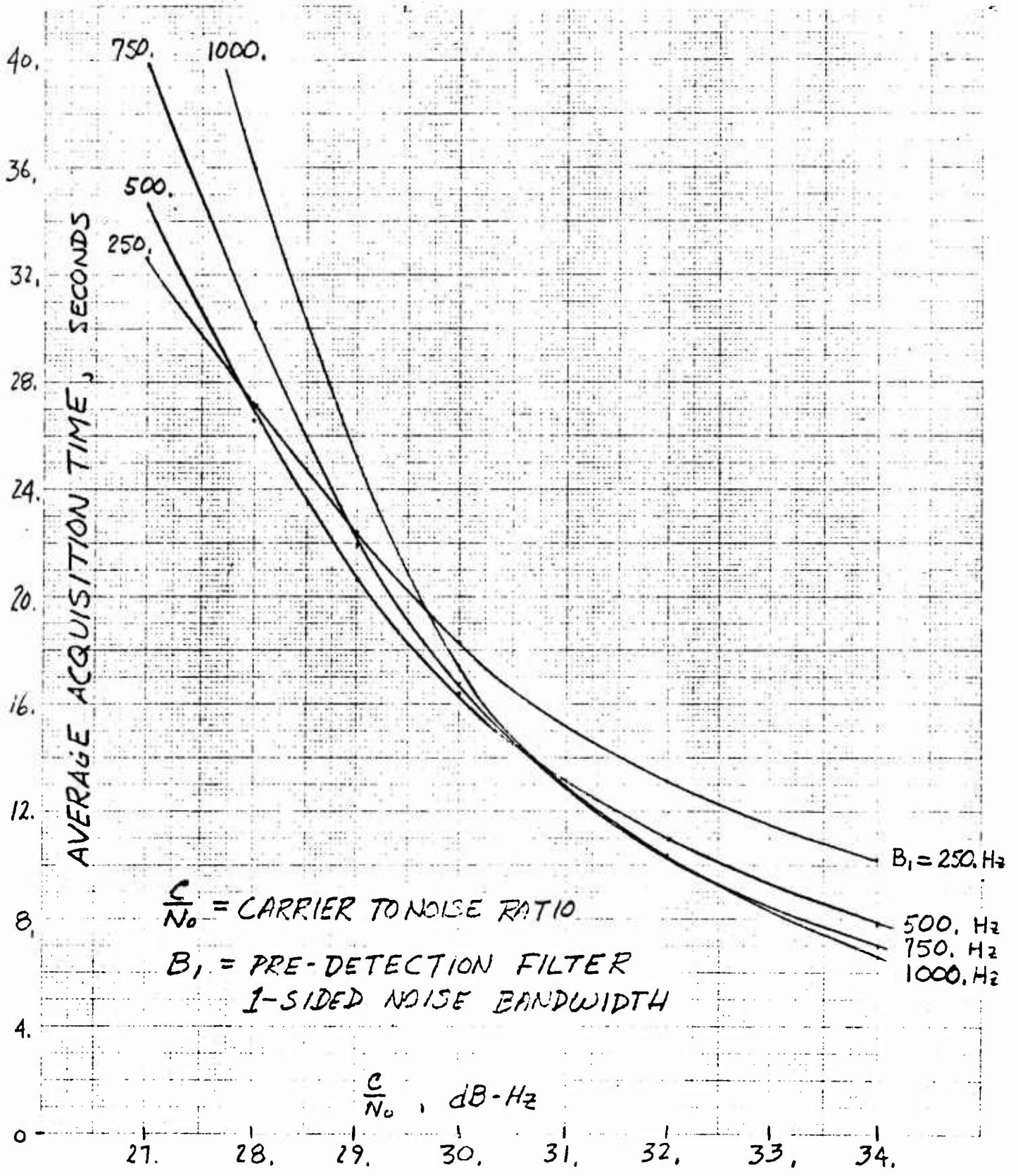
Figure 2. Optimized Lock Detector Acquisition Time

368
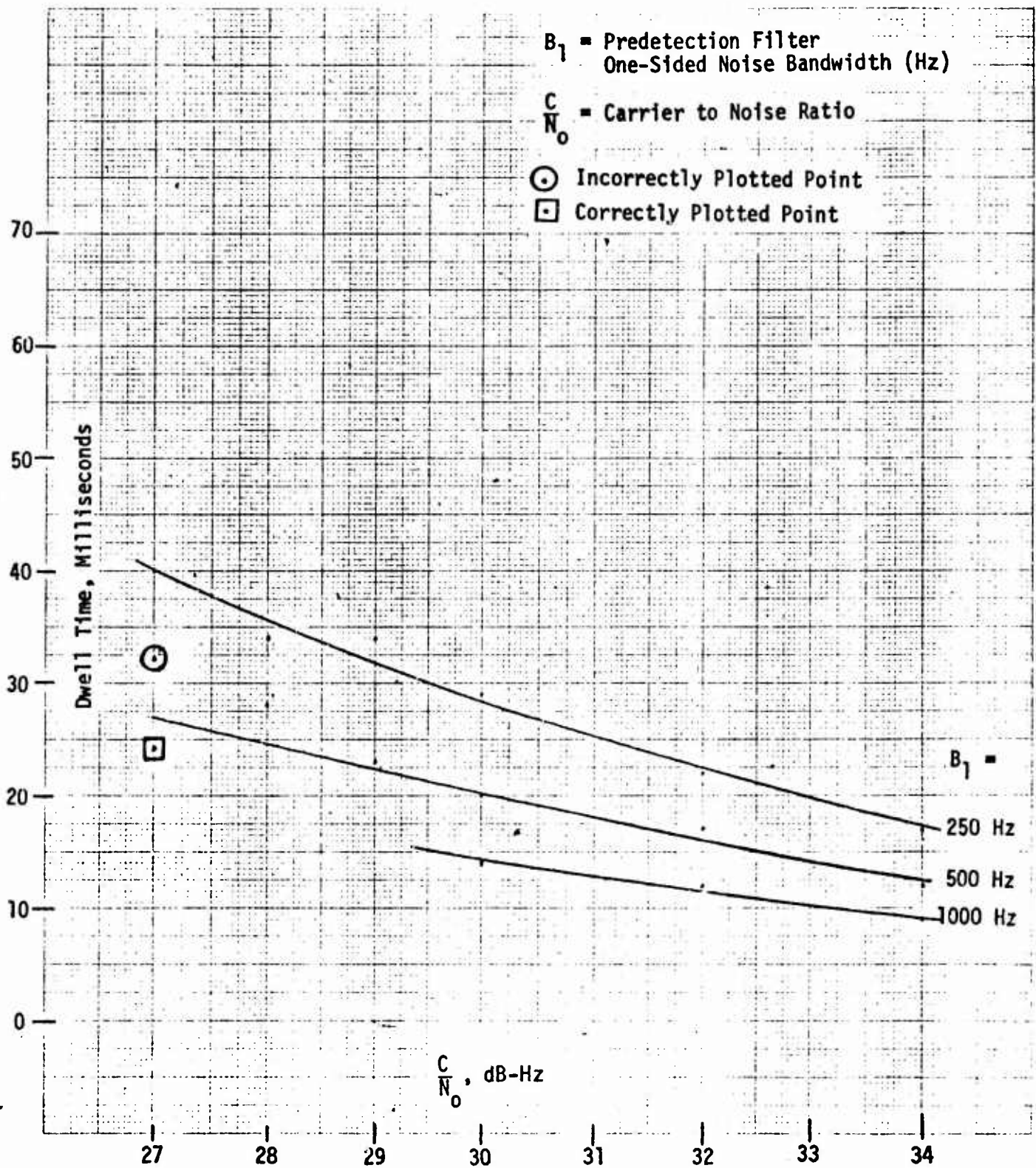
Figure 3. Dwell Times Required

369
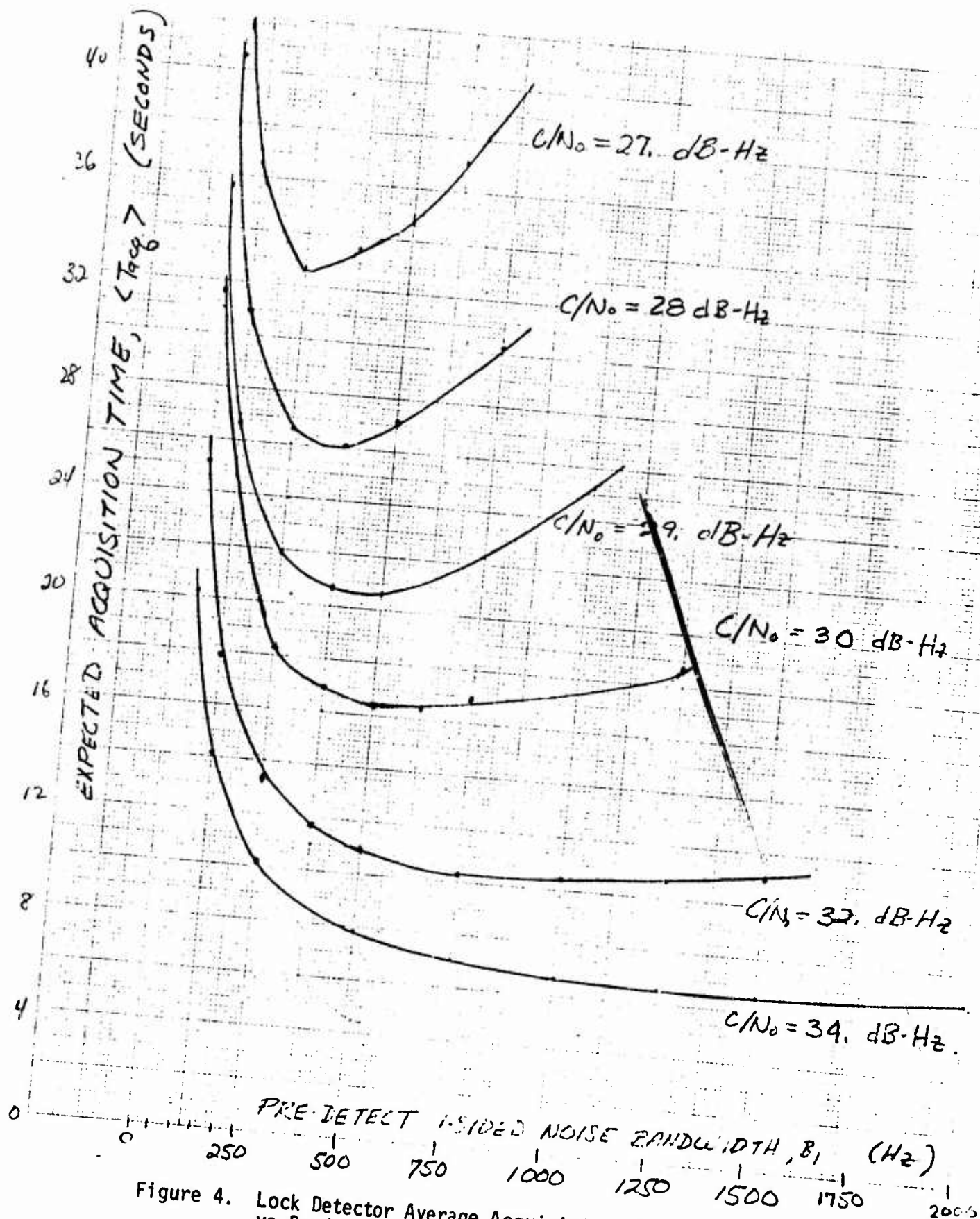
Figure 4.   Lock Detector Average Acquisition Time
vs Predetection Filter Noise Bandwidth – Optimized

370
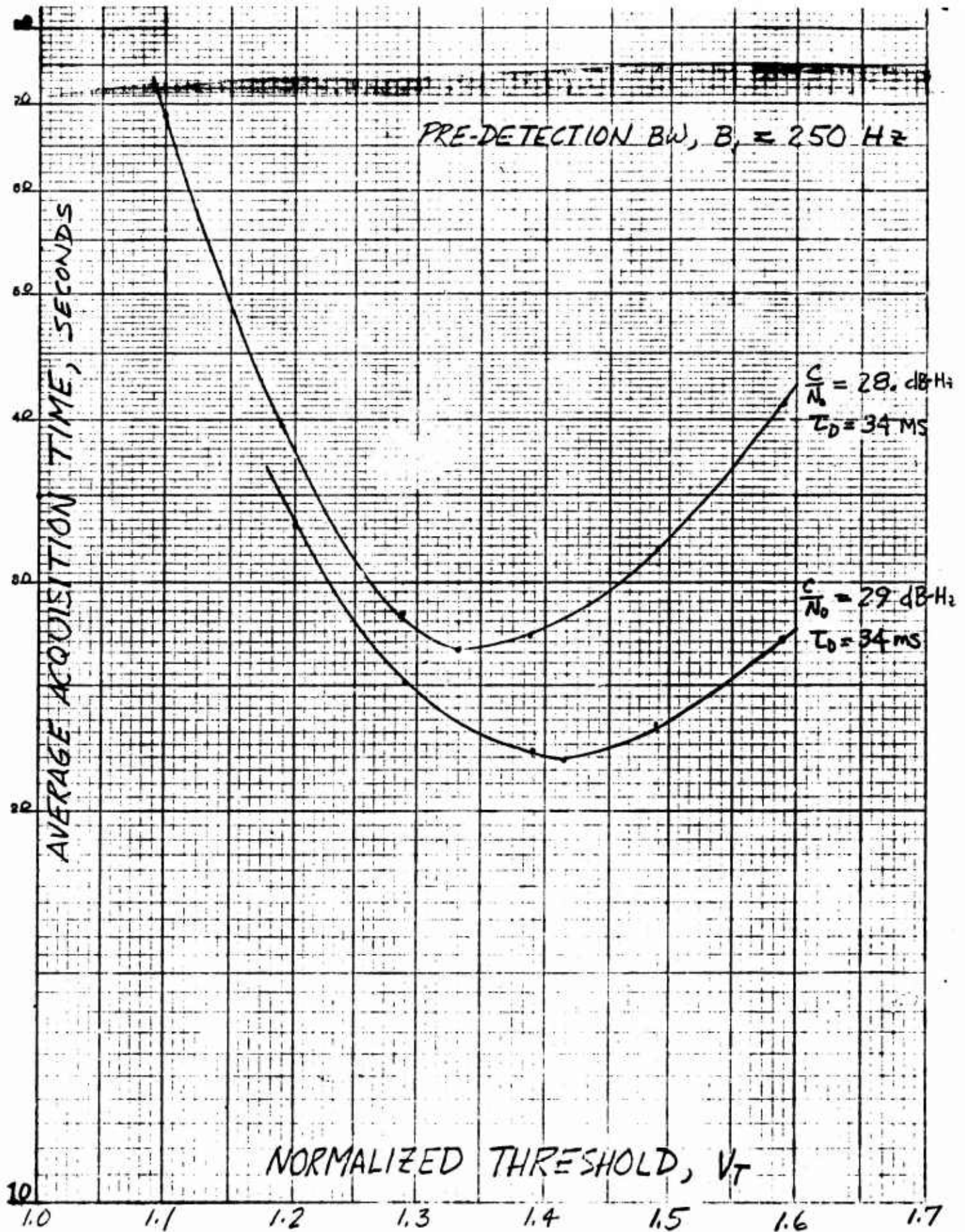
Figure 5. Acquisition Time Sensitivity to Threshold Voltage
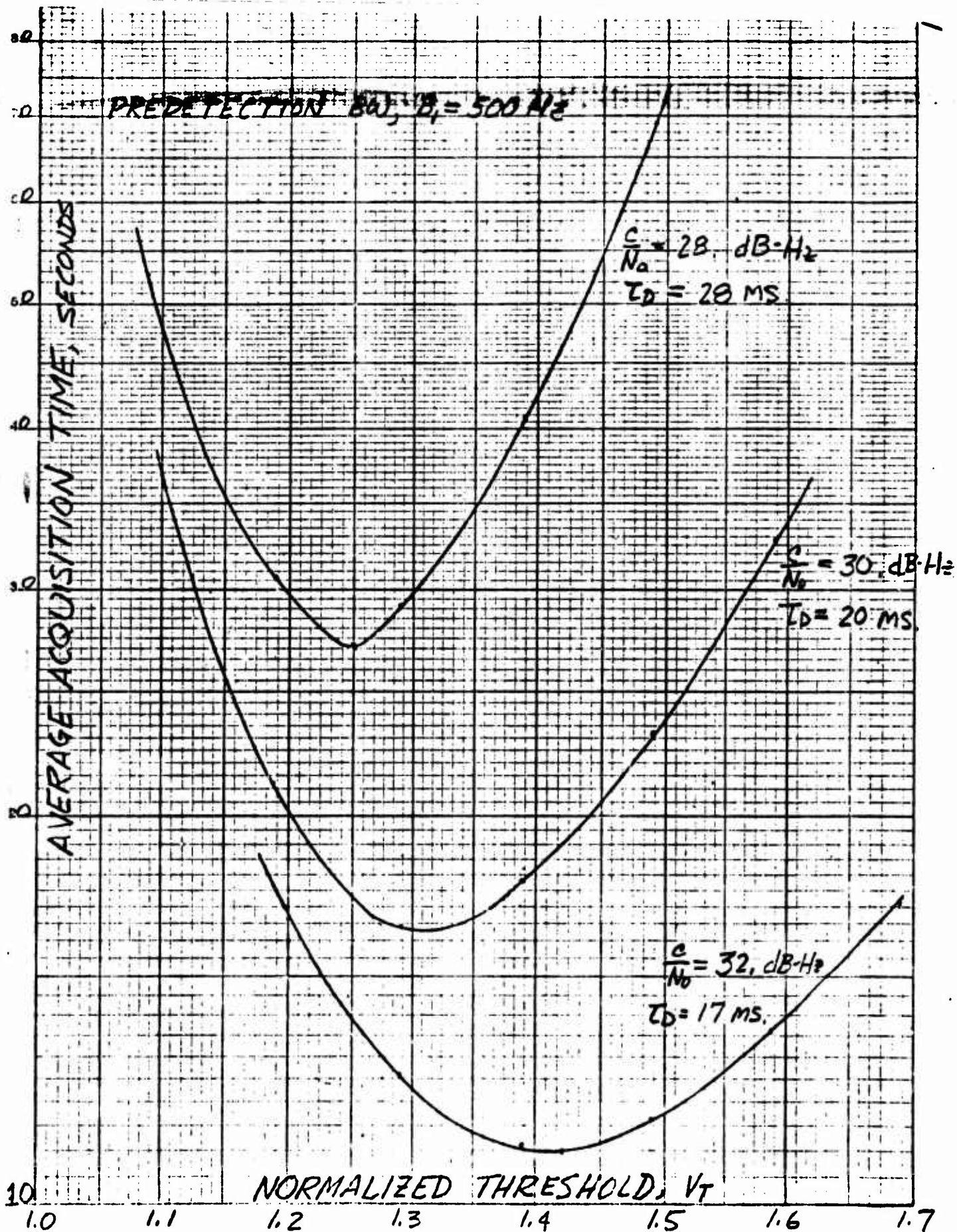
Figure 6. Acquisition Time Sensitivity to Threshold Voltage

372
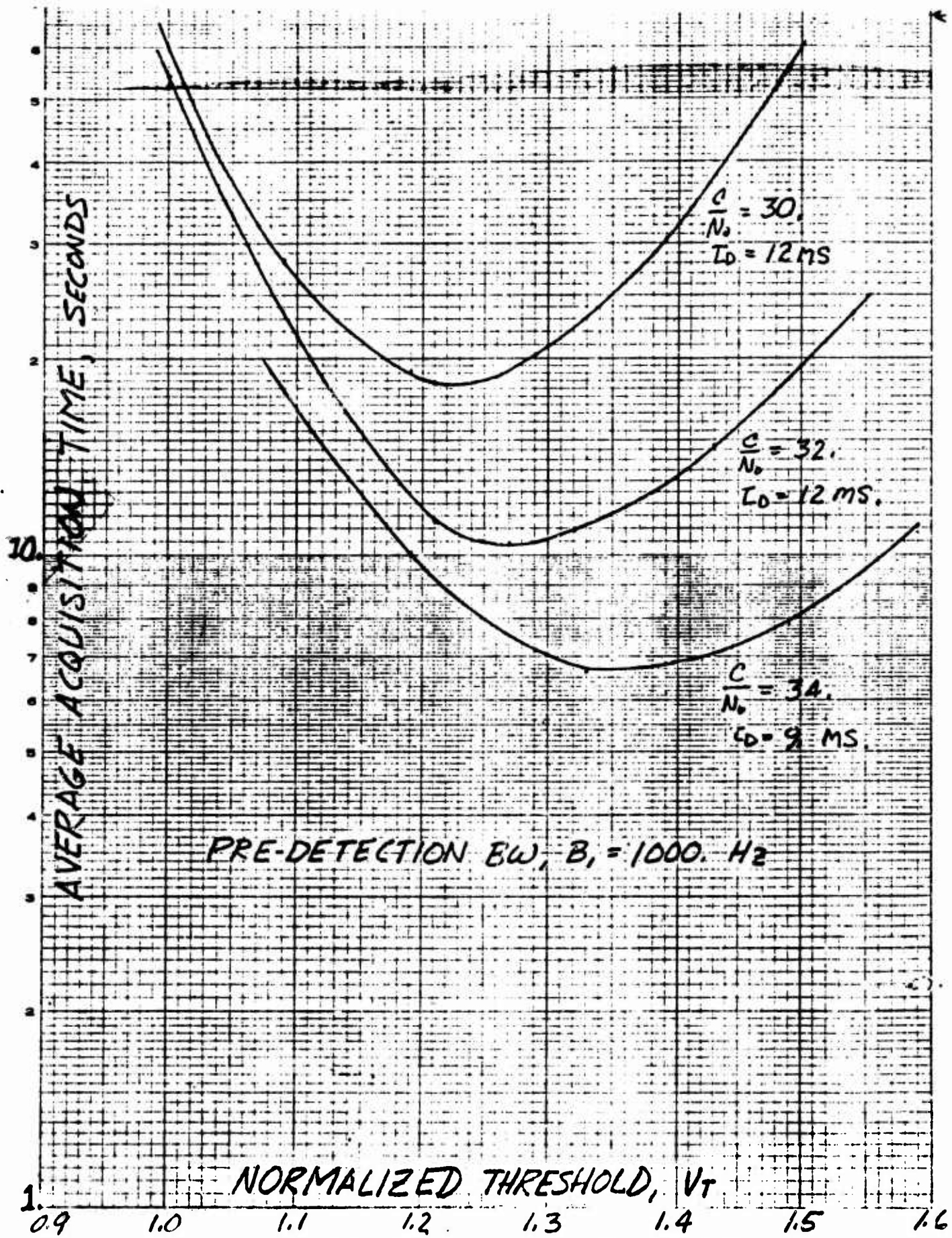
Figure 7. Acquisition Time Sensitivity to Threshold Voltage

373

Table 1. Table of Values for P_{FD}, P_{MD}, k

C/No	B_1 (H_z)	Tacq (sec)	t_D (ms)	P_{FA}	P_{MD}	k
27.	62.5	46.31	75.	.021	.064	3.
	125..	36.53	57.	.021	.082	3.
	250.	32.74	40.	.056	.134	4.
	375.	35.53	33.	.055	.239	4.
	500.	35.67	24.	.097	.324	5.
	625.	37.13	19.	.098	.44	5.
29.	62.5	35.74	59.	.021	.054	3.
	125.	26.69	43.	.020	.067	3.
	250.	21.95	34.	.021	.085	3.
	375.	20.73	25.	.056	.055	4.
	500.	20.69	23.	.055	.180	4.
	750.	22.32	16.	.097	.295	5.
34.	62.5	20.32	34.	.021	.047	3.
	125.	14.13	24.	.021	.0397	3.
	250.	10.17	17.	.021	.048	3.
	500.	7.82	12.	.020	.092	3.
	750.	7.02	11.	.020	.082	3.
	1000.	6.69	9.	.045	.105	4.
	1250.	6.53	8.	.056	.132	4.
	1500.	6.57	8.	.052	.142	4.
	2000.	6.83	7.	.051	.225	4.
	2500.	7.11	5.	.098	.30	5.

Table 1A

C/N$_o$	B$_1$(Hz)	(sec) Tacq	m(s) t$_D$	P$_{FA}$	P$_{MD}$	k
28	250	26.6	34	4.8×10^{-2}	.12	4
	500	27.2	28	.051	.22	4
	750	29.3	16	.097	.41	5
30	250	18.3	29	.02	.077	3
	500	16.4	20	.056	.135	4
	750	16.9	18	.054	.20	4
	1250	18.8	10	.093	.429	5
32	250	13.4	22	.021	.056	3
	500	11.0	17	.021	.087	3
	750	10.4	13	.054	.13	4
	1000	10.4	12	.052	.17	4
	1250	10.8	10	.054	.27	4
	1500	11.2	8	.097	.30	5

The false alarm penalty used depends on the largest acceptable probability that k successive false alarms occur. Each observation of the lock detector is essentially an independent decision. Therefore,

21)
$$E = (P_{FA})^k$$

where E = probability of k successive false alarms.

The criterion selected was that E be equal or less than 10^{-5}. Table 2 shows some typical values of minimized average acquisition for various values of E.

The post detection filter noise bandwidth is selected from the dwell time required. It was found that when $B_2 t_D = 0.3$, the smallest average acquisition time is obtained. Therefore, the post detection filter noise bandwidth (in Hz) for this study is in each case

22)
$$B_2 = \frac{0.3}{t_D}$$

where t_D = dwell time in seconds.

7. SELECTION OF RECEIVER DESIGN PARAMETERS

Although the design value of C/N_0 has not been selected at this time, it is useful to show how to compute hardware design parameters for this receiver. Suppose, for example, that a C-code value of $C/N_0 = 30.$ dB-Hz is selected for the receiver design point. Then from Figure 4, it is seen that a predetection noise bandwidth of $B_1 = 500$ Hz will minimize the average acquisition time. (This will result in an average acquisition time of 16.4 seconds.)

Since the modulation bandwidth of the data is about $\pm$ 200 Hz and the expected frequency uncertainties are shown in reference 8 to be less than 200 Hz, a 500 Hz predetection noise bandwidth is sufficiently large to pass the carrier and its modulation.

From Figure 3, we see that for $C/N_0 = 30.$dB-Hz and $B_1 = 500$ H$_z$, the dwell time should be set to $t_D = 21$ ms. From equation 22, we obtain a post detection noise bandwidth of $B_2 = 14.3$ Hz. From Table 1 we see that the penalty for false alarms, k, should be k=4.

Table 2. Sensitivity of <Tacq> to E

$C/No = 30.$ dB-H_z

$B_1 = 500.$ H_z

E	<Tacq> min (sec)	$\tau D^{(ms)}$	P_{FA}	P_{MD}	k
10^{-6}	16.79	22.	.031	.141	4.
10^{-5}	16.41	20.	.056	.135	4.
10^{-4}	15.85	20.	.046	.154	3.
10^{-3}	15.40	17.	.097	.157	3.
10^{-2}	14.24	17.	.097	.157	2.

The threshold voltage, V_T, is very important. From Figure 5, we see that the normalized threshold, V_T, should be 1.32. To compute the absolute voltage, v_T, we need to know the rms noise voltage, m_R, at the input to the threshold detector with signal absent. This value is established by design of the AGC circuit. Then the absolute reference voltage is

23)
$$v_T = m_R \, V_T$$

Suppose m_R = 2 volts RMS. Then v_T = 1.32 x 2 = 2.64 volts.

Finally, the time constants for the pre and post detection filters must be computed. For a single pole low pass filter, the noise bandwidth, B, is given by

24)
$$B = \frac{1}{4T_c}$$

where
T_c = RC time constant

B = single-sided noise bandwidth

Thus, the predetection filter time constant is T_{c_1} = 0.5 milliseconds, and the post detection filter time constant is T_{c_2} = 17.5 milliseconds. Table 3 summarizes the selection of parameters for the design example given above.

8. CONCLUDING REMARKS

This memo has presented the analytic ideas necessary to design the code correlation lock detector for the DNSDP receiver so that the acquisition time is minimized. A design example was worked out which may very well serve as our baseline design. However, a few words of caution are in order. First, the analytic model for the probability density of the lock detector output voltage, V, is an approximation. It is not known by the author how well this model would fit actual test data. Therefore, during the development phase, some experimentation should be planned with a breadboard lock detector

378

Table 3. Selection of Design Parameters

Requirements

$$C/No = 30. \; db - H_z$$

$$B_1 = 500. \; H_z$$

$$E \leq 10^{-5}$$

Receiver Parameters

$$\tau_D = 21. \; ms$$

$$V_T = 1.32$$

$$B_2 = 14.3 \; H_z$$

$$Tc_1 = 0.50 \; ms$$

$$Tc_2 = 17.5 \; ms$$

$$k = 4$$

Receiver Performance

$$\langle Tacq \rangle = 16.4 \; seconds$$

to confirm these results. Second, the obvious sensitivity of acquisition
time to threshold voltage indicates that both the reference voltage and
the receiver gain must be held to small tolerances. This implies a "tight"
AGC loop design. Finally, the algorithm assumed here for acquiring lock
in the presence of false alarms and missed detections of the PN code is
not the only possible algorithm. It is possible that additional study
would reveal methods of reducing the minimum time to acquire the code.

REFERENCES

1. J. R. Gilder, "Performance Comparison of the Noncoherent Lock
   Detector for Baseband and IF Operation," DNSDP-JRG-078,
   26 September 1973.

2. Kac, M. & Siegert, A.J.F., "On the Theory of Noise in Radio Receivers
   with Square Law Detectors," Journal of Applied Physics, Vol. 18,
   April 1947, pp 383-397.

3. Emerson, R.C., "First Probability Density with Square Law Detectors,"
   Journal of Applied Physics, Vol. 24, September 1953, pp 1168-1176.

4. Marcum, J.I., "Mathematical Appendix," Rand Corporation Research
   Report. RM-753, July 1, 1948.

5. Skolnik, M.I., "Introduction to Radar Systems," McGraw-Hill, 1962.

6. Bussgang, J.J., Nesbeda, P., and Safran, H., "A Unified Analysis of
   Range Performance of CW, Pulse, and Pulse Doppler Radar," Proc. of
   IRE, October 1959, pp 1753-1762.

7. J. R. Gilder, "Performance Analysis of the Noncoherent Lock Detector
   for the DNSDP Receiver, with Numerical Results." DNSDP-JRG-202.

8. M. Deckett, "Analysis and Simulation of the C-code Acquisition Time,"
   DNSDP-MD-160, 9 November 1973.

ATTACHMENT 1 TO APPENDIX 13

TRANSIENT RESPONSE OF THE PREDICTION FILTER

A simplified block diagram of the lock detector is shown in Figure A1. When the signal S(t) is composed of noise only, the outputs R(t) and V(t) have some steady state RMS values. However, when a signal, A sin $(w_c t)$, is applied at the input at time zero, the predetection low pass filters must charge up before the output R(t) reaches a steady state value. (The charging effect of the post detection filter on V(t) is accounted for in the lock detector performance model of Bussgang, et. al.). This analysis presents a model for the charging effect on R(t), and therefore the effective SNR, X(t), at the input to the post detection filter.

The input signal component of S(t) is (ignoring modulation)

A1) $$A \sin (w_c t)$$

This signal is mixed with the in-phase and quadrature components of the reference frequency to obtain at the input to the predetection filters.

A2) In-phase: $$A \cos (w_c - w_R)t$$

A3) Quad: $$A \sin (w_c - w_R)t$$

The transfer function of the two identical predetection filters is:

A4) $$H(s) = \frac{\alpha}{S + \alpha}$$

where

$$\alpha = \frac{1}{RC}$$

The predetection filter outputs $e(t)$ are:

A5) $$e_s(t) = \frac{A\,U(t)}{1 + (\beta/\alpha)^2} \left\{ (\beta/\alpha)e^{-\alpha t} + \sin \beta t - (\beta/\alpha)\cos(\beta t) \right\}$$

A6) $$e_c(t) = \frac{A\,U(t)}{1 + (\beta/\alpha)^2} \left\{ \cos(\beta t) + (\beta/\alpha)\sin(\beta t) - e^{-\alpha t} \right\}$$

382
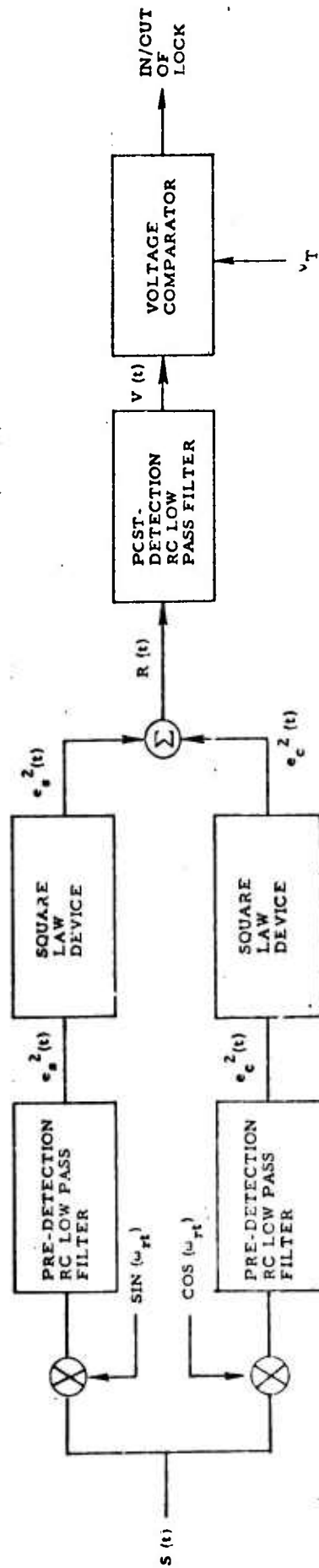
Figure A1. Lock Detector-Block Diagram

where

U(t) = unit step response

$\beta = w_c - w_r$

Squaring $e_s(t)$ and $e_c(t)$ and then adding the squares

A7)
$$R(t) = \frac{A^2 U(t)}{1+(\beta/\alpha)^2} \left\{ 1 - 2e^{-\alpha t} \cos(\beta t) + e^{-2\alpha t} \right\}$$

The value $R(t)$ above is the transient response of the lock detector to the signal component of the input. Since the noise component of the signal is presumed to have achieved a steady state RMS value at the output, the signal to noise ratio, $X(t)$, is

A8)
$$R(t) = \frac{C}{2N_o B_1} \left\{ \left(\frac{1}{1+(\beta/\alpha)^2} \right) \left(1 - 2e^{-\alpha t} \cos(\beta t) + e^{-2\alpha t} \right) \right\}$$

where

C = carrier power

B_1 = the single sided noise bandwidth of each predetection filter.

N_o = input noise spectral density.

The noise bandwidth, B_1, can be found from the definition of noise bandwidth.

A9)
$$B \triangleq \frac{\frac{1}{2\pi} \int_0^\infty |H(s)|^2 \, ds}{|H(s)|^2_{max}}$$

Substituting the transfer function for the single pole low pass filter, equation A4, into equation A9 gives:

A10)
$$B_1 = \frac{\alpha}{4} = \frac{1}{4RC}$$

384

APPENDIX 14

RECEIVER SCHEMATIC DRAWINGS

This appendix contains the receiver schematic drawings which, because of their size, are more conveniently bound at the end of this book.   The drawings here are:

SK   100   002
SK   100   101
SK   100   200   Sheets 1-5
SK   100   300   Sheets 1 and 2
SK   100   400   Sheets 1 and 2.

NOTES:

BTP = BITE TEST POINT

△ = ONE-HALF MODULE. THIS MODULE
CIRCUITS FOR TWO CHANNELS

PN CODE GENERATORS

CODE SEARCH CONTROL LOGIC

C-CODE EPOCH DETECTOR

C-CODE → EPOCH PULSES

DITHER CLOCK

TAU DITHER

DITHERED OUTPUT

CODE SELECT CMD

C/P CODE SELECT

P-CODE GEN.

P-CODE CLOCK

CODE OUTPUT

SEARCH ENABLE CMD FROM COMPUTER

C-CODE GENERATOR

RECEIVER EQUIPMENT

COMPUTER EQUIPMENT

÷10

C/P CODE CLOCK SELECT

CODE CLOCK TO TRACK MEAS. MODULE

P CODE NUM CMDS (4 CHANNELS)

COMPUTER INPUT UNIT

TRANSFER RESPONSE

TAU DITHER REF

AFL SLEW CMDS (4)

10.23 MHz CODE CLOCK

P-CODE HANDOVER LOGIC

P-CODE GENERATOR

SECURITY PROCESSOR

BYPASS SWITCH

DISCRETE CMDS

TRANSFER CMD

LOOP FILTER

RESET

TOD READ CMD

INSTRUCTION WORDS

CPU

MEMORY

DATA BIT SYNC DETECTOR

REF CLOCK

BIT DATA SYNC BITS

HANDOVER CMD FROM COMPUTER

BIT SYNC CLOCK

SATELLITE DA BITS (4 CHANNELS)

COMPUTER OUTPUT UNIT

DISCRETE SIGNALS

BIT SYNC (4)

A/D CONTROL

BRIDGE GATE GEN.

TRACKING, JAM LEVEL, AND STATUS BUFFER INPUTS

DMA DATA LINES

PREFILTER

SIGNAL MULTIPLEXER

SYNC DECISION LOGIC

BIT SYNC SLEW PULSE

TOD INTERRUPT

TOD INTERRUPT

A/D

BIT SYNC

READOUT CLOCK

DMA ADDRESS LINES

DATA BITS LEVEL BUFFER

BIT SYNC LOCK STATUS

ALC INPUT

DIFFERENTIAL DECODER

DATA OUTPUT

TO DATA BITS COMPUTER

DATA OUTPUT TO PN GEN MODULE

CHANNEL 1 IF/DIGITAL PROCESSOR

COMPUTER I/O AND RECEIVER CONTROL

DETECTION

BTP = BITE TEST POINT

= ONE-HALF MODULE. THIS MODULE CONTAINS CIRCUITS FOR TWO CHANNELS

NOTES:

BTP = BITE TEST POINT

⚠ ONE-HALF MODULE THIS MODULE CONTAINS CIRCUITS FOR TWO CHANNELS

2

REVISIONS

ZONE	LTR	DESCRIPTION	DATE	APPROVED

DITHER OUTPUT TO CHANNEL B PN DEMOD

DITHER CLOCK

SELECT CMD

P-CODE GEN

TAU DITHER

C/P CODE SELECT

PN CODE OUTPUT TO CH. A PN DEMOD

Z CODE CLOCK

L CODE AND DER TRACKING PS

COARSE RANGE BUFFER

T.O.D READ CMD

CODE UPDATE

SLEW COUNTER

READY WORD FILL

CODE SLEW COMMAND

CHANNEL A P-CODE LOGIC

SIGNAL ROUTING LOGIC

CH A P-CODE CLOCK

P-CODE GEN

COARSE RANGE BUFFER

BIT SYNC

SYNC

COARSE RANGE COUNTER

ENABLE PREPOSITION

CH A CARRIER PREPOSITION CONTROL

CH A CODE UP-DATE LOGIC

COMPUTER INPUT UNIT

COMPUTER PROGRAM CONTROL

TRANSFER

TRANSFER RESPONSE

P-CODE

CH B CARRIER PREPOSITION CONTROL

CHANNEL A L-CODE GEN

SIGNAL L-CODE CLOCK ROUTING LOGIC

P-CODE FLYWHEEL STORAGE

SLEW UPDATE SLEW COUNTER

ENABLE SEARCH CMD

RECEIVER CODE CMDS

RECEIVER CONTROL UNIT

CONTROL LINES

CONTROL WORDS

CODE SEARCH LOCK STATUS

C-CODE SEARCH CONTROL

T.O.D. INTERRUPT

DITHER CLOCK

DITHERED OUTPUT TO CH B PN DEMOD

CPU

MEMORY

C-CODE FLYWHEEL STORAGE

CODE SEARCH LOGIC STATUS

ENABLE SEARCH CMD

CHANNEL B C-CODE GENERATOR

C/P CODE SELECT

TAU DITHER

Z CODE CLOCK

PN CODE OUTPUT TO CH. B PN DEMOD

CHANNEL B C-CODE LOGIC

P-CODE SEARCH CONTROL

READY WORD FILL

C-CODE EPOCH DETECTOR

B CODE AND ER TRACKING LOOPS

SECURITY ENCRYPTOR

BI-PHASE SWITCH

SQUARE WAVE GEN

÷6

BUFFER REGISTERS

BIT SYNC LOCK STATUS

BIT SYNC

DATA BITS

COMPUTER OUTPUT UNIT

DMA DATA

DMA ADDRESS

DMA REQUEST

DMA STROBE

P CODE HANDOVER LOGIC

CODE GEN × 1 × 2

BIT SYNC DETECTOR

÷4

C-CODE BIT SYNC

FRAME SYNC

T.O.D INTERRUPT

READOUT CLOCK

POWER ON RESET (POR) FLAG

DATA READY FLAG SET

DATA READY FLAG RESET

DATA ERROR FLAG

TOD INTERR

POR FLAG RESET

PN CODE GENERATOR

BIT SYNC SELECT

A/D CONTROL

DATA SELECT

PREDET FILTER

SIGNAL MULTIPLEXER

A/D

SYNC DECISION LOGIC

C/P SELECT

ALC INPUT

BIT DECISION

DIFFERENTIAL DECODER

DATA BITS

JAM LEVEL BUFFER

COMPUTER I/O AND RECEIVER CONTROL

RECEIVER EQUIPMENT

COMPUTER EQUIPMENT

BIT SYNCHRONIZER AND DETECTION

BTP = BITE TEST POINT

ONE-HALF MODULE THIS MODULE CONTAINS CIRCUITS FOR TWO CHANNELS

B SCHECHTER	2-5-74	
J GELDER	2-5-74	

TRW

SEQUENTIAL GPS RECEIVER TYPE II CLASSES D,E

D | 11982 | SK-100002

15 PLUG-IN MODULES $\frac{1}{2} \times 4 \times 4$

PRE-AMP/MIXER (1)
FREQUENCY SYNTH. (1)
IF AMP/FILTER DET. (2)
PN DEMODULATOR (2)
IF AMP/MIXER (2)
LOOP FILTER/CODE
ERR. DET. (2)
BIT RF GENERATOR (1)
BIT LOGIC (1)
DIGITAL MEASUREMENTS (2)
PROCESSOR INTERFACE (1)

CARD CAGE
ALTERNATE CONFIG.

GROWTH

PROCESSOR (PLUG-IN 1.8)

XTAL

EST WT 2.0*

EST WT 1.25*

12.50

FAULT INDICATORS
MODULES (15)

DUST COVER

5.00 PANEL
4.87 DUST COVER

7.62

DUST COVER
RUBBER-¼ WIDE   MODULE HOLD-DOWN
NYLON STRIP-¼ WIDE

CARD CAGE &TC CARDS
ALTERNATE CONFIGURATION

HANDLE-SPRING
RETURN-90° TRAVEL

EST WT 5.0*

FAULT INDICATOR
LATCH- FLAG TYPE

ELAPSED TIME
INDICATOR

INTER CONNECT
WIREWRAP & I/O CONNECTOR

POWER SUPPLY
STOWED POSITION
(2 x 4 x 5)

OPEN POSITION

CLAMP

CHASSIS

STRESS RELIEF
SERVICE LOOP

EST WT = 18.

FIG. 1

2

GROWTH ── PROCESSOR (PLUG-IN 1.5×4×6.5)

XTAL-OSC 2.5×3.3×#.7

EST WT 2.0*

EST WT 1.25*

DUST COVER

CARD CAGE & PC CARDS
ALTERNATE CONFIGURATION

CLAMP   CHASSIS

STRESS RELIEF
SERVICE LOOP

EST WT = 18.5 LBS

FIG. 1

BACK PANEL
CONNECTOR

HOLD-DOWN RECEPTACLES

1.

RF/IF MODULE

DIGITAL PC CARD

PROCESSOR

XTAL-OSC

ESTIMATED - CLASS 'C'

SIZE $4\frac{7}{8}$ W x $7\frac{5}{8}$ H x $12\frac{9}{8}$ L

VOL   470 CU IN

WEIGHT   18.5 LBS.

DISSIPATION   30 WATTS

POWER SUPPLY
OPEN TEST POSITION

SEQUENTIAL DNSS RECEIVER   FIG. 2

XTAL-OSC

ESTIMATED - CLASS "C"

SIZE $4\frac{7}{8}$ W × $7\frac{5}{8}$ H × $12\frac{9}{16}$ L

VOL   470 CU IN

WEIGHT 18.5 LBS.

DISSIPATION   30 WATTS

ISS RECEIVER   FIG. 2
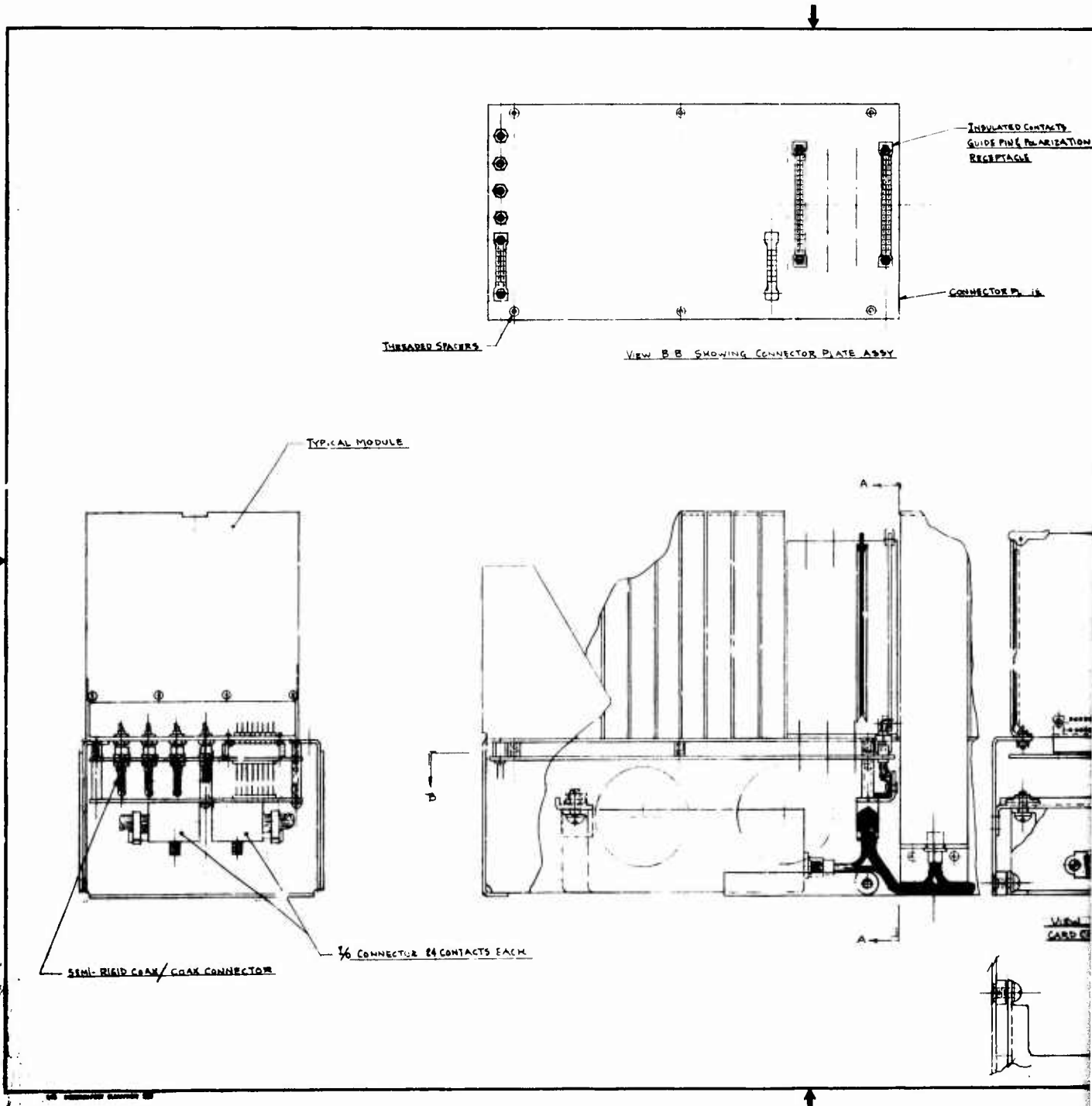
D	11982	SK 100200
		2 of 5

COVER

SUBSTRATE

WEB

COAX PLUG-IN
CONNECTOR

TYPICAL 4-SUBSTRATE MODULE PACKAGE

2

WEB

HOUSING

CONNECTOR

GUIDE PIN

COAX PLUG-IN
CONNECTOR

ATE MODULE PACKAGE   FIG.3
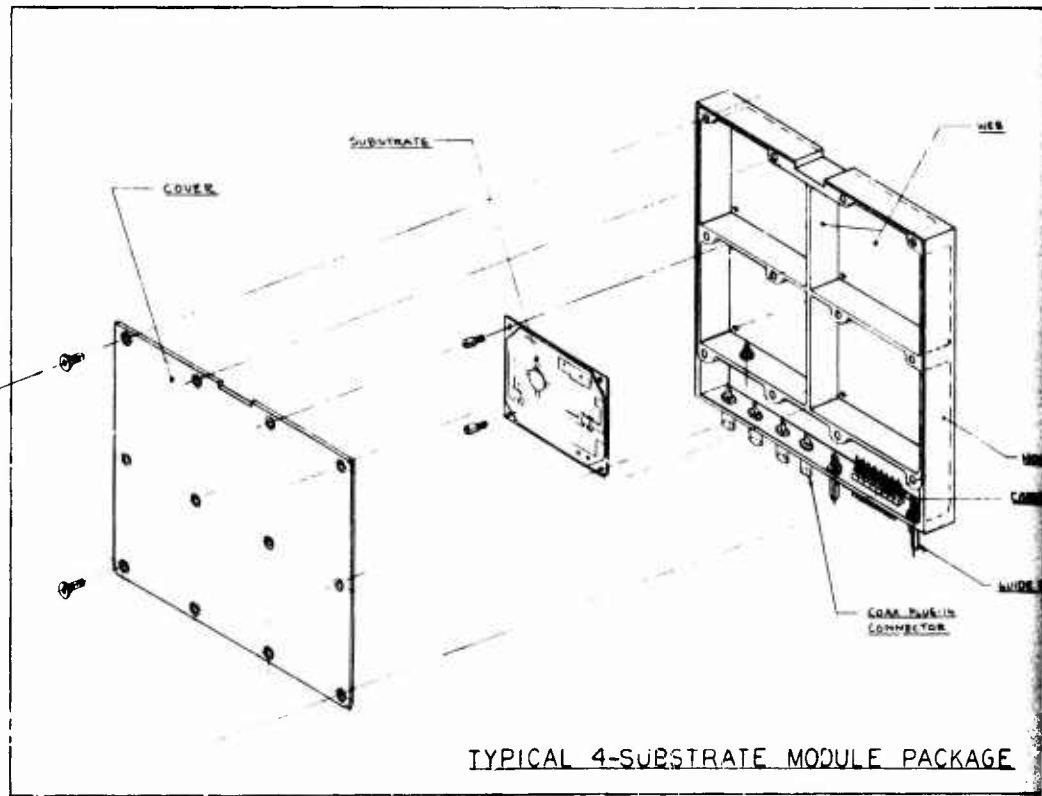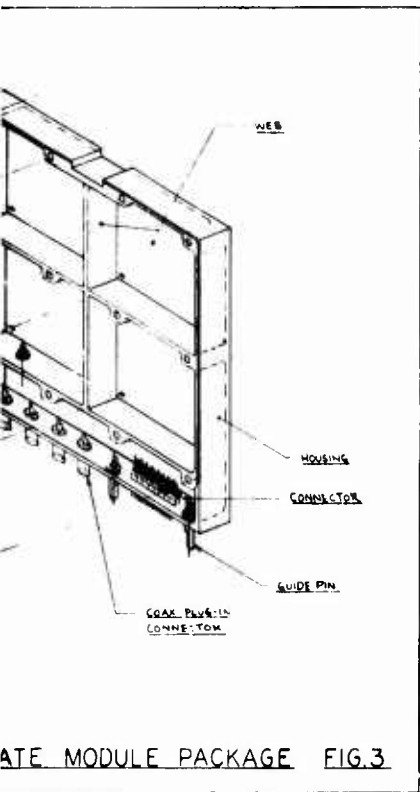
| D | 11982 | SK-100200 |

Very poor copy

2

py

1

INSULATED CONTACTS
GUIDE PINS POLARIZATION
RECEPTACLE

CONNECTOR PL. 18

THREADED SPACERS

VIEW B B SHOWING CONNECTOR PLATE ASSY

TYPICAL MODULE

A

B

A

SEMI-RIGID COAX/COAX CONNECTOR

1/6 CONNECTOR 24 CONTACTS EACH

2

INSULATED CONTACT
GUIDE PIN & POLARIZATION
RECEPTACLE

CONNECTOR PLATE

4 x ... PC CARD

CARD EXTRACTOR

CARD CAGE AND CARD GUIDE
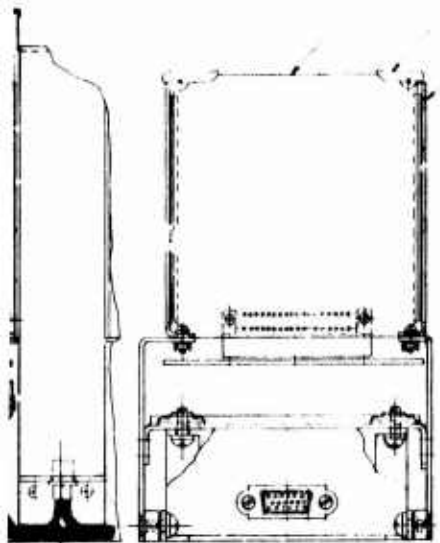
VIEW A-A SHOWING PC CARD,
CARD CAGE, & MTG. OF POWER SUPPLY
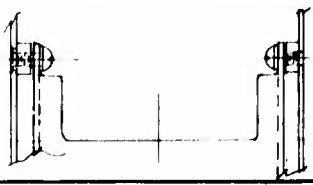
FIG.5·SHOWING CARD CAGE,
PC CARDS, AND WIRING
INTERCONNECT CONCEPT

| D | 11982 | SK 100200 |

_1_

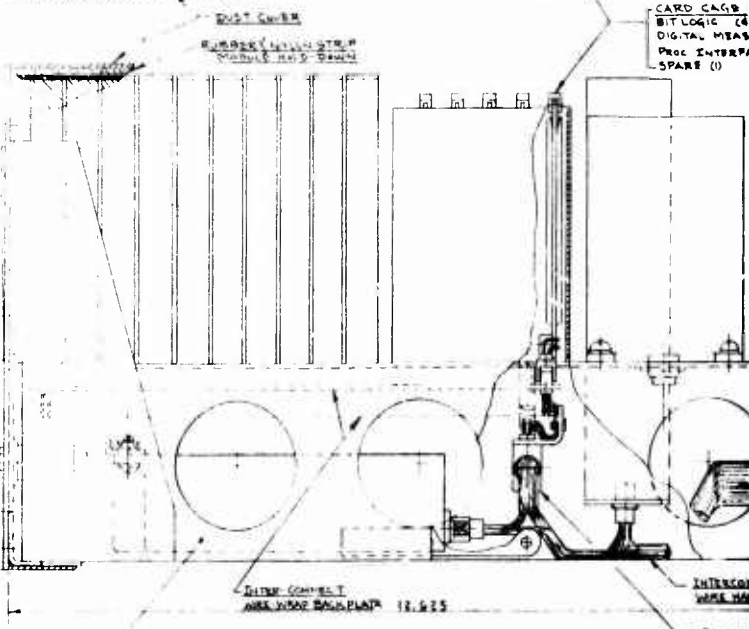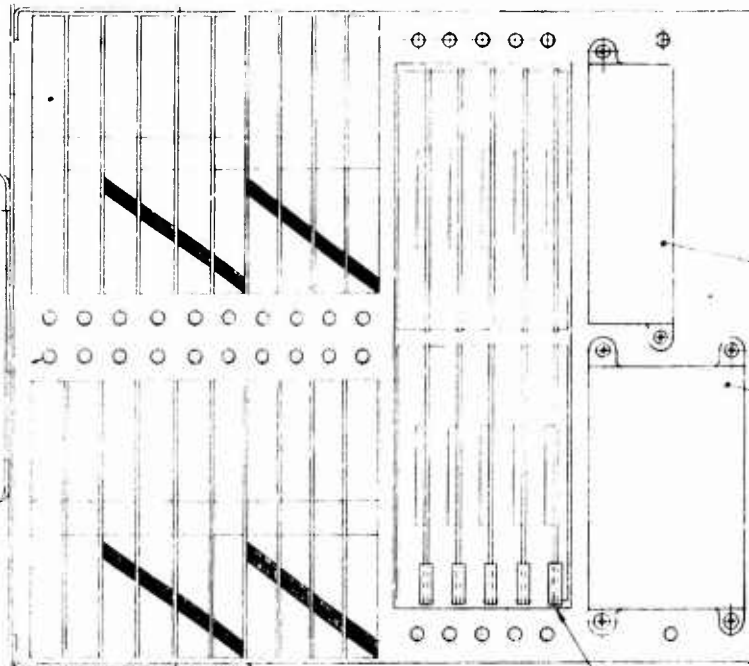20 PLUG-IN MODULES
SIZE - ½ × 4 × 4

TYPE	QUANTITY
PRE-AMP/MIXER	(1)
FREQUENCY SYNTHESIZER	(1)
IF AMP/FILTER DETECTOR	(4)
PN DEMODULATOR	(4)
IF AMP/MIXER	(4)
LOOP FILTER/CODE & PRR	
DETECTOR	(4)
BIT RF GENERATOR	(1)
SPARE	(1)

FAULT INDICATORS
RESET-TYPE

HANDLE-SPRING
RETURN - 90° TRAVEL

10.650 PANEL

DUST COVER

RUBBER/NYLON STRIP
MODULE HOLD DOWN

CARD CAGE
BIT LOGIC (4)
DIGITAL MEAS.
PROC INTERFACE
SPARE (1)

7.625

FAULT
INDICATOR

SPARE
FUSE

FUSE

TIME
INDICATOR

INTERCONNECT
WIRE HARNESS

FILTER CONNECT
WIRE WRAP BACK PLATE 12.625

POWER SUPPLY (2) 15.40 × 5.0
EST.WT 3.0 EACH

PROCESSOR
13 x 4 x 6.5
EST WT 2.0 #

XTAL - OSCILLATOR
2.5 x 3.3 x 3.7
EST WT 1.25 #

RACK & PANEL
CONNECTORS (2)

CARD CAGE
BIT LOGIC (4)
DIGITAL MEAS. (4)
PROC INTERFACE (1)
SPARE (1)

INTERCONNECT
WIRE HARNESS

½ CONNECTOR

FOUR CHANNEL DNSS RECEIVER

	DWG. IDENT NO.		
D	11982	SKS-100300	
SCALE			SHEET 1 OF 2

1

HF/IF MODULE

SIGNAL
I.C. CARDS

PROCESSOR

XTAL-OSC

ESTIMATED - CLASS A/B/F.

SIZE $10\frac{1}{8}$ W × $7\frac{5}{8}$ H × $12\frac{9}{16}$ L

VOL. 1000 CU.IN.

WEIGHT 30.0 LBS

DISSIPATION 60 WATTS

POWER SUPPLY
OPEN TEST POSITION

FOUR CHANNEL DNSS RECEIVER
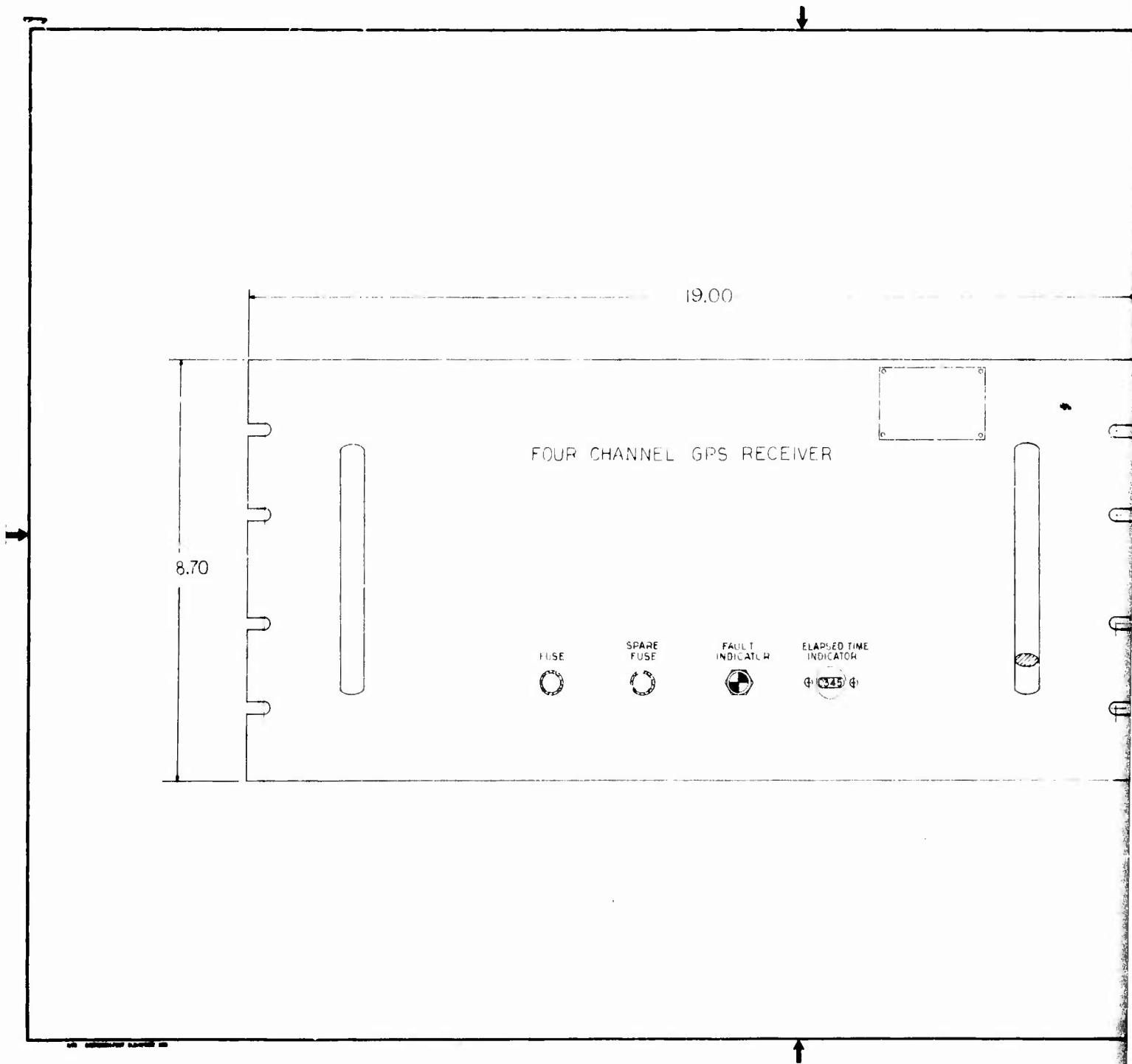
1

2

PROCESSOR

XTAL-OSC

ESTIMATED-CLASS A/B/F

SIZE $10\frac{1}{8}$ W x $7\frac{5}{8}$ H x $12\frac{9}{16}$ L

VOL   1000 CU.IN.

WEIGHT 30.0 LBS

DISSIPATION 60 WATTS
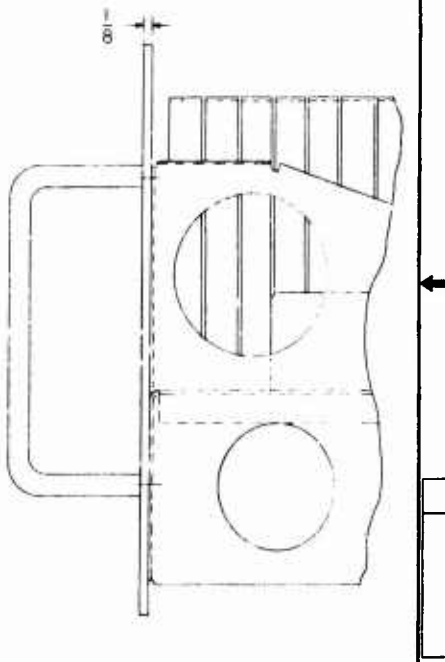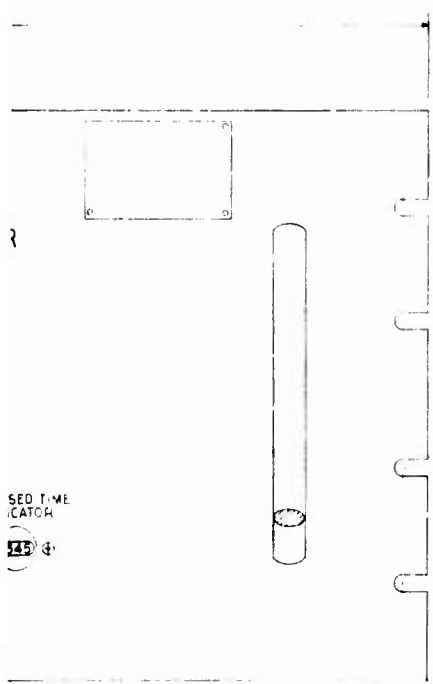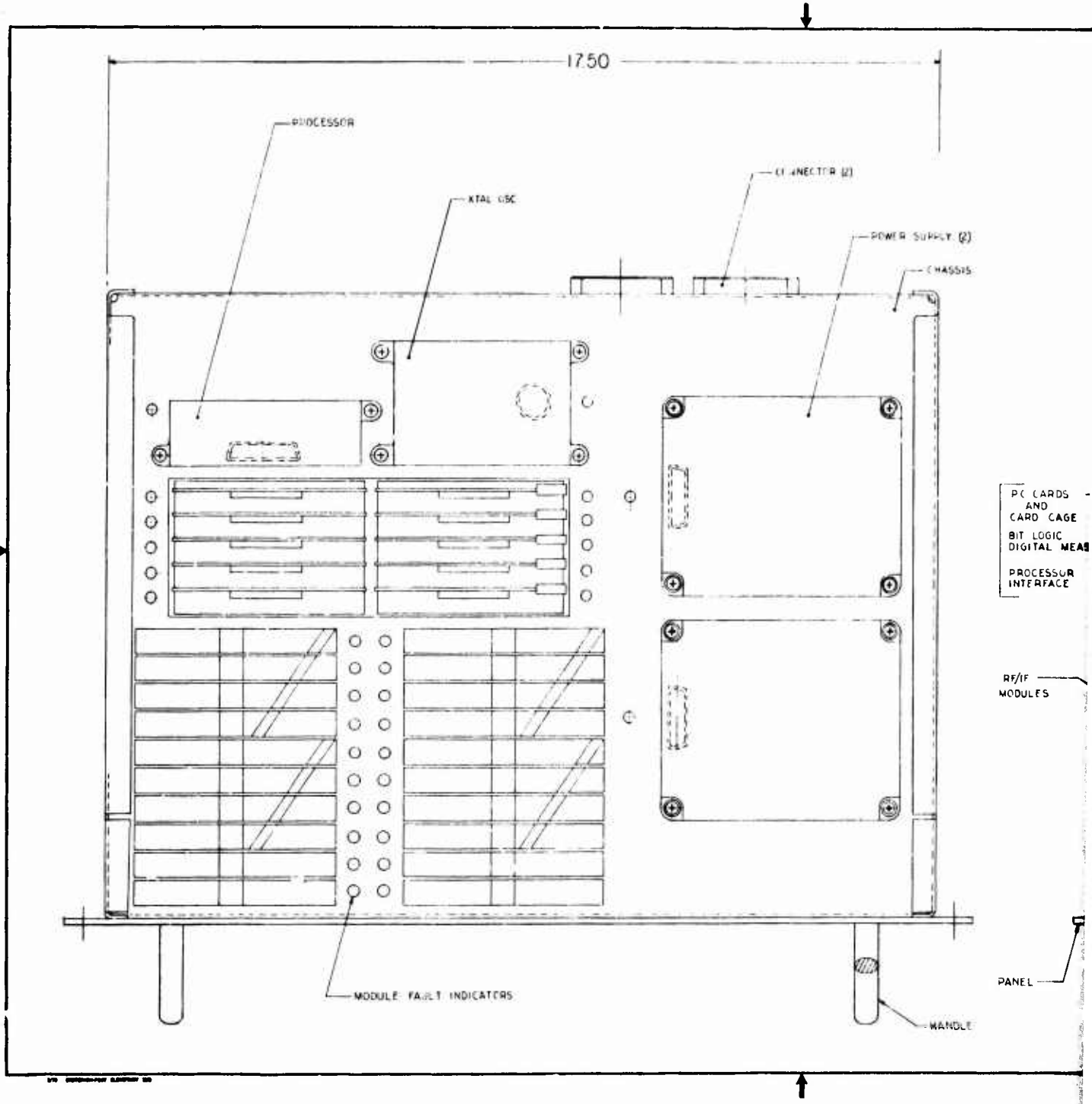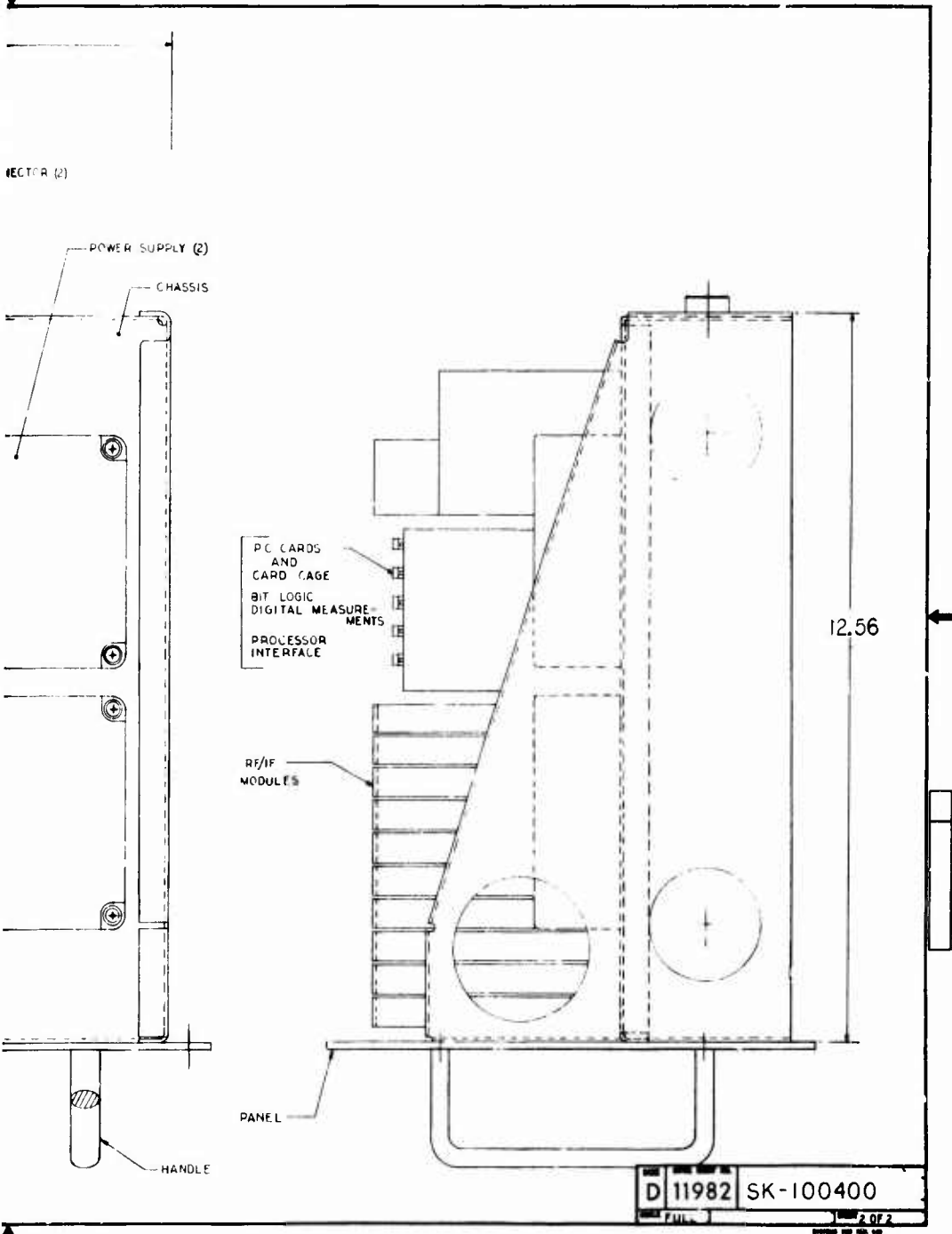
ANNEL DNSS RECEIVER

D	11982	SK 100300	
		2 of 2	

1

19.00

8.70

FOUR CHANNEL GPS RECEIVER

FUSE   SPARE   FAULT   ELAPSED TIME
         FUSE   INDICATOR INDICATOR

345

1/8

REVISIONS

ZONE	LTR	DESCRIPTION	DATE	APPROVED

SED TIME
iCATOR

CONTRACT NO.		
B. SCHECHTER	2-15-74	
CHECKED		
STRUCTURES		
B. SCHECHTER	2 15 74	
SUPERVISED		
PROJECT		
OTHER APPROVALS		

TRW
ONE SPACE PARK · REDONDO BEACH, CALIFORNIA

FOUR CHANNEL GPS RECEIVER

SIZE	CODE IDENT NO.	
D	11982	SK-100400
SCALE FULL		SHEET 1 OF 2

2

IECTOR (2)

POWER SUPPLY (2)

CHASSIS

PC CARDS
AND
CARD CAGE

BIT LOGIC
DIGITAL MEASURE-
MENTS

PROCESSOR
INTERFACE

12.56

RF/IF
MODULES

PANEL

HANDLE

D	11982	SK-100400
FULL		2 OF 2

DOCUMENT CONTROL DATA - R & D

(Security classification of title, body of abstract and indexing annotation must be entered when the overall report is classified)

1. ORIGINATING ACTIVITY *(Corporate author)*	2a. REPORT SECURITY CLASSIFICATION
Philco-Ford Corp, WDL Division Palo Alto, Calif. 94303	Unclassified
	2b. GROUP

3. REPORT TITLE

Global Positioning System (GPS), Part II, Volume B,
User Segment Trades and Analyses.

4. DESCRIPTIVE NOTES *(Type of report and inclusive dates)*

Final Report for GPS System Definition Study

5. AUTHOR(S) *(First name, middle initial, last name)*

6. REPORT DATE	7a. TOTAL NO. OF PAGES	7b. NO. OF REFS
28 Feb 1974	(2)	

8a. CONTRACT OR GRANT NO.	9a. ORIGINATOR'S REPORT NUMBER(S)
F04701-73-C-0296	WDL-TR5491-74-2-Vol-B
b. PROJECT NO.	
c.	9b. OTHER REPORT NO(S) *(Any other numbers that may be assigned this report)*
d.	SAMSO TR-74-183-74-2-Vol-B

10. DISTRIBUTION STATEMENT

DISTRIBUTION STATEMENT B

11. SUPPLEMENTARY NOTES	12. SPONSORING MILITARY ACTIVITY
	HQ Space and Missile Systems Organization P.O. Box 92960, Worldway Postal Center Los Angeles, Calif. 90009

13. ABSTRACT

This report presents detailed descriptions of the user equipment navigation
signal structure, receiver mechanization and ionospheric correction techniques
at L-band.

14 KEY WORDS	LINK A		LINK B		LINK C	
	ROLE	WT	ROLE	WT	ROLE	WT
Global Positioning System						
Data Message						
Ionospheric Correction						
Pseudo-Random Code Generation						
Spread Spectrum						